MODULATION OF MACROPHAGE FUNCTION AND IMMUNE RESPONSE BY A HELMINTH-DERIVED CYSTEINE PROTEASE

A thesis submitted for the Degree of
Doctor of Philosophy

by

Stephanie Nicole Dowdell B.Sc. (Hons)

School of Medical and Molecular Biosciences
Faculty of Science
University of Technology Sydney, Australia
2013

CERTIFICATE OF AUTHORSHIP/ORIGINALITY

I certify that the work in this thesis has not previously been submitted for a degree nor has it been submitted as part of requirements for a degree except as fully acknowledged within the text.

I also certify that this thesis has been written by me. Any help that I have received in my research work and the preparation of the thesis itself has been acknowledged. In addition, I certify that all information sources and literature used are indicated in the thesis.

_____

Stephanie Nicole Dowdell

2013

ACKNOWLEDGEMENTS

There are a number of people that I would like to thank, who have provided support for me during the completion of my thesis. My PhD project originally focused on a different topic, however, after more than a years' worth of work, results were ultimately not reproducible. I am therefore thankful for my supervisors, Associate Professor Bronwyn O'Brien, Dr Najah Nassif and Dr Andrew Hutchinson, who established a new project for me and shared their expertise and knowledge. Thank you also to Dr Lisa Sedger for advice and critical scientific discussions, I'm forever grateful.

Thank you to Dr Nicholas Archer, who taught me so much during the early years, your support and friendship has been invaluable. My fellow postgraduate students, particularly Charmain Castel with our cups of tea each morning, have been a godsend and I know that I have made friends for life during my time at UTS. Thanks also to my best friend Helen Thompson, who provided encouragement and a listening ear when I needed it most.

To the Helmedix group, including Dr Sheila Donnelly, Dr Mark Robinson, Dr John Dalton, Joyce To, Raquel Alvarado and Maria Lund. Thank you for your expertise, your discussions and advice. It's been a pleasure working with all of you, especially Raquel and Maria, and I wish you all great success with the current research focus.

Finally and most importantly, to my parents, Rosalyn and Robert Dowdell, who have stood by me through these long years, picking me up at the low points and cheering me on during the highs. Without your love and support, this would not have been possible. This thesis is dedicated to you. I will never be able to thank you enough.

PUBLICATIONS IN PEER-REVIEWED JOURNALS

Mark W. Robinson, Raquel Alvarado, Joyce To, Andrew T. Hutchinson, **Stephanie N. Dowdell**, Maria Lund, Lynne Turnbull, Bronwyn A. O'Brien, John P. Dalton and Sheila Donnelly. (2012). 'A helminth cathelicidin-like protein suppresses antigen processing and presentation in macrophages via inhibition of lysosomal vATPase', *The FASEB Journal*, 26(11): 4614-27.

PAPERS PRESENTED AT SCIENTIFIC CONFERENCES

Andrew T. Hutchinson & **Stephanie N. Dowdell**, Maria Lund, Mark W. Robinson, John P. Dalton, Bronwyn A. O'Brien, Sheila Donnelly. (2010). 'A helminth cysteine protease inhibits TRIF-dependent LPS activation of human macrophages.' Australasian Society of Immunology Scientific Meeting. Perth. (Oral presentation).

Stephanie N. Dowdell, Lynne Turnbull, Cynthia B. Whitchurch, Bronwyn A. O'Brien, Andrew T. Hutchinson. (2010). 'TLR4 endosomes are localised to tunnelling nanotubes in human macrophages.' Australasian Society of Immunology Scientific Meeting. Perth. (Poster presentation).

Stephanie N. Dowdell, Lynne Turnbull, Cynthia B. Whitchurch, Bronwyn A. O'Brien, Andrew T. Hutchinson. (2010). 'TLR4 endosomes are localised to tunnelling nanotubes in human macrophages.' RNSH/UTS Scientific Research Meeting. Sydney. (Oral presentation).

Stephanie N. Dowdell, Najah Nassif, Bronwyn A. O'Brien. (2008). 'Functional Studies of *SLC11A1* gene polymorphisms.' RNSH/UTS Scientific Research Meeting. Sydney. (Oral presentation).

AWARDS

Awarded the Poster Prize for the 2011 Science Research Day at the University of Technology, Sydney.

TABLE OF CONTENTS

LIST OF FIGURES

LIST OF TABLES

LIST OF ABBREVIATIONS

ΔCt	Change in cycle threshold
A	Absorbance
ADCC	Antibody-dependent cell-mediated cytotoxicity
AF	Alexa Fluor
AP-1	Activating protein-1
APCs	Antigen presenting cells
Arg1	Arginase 1
bp	Base pair
BSA	Bovine serum albumin
CBA	Cytokine bead array
CD	Cluster of differentiation
cDNA	Complementary deoxyribonucleic acid
C_t	Threshold cycle
CTLA	Cytotoxic T lymphocyte antigen
Cy5	Cyano 5
DAPI	4',6'-diamidino-2-phenylindole
DCs	Dendritic cells
DNA	Deoxyribonucleic acid
DNase	Deoxyribonuclease
dNTP	Deoxyribonucleoside triphosphate (or deoxyribonucleotide)
dsRNA	Double stranded ribonucleic acid
EDTA	Ethylenediaminetetraacetic acid
EEA-1	Early endosome antigen-1
ERK	Extracellular signal-related kinase
ES	Excretory/secretory
FACS	Fluorescence activated cell sorting
FBS	Foetal bovine serum
FhCL1	*Fasciola hepatica* cathepsin L1
FhES	*Fasciola hepatica* excretory/secretory products
FITC	Fluoroscein isothiocyanate
Fizz1	Resistin like alpha
Foxp3	Forkhead box p3
FSC	Forward Scatter
FSW	FACS Staining Wash
GAD	Glutamate decarboxylase
GAPDH	Glyceraldehyde-3-phosphate dehydrogenase
HDM-1	Helminth defence molecule 1
HLA	Human leukocyte antigen
IBD	Inflammatory bowel disease
IFN	Interferon
Ig	Immunoglobulin
IκBα	Nuclear factor of κ light polypeptide gene enhancer in B-cells inhibitor, α
IKK	IκB kinase
IL	Interleukin
IMDM	Iscove's modified Dulbecco's medium

iNOS	Inducible nitric oxide synthase
IRAK	IL-1R-associated kinase
IRF	Interferon regulatory factor
JNK	c-Jun NH2-terminal kinases
kDa	Kilo dalton
KEGG	Kyoto encyclopedia of genes and genomes
LBP	LPS-binding protein
LNFPIII	Lacto-N-fucopentaose III
LPS	Lipopolysaccharide
mAb	Monoclonal antibody
MAPK	Mitogen-activated protein kinase
MD-2	Myeloid differentiation protein-2
MFI	Mean fluorescence intensity
MHC	Major histocompatibility complex
MMSCs	Mesenchymal multipotent stromal cells
mRNA	Messenger ribonucleic acid
MyD88	Myeloid differentiation primary response gene 88
NF-κB	Nuclear factor κ B
NO	Nitric oxide
NOD	Non-obese diabetic
O/N	Overnight
p	Phosphorylated
PBS	Phosphate buffered saline
PCR	Polymerase chain reaction
Poly (I·C)	Polyinosinic:polycytidylic acid
Prx	Peroxiredoxin
RT-qPCR	Reverse transcriptase-quantitative polymerase chain reaction
RNA	Ribonucleic acid
RNase	Ribonuclease
RPL36AL	Ribosomal protein L36A like
RPMI	Roswell Park Memorial Institute
RT	Room temperature
RT-PCR	Reverse transcriptase-polymerase chain reaction
SD	Standard deviation
SDS-PAGE	Sodium dodecyl sulphate-polyacrylamide gel electrophoresis
SEA	Soluble egg antigen
SSC	Side scatter
T1D	Type 1 diabetes
TBK	TRAF-family-member-associated NF-κB activator binding kinase
TGF	Transforming growth factor
Th	T helper
TIR	Toll-interleukin-1 receptor
TIRAP	Toll-interleukin-1 receptor domain containing adaptor protein
TLR	Toll-like receptor
TNF	Tumour necrosis factor
TRAF	Tumour necrosis factor receptor-associated factor
TRAM	TRIF-related adaptor molecule
TRIF	Toll-interleukin-1 receptor-domain-containing adaptor-inducing interferon-β
Ym1	Chitinase 3-like 3

ABSTRACT

Helminth-derived excretory/secretory (ES) products have been demonstrated to mediate the anti-inflammatory/regulatory environment associated with helminth infection (for a review see Allen *et al.* 2011). The ES products of helminths have been exploited for therapeutic benefit in both murine and human models of autoimmune diseases (Zaccone *et al.* 2003; Zheng *et al.* 2008; Motomura *et al.* 2009; Ruyssers *et al.* 2009; Johnston *et al.* 2010; Cancado *et al.* 2011; Carranza *et al.* 2012; Kuijk *et al.* 2012). In our laboratory, the ES products of the liver fluke trematode, *Fasciola hepatica*, have been shown to prevent autoimmune type 1 diabetes in a murine model (Lund *et al.* in preparation). Disease prevention was associated with the initiation and perpetuation of anti-inflammatory/regulatory immune responses, including the generation of alternatively activated macrophages, regulatory T cells and regulatory B cell populations (Lund *et al.* in preparation). Nevertheless, the individual molecular components within the ES responsible for these phenomenon are unknown. Therefore, HPLC fractionation of the ES products of *Fasciola hepatica* was undertaken. This revealed a number of components with immune-modulatory effects. One of these *Fasciola hepatica* products is a cysteine protease, cathepsin L1 (FhCL1), and in fact it comprises a large proportion of the total ES products. In mice, FhCL1 suppresses pro-inflammatory immune responses through cleavage of toll-like receptor (TLR)-3, resulting in modulation of cell signalling in peritoneal macrophages (Donnelly *et al.* 2010).

This thesis therefore examines the effect of FhCL1 in human monocyte-derived macrophages. FhCL1 was shown to enhance expression of pro-inflammatory cytokines IL-6 and IL-8 in response to lipopolysaccharide. This was associated with the up-regulation of surface CD14, and the activation of TLR4 cell signalling via both the myeloid differentiation primary response gene 88 (MyD88)-dependent and toll-interleukin-1 receptor-domain-containing adaptor-inducing interferon-β (TRIF)-dependent signalling pathways. Furthermore, expression of IL-10 and co-stimulatory molecule CD86 was down-regulated in FhCL1-treated human monocyte-derived macrophages, and this was attributed to suppression of late endosomal TRIF-dependent signalling, with down-regulation of TRAF3. Although, FhCL1 modulated TLR

signalling in human and murine macrophages, and suppressed TRIF-dependent signalling in both human and mouse macrophages, FhCL1 enhanced pro-inflammatory cytokine expression in human monocyte-derived macrophages. Therefore, FhCL1 modulates immune responses in human monocyte-derived macrophages, albeit differently from murine peritoneal macrophages. Furthermore, while FhCL1 degraded TLR3 in murine peritoneal macrophages, FhCL1 had no effect on TLR3 or TLR4 expression or localisation in human monocyte-derived macrophages. However, treatment with FhCL1 was shown to suppress the uptake of lipopolysaccharide (LPS) by human macrophages, which appeared to correlate with altered α-tubulin localisation. Thus suppressed uptake of LPS correlates with the suppression of TRIF-dependent late endosomal signalling.

Nanotubes are cellular protrusions which connect cells and are utilised for the transport of cellular components between cells (reviewed in Gerdes *et al.* 2008; and Gurke *et al.* 2008). An incidental finding of this study was the observation of nanotubes connecting monocyte-derived macrophages in culture, and the documented trafficking of TLR4 between human macrophages, through these nanotubes. Interestingly, LPS stimulation enhanced the movement of TLR4 into nanotubes, but this was partially suppressed by FhCL1.

Taken together, the work presented in this thesis provides insight into the mechanism of action of FhCL1 in human monocyte-derived macrophages. Investigating the immune-modulatory effects of individual helminth-derived molecules is an important step in understanding the mechanisms by which helminths modulate host immune responses. Ultimately, such products may be harnessed as potential therapeutic agents in various situations, depending on their effect on the immune system.

CHAPTER 1:

GENERAL INTRODUCTION

1.1 MODULATION OF IMMUNE RESPONSE – AUTOIMMUNE DISEASE

Immunological tolerance to self-antigens prevents immune reactions against self-tissues and organs. This is essentially established through two mechanisms: (1) the elimination of self-reactive T cells within the thymus, known as central tolerance (for a review see Sprent *et al.* 2001); and (2) the deletion and/or suppression of self-reactive lymphocytes within circulation, including suppression by regulatory T cells, known as peripheral tolerance (reviewed in Walker *et al.* 2002). However, failure to induce tolerance may result in the destruction of self-tissue and the onset of autoimmunity. The pathogenesis of autoimmune diseases such as type 1 diabetes (T1D), multiple sclerosis (MS), rheumatoid arthritis and inflammatory bowel disease (IBD) are mediated by both innate immune cells, such as dendritic cells (DCs) and macrophages, and adaptive immune cells, including T helper (Th) cells and B cells, and the roles these cells play in autoimmune diseases are summarised below.

1.1.1 ACTIVATION OF DENDRITIC CELLS

Inflammatory stimuli, such as tissue damage or lipopolysaccharide (LPS)/endotoxin, as well as ligation with T cell surface receptor CD40, induces the maturation of DCs into a pro-inflammatory DC phenotype, known as DC1 (Rissoan *et al.* 1999). The 'type 1' DC phenotype is characterised by the secretion of pro-inflammatory cytokines such as interleukin (IL)-12, IL-6, IL-1α and IL-1β, and up-regulation of T cell co-stimulatory molecules such as CD80 and CD86 on the cell surface (Cella *et al.* 1996; Reis e Sousa *et al.* 1997; Rissoan *et al.* 1999).

Increased numbers of activated DCs have been observed in autoimmune diseases in humans and mice, including rheumatoid arthritis (Zvaifler *et al.* 1985; Waalen *et al.* 1988; Thomas *et al.* 1994), T1D (Jansen *et al.* 1994) and MS (experimental autoimmune encephalomyelitis (EAE)) (Serafini *et al.* 2000), suggesting they play a significant role in the onset of autoimmunity. Evidence for the role of DCs in the onset of autoimmunity is shown by the transfer of DCs isolated from mice with acute autoimmune disease inducing autoimmunity in the recipient, presumably due to their presentation of self-antigen (Ludewig *et al.* 1998; Dittel *et al.* 1999). For example, the transfer of DCs presenting myelin basic protein resulted in the induction of EAE in

irradiated mice following the transfer of transgenic T cells expressing T cell receptors capable of recognising myelin basic protein self-antigen (Dittel *et al.* 1999).

DCs are also major producers of pro-inflammatory cytokines which can promote the activation of T cells. Non obese diabetic (NOD) mice spontaneously develop T1D, with mononuclear infiltration of the pancreatic islets as early as 3-4 weeks of age (Makino *et al.* 1980; Kikutani *et al.* 1992). Within pancreatic islets, DCs produce tumour necrosis factor (TNF), which is cytotoxic to insulin-producing β-cells (Dahlen *et al.* 1998). Similarly, DCs from MS patients express higher levels of pro-inflammatory cytokines, interferon (IFN)-γ, TNF and IL-6 when compared to DCs from healthy subjects (Huang *et al.* 1999), and are associated with the stimulation of Th1 cells (Rissoan *et al.* 1999). Therefore, the expression of pro-inflammatory cytokines by DCs appears to be important in the development of autoimmune and inflammatory diseases.

1.1.2 CLASSICALLY ACTIVATED MACROPHAGES

Under inflammatory conditions, and in response to IFN-γ and TNF, macrophages adopt a classically activated phenotype (for a review see Fujiwara *et al.* 2005). Following activation, classically activated "M1" macrophages express pro-inflammatory cytokines, including IL-1, IL-6, IL-23 and IL-12, which plays a role in the initiation and perpetuation of inflammatory and autoimmune disease through tissue damage and the expansion of Th1 and Th17 cells (for reviews see Edwards *et al.* 2006; and Mosser *et al.* 2008).

For example, several populations of macrophages are involved in the pathogenesis of MS, and despite the blood brain barrier, 'blood-borne' macrophages are capable of migrating into the brain where they cause local inflammation through the production and secretion of proteases, prostaglandins, oxygen radicals, nitric oxide (NO), IL-1, IL-6 and TNF (reviewed in Hartung *et al.* 1992). Ultimately, this results in tissue damage including demyelination of nerve cells (Cammer *et al.* 1978; Chia *et al.* 1983; Konat *et al.* 1985; Brosnan *et al.* 1988; Selmaj *et al.* 1988).

Classically activated macrophages also play a role in the pathogenesis of TID. Antigen presenting cells (APCs) and self-reactive T cells infiltrate the islets of Langerhans within the pancreas and cause destruction of the insulin-producing β cells (for a review see Anderson *et al.* 2005). Within the pancreas, activated macrophages secrete cytokines such as TNF (Dahlen *et al.* 1998), which are toxic to β cells in the presence of IFN-γ (Baquerizo *et al.* 1990; Rabinovitch *et al.* 1990). Likewise, macrophages represent a major source of many cytokines, including IL-1β, TNF, IL-6, IL-8, IL-10, IL-12 and IL-18 in the inflamed mucosa during IBD pathogenesis (Sartor *et al.* 2005), establishing a predominately Th1/Th17 mediated immune environment. Lastly, classically activated macrophages in the synovial fluid in patients with rheumatoid arthritis secrete IL-15, a cytokine with chemoattractant properties for memory T cells, which promotes infiltration and proliferation of inflammatory T cells within the joint synovium, contributing to the pathogenesis of rheumatoid arthritis (McInnes *et al.* 1996). Furthermore, IL-15 activation of synovial T cells induces the production of IL-1α, IL-1β, TNF, IL-8, metalloproteinases and monocyte chemotactic protein-1 by macrophages, promoting the recruitment and activation of inflammatory cells (Badolato *et al.* 1997; McInnes *et al.* 1997; Sebbag *et al.* 1997). Macrophages also play a role in the presentation of type II collagen (Michaelsson *et al.* 1995), an auto-antigen of rheumatoid arthritis (Londei *et al.* 1989; Tarkowski *et al.* 1989; Trentham *et al.* 1993). Therefore the production of pro-inflammatory cytokines and the presentation of antigen by classically activated macrophages plays a significant role in the development of autoimmunity.

1.1.3 TH1/TH17 POLARISATION

Self-reactive T lymphocytes are activated in the presence of pro-inflammatory cytokines produced by APCs and are polarised to a Th1/Th17 phenotype (for a review see Zhu *et al.* 2008). In the presence of antigen presented by APCs and a pro-inflammatory cytokine milieu, Th cells differentiate into Th1 cells which are characterised by the production of IFN-γ, IL-2 and granulocyte macrophage colony stimulating factor (Mosmann *et al.* 1986; Hsieh *et al.* 1993). Alternatively, in the presence of IL-6, IL-21, IL-23 and transforming growth factor (TGF)- β produced by APCs, naïve Th cells differentiate into Th17 cells (Bettelli *et al.* 2006; Korn *et al.* 2007). Th17 cells are characterised by the expression of IL-17A, as well as IL-17F,

IL-21 and IL-22 (Langrish *et al.* 2005; Nurieva *et al.* 2007). These cells are potent inducers of tissue inflammation, and are associated with autoimmunity (reviewed in Korn *et al.* 2009).

Autoimmunity is often associated with increased expression of pro-inflammatory cytokines. For example, T cell populations in the lamina propria of patients suffering Crohn's disease secrete higher levels of IFN-γ compared to cells from unaffected individuals (Fuss *et al.* 1996). Likewise, within the joint synovium of individuals with rheumatoid arthritis, Th1 cell populations predominate, producing large amounts of IFN-γ (Miltenburg *et al.* 1992; Quayle *et al.* 1993). The pro-inflammatory cytokine milieu established by activated Th1 and Th17 cells contributes to autoimmunity (for reviews see Skapenko *et al.* 2005; and Korn *et al.* 2009) through either direct effects on tissues, with some cytokines being toxic to cells (Dahlen *et al.* 1998), or by activating other immune cells which cause inflammation, cell death and tissue damage.

The pro-inflammatory milieu associated with the induction of Th17 cells is also associated with the suppression of regulatory T cells, which favours the development of autoimmunity (for a review see Korn *et al.* 2009). Typically, TGF-β induces regulatory T cell differentiation (Chen *et al.* 2003), however in the presence of the pro-inflammatory cytokine IL-6, TGF-β-driven induction of Forkhead box P3 (Foxp3) is suppressed. Foxp3 is a transcription factor that acts primarily as a transcriptional repressor (Schubert *et al.* 2001), and it is a potent control factor of regulatory T cells (Fontenot *et al.* 2003; Hori *et al.* 2003). As a result of the suppression of Foxp3, Th17 cells are induced (Bettelli *et al.* 2006) and in the absence of regulatory T cells mice succumb to multiple autoimmune diseases (Asano *et al.* 1996), demonstrating the active role of Tregs in maintaining tolerance. Autoimmune diseases such as systemic lupus erythematosus (Crispin *et al.* 2003; Liu *et al.* 2004) and Kawasaki disease (Furuno *et al.* 2004) are associated with reduced regulatory T cell numbers relative to healthy subjects. Thus, low levels of regulatory T cells were frequently associated with increased autoimmune disease activity and poorer prognosis. Genetic defects in regulatory T cell populations are another contributing factor to the development of autoimmunity. For example, polymorphisms in Foxp3 are strongly linked with immune dysregulation (Wildin *et al.* 2002) with individuals encoding a promoter region polymorphism being more susceptible to T1D (Bassuny *et al.* 2003).

Autoimmune disease pathogenesis is also associated with changes in T cell anergy, a state of T cell unresponsiveness. In this regard, cytotoxic T lymphocyte antigen (CTLA)-4 is an essential controller of T cell activation, acting as a repressor of T cell activation and inducing T cell anergy (McCoy *et al.* 1999). Therefore, knockout of CTLA-4 is associated with systemic autoimmunity in mice, due to failure to induce anergy in T cells (Tivol *et al.* 1995; Ueda *et al.* 2003). Anergy of Th2/regulatory T cell populations is also responsible for the development of autoimmunity in some cases. For example, several immune deficiencies contribute to the onset of T1D in the NOD mouse, including the induction of anergy in Th2/regulatory T cell populations (Zipris *et al.* 1991; Rapoport *et al.* 1993; Jaramillo *et al.* 1994). The induction of anergy may lead to a breakdown of tolerance and the concomitant expansion of self-reactive Th1 populations and this has been associated with increased susceptibility to diabetes (Jaramillo *et al.* 1994).

1.1.4 PRODUCTION OF AUTOANTIBODIES BY B CELLS

B cells play an important role in the pathogenesis of autoimmune disease. As APCs, B cells present antigen to T cells and are a source of pro-inflammatory cytokines which contributes to autoimmunity (reviewed in Dorner *et al.* 2009). The recognition of self-antigen results in plasma B cell populations that produce autoantibodies, which are associated with the destruction of self-tissue (reviewed in Dorner *et al.* 2009). By binding self-antigen on the surface of cells, autoantibodies induce antibody-dependent cell-mediated cytotoxicity (ADCC), where the Fc receptor on the surface of effector cells mediates the release of cytotoxic molecules and targeted destruction of self-tissue, as observed in autoimmune thyroid disease (Rebuffat *et al.* 2008). The binding of antibodies with self-antigen also activates the classical complement pathway which results in the formation of a membrane pore and the destruction of cells, such as in the case of rheumatoid arthritis (Ruddy *et al.* 1975) and Sjögren's syndrome (Hansen *et al.* 2003). Autoantibodies are also present in MS and target myelin components as well as axonal antigens and oligodendrocyte precursors (Niehaus *et al.* 2000; Kanter *et al.* 2006; Mathey *et al.* 2007; Meinl *et al.* 2011). This is often associated with destruction of axons, which occurs in a complement-dependent manner (Elliott *et al.* 2012).

Autoimmunity is sometimes associated with particular antibody isotypes, namely immunoglobulin (Ig)G1 and IgG3. This is due to their high affinity for Fc receptors on effector cells and their ability to activate complement (Canfield *et al.* 1991). Isotype class switching is stimulated by T helper cells and is dependent upon cytokines and CD40 ligation (reviewed in Esser *et al.* 1990). In T1D, the presence of autoantibodies against insulin, islet antigen-2 and glutamate decarboxylase (GAD)-65 has been reported (Rewers *et al.* 1996; Ziegler *et al.* 1999; Kimpimaki *et al.* 2001) and these antibodies are associated with an increased risk of developing T1D (Verge *et al.* 1996). This was demonstrated in a large scale U.S. study where first-degree relatives of individuals with T1D had a 68% 5-year risk of developing T1D when they had two or more autoantibodies (Verge *et al.* 1996). However, investigations into the predominant antibody isotypes present during T1D are inconsistent, but are suggestive of a predominance of IgG1 and IgG3 autoantibodies (reviewed in Pihoker *et al.* 2005). For example, a study investigating antibody isotype in the siblings of individuals with T1D found that the earliest peak in antibody isotype for antibodies against GADA, insulin and islet antigen-2 was IgG1 (Bonifacio *et al.* 1999). Likewise, a twin study investigating the antibody isotype in the non-diabetic twin observed that for the 15 twins that subsequently developed diabetes, an IgG1 antibody specific for islet antigen-2 and GAD predominated, both prior to and upon diagnosis of T1D (Hawa *et al.* 2000).

1.1.5 TOLL-LIKE RECEPTORS AND AUTOIMMUNITY

Autoimmune diseases are also hypothesised to be associated with polymorphisms in or altered expression of pattern recognition receptors such as Toll-like receptors (TLRs) (reviewed in Mills 2011). Toll-like receptors are expressed by a wide variety of cells, but particularly APCs, and recognise specific molecular patterns (known as pathogen associated molecular patterns) which are present in microbial, viral and parasite products (for a review see Akira *et al.* 2006). While TLRs all recognise different ligands, they broadly recognise either nucleic acids, in the case of TLR3 (Alexopoulou *et al.* 2001), TLR7 (Diebold *et al.* 2004), TLR8 (Heil *et al.* 2004) and TLR9 (Lund *et al.* 2003; Hochrein *et al.* 2004; Krug *et al.* 2004a; Krug *et al.* 2004b; Tabeta *et al.* 2004) or lipoproteins, in the case of TLR1 (Takeuchi *et al.* 2002), TLR2 (Aliprantis *et al.* 1999; Hirschfeld *et al.* 1999; Lien *et al.* 1999), TLR6 (Takeuchi *et al.* 2001), TLR4 (Poltorak *et al.* 1998) and TLR5 (Hayashi *et al.* 2001) (summarised in Figure 1.1).

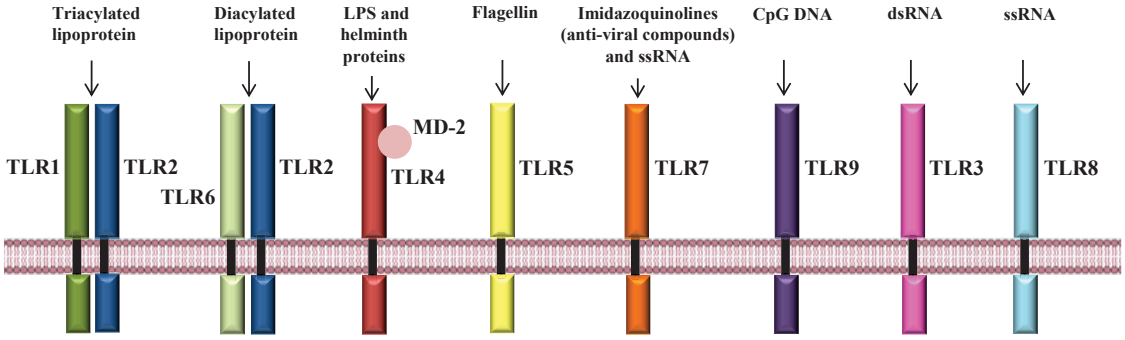

Figure 1.1: Toll-like receptors and their ligands.
Toll-like receptors (TLR) recognise bacterial (TLR1-7 and TLR9), viral (TLR3, 7-9) and helminth (TLR2-4) components based on specific molecular patterns of their components. These components include lipoproteins and nucleic acids. (Adapted from Takeda *et al.* 2004).

Following recognition of their ligands, TLR signalling pathways are activated, inducing pro-inflammatory responses and the expression of co-stimulatory molecules (for reviews see Akira *et al.* 2004; and Takeda *et al.* 2004). However, dysregulated induction of TLR-mediated pro-inflammatory responses is associated with the development of inflammatory disorders and autoimmune disease (reviewed in Mills 2011). Firstly, polymorphisms within the TLR genes may be associated with differences in the responsiveness of TLRs to ligands and thus may alter the outcome of activation. Association studies have linked polymorphisms in TLR2 with T1D (Park *et al.* 2004) and polymorphisms in TLR4 and TLR9 with Crohn's Disease patients (Hong *et al.* 2007). Secondly, within tissues that typically down-regulate TLRs due to continual exposure to microflora, infiltration of the tissue or organ by cells expressing TLRs can contribute to organ-specific inflammation during autoimmunity. For example, the intestinal tract down-regulates TLRs and CD14 to prevent excessive inflammation in the microflora-populated intestine (Smith *et al.* 1997; Smith *et al.* 2001; Smythies *et al.* 2005). However, the presence of TLRs and CD14 on APCs which have migrated into the intestinal tract during inflammation results in expression of pro-inflammatory cytokines to the detriment of the intestinal tissue and contributes to inflammatory processes (Hausmann *et al.* 2002). Additionally, TLR signalling is activated in some autoimmune diseases, including T1D, which contributes to the inflammation associated with T1D (Devaraj *et al.* 2007). Similarly, the presence of ligands of TLR4 such as heat shock protein 60, hyaluronic acid and fibronectin within the joint synovium of rheumatoid arthritis sufferers may activate TLR4 on the surface of macrophages and

drive expression of the pro-inflammatory cytokines associated with rheumatoid arthritis (Ohashi *et al.* 2000; Okamura *et al.* 2001; Termeer *et al.* 2002). Lastly, the knockout of TLRs in mice confirms the role TLRs play in the development of autoimmunity, as TLR knockout mice demonstrate reduced susceptibility or delayed onset of autoimmune diseases, for example, knockout of TLR2 inhibited T1D onset (Kim *et al.* 2007), knockout of TLR2 or TLR4 decreased the severity of or prevented rheumatoid arthritis (Frasnelli *et al.* 2005; Abdollahi-Roodsaz *et al.* 2008) and TLR9 knockout delayed the onset of EAE (Prinz *et al.* 2006).

1.1.6 INCIDENCE OF AUTOIMMUNITY

In recent decades the incidence of autoimmune diseases, including T1D, has increased rapidly. In the first half of the 20th century, T1D incidence was stable and relatively low, reported to range from 2-7 per 100,000 in the United States, Denmark and Norway between 1900 to 1920 (Gale 2002). However, a clear increase in T1D incidence began after the middle of the century. For example, in the U.S. the incidence of T1D rose from 6.6/100,000 per year in 1950-1952 to 11.3/100,000 per year in 1959-1961 (Gale 2002). By the end of the 20th century national registries for T1D had been established and the incidence of T1D continued to increase by approximately 3% each year (Gale 2002). The incidence of T1D varies dramatically within and between countries, and for the period between 1990 and 1994, incidence rates ranged from 0.1 per 100,000 per annum in China and Venezuela to 36.8 per 100,000 in Sardinia and over 40.9 per 100,000 in Finland (DIAMOND Project Group 2006).

Similarly, the incidence of MS has also risen during the 20th century (Alonso *et al.* 2008). Studies have shown that MS incidence rates are higher in women compared to men and a meta-analysis pooling incidence studies published between 1966 and 2007 showed that prior to 1980 the incidence of MS in women was 3.4 per 100,000 which increased to 4.7 per 100,000 from 1980 to 2007 (Alonso *et al.* 2008). Comparatively, the incidence in men prior to 1980 was 1.9 per 100,000 which rose to 2.4 per 100,000 after 1980 (Alonso *et al.* 2008). The World Health Organization reported that the median global incidence of MS is 2.5 per 100,000 when incidence was not separated by gender, with the lowest incidence in Africa (0.1 per 100,000) and the highest median incidence in Europe (3.8 per 100,000) (World Health Organization 2008). The rapid

increase in autoimmune disease in recent years suggests that something has changed in the environment to alter susceptibility to autoimmune disease (Karvonen *et al.* 1993; Kolb *et al.* 1994) and it was noted that NOD mice reared under specific pathogen free conditions had higher T1D incidence suggesting that exposure to pathogens had a protective effect against autoimmune disease (Like *et al.* 1991; Wilberz *et al.* 1991).

1.2 MODULATION OF IMMUNE RESPONSE – HELMINTH PARASITE INFECTION

In contrast to the increasing incidence rates of autoimmune disease, the prevalence of parasitic worm (helminth) infection has declined globally in recent decades. This is largely due to national control programs and improvements in healthcare and sanitation (de Silva *et al.* 2003; Ziegelbauer *et al.* 2012). Helminths can be separated into three main classes, nematodes (also known as roundworms), trematodes (also known as flatworms), and cestodes (also known as tapeworms) and infection is associated with a variety of infectious diseases and tissue damage. For example, fasciolosis which results from infection with the trematode *Fasciola hepatica*, results in damage to the liver which can ultimately lead to fibrosis (reviewed in Marcos *et al.* 2008).

Helminths live within and feed off living hosts, and during infection they release a collection of molecules, termed excretory/secretory (ES) products (for reviews see Lightowlers *et al.* 1988; and Hewitson *et al.* 2009). The composition of ES products is specific to each species and can differ depending on the phase of the life cycle, but generally consist of proteins, glycoproteins and glycolipids, including surface antigen molecules and enzymes (Robinson *et al.* 2005; Delcroix *et al.* 2007; Guillou *et al.* 2007; Mulvenna *et al.* 2009; Hewitson *et al.* 2011). Parasite ES products such as cysteine proteases are believed to facilitate invasion and digestion of host tissues, to aide parasite migration and feeding (Smith *et al.* 1993b). However, during infection ES molecules also act upon host immune cells such as APCs, including DCs and macrophages (Rodriguez-Sosa *et al.* 2002; Nair *et al.* 2003; Raes *et al.* 2005; Segura *et al.* 2007; Donnelly *et al.* 2008; Hamilton *et al.* 2009). In the presence of parasites, the cytokine milieu secreted by APCs promotes the differentiation of Th2 cells and inhibits Th1 cell subsets (Grencis *et al.* 1991; Herbert *et al.* 2004; Jankovic *et al.* 2004). Furthermore, the production of Resistin-like molecule (RELM)α and arginase 1 (Arg1) by macrophages

(Nair *et al.* 2009; Pesce *et al.* 2009) and RELMβ by epithelial cells (Herbert *et al.* 2009), promotes wound repair and the containment of parasites, by promoting extracellular matrix production or by preventing helminth feeding (reviewed in Allen *et al.* 2011). See Figure 1.2 for a summary of the mechanisms by which helminths modulate immune responses, which are expanded upon in subsequent sections.

1.2.1 T HELPER 2 AND REGULATORY T CELL POLARISATION AND PERIPHERAL TOLERANCE

In contrast to the polarisation of pro-inflammatory Th1 and Th17 cells during autoimmune disease pathogenesis, infection with helminths results in the polarisation of naïve Th cells into anti-inflammatory Th2 populations. The induction of a Th2 response is common to most helminth species. For example, after infection with *F. hepatica* metacercarie, BALB/c mice exhibited Th2 cell responses, with increased expression of IL-4 and IL-5 and low levels of IL-12 and IFN-γ (O'Neill *et al.* 2000). Likewise, the ES products of *Schistosoma mansoni* also induce polarisation of Th2 responses, coincident with egg production by adult worms, in both humans and murine models (Jankovic *et al.* 2004; Pearce 2005). Furthermore, *Trichinella spiralis* infection in NIH or B10.G mice is associated with up-regulation of IL-3, IL-4, IL-5 and IL-9, indicative of Th2 cell activation (Grencis *et al.* 1991).

Along with the induction of Th2 effector cells during helminth infection, the anti-inflammatory milieu induces populations of regulatory T cells that secrete IL-10 and TGF-β (Taylor *et al.* 2005). During early stages of *Litomosoides sigmodontis* infection, an increase in $CD4^+$ T cells occurs within the pleural cavity and lymph nodes close to the site of infection (Taylor *et al.* 2009b). Within these expanded $CD4^+$ T cell populations, there is a significant expansion of $CD4^+Foxp3^+$ regulatory T cells (Taylor *et al.* 2009b). Likewise, infection with *Heligmosomoides polygyrus bakeri* promotes the production of regulatory cytokines and regulatory $CD8^+$ T cells within the intestinal mucosa of infected mice (Metwali *et al.* 2006; Setiawan *et al.* 2007). Regulatory T cells suppress immune responses through contact-dependent mechanisms such as surface receptor interaction and contact-independent mechanisms such as the expression of cytokines and through competition for limited antigen or cytokine (reviewed in Sojka *et al.* 2008).

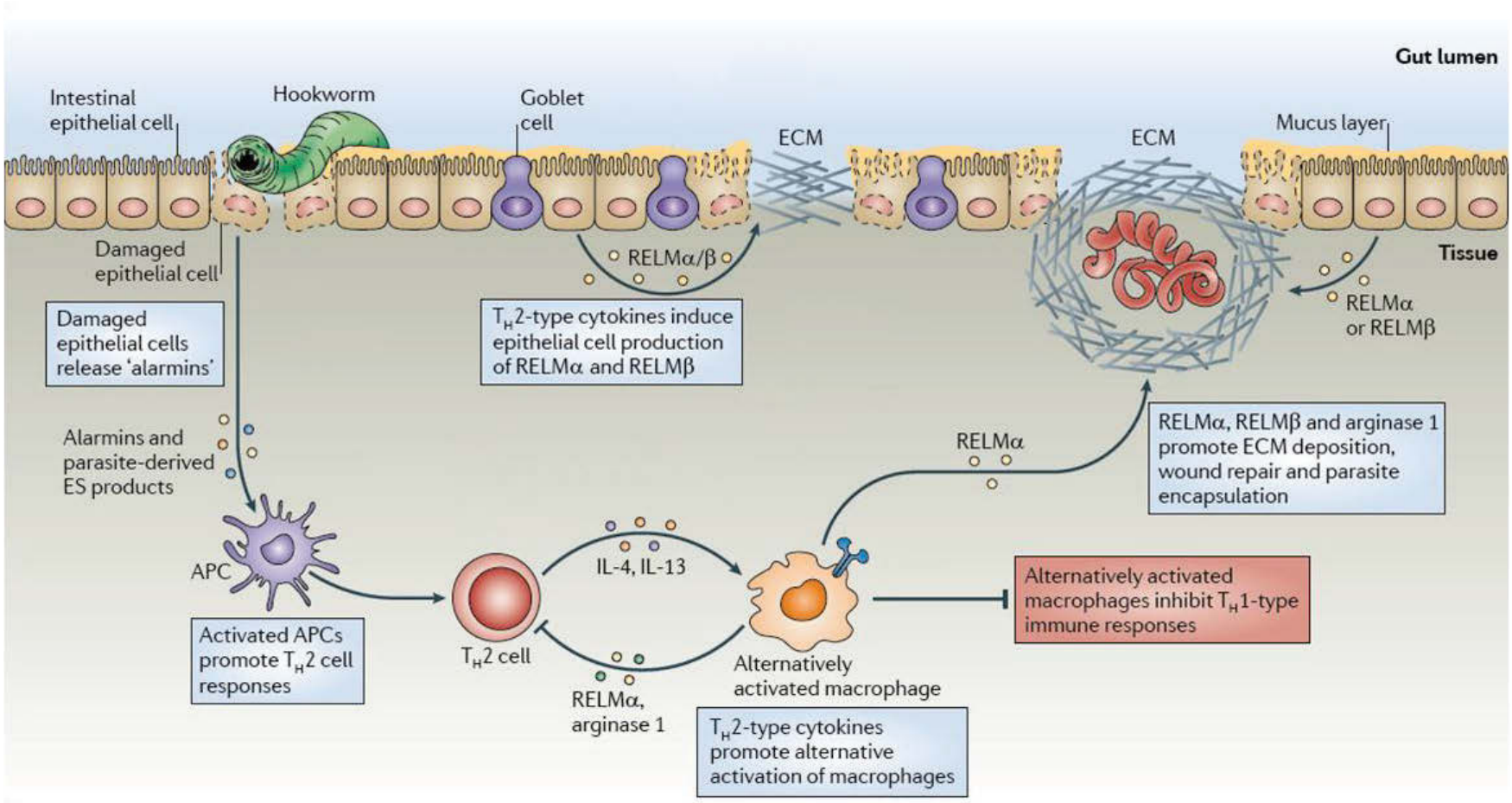

Figure 1.2: The induction of Type 2 immunity during helminth infection.
The migration of helminths through tissues results in cell death and the release of alarmins. These molecules, in conjunction with parasite-derived excretory/secretory (ES) products, promote a type 2 response by activating antigen presenting cells (APCs), including dendritic cells and macrophages, which promote Th2 cell responses and inhibit Th1 and classically activated macrophage responses. The production of resistin-like molecule (RELM)-α and RELMβ by epithelial cells, along with arginase 1, promote production of extracellular matrix (ECM) for tissue repair and for the containment of helminths through encapsulation. (Adapted from Allen *et al.* 2011).

The suppression of host immune response against helminths by regulatory T cells is essential for helminth survival. For example, neutralisation of regulatory T cells through antibodies against both regulatory T cell surface marker, CD25, and T effector cell costimulatory molecule GITR (glucocorticoid-induced TNFR-related protein), results in the efficient clearance of established *Litomosoides sigmodontis* infection (Maizels *et al.* 2004). This suggests that regulatory T cells are essential for dampening the immune response and hence maintaining helminth infection.

The differentiation of Th cells is dependent upon the cytokine milieu and defined Th cell subsets are mutually exclusive, with the activation and differentiation of one subset suppressing the differentiation of other Th subsets. For example, Th1 and Th2 subsets are mutually exclusive, with the expression of IFN-γ by Th1 cells suppressing Th2 differentiation and IL-4 production by Th2 cells suppressing Th1 differentiation (Hsieh *et al.* 1992; Seder *et al.* 1992). Secretion of IFN-γ by Th1 cells and IL-4 by Th2 cells also inhibits Th17 differentiation (Harrington *et al.* 2005; Park *et al.* 2005). The secretion of TGF-β by regulatory T cells suppresses Th1, Th2 and Th17 responses, regulating immune responses (Gorelik *et al.* 2000; Xu *et al.* 2003; Zhou *et al.* 2008). The polarisation of Th2 cells, along with the induction of regulatory T cells by helminths is termed a 'modified type 2 profile', and the immunological milieu established is associated with inhibition of pro-inflammatory Th1/Th17 cell populations (Figure 1.3).

While helminth infection is commonly associated with induction of Th2/regulatory T cells, some parasites are associated with the induction of T cell anergy. In both humans and mice, the chronic phase of filarial parasite or schistosomal infection is frequently marked by T cell anergy, which is associated with reduced T cell/lymphocyte proliferation as well as elevated inhibitory molecules on T cells, such as GRAIL (Gene relating to anergy in lymphocytes) and CTLA-4, as well as programmed death ligand 1 (PD-L1) on the surface of macrophages. For example, during *Litomosoides sigmodontis* infection in BALB/c mice, effector T cells at the site of infection were hyporesponsive, failing to respond to *Litomosoides sigmodontis* antigen (Taylor *et al.* 2007). This hyporesponsiveness was not associated with the induction of regulatory T cells during *Litomosoides sigmodontis* infection, as ablation of regulatory T cells had no effect on the responsiveness of effector T cells. Instead, T cell anergy induced during

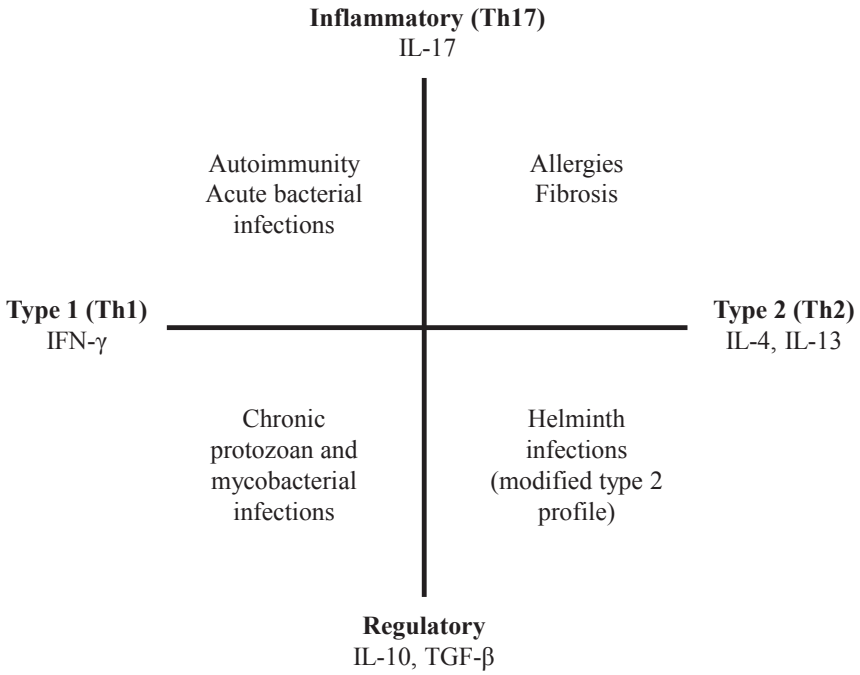

Figure 1.3: T cell subsets and disease association.
Each subset of T cells is associated with a distinct set of cytokines. During infection, autoimmune reactions or allergic reactions, the cytokines and T cell populations induced results in inhibition of the opposing immune response, for example, the induction of a Th2/regulatory T cell response during helminth infection inhibits Th1/Th17 responses. (Adapted from Diaz *et al.* 2007).

Litomosoides sigmodontis infection was associated with elevated expression of inhibitory molecules, such as CTLA-4, on the surface of T cells (Taylor *et al.* 2007). By competing with the positive co-stimulatory molecule CD28 for binding CD80 and CD86, CTLA-4 inhibits T cell activation (Teft *et al.* 2006). When CD80 and CD86 are engaged, CTLA-4 acts as a negative regulator for T cell activation and suppresses T cell responses (Teft *et al.* 2006). PD-L1 typically interacts with programmed death 1 (PD-1) on T cells resulting in negative regulation of lymphocyte activation (Freeman *et al.* 2000). During infection with *S. mansoni*, PD-L1 was up-regulated on the surface of macrophages and when these macrophages were cultured with naïve $CD4^+$ and $CD8^+$ T cells, there was a marked impairment of T cell proliferation, indicative of anergy (Smith *et al.* 2004). Lastly, during chronic *S. mansoni* infection, the number of Th2 cells plateaus after the acute phase of infection, and proliferation of Th2 cells declines (Taylor *et al.* 2009a). The hyporesponsive state of T cells was not associated with continued inhibitory signals via APCs, indicative of adaptive tolerance, instead, repeated antigen stimulation resulted in the up-regulation of Grail which is important for the induction of T cell anergy (Seroogy *et al.* 2004; Taylor *et al.* 2009a).

1.2.2 ANTIBODY ISOTYPE SWITCHING AND INDUCTION OF REGULATORY B CELLS

IgG1 and IgG3 autoantibodies, with high affinity for Fc receptors and complement (Canfield *et al.* 1991), are the predominant antibody isotype produced during autoimmune disease pathogenesis in humans (reviewed in Pihoker *et al.* 2005). However, helminth infection in humans is usually associated with B cells switching their antibody isotype to IgG4 or IgE (Ottesen *et al.* 1985; Hussain *et al.* 1986). The IgG4 isotype is non cytolytic and has low affinity for Fc receptors (van der Zee *et al.* 1986) and this is believed to be one of the main mechanisms by which it enhances immune evasion by filarial parasites (reviewed in Adjobimey *et al.* 2010). This limits host effector activity by preventing the induction of ADCC (Dafa'alla *et al.* 1992; van der Neut Kolfschoten *et al.* 2007) and appears to be important in filarial helminth infection. For example, IgG4 represents 88% of the total IgG in *Brugia malayi* infection and this is associated with asymptomatic infection (Kurniawan *et al.* 1993). Moreover, individuals with symptomatic infection (elephantitis) produce higher levels of IgG1, IgG2 and IgG3, and lower titres of IgG4 than asymptomatic individuals, indicating a possible protective role for IgG4 in filariasis (Kurniawan *et al.* 1993). Another example of the benefits of IgG4 to parasites is in patients with *Wuchereria bancrofti* filariasis in whom IgG4 correlates with the prevention of histamine release (Hussain *et al.* 1992). In fact, histamine inhibition could be prevented by the removal of IgG4 from the sera of patients (Hussain *et al.* 1992).

IgE is also induced during helminth infection (Jarrett *et al.* 1974; Carson *et al.* 1975; Ishizaka *et al.* 1976; Turner *et al.* 1979; Hussain *et al.* 1981; Yamada *et al.* 1992) and is recognised by Fc receptors on the surface of certain myeloid cells such as mast cells (Stanworth *et al.* 1968; Ishizaka *et al.* 1970). While IgE typically results in mast cell and eosinophil degranulation, contributing to the destruction of helminths, the majority of IgE produced during helminth infection is not specific to helminth antigens (Jarrett *et al.* 1974; Carson *et al.* 1975; Ishizaka *et al.* 1976; Turner *et al.* 1979; Yamada *et al.* 1992). Thus, it has been suggested that the presence of non-specific IgE may saturate Fc binding sites on the surface of mast cells and basophils and provide protection from degranulation targeted to helminths (reviewed in Erb 2007).

Helminths also induce regulatory B cells (Gillan *et al.* 2005; reviewed in Hussaarts *et al.* 2011), which are populations of B cells characterised by the expression of IL-10, and they are associated with the suppression of pro-inflammatory immune responses (reviewed in Mizoguchi *et al.* 2006). For example, BALB/c mice infected with the nematode *Brugia pahangi* promote Th2 responses, with up-regulation of IL-4, IL-5 and IL-10, but when B cells were removed from splenocyte cultures, the levels of IL-4, IL-5 and IL-10 were decreased, while IFN-γ expression was increased (Gillan *et al.* 2005). In this example, B cells accounted for approximately 60% of IL-10 and the production of IL-10 correlated with reduced antigen presenting ability of the B cells through down-regulation of co-stimulatory molecules, likely suppressing $CD4^+$ T helper cell activation and expansion (Gillan *et al.* 2005). Furthermore, Th1 inflammatory responses were expanded in *S. mansoni*-infected μMT mice (which are deficient in B cells), indicating that B cells are directly required for the suppression of Th1 cells (Ferru *et al.* 1998). The production of IL-10 by regulatory B cells also recruits regulatory T cells, as demonstrated by infection with *S. mansoni* in BALB/c mice (Amu *et al.* 2010).

1.2.3 MODULATION OF DENDRITIC CELL MATURATION AND FUNCTION

Helminth infection inhibits the maturation of DCs and alters their activation status, driving their polarisation to a tolerogenic (DC2) phenotype. Tolerogenic DCs are associated with the activation of regulatory T cells and Th2 cells as well as suppression of pro-inflammatory responses (Rissoan *et al.* 1999; reviewed in Maizels *et al.* 2004). Infection with live helminths or treatment with helminth ES products typically does not activate DCs and results in no change in the expression of co-stimulatory surface markers from unstimulated DCs, or induces the down-regulation of co-stimulatory molecules, indicative of an immature DC phenotype (O'Doherty *et al.* 1994; Jonuleit *et al.* 2000; Jankovic *et al.* 2004). For example, infection of BALB/c and C57BL/6J mice with the tegumental antigen of *F. hepatica* down-regulates co-stimulatory markers CD80, CD86 and CD40 on DCs (Hamilton *et al.* 2009). This suppressed maturation profile was associated with suppressed production of cytokines, including IL-12p70, IL-6, IL-10, TNF (Hamilton *et al.* 2009). Similarly, the *H. polygyrus* ES products reduced CD40 and CD86 expression on the surface of murine DCs, as well as major histocompatibility complex class II (MHC-II) (Segura *et al.* 2007). Bone marrow-

derived DCs treated with *H. polygyrus* ES products also failed to induce cytokine production, suggesting that these cells were not activated by the ES products (Segura *et al.* 2007). Glycoprotein ES-62 from *Acanthocheilonema viteae* also induces tolerogenic DCs in BALB/c mice, with no change in CD40, CD80, CD86 or CD54 (Whelan *et al.* 2000), indicative of suppressed maturation. This is associated with the induction of Th2-like responses by DCs, with increased IL-4 expression and decreased IFN-γ (Whelan *et al.* 2000). Likewise, the soluble egg antigen (SEA) of *S. mansoni* decreases or has no effect on DC maturation markers (MacDonald *et al.* 2001; Cervi *et al.* 2004; Jankovic *et al.* 2004). Therefore, helminths or their ES products generally suppress DC maturation and cytokine profiles.

Helminth molecules have also been observed to modulate antigen presentation by APCs. Cysteine proteases are involved in the degradation of proteins taken up within the endosomal/lysosomal compartments of APCs for presentation on MHC-II molecules (reviewed in Obermajer *et al.* 2006). Nematode cystatins, have been demonstrated to inhibit the degradation of proteins by interfering with cysteine proteases (reviewed in Hartmann *et al.* 2003). For example, recombinant cystatin of *Nippostrongylus brasiliensis* has been demonstrated to inhibit antigen processing of ovalbumin (OVA) by host cysteine proteases which appears to be due to inhibition of host cell cathepsin B and cathepsin L (Dainichi *et al.* 2001). Similar findings have been reported for recombinant cystatin from *Onchocerca volvulus* and *Haemonchus contortus* (Newlands *et al.* 2001; Schonemeyer *et al.* 2001). By preventing the processing of antigen, fewer helminth proteins are loaded onto MHC-II molecules, which diminishes antigen-specific host immune responses (Dainichi *et al.* 2001).

1.2.4 ALTERNATIVE MACROPHAGE ACTIVATION

Helminth infection induces alternatively activated (M2) macrophages, which can be separated into a spectrum of phenotypes including wound-healing macrophages and regulatory macrophages (Figure 1.4) (Mosser *et al.* 2008; reviewed in Murray *et al.* 2011). In the presence of IL-4 and IL-13 produced by Th2 cells, macrophages adopt an anti-inflammatory wound-healing M2 macrophage phenotype (reviewed in Martinez *et al.* 2009). Wound healing M2 macrophages promote tissue remodelling and repair, increasing expression of fibronectin (Gratchev *et al.* 2001; Martinez *et al.* 2006), which

is essential in cell adhesion, migration, wound healing associated with helminth migration, and encapsulation of helminths (Martin *et al.* 2005; Kreider *et al.* 2007). Along with promoting wound repair, wound healing M2 macrophages produce minimal amounts of pro-inflammatory cytokines and do not produce NO (Edwards *et al.* 2006). On the other hand, expression of IL-10 by regulatory T cells promotes the activation of regulatory M2 macrophages (Figure 1.4). Regulatory macrophages are associated with high expression of IL-10 and TGF-β and suppression of IL-12 (Gerber *et al.* 2001; Anderson *et al.* 2002; Edwards *et al.* 2006). When regulatory macrophages present antigen to co-cultured naïve T cells, Th2 cell polarisation, with IL-4 expression, is induced (Anderson *et al.* 2002; Edwards *et al.* 2006).

Human and murine M2 macrophages up-regulate surface receptors indicative of their alternatively activated phenotype. Human M2 macrophages are identified by the up-regulation of mannose receptor 1 (CD206), haemoglobin scavenger receptor (CD163), macrophage scavenger receptor 1, C-type lectin-like receptor Dectin-1, Dendritic Cell-Specific Intercellular adhesion molecule-3-Grabbing Non-integrin (DC-SIGN, also known as CD209), C-type lectin domain superfamily (CLECSF)-6, C-type lectin DCL-1 and CLECSF13 (Martinez *et al.* 2006). Murine M2 macrophages are associated with up-regulation of Arg1, Chitinase 3-like 3 (Ym1) and Resistin-like molecule alpha (Fizz1, found in inflammatory zone-1) (Stein *et al.* 1992; Raes *et al.* 2002; Zhu *et al.* 2004).

The induction of M2 macrophages is common to many helminths infections (for a review see Allen *et al.* 2011). Studies within our laboratory have shown that infection of BALB/c mice with *F. hepatica*, or administration of the excretory/secretory products of *F. hepatica* (FhES), induces alternative activation of macrophages. Following infection with *F. hepatica* metacercariae, alternatively activated macrophages are recruited to the peritoneal cavity of BALB/c mice, identified by the up-regulation of Ym1, Fizz1 and Arg1 (Donnelly *et al.* 2005; Donnelly *et al.* 2008). Additionally, the FhES immune-modulatory component peroxiredoxin (Prx) also induces alternative macrophage activation, characterised by the expression of Ym1 (Donnelly *et al.* 2008).

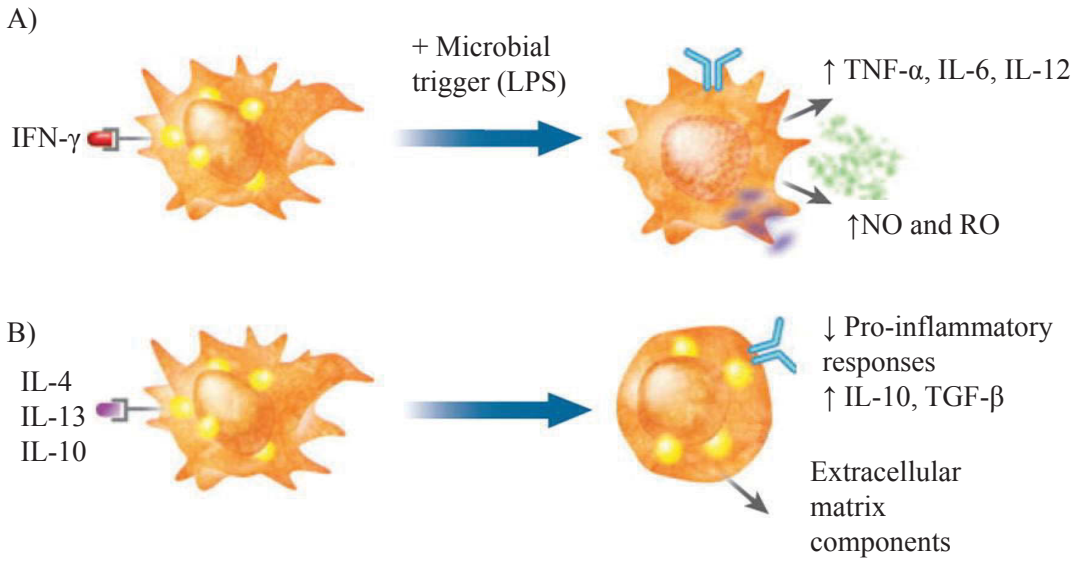

Figure 1.4: Macrophage activation phenotypes.
The cytokine milieu established by T helper cells activates macrophage populations into phenotypes along a spectrum of activation, but are commonly characterised as either A) classically activated or B) alternatively activated. In the presence of pro-inflammatory cytokines and microbial triggers such as lipopolysaccharide (LPS), macrophages are classically activated, associated with increased production of pro-inflammatory cytokines, as well as nitric oxide (NO) and reactive oxygen species (RO). During helminth infection, the expression of anti-inflammatory cytokines promotes alternative macrophage activation, which induces anti-inflammatory immune responses and promote tissue repair through the production of extracellular matrix proteins. (Adapted from Odegaard *et al.* 2011).

Alternative macrophage activation is essential for protection against organ injury during acute schistosomiasis. Despite infection establishing a Th2 response, IL-4Rα-deficient BALB/c mice succumbed to infection due to being unable to activate IL-4/IL-13-dependent M2 macrophages (Herbert *et al.* 2004). This was associated with increased IFN-γ expression, reduced expulsion of *S. mansoni* eggs, as well as inflammation of the liver and intestine. Thus, induction of M2 macrophages is essential for limiting tissue damage and ensuring host survival during *S. mansoni* infection (Herbert *et al.* 2004). The ES product lacto-N-fucopentaose III (LNFPIII) from *S. mansoni* is also associated with the induction of IL-4/IL-13-dependent M2 macrophages in mice, and when M2 macrophages were transferred to naïve recipients they promote the production of IL-10 and IL-13 by recipient T cells, thus promoting an anti-inflammatory cytokine milieu (Atochina *et al.* 2008).

Alternative macrophage activation is also associated with infection with the tapeworm, *Taenia crassiceps* (Raes *et al.* 2005; Terrazas *et al.* 2005). Chronic infection of *Taenia*

crassiceps in BALB/c mice induces alternatively activated macrophages which produce high levels of anti-inflammatory IL-6 and prostaglandin E2; and suppressed IL-12 and NO (Rodriguez-Sosa *et al.* 2002). These alternatively activated macrophages induced expression of IL-4 from $CD4^+$ T cells, promoting a Th2 response (Rodriguez-Sosa *et al.* 2002).

Infection with nematode parasites such as *B. malayi*, *Litomosoides sigmodontis*, *Nippostrongylus brasiliensis* and *H. polygyrus* also induces alternatively activated macrophages (Loke *et al.* 2000a; Loke *et al.* 2000b; Loke *et al.* 2002; Nair *et al.* 2003; Nair *et al.* 2005; Anthony *et al.* 2006; reviewed in Nair *et al.* 2006; Taylor *et al.* 2006). Alternatively activated macrophages isolated from *B. malayi* infected mice suppressed T cell proliferation during co-culture through a cell contact mediated mechanism (Loke *et al.* 2000b), and upon secondary stimulation T cells differentiated into IL-4-producing Th2 cells (Loke *et al.* 2000a; Loke *et al.* 2000b). The recombinant ES product TsP53 from nematode *T. spiralis* is also associated with the induction of M2 macrophages, characterised by up-regulation of Arg1 and Fizz1 in mice (Du *et al.* 2011). This was associated with reduced pro-inflammatory Th1 cytokines IFN-γ, TNF and IL-6, with enhanced anti-inflammatory/regulatory Th2 cytokines IL-4, IL-13, IL-10 and TGF-β (Du *et al.* 2011). In summary, the induction of M2 macrophages by helminths and their products promotes anti-inflammatory responses, resulting in suppression of the pro-inflammatory responses induced by Th1 cells.

1.2.5 MODULATION OF TOLL-LIKE RECEPTOR SIGNALLING BY HELMINTHS

Given the induction of cell activation and the resultant expression of pro-inflammatory cytokines by TLR signalling pathways, modulation of TLRs or their signalling pathways is a common method of helminth immune modulation (Table 1.1). One way this is achieved is through the ES products of helminths binding directly to TLRs. For example, TLR2, which recognises lipid antigens in association with TLR1 and TLR6 (Aliprantis *et al.* 1999; Lien *et al.* 1999; Takeuchi *et al.* 2001; Takeuchi *et al.* 2002), is activated in the presence of lyso-phosphatidylserine from *S. mansoni* (Takeuchi *et al.* 2002; van der Kleij *et al.* 2002). The activation of TLR2 resulted in mature murine DCs promoting the development of IL-10-producing regulatory T cells, contributing to the

Table 1.1: The effect of helminths and helminth-derived molecules on TLRs.

Helminth/ Helminth product	Helminth species	Toll-like receptor	Cytokine profile	Immunological outcome	Reference
Lacto-N-fucopentaose III	*S. mansoni*	TLR4	↓IFN-γ ↑IL-4	DC2 and Th2	(Thomas *et al.* 2003)
ES-62	*A. viteae*	TLR4	↓IL-12	Th2	(Goodridge *et al.* 2005)
Double stranded RNA	*S. mansoni*	TLR3	↑TNF ↑IL-12p40	Th1	(Aksoy *et al.* 2005; Vanhoutte *et al.* 2007)
Whole microfilarieae	*B. malayi*	↓TLR3, 4, 5, 7	↓IFN-α ↓IL-12 ↓MIP-1α* ↓IL-1α	Dampened pro-inflammatory response	(Semnani *et al.* 2008)
Cathepsin L1	*F. hepatica*	Cleavage of TLR3	↓IFN-β ↓TNF ↓IL-6 ↓IL-12	Dampened TRIF [1]-signalling	(Donnelly *et al.* 2010)
Lysophosphatidyl serine and phosphatidylserine	*A. lumbricoides* and *S. mansoni*	TLR2	↓TNF ↓IL-12	Regulatory T cells Th2	(van der Kleij *et al.* 2002; van Riet *et al.* 2009)
ES products	*H. polygyrus*	Unknown	↓IL-10 ↓IL-12 ↓IL-6 ↓MCP-1** ↓IL-1β ↓RANTES† ↓TNF	Regulatory T cells	(Segura *et al.* 2007)

* Macrophage inflammatory protein-1α; ** Monocyte chemotactic protein-1 † Regulated on activation, normal T cell expressed and secreted.
[1] Toll-interleukin-1 receptor-domain-containing adaptor-inducing interferon-β

regulatory environment established during helminth infection (van der Kleij *et al.* 2002). Toll-like receptor 4, which recognises lipoproteins including bacterial LPS (Beutler 2000), also binds the helminth ES products, such as LNFPIII from *S. mansoni* and filarial phosphorylcholine-containing ES-62 secreted by *A. viteae* (Thomas *et al.* 2003; Goodridge *et al.* 2005). By binding TLR4 and altering signalling pathways, ES-62 ultimately prevents IL-12 production in restimulated murine macrophages (Goodridge *et al.* 2005). While the precise method of immune modulation by *A. viteae* has not been determined, ES-62 prevents Myeloid differentiation primary response gene 88 (MyD88) signalling, which is common to multiple TLRs (Goodridge *et al.* 2005). Likewise, following TLR4 activation by LNFPIII, DCs are polarised into a tolerogenic phenotype which induces naïve $CD4^+$ T cells to differentiate into Th2 cells, promoting the protective anti-inflammatory milieu required for the protection of both host and parasite (Thomas *et al.* 2003). Lastly, TLR3, which recognises nucleic acids, binds double stranded (ds)RNA including not only viral, but also helminth, such as from *S. mansoni* (Alexopoulou *et al.* 2001; Aksoy *et al.* 2005). Unlike the other helminth proteins which modulate TLR signalling and induce anti-inflammatory or regulatory responses, *S. mansoni* dsRNA enhances Th1 responses in mice, resulting in increased IFN-γ, TNF and IL-12p40 expression (Aksoy *et al.* 2005; Vanhoutte *et al.* 2007).

Typically, recognition and binding of ligands with TLRs initiates intracellular signalling via one of two pathways (for a review see Akira *et al.* 2004). At the cell surface, toll-like receptors 1, 2, 4, 5 and 6 all recruit MyD88 (Medzhitov *et al.* 1998) and initiate cell activation either via phosphorylation and degradation of Nuclear factor of kappa light polypeptide gene enhancer in B-cells inhibitor, alpha (IκBα) which results in the activation of nuclear factor-κB (NF-κB), or alternately via the mitogen-activated protein kinase (MAPK) pathways (for a review see Akira *et al.* 2004). The MAPK pathways include extracellular signal-related kinase (ERK), p38 and c-Jun NH2-terminal kinase (JNK) pathways which result in the activation of activating protein-1 (AP-1) (Figure 1.5) (reviewed in Roux *et al.* 2004). On the other hand, TLR3, 4, 7, 8 and 9 signal from within late endosomes where they reside within cells (Heil *et al.* 2003; Lee *et al.* 2003; Matsumoto *et al.* 2003; Latz *et al.* 2004; Sioud 2005; Kagan *et al.* 2008). TLR7, 8 and 9 signal through MyD88 (Heil *et al.* 2004; Latz *et al.* 2004), while both TLR3 and 4 activate the Toll-interleukin-1 receptor-domain-containing adaptor-inducing interferon-β (TRIF) pathway (Yamamoto *et al.* 2003). The TRIF-dependent pathway can induce

late NF-κB signalling via TNF receptor-associated factor (TRAF)-6 signalling, or induces the expression of type 1 interferons via phosphorylation of Interferon Regulatory Factor (IRF)-3 and IRF7 (Sato *et al.* 2003) (Figure 1.5). Activation of these signalling molecules leads to production of inflammatory cytokines including TNF, IL-1β, IL-6 and IL-12, as well as T cell co-stimulatory molecules and chemotactic factors, activating APCs such as macrophages to a classically activated phenotype and inducing Th1 adaptive immune responses (Medzhitov *et al.* 1997; Aderem *et al.* 2000).

Toll-like receptor signalling molecules are also a target of helminth immune-modulation (reviewed in Venugopal *et al.* 2009). Firstly, down-regulation of TLRs by helminths modulates cell signalling (Venugopal *et al.* 2009). The microfilarial parasite *B. malayi* down-regulates TLR3, 4, 5 and 7 messenger (m)RNA expression as well as MyD88 mRNA expression in human DCs (Semnani *et al.* 2008). This results in decreased production of pro-inflammatory cytokines, IFN-γ, IL-12, macrophage inflammatory protein (MIP)-1α and IL-1α (Semnani *et al.* 2008). Similarly, *F. hepatica* cysteine protease, cathepsin L1 (FhCL1) cleaves TLR3 in murine macrophages, preventing signalling via the TRIF-dependent pathway in response to TLR-ligands LPS and Polyinosinic:polycytidylic acid (Poly (I·C)), and down-regulation of pro-inflammatory cytokines IFN-β, TNF, IL-6 and IL-12 (Donnelly *et al.* 2010).

Helminth-derived products also modulate the down-stream responses to TLR-ligands. For example, the *H. polygyrus* ES products and the *S. mansoni* SEA suppress TLR signalling in DCs and impair activation in response to TLR-ligands. The *H. polygyrus* ES causes DCs to down-regulate maturation markers CD86, CD40 and MHC-II in response to LPS, CpG DNA and Poly (I·C), indicative of tolerogenic DCs (Segura *et al.* 2007). Likewise, *S. mansoni* SEA also induced tolerogenic DCs, with decreased surface expression of CD86, CD80, CD83 in response to LPS or Poly(I·C) (van Liempt *et al.* 2007). In response to TLR-ligands, murine DCs down-regulated expression of IL-10, IL-12p70, IL-6, monocyte chemotactic protein (MCP)-1, IL-1β, RANTES (Regulated on activation, normal T cell expressed and secreted) and TNF, demonstrating sustained down-stream suppression of TLR cell signalling pathways (Segura *et al.* 2007; van Liempt *et al.* 2007).

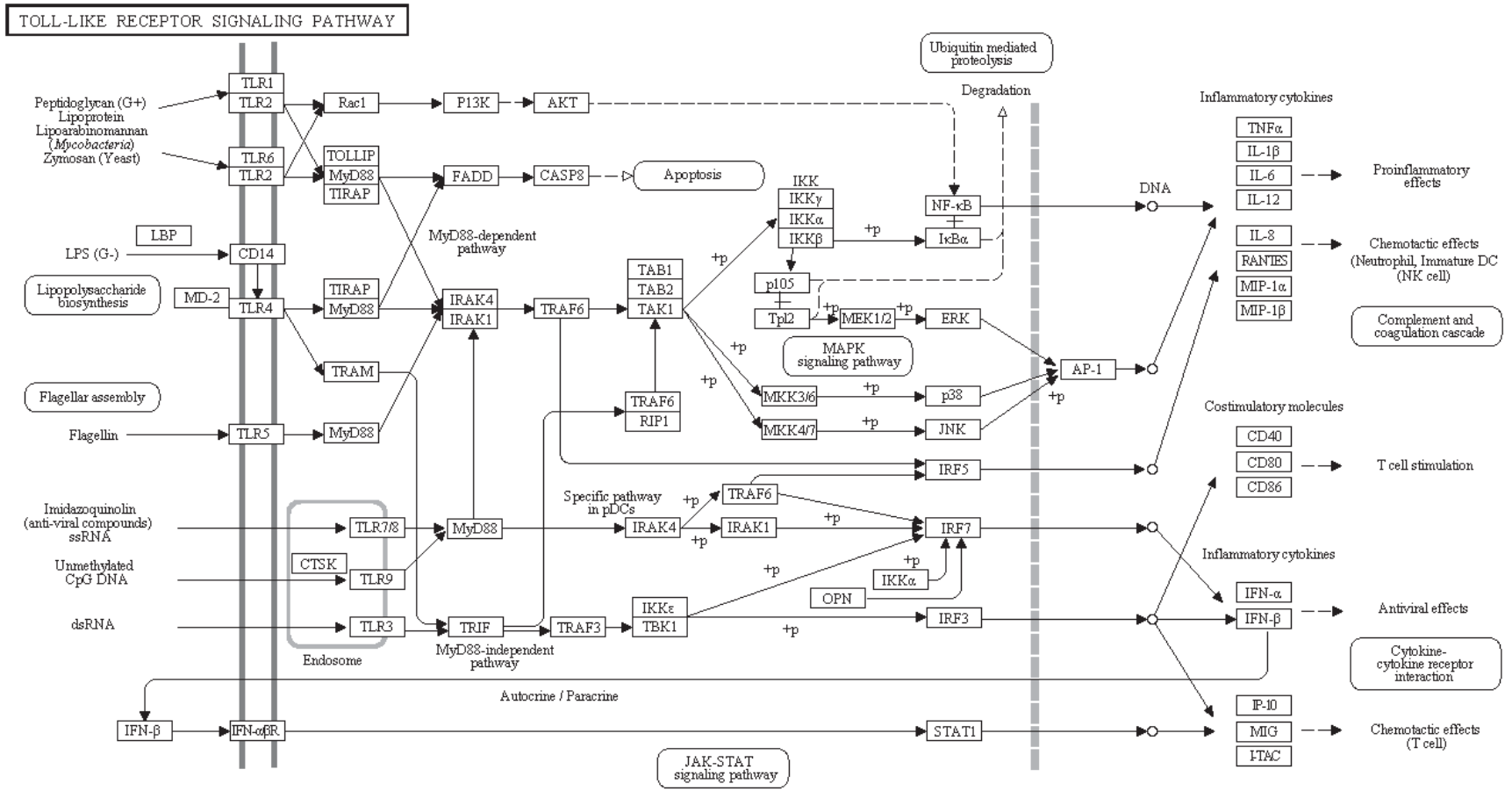

Figure 1.5: Toll-like receptor signalling pathways.
Toll-like receptors (TLRs) are membrane-bound pattern recognition molecules expressed on innate immune cells including macrophages and dendritic cells and recognise microbial, viral and helminth pathogens. Recognition of antigens induces rapid activation of innate immunity through the production of pro-inflammatory cytokines and up-regulation of co-stimulatory molecules. TLR signalling pathways are separated into two groups. Firstly, the Myeloid differentiation primary response gene 88 (MyD88)-dependent pathway that leads to the early activation of NF-κB and activating protein-1 (AP-1) is induced, resulting in expression of pro-inflammatory cytokines, while the MyD88-independent, Toll-interleukin-1 receptor-domain-containing adaptor-inducing interferon-β (TRIF)-dependent pathway is associated with the late activation of NF-κB and AP-1, along with the induction of type I IFNs and IFN-inducible genes. (Kyoto Encyclopedia of Genes and Genome (KEGG) pathway, 2010).

Due to the migration of helminths through epithelial cells, infection is often associated with the release of bacteria, however, perhaps paradoxically, parasite infection is almost completely asymptomatic (Yazdanbakhsh 1999; Maizels *et al.* 2004). This provides further evidence that helminths modulate the TLR signalling pathways through which bacterial products are recognised. For example, infection with *F. hepatica* begins with the burrowing of parasites through the gut wall into the peritoneal cavity, migrating towards the liver (Krull *et al.* 1943; reviewed in Andrews 1999). The growth of *F. hepatica* within the bile ducts causes biliary obstruction and liver injury, and is associated with the presence of bacteria in the bile, including *Escherichia coli* (Ogunrinade *et al.* 1982; Foster 1984; Valero *et al.* 2006). Investigations by our group into the role of individual proteins within the FhES identified molecules that have been observed to modulate TLR signalling in response to bacterial LPS. The recently described helminth defence molecule (HDM)-1 binds to LPS, preventing its interaction with LPS-binding protein and CD14, impairing signalling through the TLR4 pathway and preventing LPS-induced inflammatory responses in mice (Robinson *et al.* 2011b). The cleavage of TLR3 in murine macrophages by FhCL1 also plays a role in the prevention of bacteria-induced responses, suppressing the expression of pro-inflammatory cytokines including IL-6, IL-12, inducible nitric oxide synthase (iNOS) and TNF in response to LPS (Donnelly *et al.* 2010).

Although much of this knowledge comes from studies involving experimentally infected mice, there is also strong evidence for helminths suppressing responses to TLR ligands in humans. For example, cytokine responses to both TLR2 and TLR4 ligands, lysophosphatidyl serine and LPS were lower in peripheral blood mononuclear cells isolated from schistosome infected children when compared to those isolated from uninfected children, suggestive of suppressed TLR signalling (van der Kleij *et al.* 2004). Furthermore, *S. haematobium* down-regulates responses to TLR ligands through the continual exposure of the host to LPS as a result of microbial release during migratory phases of the parasite's lifecycle (van der Kleij *et al.* 2004). Cytokine responses to TLR2, TLR4, TLR5 and TLR9 ligands, lipoprotein, LPS, Flagellin and CpG DNA respectively, were also lower in monocytes isolated from peripheral blood mononuclear cells from *B. malayi* infected individuals (Babu *et al.* 2005). Ultimately, helminth parasites require the survival of their host, which can be compromised by the release of bacteria, thus it is conceivable that helminths and their ES products ensure their survival

while also playing a protective role for the host, through the modulation of TLR signalling pathways.

In summary, helminth infection is generally associated with the induction of an anti-inflammatory/regulatory immune environment. While helminth molecules induce Th2/regulatory T cell responses by a number of different mechanisms, modulation of TLR signalling is central to immune modulation by many helminths. Through the induction of tolerogenic DCs, helminths down-regulate co-stimulatory molecules and prevent TLR stimulation in response to traditionally pro-inflammatory stimuli including LPS and Poly I·C (Segura *et al.* 2007; van Liempt *et al.* 2007). The decreased expression of pro-inflammatory cytokines by DCs suppresses Th1 differentiation and promotes Th2/regulatory T cell polarisation (Segura *et al.* 2007; van Liempt *et al.* 2007). Similarly, by down-regulating or cleaving TLRs in DC and macrophages, helminth products suppress pro-inflammatory immune responses and prevent Th1 cell activation (Semnani *et al.* 2008; Donnelly *et al.* 2010). The suppression of pro-inflammatory responses, and the induction of Th2/regulatory T cell responses, IL-10 producing regulatory B cells, tolerogenic DCs and alternatively activated macrophages by helminths simultaneously aids helminth survival and protects the host from extensive tissue pathology associated with the migration of helminths through tissues (reviewed in Allen *et al.* 2011).

1.2.6 THE THERAPEUTIC POTENTIAL OF HELMINTH PRODUCTS

The opposing immunological milieu established during helminth infection and autoimmunity is suggestive of helminths providing protection against the development of autoimmune and inflammatory diseases. Furthermore, an inverse global distribution pattern exists between helminth infection and autoimmune disease prevalence, with helminth infection endemic in tropical equatorial regions (Crompton *et al.* 1987; Bundy *et al.* 1989; Chan *et al.* 1994; de Silva *et al.* 2003), while autoimmune diseases, such as T1D and MS, have the highest prevalence rates outside equatorial regions (DIAMOND Project Group 2006; World Health Organization 2008). In fact, comparisons between the prevalence of MS and *Trichuris trichiura* infection showed that *T. trichiura* infection was negatively correlated with the prevalence of MS (Fleming *et al.* 2006). The inverse correlation and opposing immunological milieu has subsequently lead to

the immune-modulatory effects of helminths and their products being examined for their potential therapeutic effects in both human and murine models of autoimmunity.

Many studies have investigated the effect of live helminth infection on the progression of autoimmune disease and have established that infection with helminths from the trematode, nematode and cestode species all have therapeutic benefit in certain circumstances (Table 1.2). Infection with live cerceriae or ova is commonly associated with the polarisation of Th2 cells, regulatory T cells and regulatory B cells with induction of alternatively activated macrophages or tolerogenic DCs (Table 1.2). The anti-inflammatory immune response established during helminth infection suppresses Th1/Th17 immune responses established during autoimmune/inflammatory disease and as such, alleviates the symptoms, reduces the severity, or prevents the development of autoimmune/inflammatory diseases such as IBD, MS, T1D and rheumatoid arthritis in both human and murine disease models (summarised in Table 1.2).

However, live helminth infection is problematic due to the resultant tissue damage and pathology associated with the migration of the parasite through host tissues (reviewed in Ruyssers *et al.* 2008). Therefore, because the ES products of helminths are responsible for immune modulation, without the resultant tissue damage associated with live helminth infection, many studies have focused on the therapeutic potential of dead ova or the ES products of helminths, as well as soluble egg or worm extracts, and have observed amelioration or prevention of autoimmunity (Table 1.2).

For example, *F. hepatica* infection is characterised by a switch to an alternatively activated macrophage phenotype as early as 24 h post infection in mice (Donnelly *et al.* 2005). Following the switch in the innate immune response, a Th2 response is induced approximately 7 days after the induction of alternative macrophage activation (Donnelly *et al.* 2005). Investigations into the immune-modulatory effect of whole FhES in murine models demonstrated that collectively the ES products are capable of suppressing Th1-mediated delayed type hypersensitivity to both specific and non-specific antigen (Cervi *et al.* 1996). Further investigations demonstrated that alternatively activated macrophages, identified by the production of Fizz1, Ym1 and Arg1, were recruited to the peritoneum of mice treated with whole FhES, and *ex vivo* cultures of spleen cells from these mice were shown to secrete IL-4 and IL-5 with an absence of IFN-γ, similar

Table 1.2: The use of helminths and their products in the prophylactic and therapeutic treatment of murine and human autoimmune and inflammatory diseases.

Helminth life stage or product*	Disease	Disease modulation	Immune profile	Reference
Trematode				
Fasciola hepatica				
ES products	Type 1 diabetes	Prevention	↓IFN-γ ↑IgG1:IgG2a Breg [1] ↑M2 macrophages	(Lund *et al.* in preparation)
	Rheumatoid arthritis	↓ Severity	↑Treg [2] ↑DC2 ↑IL-10 ↑TGF-β ↓TNF ↓IL-12 ↓IL-6 ↓IL-23	(Carranza *et al.* 2012)
Peroxiredoxin (Prx)	Not tested	-	↑M2 macrophages ↑IL-4 ↑IL-5 ↑IL-13	(Donnelly *et al.* 2008)
Cathepsin L (FhCL1)	Septic shock	Protection	Cleavage of TLR3 ↓TNF ↓IL-6 ↓IL-12 ↓Nitrite	(Donnelly *et al.* 2010)
Helminth defence molecule-1 (HDM-1)	Systemic inflammation	Protection	Binds LPS ↓TNF ↓IL-1β	(Robinson *et al.* 2011b)
	Not tested	-	Prevents antigen processing/ presentation in macrophages	(Robinson *et al.* 2012)
Schistosoma japonicum				
Live cerceriae	Rheumatoid arthritis	Prevention	↓IFN-γ ↑IL-4 ↑IL-10	(He *et al.* 2010)
Dead ova	Inflammatory bowel disease	Attenuation	↓IFN-γ ↑IL-4 ↑IL-5 ↑IL-10 ↑Treg	(Mo *et al.* 2007)
Ova soluble extract	Experimental autoimmune encephalomyelitis	↓ Severity	↓IFN-γ ↑IL-4	(Zheng *et al.* 2008)
Schistosoma mansoni				
Live cerceriae	Rheumatoid arthritis	↓ Severity	↓IFN-γ ↓TNF ↓IL-17 ↑IL-4 ↑IL-10	(Osada *et al.* 2009)
	Experimental	↓ Severity	↓IFN-γ	(La Flamme *et al.*

	autoimmune encephalomyelitis		↓TNF ↓IL-12	2003)
	Type 1 diabetes	Prevention	↑IL-4 ↑IL-5 ↑IL-10 ↓IL-2 ↓IFN-γ	(Grzych *et al.* 1991; Cooke *et al.* 1999)
Live cerceriae	Inflammatory bowel disease	Prevention	↑IL-10 ↑TGF-β	(Smith *et al.* 2007)
Dead ova	Inflammatory bowel disease	Prevention	↓IFN-γ ↑IL-4 ↑IL-10	(Elliott *et al.* 2003)
Soluble Egg Antigen (SEA)	Type 1 diabetes	Prevention	↑M2 macrophages ↑Treg ↑IL-2 ↑IL-4 ↑IL-5 ↑IL-6 ↑IL-10 ↑IL-12 ↑IL-13 ↑TGF-β	(Maron *et al.* 1998; Zaccone *et al.* 2003; Donnelly *et al.* 2008; Zaccone *et al.* 2009; Zaccone *et al.* 2010)
Soluble Worm extract	Type 1 diabetes	Prevention	↑IL-4 ↑IL-5 ↑IL-10 ↑IL-13 ↑IFN-γ	(Zaccone *et al.* 2003; Donnelly *et al.* 2008)
	Inflammatory bowel disease	Curative	↓IFN-γ ↓IL-17 ↑IL-10 ↑TGF-β	(Ruyssers *et al.* 2009)
Peroxiredoxin (Prx)	Not tested	-	↑M2 macrophages ↑IL-4 ↓IFN-γ	(Donnelly *et al.* 2008)
Cathepsin L	Not tested	-	↓TNF ↓IL-6 ↓IL-12 ↓Nitrite	(Donnelly *et al.* 2010)
Omega-1 (ω-1)	Not tested	-	↑DC2 ↑IL-4 ↑IL-5 ↑IL-10 ↑IL-13 ↑Treg ↑IFN-γ ↑IL-17	(Steinfelder *et al.* 2009; Zaccone *et al.* 2011)
	Not tested	-	↓IFN-γ ↓IL-12 ↑IL-4	(Everts *et al.* 2009)

Lacto-N-fucopentaose III (LNFPIII)	Psoriasis Type 1 diabetes Experimental autoimmune encephalomyelitis	Prevention Protection Protection	↑M2 macrophages ↓IFN-γ ↑IL-4 ↑IL-10 ↑IL-13 ↑DC2	(Thomas *et al.* 2003; Atochina *et al.* 2008; Harn *et al.* 2009)
Chemokine binding protein (smCKBP)	Experimental autoimmune encephalomyelitis Rheumatoid arthritis Acute pulmonary inflammation	No effect No effect ↓ Severity	Binds chemokines blocking their pro-inflammatory properties	(Smith *et al.* 2005)
IPSE/α-1 glycoprotein	Not tested	-	↑IL-4	(Schramm *et al.* 2007)
dsRNA	Not tested	-	DC activation through TLR3 promoting Th1 responses	(Aksoy *et al.* 2005; Vanhoutte *et al.* 2007)
Lysophosphatidyls-erine and phosphatidylserine	Not tested	-	TLR2-dependent activation of DC ↓IL-12 ↓IL-23 ↑Treg ↑IL-4 ↑IL-10	(van der Kleij *et al.* 2002; van Riet *et al.* 2009)
Nematode				
Acanthocheilonema viteae				
ES-62	Collagen-induced arthritis	↓ Severity	TLR4-dependent DC and macrophage activation ↓IL-12 ↓TNF ↓IFN-γ ↓IL-6 ↑IL-10	(McInnes *et al.* 2003; Goodridge *et al.* 2005)
Cystatin	Colitis	↓ Severity	↑IL-10 ↑IL-12 ↑M2 macrophages ↑Treg	(Schnoeller *et al.* 2008; Klotz *et al.* 2011)
Ancylostoma caninum				
ES products	Inflammatory bowel disease	Curative	Not investigated	(Ruyssers *et al.* 2009)
Ancylostoma ceylanicum				
ES products	Inflammatory bowel disease	↓ Severity	↓IFN-γ ↓TNF ↓IL-17	(Cancado *et al.* 2011)
Ascaris lumbricoides				
	Multiple sclerosis	↓ Severity	↑Treg ↓IL-12 ↓IFN-γ ↑IL-10 ↑TGF-β	(Correale *et al.* 2007)
Phosphatidylserine	Not tested	-	TLR2-dependent activation of DC ↓IL-12	(van Riet *et al.* 2009)

			↓IL-23 ↑IL-4	
Ascaris simplex				
rAs-MIF (Migration Inhibitory Factor)	Colitis	↓ Severity	↑IL-10 production by DCs ↑TGF-β ↑Treg ↓IFN-γ ↓IL-6 ↓IL-13	(Cho *et al.* 2011)
Dirofilaria immitis				
DiAg	Type 1 diabetes	Prevention	↑IL-4 ↑IL-10 ↑Antigen non-specific IgE production	(Imai *et al.* 2001; Imai *et al.* 2004)
Enterobius vermicularis				
	Multiple sclerosis	↓ Severity	↑Treg ↓IL-12 ↓IFN-γ ↑IL-10 ↑TGF-β	(Correale *et al.* 2007)
Heligmosomoides polygyrus				
Live cerceriae	Inflammatory bowel disease	↓ Severity/ Reversal/ Prevention	↓IFN-γ ↓TNF ↓IL-1β ↓IL-17 ↓IL-12 ↑IL-4 ↑IL-5 ↑IL-10 ↑IL-13 ↑TGF-β ↑Treg	(Fox *et al.* 2000; Elliott *et al.* 2004; Metwali *et al.* 2006; Setiawan *et al.* 2007; Elliott *et al.* 2008; Sutton *et al.* 2008; Hang *et al.* 2010)
	Type 1 diabetes	Prevention	↑Ag non-specific IgE ↑/↓IFN-γ ↑IL-4 ↑IL-10 ↑IL-13	(Saunders *et al.* 2007a; Liu *et al.* 2009)
	Experimental autoimmune encephalomyelitis	Reversal	↑IL-10 ↑TGF-β ↑IL-6 ↓IL-12 ↓IL-17A ↓IL-2	(Donskow-Lysoniewska *et al.* 2012)
Adult worm homogenate	Not tested	-	↑IL-4 ↑IL-10	(Rzepecka *et al.* 2009)
Calreticulin	Not tested	-	↑IL-4 ↑IL-10	(Rzepecka *et al.* 2009)
Litomosomoides sigmodontis				
Third stage larvae	Type 1 diabetes	Prevention	↑Treg ↑TGF-β ↑IL-4 ↑IL-5 ↑IL-13	(Hubner *et al.* 2009; Hubner *et al.* 2012)

			↓IFN-γ	
Necator americanus				
Live cercariae	Inflammatory bowel disease	↓ Severity	Not investigated	(Croese *et al.* 2006)
Third stage larvae	Celiac disease	Trend towards ↓ severity	↓IFN-γ ↓IL-17A ↑IL-10 ↑IL-5 ↑IL-13	(Daveson *et al.* 2011; McSorley *et al.* 2011)
Nippostrongylus brasiliensis				
Third stage larvae	Rheumatoid arthritis	↓ Severity	↑IL-4	(Salinas-Carmona *et al.* 2009)
Strongyloides stercolaris				
	Multiple sclerosis	↓ Severity	↑Treg ↓IL-12 ↓IFN-γ ↑IL-10 ↑TGF-β	(Correale *et al.* 2007)
Trichinella spiralis				
Live cercariae	Inflammatory bowel disease	↓ Severity	↓IL-12 ↓IFN-γ ↑IL-4 ↑IL-13	(Khan *et al.* 2002; Motomura *et al.* 2009)
	Type 1 diabetes	Prevention	↑Ag non-specific IgE ↑IFN-γ ↑IL-4	(Saunders *et al.* 2007b)
Soluble worm/larval products	Experimental autoimmune encephalomyelitis	↓ Severity	↓TNF ↓IL-12 ↓Th17	(Kuijk *et al.* 2012)
	Inflammatory bowel disease	↓ Severity	↓IL-1β ↓iNOS ↑IL-13 ↑TGF-β	(Motomura *et al.* 2009)
TsP53	Colitis	↓ Severity	↑M2 macrophages ↓IFN-γ ↓TNF ↑IL-4 ↑IL-13 ↓IL-10 ↓TGF-β	(Du *et al.* 2011)
Trichuris suis				
Live ova	Inflammatory bowel disease	↓ Severity	Not investigated	(Summers *et al.* 2003; Summers *et al.* 2005)
Live ova	Multiple sclerosis	↓ Severity	↑IL-4 ↑IL-10	(Fleming *et al.* 2011)
Soluble worm/larval products	Experimental autoimmune encephalomyelitis	↓ Severity	↓TNF ↓IL-12 ↓IL-17 ↑IL-4	(Kuijk *et al.* 2012)
Trichuris trichiura				
Liva ova	Inflammatory bowel disease	Remission	↑IL-22 and IL-4 producing T cells	(Broadhurst *et al.* 2010)
	Multiple sclerosis	↓ Severity	↑Treg ↓IL-12	(Correale *et al.* 2007)

			↓IFN-γ ↑IL-10 ↑TGF-β	
Cestode				
Hymenolepis diminuta				
Live cerceriae	Inflammatory bowel disease	Prevention	Not investigated	(Reardon *et al.* 2001)
Live/dead cysticercoids	Rheumatoid arthritis	↓ Severity	↓IL-12 ↓TNF ↑IL-4 ↑IL-10	(Shi *et al.* 2011)
ES products	Inflammatory bowel disease	↓ Severity	↓TNF ↑IL-4 ↑IL-10	(Johnston *et al.* 2010)
Hymenolepsis nana	Multiple sclerosis	↓ Severity	↑Treg ↓IL-12 ↓IFN-γ ↑IL-10 ↑TGF-β	(Correale *et al.* 2007)

* presented where available
[1] regulatory B cells, [2] regulatory T cells

to active infection (Donnelly *et al.* 2005). Furthermore, in the NOD mouse model, Lund *et al.* observed prevention of diabetes development when the FhES products were administered concurrent with type 1 disease onset (Lund *et al.* in preparation). Along with decreased expression of pro-inflammatory IFN-γ, this was associated with increases in an IL-10 secreting regulatory B cell population (Lund *et al.* in preparation). There was also a switch in autoantibody isotype from secretion of IgG2a, which is induced by IFN-γ and thus associated with Th1 responses (Snapper *et al.* 1987b; Finkelman *et al.* 1988; Snapper *et al.* 1988) to IgG1 which is induced by IL-4 and thus associated with Th2 responses (Snapper *et al.* 1987a).

Recent research has taken a reductionist approach, fractionating ES products and soluble helminth extracts to identify the individual components and assess their immune-modulatory effects. The composition of ES products varies depending on the helminth species and the individual molecules have a variety of immune-modulatory effects (Table 1.2). While the majority of components induce immune responses that are similar to whole helminth infection, i.e. primarily promoting anti-inflammatory immune responses, some of the components are associated instead with the induction of pro-inflammatory immune responses.

Fractionation of the FhES by sodium dodecyl sulphate-polyacrylamide gel electrophoresis (SDS-PAGE) revealed that it is a mixture of proteins (Figure 1.6A) (Donnelly *et al.* 2008). Although compared to the ES products of *S. mansoni* (Everts *et al.* 2009) it has a relatively simple composition (Figure 1.6B). When the FhES was fractionated using size exclusion chromatography, the products separated into two main peaks (Figure 1.6C) (Donnelly *et al.* 2008). Proteomic analysis has shown that the first peak is composed mainly of Prx and a defensin-like molecule termed HDM-1 (Donnelly *et al.* 2005; Robinson *et al.* 2011b), while the second peak contains a cysteine protease, FhCL1 (Collins *et al.* 2004).

Recombinant Prx, FhCL1 and peptides of HDM-1 have been created to determine the effects of these molecules. Investigations in our laboratory have determined that Prx induces similar effects on murine macrophages as whole FhES, inducing Th2 responses due to alternative activation of macrophages (Donnelly *et al.* 2005). In contrast, both HDM-1 and FhCL1 were associated with the suppression of pro-inflammatory responses without inducing an anti-inflammatory response (Donnelly *et al.* 2010; Robinson *et al.* 2011b). HDM-1 binds LPS, preventing it from binding to LPS binding protein (LBP) on the surface of macrophages. By binding LPS, HDM-1 suppressed the release of macrophage inflammatory mediators and protected mice from LPS-induced inflammation (Robinson *et al.* 2011b). Furthermore, HDM-1 inhibited antigen processing and presentation in human macrophages by inhibiting acidification of endolysosomes (Robinson *et al.* 2012). FhCL1 is one of the most abundant proteins within the FhES products (O'Neill *et al.* 2001) and is essential for parasite migration due to its role in the breakdown of host tissues, such as fibrinogen, laminen and collagen (Berasain *et al.* 1997; McGonigle *et al.* 2008). In mice FhCL1 inhibited LPS signalling by altering the TLR signalling pathway in murine peritoneal macrophages, suppressing serum and macrophage pro-inflammatory cytokine expression, significantly down-regulating IL-6, IL-12, TNF and iNOS secretion (Donnelly *et al.* 2010). FhCL1 suppressed pro-inflammatory cytokines in part by degrading TLR3, modulating IFN-β mediated TRIF-dependent TLR signalling within endosomes (Donnelly *et al.* 2010). Investigation into the localisation of FhCL1 2 h post intraperitoneal injection, showed that FhCL1 localised within endosomes, where it likely modulated down-stream signalling and cleaved TLR3 (Donnelly *et al.* 2010). Furthermore, the degradation of

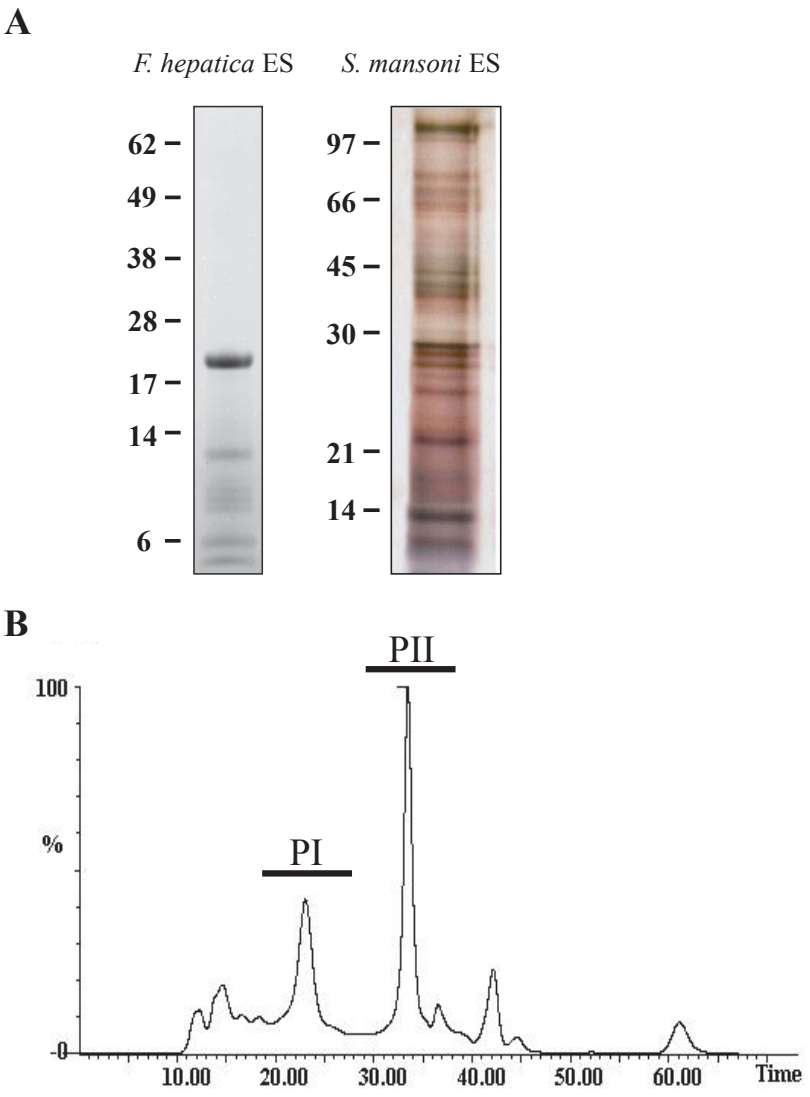

Figure 1.6: Separation of *F. hepatica* and *S. mansoni* ES products using SDS page and size exclusion chromatography.
A) SDS-PAGE analysis of the ES products of *F. hepatica* and *S. mansoni* visualised by Coomassie and silver staining respectively (Donnelly *et al.* 2008; Everts *et al.* 2009). B) Size exclusion fractionation of *F. hepatica* ES products. The time of elution is shown in minutes against the percentage of total protein. The components of the ES products were separated into two main peaks labelled peak I (PI) and peak II (PII), of which the majority is cathepsin L1 (Donnelly *et al.* 2008).

TLR3 by FhCL1 can delay the onset of and prevent LPS-induced septic shock (Donnelly *et al.* 2010). FhCL1 has also been observed to modulate maturation of murine bone marrow-derived DCs, up-regulating CD40 on the cell surface, but having no effect on CD80, CD86 and MHC class II expression, indicative of partial maturation (Dowling *et al.* 2010). In contrast to its effect on murine macrophages, FhCL1 treatment increased the expression of IL-6, IL-12 and macrophage inflammatory proteins 1 and 2 in murine DCs in a TLR4-dependent manner, though this was not in response to LPS (Dowling *et al.* 2010). FhCL1-treated DCs from BALB/c mice also suppressed the induction of Th17 cells from DO11.10 mice following adoptive transfer (Dowling *et al.* 2010). This was due to decreased secretion of IL-23 (Dowling *et al.* 2010), which is important in inducing the secretion of IL-17 from Th17 cells (Aggarwal *et al.* 2003).

Many similar findings have also been reported for *S. mansoni*. Active infection, or administration of dead ova or the soluble egg and worm antigens of *S. mansoni* suppresses pro-inflammatory responses associated with the migratory phase of infection and induces a Th2/regulatory T cell response, with induction of alternatively activated macrophages (Maron *et al.* 1998; Elliott *et al.* 2003; Donnelly *et al.* 2008; and reviewed in Lambertucci 2010) (Table 1.2). SDS-PAGE analysis of the ES products of *S. mansoni* reveal that unlike the ES of *F. hepatica*, it is a very complex mixture of proteins (Figure 1.6). The majority of products individually suppress pro-inflammatory responses, with or without inducing anti-inflammatory responses (Table 1.2). For example, similar to the ES products of *F. hepatica, S. mansoni* peroxiredoxin suppresses expression of pro-inflammatory cytokines such as IFN-γ, while promoting Th2 responses, with up-regulation of IL-4 and the induction of alternatively activated macrophages (Donnelly *et al.* 2008). In contrast to peroxiredoxin, *S. mansoni* cathepsin L suppresses pro-inflammatory cytokines such as IL-12 and iNOS, but is not associated with the induction of anti-inflammatory/Th2 responses, similar to FhCL1 (Donnelly *et al.* 2010). Lastly, the ES of *S. mansoni* has also been shown to be comprised of dsRNA, the ligand of TLR3, and as a result in contrast to other components of *S. mansoni* ES, dsRNA contributes to pro-inflammatory cytokine production, namely, TNF and IL-12p40, dependent upon signalling through TLR3 (Aksoy *et al.* 2005; Vanhoutte *et al.* 2007). Therefore, despite the collective ES products inducing a Th2 response during infection with *S. mansoni*, the individual products modulate immune responses through a variety of methods.

To date, there have been a large number of studies investigating the immune-modulatory effect of soluble helminth products and individual helminth-derived molecules on the prevention of auto-inflammatory responses in animal models. Murine models of autoimmune disease have demonstrated that by promoting the induction of anti-inflammatory immune responses with the suppression of pro-inflammatory responses, soluble helminth products and individual ES molecules improve the outcome of, or even prevent murine autoimmune diseases including, IBD, EAE, T1D and rheumatoid arthritis (Table 1.2). Furthermore, helminth-derived products show therapeutic benefit in the treatment of systemic inflammation (Table 1.2).

While the number of investigations into the use of helminths and their products in the treatment of autoimmune and inflammatory diseases in humans are limited, studies have shown that with regard to IBD, disease severity is reduced following treatment with helminths (Summers *et al.* 2005; Croese *et al.* 2006; Correale *et al.* 2007; Correale *et al.* 2008; Broadhurst *et al.* 2010) (Table 1.2). One particular study completed in humans suffering IBD used *Trichuris suis*, a porcine whipworm which can only colonise humans temporarily as humans are not the definitive host of the helminth (Beer 1976). The ova of the parasite hatch in the dueodenum but do not invade the host (Summers *et al.* 2005), thus avoiding the tissue destruction commonly associated with helminth infection. Infection with *T. suis* led to improvements in the symptoms of IBD, including reduced diarrhoea and blood in the stools, along with improvements in the mucosa of the intestine as evidenced by sigmoidoscopy (Summers *et al.* 2005).

Helminth infection has also been shown to be associated with reduced severity of MS in humans (Table 1.2). An association study found that those infected with helminths showed reduced disease severity (Correale *et al.* 2007). Individuals infected with *Hymenolepsis nana*, *T. trichiura*, *Ascaris lumbriocoides*, *Strongyloides stercolaris* or *Enterobius vermicularis* exhibited higher levels of anti-inflammatory cytokines, namely IL-10 and TGF-β, with increased regulatory T cell populations and decreased IL-12 and IFN-γ (Correale *et al.* 2007). Similarly, treatment of relapsing-remitting MS with ova from the non-pathogenic *T. suis* was associated with increased expression of IL-10 and IL-4, and improvements in lesions (Fleming *et al.* 2011). A follow-up study demonstrated that when individuals who developed symptoms of helminth-infection were given anti-parasite treatment, there was a significant increase in the clinical

symptoms of MS, along with an increased number of IFN-γ and IL-12 producing cells with a concurrent fall in regulatory T cells and cells secreting TGF-β and IL-10 (Correale *et al.* 2011). Thus in the case of relapsing-remitting MS, modulation of the immune response by parasites has therapeutic benefit to MS patients.

While active helminth infection with either live cercarieae or live ova has been associated with protection from autoimmune disease and thus has demonstrated potential in a clinical setting, active helminth infection is associated with tissue damage during maturation and migration of the helminth, making it undesirable as a therapeutic. Nevertheless, the use of unfractionated ES products of helminths has also been demonstrated to prevent or suppress murine autoimmune and inflammatory disease and holds therapeutic potential. However, it is not easy to produce ES in large volumes, and it is important to ensure continuity in ES protein composition. Moreover, it is desirable to determine the composition of ES molecules and their specific immune modulatory effects prior to their use in a clinical setting. The majority of studies investigating the immune modulatory effect of individual molecules have been performed in murine models and therefore, our laboratory is expanding upon this knowledge by investigating the effect of the recombinant FhES-derived molecules on human immune cells.

1.3 MODULATION OF IMMUNE RESPONSE – FORMATION OF NANOTUBES BETWEEN CELLS

Cells have developed a number of mechanisms that allow them to communicate with both their environment and surrounding cells. These include the secretion of various cytokines, which have effects on other cells, and cell to cell contact through engagement with cell surface receptors. These mechanisms result in the induction of cellular responses under different physiological conditions. Alternatively, cells have also been shown to be able to communicate through the formation of cellular connections termed nanotubes (Rustom *et al.* 2004). These intercellular, ultrafine structures described as protrusions of the cell membrane, stretch between two or more cells (Figure 1.7) and possess a cytoskeletal backbone (reviewed in Gurke *et al.* 2008). Nanotubes have been shown to enable the formation of cell networks, through which intracellular and surface

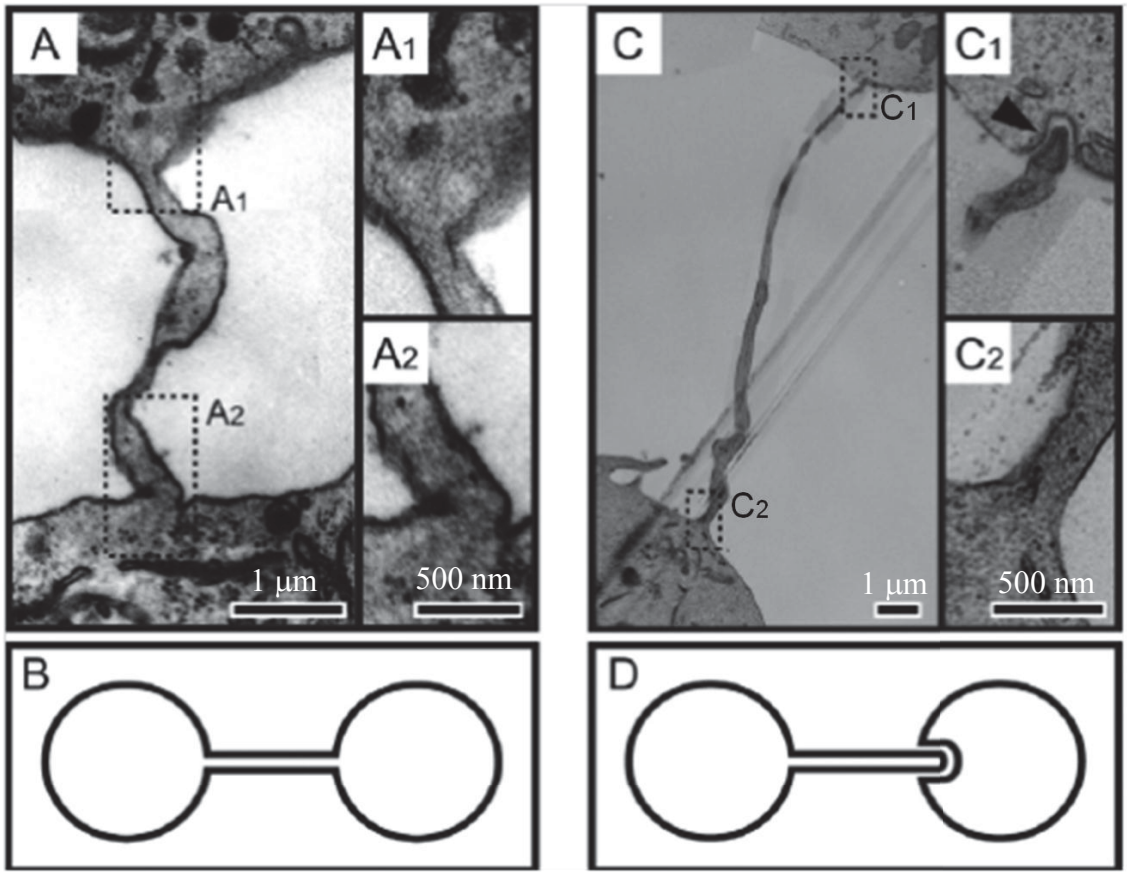

Figure 1.7: Electron microscopy images and schematic representations of the types of nanotubes.
Nanotubes are ultrafine structures which connect cells. A) In some cells, membrane continuity is observed between connected cells (Images A_1 and A_2) (Rustom *et al.* 2004). This is illustrated schematically in B. C) In other instances membrane continuity is not observed at one cell junction, instead, the nanotube formed by one cell (C_2) produces an invagination (arrowhead) into the connected cell (C_1) (Sowinski *et al.* 2008), also depicted schematically in D. (Reproduced from Gerdes *et al.* 2008).

material, along with bacterial and viral proteins (Onfelt *et al.* 2006; Sherer *et al.* 2007; Sowinski *et al.* 2008), can be passed between connected cells (reviewed in Gurke *et al.* 2008). The cellular responses elicited depend upon the type of material being shared. Thus, by forming nanotubes, connected cell populations do not require interaction of each cell with ligands or stimuli, but instead, a cellular stimulus can spread between connected cells (Watkins *et al.* 2005; Chinnery *et al.* 2008).

Nanotubes have been observed in *in vitro* cultures of a number of different cell types, forming between cells in both homogenous cultures (Onfelt *et al.* 2004; Rustom *et al.* 2004; Watkins *et al.* 2005; Zhu *et al.* 2005; Onfelt *et al.* 2006; Sowinski *et al.* 2008) and cultures of mixed cell populations (Koyanagi *et al.* 2005; Watkins *et al.* 2005; Sherer *et al.* 2007) (tabulated in Gerdes *et al.* 2008; Gurke *et al.* 2008; and Marzo *et al.* 2012). Cellular protrusions have also been documented in tissues *in situ*, where they may play important roles in intercellular communication (Domhan *et al.* 2011). Nanotubes have been observed *in situ* in several normal tissues of vertebrate and invertebrate origin. This includes primary mesenchyme sea urchin embryos (Gustafson *et al.* 1967; Miller *et al.* 1995), *Drosophila* wing and eye imaginal discs (Ramirez-Weber *et al.* 1999; Gibson *et al.* 2000; Jacinto *et al.* 2000; Chou *et al.* 2002; Demontis *et al.* 2007), and embryonic muscle (Ritzenthaler *et al.* 2000; Ritzenthaler *et al.* 2003), as well as limb buds (Ramirez-Weber *et al.* 1999), transverse thorax muscle (Misgeld *et al.* 2002), and the corneas of mice (Chinnery *et al.* 2008). Most recently, nanotubes have also been observed in human tumours (Lou *et al.* 2012).

1.3.1 MECHANISMS OF NANOTUBE FORMATION

The formation of nanotubes occurs by two mechanisms (reviewed in Marzo *et al.* 2012). Firstly, cells that have been in contact, usually following cell division, are thought to remain connected by nanotubes. Secondly, nanotubes can form *de novo* when a cellular protrusion, extended by actin polymers, contacts an adjacent cell. In the case of all non-dividing cells, such as rat pheochromocytoma cells (Rustom *et al.* 2004) and primary macrophages (Onfelt *et al.* 2006), formation of nanotubes is most likely to occur by the *de novo* mechanism, or following contact with passing cells. In this case, the movement of cells within culture brings cells into contact, and, as cells subsequently move apart, the cell membranes remain connected by nanotubes (Chauveau *et al.* 2010).

By connecting many cells by the shortest distance possible, nanotubes create intercellular networks that can span lengths of up to several cell diameters *in vitro* (Rustom *et al.* 2004; Watkins *et al.* 2005). For example, pairs of macrophages in culture can produce single nanotubes between 10 μm to over 50 μm in length (Onfelt *et al.* 2004). Nanotubes have been observed to connect cells in *in vitro* cultures without touching the substrate on which they are grown. Rather, nanotubes are raised above the surface and connect apical parts of cells (Onfelt *et al.* 2006) suggesting that nanotubes are not formed purely as a response to the culture surface, but play an important role in facilitating the formation of functional intercellular networks.

1.3.2 TYPES OF NANOTUBES

Two types of nanotubes have been observed. Nanotubes can be open-ended with a continuous membrane connecting two cells (Figure 1.7A and B), allowing the bi-directional exchange of both surface and cytoplasmic material. Alternatively, a nanotube formed by one cell can be closed on the end where it connects with the second cell forming an 'invagination' (Figure 1.7C_1 and D), whereby free diffusion of material between connected cells is prevented and only material at the cell surface is exchanged (Gerdes *et al.* 2008). The type of nanotubes formed by cells is dependent on the cell type and influences the ability of connected cells to share surface and cytoplasmic material (Rustom *et al.* 2004; Sowinski *et al.* 2008).

Nanotubes form from protrusions of the cell membrane and therefore, a cytoskeletal backbone is required in order for these protrusions to extend towards a nearby cell. Therefore, their formation and integrity can be prevented or altered in culture by the inclusion of agents that disrupt cytoskeletal components, including actin-depolymerising drugs, latrunculin B and cytochalasin D, as well as microtubulin-destabilising drugs, nocodazole and colchicine (Onfelt *et al.* 2006). While a complete analysis of the cytoskeletal components of nanotubes has not been conducted in all cases, the cytoskeletal proteins F-actin, microtubulin and myosin Va have been consistently identified (tabulated in Gurke *et al.* 2008). Interestingly, when comparing what is known about the cytoskeletal components of nanotubes formed by non-immune and immune cells, those formed between non-immune cells, including rat pheochromocytoma cells, kidney cells and astrocytes, are composed of F-actin and

myosin Va (Rustom *et al.* 2004; Zhu *et al.* 2005). On the other hand, nanotubes connecting immune cells, such as human monocyte-derived macrophages and natural killer cells, are composed of F-actin and microtubulin (Onfelt *et al.* 2006; Chauveau *et al.* 2010). On the basis of cytoskeletal composition and size, two types of nanotubes have been observed in human macrophages to date. The first, termed 'thick' nanotubes, consist of nanotubes with a diameter of ≥0.7 μm and are composed of both F-actin and α-tubulin (Onfelt *et al.* 2006). The second, termed 'thin' nanotubes, are those that have a diameter of <0.7 μm and are composed of only F-actin (Onfelt *et al.* 2006).

Both *in vitro* and *in vivo*, nanotubes have been demonstrated to transport intracellular organelles, as well as to transfer surface receptors and calcium ions in either a uni, or bidirectional manner (Rustom *et al.* 2004; Onfelt *et al.* 2006; reviewed in Gurke *et al.* 2008). The directionality of movement is dependent on the cytoskeletal composition of nanotubes, with endosomes, lysosomes, mitochondria and viral proteins generally being transported in a uni-directional, actin-dependent manner in nanotubes that did not contain microtubulin (Rustom *et al.* 2004; reviewed in Gurke *et al.* 2008; Sowinski *et al.* 2008). However, bi-directional, microtubulin-dependent movement of organelles (such as mitochondria, endosomes and lysosomes) has been observed in nanotubes composed of both F-actin and microtubulin (Onfelt *et al.* 2006).

1.3.3 FUNCTIONS OF NANOTUBES IN NON-IMMUNE CELLS

In non-immune cells, nanotubes have been observed to transport endosome-related organelles, lipid-anchored proteins, mitochondria and soluble/cytosolic proteins (Rustom *et al.* 2004; Koyanagi *et al.* 2005; Zhu *et al.* 2005; Sherer *et al.* 2007; Arkwright *et al.* 2010). Many normal cell processes require the formation of nanotubes, including wound healing (Wood *et al.* 2002; Wang *et al.* 2011a), however nanotubes have also been shown to mediate cell rescue (Plotnikov *et al.* 2010; Yasuda *et al.* 2011), facilitate the recycling of cellular components (Wang *et al.* 2011b) and induce differentiation in connected cells (Plotnikov *et al.* 2008; Plotnikov *et al.* 2010). Additionally, pathogens may utilise existing nanotubes as a way of spreading between cells to evade extracellular recognition by immune cells (Sherer *et al.* 2007).

1.3.3.1 WOUND HEALING

The formation of nanotubes has been associated with wound healing, with cellular protrusions making connection with distant tissue and bringing the edges of tissues together. The role of nanotubes in wound healing has been explored in *Drosophila melanogaster* where nanotubes were found to stretch across disrupted tissue and initiate the 'tugging' of the two edges together (Wood *et al.* 2002). Furthermore, nanotubes have been observed to transfer electrical signals between cells (reviewed in Wang *et al.* 2010; Abounit *et al.* 2012), which has been proposed to have implications in the healing processes of cells, potentially synchronising actin remodelling (Wang *et al.* 2011a).

1.3.3.2 STEM CELL-MEDIATED RESCUE

A number of disease states associated with oxidative stress are linked with lysosome permeabilisation and a collapse of lysosomal pH gradients (Patschan *et al.* 2008a; Patschan *et al.* 2008b) along with mitochondrial damage (Orrenius *et al.* 2007). In these cases, the transfer of mitochondria and lysosomes from healthy cells provides a means of replacing damaged mitochondria and restoring lysosomal pH gradients. Recent investigations observed that the formation of nanotubes between stem cells and stressed cells was responsible for stem cell mediated rescue (Plotnikov *et al.* 2010; Yasuda *et al.* 2011). In *in vitro* models, nanotubes formed between endothelial progenitor cells and endothelial cells; or between human mesenchymal multipotent stromal cells (MMSCs) and rat renal tubular cells, were responsible for the rescue of stressed cells, through the transfer of mitochondria (Plotnikov *et al.* 2010; Yasuda *et al.* 2010) to restore aerobic respiration (Spees *et al.* 2006), and/or lysosomes to improve viability and ameliorate senescence (Yasuda *et al.* 2011). In other instances, nanotubes that formed between healthy and stressed cells were always initiated by stressed cells (Zhang 2011), suggesting that nanotube formation was a response to stress (Zhang 2011). It was observed that stressed cells transferred their viable cellular contents to healthy cells, allowing for the recycling of functional organelles (Wang *et al.* 2011b).

1.3.3.3 RECYCLING OF CELLULAR CONTENTS

Nanotubes can also be used to transfer cell contents to stem cells to initiate the differentiation process (Plotnikov *et al.* 2008; Plotnikov *et al.* 2010). Nanotubes formed between rat tubular cells and MMSCs incited the differentiation of the MMSCs and it

was theorised that nanotubes were used to transfer signalling molecules from rat tubular cells to induce the differentiation of MMSCs (Plotnikov *et al.* 2008; Plotnikov *et al.* 2010). Therefore, stem cells could have the potential to replace damaged cells by the transfer of cell-specific signalling molecules.

1.3.3.4 PATHOGEN MIGRATION

While nanotubes mediate the transport of cellular contents for the purpose of cell differentiation and rescue, nanotubes may also be hijacked by pathogens as a means of spreading between cells. The transport of murine leukaemia virus via nanotubes was observed in both monkey and human kidney cells (Cos-1 and HEK293), along with rat muscle tumour cells (Sherer *et al.* 2007). Viral envelope glycoproteins congregated at the cell surface of infected cells, and uninfected cells expressing viral receptors were observed to initiate the formation of nanotubes towards infected cells. The binding of viral envelope glycoproteins to receptors at the tip of the nanotubes stabilised the contact site and allowed the transport of murine leukaemia virus along the surface of the nanotubes towards the cell body where it infected the connected cell (Sherer *et al.* 2007).

1.3.4 ROLE OF NANOTUBES IN IMMUNE CELLS

Cellular protrusions have been observed in many immune cell types, particularly APCs, where the extension of cell projections is essential for detecting pathogens which may be rapidly moving or sparsely opsonised (Flannagan *et al.* 2010). Nanotubes have been observed to be associated with a number of immune cells including monocytes and macrophages (Watkins *et al.* 2005; Onfelt *et al.* 2006), DCs (Watkins *et al.* 2005), B cells (Onfelt *et al.* 2004; Quah *et al.* 2008), natural killer cells (Chauveau *et al.* 2010) and T lymphocytes (Sowinski *et al.* 2008; Arkwright *et al.* 2010; Luchetti *et al.* 2012). Nanotubes connecting immune cells are responsible for the transport of calcium ions, surface receptors and markers, including human leukocyte antigen (HLA) molecules, along with other membrane components, cytosolic components and intracellular organelles, such as mitochondria, endosomes and lysosomes (reviewed in Gurke *et al.* 2008; and Marzo *et al.* 2012). The role of nanotubes in immune cells includes the induction of cell activation in connected cells by the transport of calcium ions (Watkins *et al.* 2005), the induction of cell death in connected target cells (Chauveau *et al.* 2010),

the transport of viral proteins (Sowinski *et al.* 2008; Eugenin *et al.* 2009; Kadiu *et al.* 2011a, 2011b), the binding and trafficking of bacteria (Onfelt *et al.* 2006), and amplification of immune responses (Chinnery *et al.* 2008).

1.3.4.1 CELL ACTIVATION

Nanotubes have been observed to induce cell activation in connected cells, in response to soluble bacterial products or mechanical stimulation, through the transport of calcium ions between cells, indicative of the first steps of cell activation (Watkins *et al.* 2005). The release of soluble *E. coli* factors into the medium of cultures containing DCs and THP-1 cells, resulted in the transport of calcium ions from human DCs to THP-1 cells connected by nanotubes (Watkins *et al.* 2005). This initiates activation and triggering immune responses in THP-1 cells (which are not activated by soluble *E. coli* factors), such as cell spreading which is a characteristic response to bacteria (Watkins *et al.* 2005).

1.3.4.2 INDUCTION OF CELL DEATH

Nanotubes are also utilised to facilitate cell death in connected cells. Natural killer cells have been observed to connect to target cells and use nanotubes to draw target cells closer, forming a cytolytic synapse resulting in the death of the target cell (Chauveau *et al.* 2010). Alternatively, natural killer cells were able to induce cell death in distant target cells connected by nanotubes and while the mechanism behind this cytolysis is unknown, it is thought to be mediated by the movement of perforin through nanotubes (Chauveau *et al.* 2010). Furthermore, as observed in non-immune cells, such as in rat astrocytes and neurons (Wang *et al.* 2011b), stressed or apoptotic human T cell populations have been observed to induce the formation of nanotubes to allow sharing of cytoplasmic and membrane material between Fas ligand-activated cells (Arkwright *et al.* 2010; Luchetti *et al.* 2012). The transfer of the cytosolic material from Fas ligand activated cells is proposed to propagate and expand the apoptotic signal between activated T cells (Luchetti *et al.* 2012).

1.3.4.3 PATHOGEN TRANSPORT

Nanotubes of immune cells transport pathogens between cells and can initiate an immune response in connected cells. Pathogens can, however, utilise nanotubes as a

means of spreading between cells. As observed in kidney cells, nanotubes connecting homogenous cultures of Jurkat T cells or primary human monocyte-derived macrophages result in the spreading of viruses between cells, as shown by the transport of human immunodeficiency virus (HIV)-1 proteins within nanotubes (Sowinski *et al.* 2008; Kadiu *et al.* 2011a, 2011b). By spreading between cells through nanotubes, the virus may minimize extracellular detection (Sowinski *et al.* 2008). Nanotubes associated with macrophages have also been shown to bind bacteria on their surface and, in some cases, transport bacteria along the surface of nanotubes towards the cell body for phagocytosis (Onfelt *et al.* 2006).

1.3.4.4 AMPLIFICATION OF IMMUNE RESPONSES

Lastly, nanotubes produced by immune cells have a proposed role in the amplification of immune responses (Chinnery *et al.* 2008). Nanotubes have recently been observed *in vivo* in mouse cornea, produced by and connecting MHC class II positive cells, putatively DCs (Chinnery *et al.* 2008). Within the immune-privileged corneal stromal tissue, these DC-like cells are present in low numbers and the formation of nanotubes allows cells to remain in contact. This potentially allows rapid and more efficient immune responses. In damaged corneal tissue and corneas exposed to the inflammatory bacterial product, LPS, a notable increase in nanotubes was observed (Chinnery *et al.* 2008), suggesting that nanotubes have an important role in cell to cell communication *in vivo*. Nanotubes may potentially provide a means of transferring antigen or antigen-receptor complexes such as MHC and TLR molecules between DCs (Chinnery *et al.* 2008).

1.4 SCOPE OF THE PROJECT

The rapid induction of an anti-inflammatory/Th2 immune response after infection by the helminth *F. hepatica* (Donnelly *et al.* 2005) and the immune modulatory effects of its main ES components (Donnelly *et al.* 2008; Donnelly *et al.* 2010; Robinson *et al.* 2011b; Carranza *et al.* 2012; Robinson *et al.* 2012), makes the FhES products candidates for the treatment of autoimmune and inflammatory diseases. In murine macrophages, the immune modulatory effect of the main FhES component, FhCL1, was found to be suppression of pro-inflammatory cytokines in a TRIF-dependent manner, due to the cleavage of TLR3 (Donnelly *et al.* 2010). This was associated with protection from septic shock (Donnelly *et al.* 2010), a fatal systemic pro-inflammatory immune response mounted against bacteria or their products. Therefore, FhCL1 represents a potential therapeutic target for the treatment of inflammatory diseases in humans. The use of helminths and their products therapeutically in humans requires an understanding of the precise mechanisms through which the specific helminth products modulate immune responses. To date, nothing is known about the effect of FhCL1 on human cells. Therefore, before progressing to pre-clinical development, the immune modulatory effects of FhCL1 must first be investigated *in vitro* in human cells. Our lab is concurrently investigating this via two distinct avenues, examining the effect of FhCL1 on human monocyte-derived macrophages, and monocyte-derived DCs. As APCs, both cell types shape the innate and adaptive immune response. This thesis focused on the effect of FhCL1 on human monocyte-derived macrophages.

This aims of this PhD research are to:

(1) Examine the effect of FhCL1 on macrophage function and phenotype by examining its effect on cell surface markers and cytokine expression.

(2) Examine the localisation of FhCL1 within monocyte-derived macrophages and further elucidate its mechanism of action by investigating key immune molecules, such as TLRs, through which FhCL1 may mediate its effects.

(3) Investigate nanotubes connecting primary human monocyte-derived macrophages, especially the effects of LPS and FhCL1, on endosomes and TLRs in connected cells.

CHAPTER 2:

MATERIALS AND METHODS

2.1 GENERAL METHODS

2.1.1 STERILITY AND CONTAINMENT

For all molecular biology work involving RNA extraction, all solutions and plasticware used were autoclaved or obtained/purchased as deoxyribonuclease (DNase)- and ribonuclease (RNase)-free, in order to prevent degradation of nucleic acids, and all samples for reverse transcriptase-quantitative polymerase chain reaction (RT-qPCR) were prepared in DNase and RNase free water. Separate work areas were designated for pre-PCR manipulations (DNA extraction, reagent pipetting) and for post-PCR work (analysis of amplicons). Sterile filtered tips (Axygen Scientific, USA) were used for PCR setup and tissue culture to prevent aerosol contamination. All tissue culture work, including purification of primary cells, were performed in a class II biohazard safety hood, under asceptic conditions, using disposable, sterile plasticware (Sarstedt, Germany).

2.2 PRODUCTION OF RECOMBINANT FUNCTIONALLY ACTIVE *F. HEPATICA* CATHEPSIN L1

A functionally active recombinant form of the *F. hepatica* cysteine protease, FhCL1, with a 6xHis-tag, was expressed in *Pichia pastoris* and purified by affinity chromatography on nickel-nitrilotriacetic acid-agarose, by D. Xu (UTS), as described in Collins *et al.* (2004). Once prepared, the recombinant FhCL1 was tested using Endosafe Endochrome-K assay (Charles River, USA), by J. To (UTS), and found to be negative for the presence of endotoxin by transferring the sample for testing (100 μL) as well as a negative control and positive standards to individual wells of a microtitre plate. Limulus amebocyte lysate reagent (100 μL) was then added to each well and a kinetic assay performed to determine the amount of time taken for absorbance to increase significantly over background levels. By creating a standard curve, the level of endotoxin within samples was determined.

Enzymatic activity of FhCL1 was blocked by incubation of FhCL1 with the cysteine proteinase inhibitor E64 ((2*S*,3*S*)-3-(*N*-{(*S*)-1-[*N*-(4-guanidinobutyl) carbamoyl] 3-methylbutyl} carbamoyl) oxirane-2-carboxylic acid) (Sigma-Aldrich, USA) (10-20 μM

E64 for 1 h, room temperature (RT)). The enzyme was confirmed to be approximately 80% inactivated in the presence of 10 μM and 20 μM E64 based on a fluorometric substrate assay performed by J. To (UTS), as described by Collins *et al.* (2004) and Stack *et al.* (2005) (data not shown). Briefly, FhCL1 was assayed in a total volume of 1 mL substrate buffer mix (2.5 mM ethylenediaminetetraacetic acid (EDTA), 2 mM dithiothreitol 0.1 M sodium phosphate buffer, pH 5.0, and 10 μM Z-Phe-Arg-NHMec). The reaction was incubated (37 ˚C, 30 min) and stopped by the addition of 200 μL of 10% acetic acid. Fluorescence was recorded at an excitation wavelength of 370 nm and an emission wavelength of 440 nm. The activity of FhCL1 was calculated from a standard curve of NHMec ranging from 0 to 10 μM and presented as nmol NHMec min^{-1} mL^{-1} (Collins *et al.* 2004; Stack *et al.* 2005).

2.2.1 REMOVAL OF ENDOTOXIN FROM FHCL1 PREPARATIONS

While recombinant FhCL1 was produced in yeast and therefore should have no/low levels of endotoxin, Triton X-114 (Sigma-Aldrich, USA) was utilised to remove any contaminating endotoxin using a protocol modified from Aida and Pabst *et al*. (1990). Briefly, Triton X-114 (10 μL) was added to FhCL1 (1 mL) and vortexed to mix. Samples were incubated on ice (30 min) with occasional vortexing before heating (37 °C, 10 min). Once samples became cloudy in colour, they were centrifuged (16100 x g, 37 °C, 10 min) to pellet Triton X-114. The aqueous phase was transferred to a new Eppendorf tube and the Triton X-114 treatment was repeated a further 3 times (a total of 4 treatments) with the addition of fresh Triton X-114 each time, except during the final cycle which removed any remaining Triton X-114. Protein concentration was determined using spectrophotometry (Section 2.2.2).

2.2.2 QUANTITATION OF PROTEIN

Prior to the use of protein samples, the protein concentration was determined by spectrophotometry (Nanodrop, ND1000, Thermo Scientific, USA) using the absorbance of an aliquot of the sample at 280 nm.

2.3 DERIVATION OF PRIMARY HUMAN MACROPHAGES

2.3.1 ISOLATION OF HUMAN MONOCYTES USING MAGNETIC SEPARATION

Whole human blood, from a total of 35 donors (Table 2.1), obtained from the Red Cross Blood Bank, was transferred into a 50 mL falcon tube and diluted 1 in 2 with Roswell Park Memorial Institute (RPMI) 1640 medium (Gibco/Life Technologies, USA). Approximately 35 mL of diluted blood was gently layered onto 15 mL of Ficoll Paque Plus (GE Healthcare Biosciences AB, Sweden) at RT, ensuring that blood and Ficoll did not mix and the blood formed a layer on top of the Ficoll. Following centrifugation (400 x g, 30 min, RT, break/accelerator low, Eppendorf 5810R) red blood cells formed a layer below the Ficoll, while white blood cells settled above the Ficoll layer beneath the serum layer. White blood cells were collected by aspiration and washed 3 times in RPMI 1640 medium. White blood cells were harvested by centrifugation (400 x g, 7 min, RT, Eppendorf 5702) and any remaining Ficoll was removed. The white blood cell pellet was resuspended in 25 mL autoMACs rinsing solution (Miltenyi Biotec, Germany) containing 1% (v/v) foetal bovine serum (FBS) (Gibco/Life Technologies, USA) and the cell number was determined using a neubauer chamber. Samples were centrifuged (400 x g, 7 min, RT, Eppendorf 5702) and white blood cells were resuspended in 80 µL of autoMACs rinsing solution per 10^7 cells. To positively select for $CD14^+$ cells, 20 µL of $CD14^+$ MicroBeads (Miltenyi Biotec, Germany) was added per 10^7 cells and, after mixing well, the samples were left to incubate (15 min, 4 °C). Samples were washed by adding 1-2 mL of buffer per 10^7 cells and up to 10^8 cells were resuspended in 500 µL of buffer.

The magnetically labelled $CD14^+$ cells were separated using a MACS LS column (Miltenyi Biotech, Germany), which was placed in the magnetic field of the midiMACS separation unit (Miltenyi Biotech, Germany). The column was washed with 3 mL of autoMACS rinsing solution and the cell suspension was added to the column, allowing unlabelled cells to pass through. Magnetically labelled cells were then washed three times with 3 mL rinsing solution and the column was removed from the separator and placed over a falcon tube for collection. After pipetting 5 mL of rinsing solution onto the column, the magnetically labelled contents were immediately flushed out by firmly

Table 2.1: Information relating to isolation, culture and testing of individual macrophage donors.

Macrophage Donor	Date of Isolation	Individual/ Pooled	Experiments
A	17 Nov 2009	Individual	3.5, 3.6, 4.6, 4.9
B	17 Nov 2009	Individual	3.5, 3.6, 3.15, 3.17, 4.6, 4.9
C	25 Jan 2010	Individual	3.5, 3.6, 3.7, 3.8, 3.17, 4.6, 4.9
D	25 Jan 2010	Individual	3.5, 3.6, 3.7, 3.8, 4.9
E	25 Jan 2010	Individual	3.5, 3.6, 3.7, 3.8, 3.13, 3.17, 4.6, 4.9
F	25 Jan 2010	Individual	3.5, 3.6, 3.7, 3.8, 3.17, 4.6, 4.9
G	9 Feb 2010	Individual	3.5, 3.6, 3.17, 4.6, 4.9
H	9 Feb 2010	Individual	3.5, 3.6, 3.13, 3.15, 3.17, 4.9
I	3 Apr 2012	Individual/ Pooled	3.10, 3.11, 3.12, 3.13, 3.14, 3.15, 4.14, 4.15, 4.16, 5.1, 5.6
J	3 Apr 2012	Individual/ Pooled	3.10, 3.11, 3.12, 3.13, 3.14, 3.15, 4.14, 4.15, 4.16, 5.1, 5.6
K	3 Apr 2012	Individual/ Pooled	3.10, 3.11, 3.12, 3.13, 3.14, 3.15, 4.14, 4.15, 4.16, 5.1, 5.6
L	3 Apr 2012	Individual/ Pooled	3.10, 3.11, 3.12, 3.13, 3.14, 3.15, 4.14, 4.15, 4.16, 5.1, 5.6
M	16 Feb 2010	Individual	3.8
N	16 Feb 2010	Individual	3.8
O	16 Feb 2010	Individual	3.8
P	16 Feb 2010	Individual	3.8
Q	22 Jun 2010	Individual	3.8, 4.10
R	22 Jun 2010	Individual	3.8, 4.10
S	8 Jul 2010	Pooled	4.7, 4.11, 5.2, 5.3, 5.4, 5.8
T	8 Jul 2010	Pooled	4.7, 4.11, 5.2, 5.3, 5.4, 5.8
U	8 Jul 2010	Pooled	4.7, 4.11, 5.2, 5.3, 5.4, 5.8
V	8 Jul 2010	Pooled	4.7, 4.11, 5.2, 5.3, 5.4, 5.8
W	29 Jul 2010	Individual	3.9, 4.1, 4.2, 4.11
X	17 Aug 2010	Pooled	3.9, 4.2
Y	17 Aug 2010	Pooled	3.9, 4.2
Z	7 Sep 2010	Pooled	4.11, 5.2, 5.7, 5.8
AA	7 Sep 2010	Pooled	4.11, 5.2, 5.7, 5.8
AB	28 Sep 2010	Pooled	4.11, 5.5
AC	28 Sep 2010	Pooled	4.11, 5.5
AD	7 Nov 2010	Pooled	4.3, 4.4
AE	7 Nov 2010	Pooled	4.3, 4.4
AF	16 Nov 2010	Pooled	4.12
AG	16 Nov 2010	Pooled	4.12
AH	16 Jun 2011	Pooled	4.12
AI	16 Jun 2011	Pooled	4.12

applying the plunger supplied with the column. Alternatively, the autoMACs automated separation unit was used (following the manufacturer's instructions) for positive selection of $CD14^+$ cells, which follows the same protocol with automated wash and collection steps.

2.3.2 CULTURE, DIFFERENTIATION AND STIMULATION OF HUMAN MACROPHAGES

Human peripheral blood monocytes ($1x10^6$) were cultured in 24 well tissue culture plates (Nunc, Denmark) in 1 mL Iscove's Modified Dulbecco's Medium (IMDM) (Gibco/Life Technologies, USA) supplemented with 2% (v/v) heat-inactivated human serum and 1% Penicillin/Streptomycin (Gibco/Life Technologies, USA). Cells matured into macrophages over a period of 5-6 days and, prior to stimulation, medium was replaced with fresh IMDM. Macrophages were cultured with 10-20 μg/mL FhCL1, with or without protease inhibitor E64 (10-20 μM) (Sigma-Aldrich, USA) for 18 h and/or stimulated with 50 ng/mL LPS (Sigma-Aldrich, USA) for between 15 min and 24 h where stated, or cultured with 2 μg/mL tubulin inhibitor, nocodazole (Sigma-Aldrich, USA) for 30 min.

2.4 ISOLATION AND TREATMENT OF RNA

2.4.1 ISOLATION OF RNA FROM PRIMARY CELLS

The TRIzol (Life Technologies, USA) method of RNA extraction was used to isolate RNA from cultures of primary human macrophages, containing approximately $1-2x10^6$ cells/mL, following the manufacturer's instructions. TRIzol (1 mL) was added to $1x10^6$ macrophage cells followed by cell disruption by pipetting. Samples were incubated (5 min, RT) to completely dissociate all nucleoproteins. Chloroform was added (200 μL per 1 mL of Trizol), samples were shaken by hand (15 s) and incubated (2-3 min, RT). Samples were centrifuged (12000 x g, 15 min, 2-8 °C, Eppendorf 5417R) to separate the phases. The upper aqueous phase was transferred to a new Eppendorf tube, being careful not to disturb the lower phases. Isopropanol was added (0.5 mL for every 1 mL of TRIzol used) and the sample was mixed by inversion and incubated (10 min, RT) prior to collection of the RNA as a pellet by centrifugation (12000 x g, 10 min, 2-8 °C, Eppendorf 5417R). Supernatants were removed and the

pellet washed once with 75% (v/v) ethanol. A pellet of RNA formed following centrifugation (7500 x g, 5 min, 2-8 °C, Eppendorf 5417R). Supernatants were removed completely by pipetting and the pellet was allowed to air dry. RNA was resuspended in 25 µL of RNase-free water and concentrations were determined using spectrophotometry (Section 2.4.2) and typically ranged from 10 to 150 ng/µL. All RNA samples were stored at -80 °C prior to DNase treatment and complementary (c)DNA synthesis.

2.4.2 QUANTITATION OF NUCLEIC ACIDS

The concentration of extracted nucleic acids was determined by spectrophotometry (Nanodrop, ND1000, Thermo Scientific, USA) where one absorbance unit (260 nm) equals 50 µg/mL DNA and 40 µg/mL RNA. The ratio of absorbance of a sample at 260 and 280 nm was used to assess the purity of the nucleic acid. A ratio of approximately 1.8 and 2.0 is considered pure for DNA and for RNA, respectively.

2.4.3 DNASE TREATMENT AND CDNA SYNTHESIS OF RNA SAMPLES

RNA was treated with DNase I (1 Unit/µL) (Life Technologies, USA). Reactions were set up on ice with 1 Unit DNase I and 1 µL 10x DNase I reaction buffer made up to a total volume of 10 µL with diethylpyrocarbonate-treated water. Samples were incubated (15 min, RT) and the reaction stopped by the addition of 25 mM EDTA (pH 8.0) (1 µL), followed by heating (10 min, 65 °C) to inactivate the DNase I. DNase treated RNA was used for cDNA synthesis using the SuperScript III First Strand Synthesis Supermix (Life Technologies, USA), following the manufacturer's instructions. Briefly, RNA (up to 5 µg) was incubated with 50 µM oligo$(dT)_{20}$ primers, annealing buffer and RNase/DNase-free water (65 °C, 5 min). First-strand reaction mix and SuperScript III/RNaseOUT Enzyme Mix were added to the reaction on ice and reverse transcription was conducted at 50 °C (50 min). The reaction was then terminated by incubation at 85 °C (5 min) before cooling (4 °C, 5 min). The synthesised cDNA was then stored at -20 °C until assayed.

2.5 PCR PROTOCOLS

2.5.1 OLIGONUCLEOTIDES FOR REAL TIME REVERSE TRANSCRIPTASE-QUANTITATIVE PCR

All primers were designed using the program Primer Select version 9.0.4 (Lasergene, DNASTAR, California, USA) and were designed to span intron/exon junctions (where possible) and amplify Interleukin (IL)-1β, IL-10, IL-12, Interferon (IFN)- β, Toll-like receptor (TLR)-3, TLR4 and the reference gene Ribosomal Protein L36A Like (RPL36AL) (Eisenberg *et al.* 2003) for RT-qPCR (Table 2.2, see Appendix 1 for primer locations). Primer sequences used for the amplification of Interferon regulatory factor (IRF)-3 were as described by Izaguirre *et al.* (2003) (Table 2.2). Amplicons for RT-qPCR were designed to be between 90 and 140 base pairs (bp) in length to allow similar amplification efficiency within the extension time used. However, primers amplifying IRF3 produced a 65 bp amplicon (Izaguirre *et al.* 2003).

Primers were purchased from Sigma-Genosys (USA) or Life Technologies (USA) and obtained in a lyophilised form. Primers were resuspended to a concentration of 200 pmol/μL in Tris EDTA buffer (10 mM Tris HCl pH 7.5 (Amresco, USA), 1 mM EDTA (Sigma-Aldrich, USA)). Working solutions were made by dilution of the 200 pmol/μL stock solution. All stock and working solutions were stored at -20 °C, until required.

2.5.2 PCR FOR OPTIMISATION

PCR amplification to optimise RT-qPCR was carried out in thin walled 8 strip PCR tubes (Axygen Scientific, USA) with a 50 μL reaction volume containing 1x PCR mix (Promega, USA) (1.25 Units/reaction *Taq* polymerase, 200 μM deoxyribonucleotides (dNTP), 1.5 mM $MgCl_2$), 20 pmol of each primer (forward and reverse) and 20 ng of cDNA. Controls for the PCR included a no reverse transcriptase reaction and a no cDNA template control in which the template was substituted with sterile water (negative control). PCR was carried out in an Eppendorf Mastercycler Gradient instrument (Eppendorf, Germany) and was initiated with an initial denaturation (95 °C, 5 min), followed by 40 cycles of denaturation (95 °C, 40 s), primer annealing (58 °C,

Table 2.2: Sequences of primers for real time RT-qPCR analysis.

Gene	Primer Name	Primer Base Sequence	Annealing Temperature (°C)	Predicted Amplicon Size (bp)
RPL36AL	HSRPL36AL-F	5'-GTTAGGCGAGAGCTGCGAAAGG-3'	61	128
	HSRPL36AL-R	5'-GGTTCTTCGGGTTTTAGGTACGTT-3'		
IL-1β	HSIL-1β-F	5'-TGAGCTCGCCAGTGAAATGATG-3'	61	118
	HSIL-1β-R	5'-CAGAGGGCAGAGGTCCAGGTC-3'		
IL-10	HSIL-10-F	5'-AGCAAGGCCGTGGAGCAGGTGA-3'	61	135
	HSIL-10-R	5'-GTCTCAGTTTCGTATCTTCATTGTC-3'		
IFN-β	HSIFN-β-F	5'-AAGCAGCAATTTTCAGTGTCAGA-3'	61	138
	HSIFN-β-R	5'-AATGCGGCGTCCTCCTTC-3'		
IL-12	HSIL-12-F	5'-CACAAAGGAGGCGAGGTTCTAAG-3'	61	157
	HSIL-12-R	5'-AGCAGGTGAAACGTCCAGAATAATT-3'		
IRF3	HSIRF3-F	5'-ACCAGCCGTGGACCAAGAG-3'	61	65
	HSIRF3-R	5'-TACCAAGGCCCTGAGGCAC-3'		
TLR3	HSTLR3-F	5'-AGACCCATTATGCAAAAGATTCAA-3'	57	131
	HSTLR3-R	5'-GCAAACAGAGTGCATGGTTCAG -3'		
TLR4	HSTLR4-F	5'-CCGACAACCTCCCCTTCTC-3'	61	130
	HSTLR4-R	5'-GTCTGGATTTCACACCTGGATAA-3'		

40 s) and extension (72 °C, 40 s) followed by a final extension step (72 °C, 10 min). After amplification, an aliquot (10 μL) of the reaction products was examined by electrophoresis on a 2.5% (w/v) Tris acetic acid EDTA (TAE) agarose gel.

Optimisation of primer annealing temperature for RT-qPCR was carried out in a 25 μL reaction volume, containing 1x PCR mix (Promega, USA) (0.625 units/reaction *Taq* polymerase, 100 μM dNTP, 0.75 mM $MgCl_2$), 20 pmol of each primer (forward and reverse) and 10ng of the synthesised cDNA (Section 2.4.3). A no cDNA template (negative) control was included in all runs. PCR conditions were as previously described but with a temperature gradient of 55-66 °C to determine optimal amplification conditions. PCR products (10 μL) were analysed by electrophoresis on 2.5% (w/v) agarose gels (Section 2.5.3) to confirm that the amplified products were within the expected size ranges (93 to 157 bp) (Table 2.2). The best quality amplifications were those which showed the correct size product, the highest intensity fluorescence levels, and the absence of any non-specific amplification.

2.5.3 AGAROSE GEL ELECTROPHORESIS AND VISUALISATION OF NUCLEIC ACIDS

In order to visualise PCR products and RNA, nucleic acid samples were electrophoresed in agarose gels. Gels varied from 2.5-3% (w/v) agarose (Amresco, USA), depending on the sizes of the products being analysed. Gels were electrophoresed in 1x TAE buffer (40 mM Tris (Amresco, USA), 20 mM acetic acid (Sigma-Aldrich, USA), 1 mM EDTA (Sigma-Aldrich, USA)) containing 0.5 μg/mL ethidium bromide (Sigma-Aldrich, USA) or GelRed (Biotium, USA). Prior to electrophoresis, 0.3-0.5 vol of 6x loading buffer (60% sucrose (Sigma-Aldrich, USA), 50 mM Tris pH 8.0, 10 mM EDTA and 0.01% (w/v) bromophenol blue (Sigma-Aldrich, USA)) was added to all DNA samples and 0.5 vol RNA loading buffer (20% glycerol (Amresco, USA), 2.7% formaldehyde (Sigma-Aldrich, USA), 4 mM EDTA, 30.84% (v/v) formamide (Sigma-Aldrich, USA) and 1.6% (w/v) bromophenol blue) was added to all RNA samples. Molecular weight standards were electrophoresed alongside PCR products to aid in the determination of amplicon sizes. The quantitative DNA size standards used were Hyperladder 1, Hyperladder IV and Hyperladder V (Bioline, UK) as well as the 100 bp and 1 kilobase DNA ladders (New England Biolabs, USA). The RNA size standard used was a non-

quantitative ladder consisting of nine RNA transcripts that range in size from 281 nucleotides up to 6583 nucleotides (Promega, USA). Agarose gels were electrophoresed at 80V for 40-60 min. After electrophoresis, nucleic acid samples were visualised using a Uvitech Transilluminator (Integrated Sciences, Australia). Images were captured using Carestream Molecular Imaging Software version 5.0.2.30 (Carestream Health Inc., USA) using a Kodak EDA 290 digital camera. For RNA gels, the presence of 28S and 18S ribosomal RNA bands and a smear of mRNA extending above the 28S band and below the 18S band indicated high quality RNA preparations.

2.5.4 REAL TIME RT-QPCR ANALYSIS

Following optimisation of primer annealing temperature, primer concentrations for each primer pair were optimised for RT-qPCR to ensure they were at non-limiting concentrations for amplification, while limiting the formation of primer dimer. A primer matrix was performed which included triplicate reactions of all combinations of forward and reverse primer concentrations (9.0, 6.0, 3.0 and 0.5 μM) to determine the optimal forward and reverse primer concentrations for amplification of RPL36AL, IL-1β, IL-10, IL-12B, IFN-β, IRF3, TLR3 and TLR4 genes. Optimal primer concentrations were those which produced the highest end fluorescence and the lowest threshold cycle (C_t) value. Additionally, to confirm the amplification of PCR product was quantitative, PCR was performed on serial two-fold dilutions of cDNA template and fluorescence intensity profiles were compared to confirm that decreased template corresponded with decreased product.

Real time RT-qPCR was carried out in a 25 μL volume, containing 1x SYBR GreenER qPCR SuperMix (Life Technologies, USA). The PCR was set up in Twin.tec skirted PCR plates (Eppendorf, Germany) and sealed with heat sealing film (Eppendorf, Germany). Each reaction included 10 ng of cDNA. For each real time PCR experiment a no template (negative) control containing sterile water was included for each gene examined. Real time RT-qPCR was carried out using an Eppendorf Mastercycler EP *realplex* (Eppendorf, Germany). The PCR protocol began with an incubation with uracil N-glycosylase (50 °C, 2 min) followed by an initial DNA denaturation step (95 °C, 5 min) and then 40 cycles of denaturation (95 °C, 30 s), primer annealing (57 or 61 °C as described in Table 2.2, 30 s) and extension (72 °C, 30 s). This was followed by a

melt analysis (10 min, approximately 3.5 °C/min) of the PCR products to confirm purity of the amplicon ensuring that a single, homogenous product had been amplified, as indicated by a single peak in the melt curve. Amplification plots were used to analyse the amplification efficiency and determine the C_t value.

2.5.5 REAL TIME RT-QPCR ANALYSIS USING TAQMAN ASSAYS

For mRNA expression analysis of ERK1, ERK2 and TRAF3, pre-validated Taqman primer and probe assays (Applied Biosystems/Life Technologies, USA) were used, which included unlabelled forward and reverse primer pairs, along with a Fluorescein amidite-labelled Taqman major groove binder probe. A Taqman assay for Glyceraldehyde-3-phosphate dehydrogenase (GAPDH) was included as a reference gene. PCR was performed following the manufacturer's instructions. Briefly, RT-qPCR was performed in singleplex 20 μL reaction volumes containing 2x Taqman Gene Expression Master Mix (AmpliTaq Gold® DNA Polymerase), 20x Taqman gene expression assay specific to each target gene, which included forward and reverse unlabelled PCR primers (150 nM final 1x reaction concentration) and a Fluorescein amidite-labelled Taqman probe (250 nM final 1x reaction concentration); and 10 ng cDNA. Controls for the PCR included a no template control in which the template was substituted with sterile water (negative control). PCR was carried out using an Eppendorf Mastercycler EP *realplex* (Eppendorf, Germany). The PCR protocol began with an incubation with uracil N-glycosylase (50 °C, 2 min) followed by an initial DNA denaturation step (95 °C, 10 min) and then 40 cycles of denaturation (95 °C, 15 s) and primer annealing plus extension (60 °C, 1 min). Amplification plots were used to analyse the amplification efficiency and determine the C_t.

2.5.6 QUANTITATION OF DIFFERENCES IN TARGET GENE EXPRESSION IN HUMAN MACROPHAGES FOLLOWING TREATMENT

Quantitation of expression of the target genes IL-1β, IL-10, IL-12B, IFN-β, ERK1, ERK2, TRAF3, IRF3, TLR3 and TLR4 was carried out using a relative quantitative approach, utilising the reference genes RPL36AL or GAPDH. All reactions were set up in triplicate and C_t values for each gene represented the average of three C_t values. The ΔC_t calculation refers to the change in threshold cycle value between the target gene and the reference gene within each cell treatment (Livak *et al.* 2001).

Mean $\Delta C_t = C_{t\ target} - C_{t\ reference}$

The expression of target genes was then compared between different cell treatments for the same donor using the $\Delta\Delta C_t$ calculation, which calculates the change in the threshold cycle value between the target gene and the reference gene, between the two cell treatments (Livak *et al.* 2001).

$\Delta\Delta C_t$ = Mean ΔC_t (treated) – Mean ΔC_t (Untreated)

The fold change in expression between cell treatments was determined using the $\Delta\Delta C_t$ calculation where fold change is determined by the calculation: $2^{-\Delta\Delta Ct}$.

2.5.7 PURIFICATION AND SEQUENCE ANALYSIS OF PCR PRODUCTS

PCR products which were well separated and where no other bands were observed on agarose gel electrophoresis, were purified for sequencing analysis using the Purelink PCR Purification spin column kit (Life Technologies, USA), following the manufacturer's protocol. In brief, 4 volumes of binding buffer with isopropanol were added to 1 volume of PCR product (50 μL). The sample was loaded into a spin column and centrifuged (10,000 x g, 1 min, RT, Eppendorf 5415D). The flowthrough was discarded and DNA was washed by adding 650 μL of wash buffer with ethanol and centrifuged (10,000 x g, 1 min, RT, Eppendorf 5415D). To remove any remaining wash buffer, the flowthrough was discarded and the column centrifuged at maximum speed (16,100 x g, 1 min, RT, Eppendorf 5415D). The PCR products were eluted in a volume of 50 μL of Tris EDTA buffer by centrifugation (16,100 x g, 1 min, RT, Eppendorf 5415D). Spectrophotometric determination was carried out on an aliquot (2 μL) to determine the concentration of the purified PCR product. The efficiency of purification was confirmed by agarose gel electrophoresis (2.5%) which also served to confirm the yield of DNA from a 5-10 μL aliquot by comparison to quantitative molecular weight markers electrophoresed simultaneously. Purified PCR products were stored at -20 °C until required.

Purified PCR products were prepared for sequencing based on the concentration of DNA in each sample according to the specifications of the Sydney University and Prince Alfred Molecular Analysis Centre (SUPAMAC, Australia) or MACROGEN

(Korea). Sequencing was carried out with the forward and reverse primers in separate reactions to allow for double-strand sequence verification.

The data returned following sequencing was in the form of raw sequence data and sequencing electropherograms. The program Chromas Lite Version 2.01 (Technelysium, 2005) was used to visualise the electropherograms, from which the base sequence of the amplified PCR product could be matched to the known sequence of the target gene to confirm amplification of the target product using NCBI BLAST Search (using standard search conditions).

2.6 FLOW CYTOMETRY

2.6.1 FLOW CYTOMETRY STAINING PROTOCOL

When working with monocytes purified from peripheral blood mononuclear cells (Section 2.3.1), cells were transferred to microfuge tubes (Axygen Scientific, USA), pelleted and washed with fluorescence activated cell sorting (FACS) staining wash (FSW), which contained phosphate buffered saline (PBS) and 1% (w/v) bovine serum albumin (BSA) (Research Organics, USA). For macrophages, single cell suspensions were prepared by scraping cells from the bottom of wells using a pipette tip (Axygen Scientific, USA) and transferred to microfuge tubes, before being washed with FSW. Cell pellets were stained with a cocktail of directly-conjugated fluorescent antibodies in a total volume of 50 μL for 30 min on ice, protected from light, or by two step staining, with a non-conjugated primary antibody (50 μL for 30 min on ice) and a conjugated fluorescent secondary antibody for 1 h on ice, protected from light. Details of all antibodies used are provided in Table 2.3. Cells were then washed three times in FSW (750 μL for each wash) and collected by pulse centrifugation (8 s in a microcentrifuge) after each wash, before resuspension in FSW (400 μL) on ice. Flow cytometry was performed using the BD LSR II Flow Cytometer (BD Bioscience, USA) by Dr. A. Hutchinson and M. Lund (University of Technology, Sydney). After gating on live cells based on forward and side scatter plots, the cells were analysed using a four laser (350nm, 405nm, 488nm and 633nm) LSRII flow cytometer. Automatic compensation was performed using FACSDiva software version 6.1.3 (BD Bioscience, USA), using single colour controls, before each experiment such that single labelled cells showed

fluorescence in one channel only. Typically 3-5x10^4 events were acquired. From the forward and side scatter histogram, a gate was placed around the single cell population of interest and events within the gate were further analysed according to fluorescence intensity. Data analysis was completed using CellQuest Pro version 6.0 (BD Biosciences, USA).

Table 2.3: Antibodies used for flow cytometry experiments.

Antibody conjugate [1]	Ig Species	Clone name	Concentration [4]	Supplier
CD14 Pacific Blue	Mouse mAb [3]	TüK4	5 μL	Life Technologies
CD86 PE-Cy5	Mouse mAb	2331 (FUN-1)	20 μL	BD Pharmingen
CD163 APC	Mouse mAb	215927	10 μL	R and D Systems
CD206 FITC	Mouse mAb	clone: 19.2	20 μL	BD Pharmingen
HLA-DR PerCP	Mouse mAb	Clone: TU36	5 μL	Life Technologies
TLR4	Mouse mAb	76B357.1	1.25 μg/mL	Abcam
IgG1	Mouse mAb	MopC-21	250 ng/mL	Sigma
Anti-Mouse IgG AF488 [2]	Goat		2 μg/mL	Life Technologies

[1] PE: Phycoerythrin, Cy5: Cyano 5, FITC: Fluorescein isothiocyanate, PerCP: Peridinin Chlorophyll Protein Complex, APC: Allophycocyanin
[2] AF: Alexa Fluor
[3] monoclonal antibody
[4] per 1x10^6 cells

2.6.2 QUANTITATION OF CYTOKINE SECRETION BY CYTOKINE BEAD ARRAY ANALYSIS

To assess the levels of secreted cytokines in the supernatant of cultured human macrophages, cells were pelleted by centrifugation (400 x g, 7 min, RT, Eppendorf 5415D) and the supernatants collected. The BD Human Inflammatory Cytokine Bead Array (CBA) kit (BD Bioscience, San Diego, USA) was used to measure levels of IL-8, IL-1β, IL-6, IL-10, TNF and IL-12 p70 in culture supernatant.

The CBA was performed according to the manufacturer's instructions. Lyophilised recombinant cytokine standards were reconstituted and serially diluted (0 – 5000 pg/mL). Samples collected from primary human macrophages were diluted 1 in 2 in assay diluent. Individual bead populations were mixed (25 μL/sample) and added to standards and samples, which were then incubated with detection reagent (2 h, RT), protected from light. Samples were then centrifuged (400 x g, 5 min, RT,

Eppendorf 5415D) to pellet beads and any unbound analytes and supernatants were washed away. Samples were resuspended (300 μL) and analysed on the LSRII Flow Cytometer (BD Bioscience, USA) by Dr. A. Hutchinson or M. Lund. The cells were analysed with the following channels: excitation laser 488 nm, emission filters 488/10 nm for forward scatter (FSC) and side scatter (SSC), 530/30 nm for the detection of fluoroscein isothiocyanate (FITC), 575/26 nm for the detection of phycoerythrin (PE) and 670/14 for the detection of bead populations. Generally, 1800 events were acquired for each sample. A gate (R1) was placed on singlet bead populations using the supplied Cytometer Setup Beads tube A and events within R1 were further analysed according to fluorescence intensity. Each bead population has distinct fluorescence intensity that is resolved in the red channel, allowing for the separation of bead populations according to the individual cytokines bound. Quantitation of each cytokine is based on the presence of the phycoerythrin-labelled fluorescence detector antibody. Data was exported as FCS2 files from the FACSDiva software version 6.1.3 (BD Biosciences, USA) and imported into CellQuest Pro version 6.0 (BD Biosciences, USA) for analysis. A standard curve was constructed using the mean fluorescence intensities of each standard analysed, and concentrations of unknowns were then determined by non-linear regression using Graphpad Prism 5 software version 5.02 (GraphPad software, USA).

2.7 MICROSCOPY

2.7.1 PREPARATION AND STAINING OF PRIMARY HUMAN MACROPHAGES FOR CONFOCAL MICROSCOPY

Once isolated, primary human monocytes were cultured in IMDM with 2% (v/v) heat inactivated human serum to stimulate differentiation into macrophages. For visualisation of cells using confocal microscopy 0.5-1x10^6 cells were cultured in 35mm diameter dishes, which had a 23mm diameter indentation (World Precision Instruments Inc, USA). Cells matured over a period of 5-6 days and, prior to stimulation, media was replaced with fresh IMDM. Cells were treated with 10 μg/mL FhCL1 or the same volume of PBS for varying time periods, prior to fixation.

Cells were washed with 2 mL warm PBS (37 °C) for 1-5 min before fixation with 1 mL ice cold 4% (v/v) paraformaldehyde (Sigma-Aldrich, USA) for 30 min (RT). Following incubation with 4% (v/v) paraformaldehyde, cells were washed three times with PBS

(1-2 mL) (RT, 1-5 min). Samples were then blocked and stained or were stored in PBS at 4 °C sealed in parafilm, to prevent dehydration, until required. Samples were permeabilised with 0.1% Triton X (Sigma-Aldrich, USA) (2 mL) for 1 min. Cells were then washed three times (1-2 mL) with PBS (RT, 5 min), with all subsequent wash steps following this method. Excess aldehyde from fixation steps was quenched with 100 mM glycine (Amresco, USA) in PBS (2 mL, 5 min) and cells were washed in PBS. Samples were blocked overnight (O/N) (4 °C) on a rocking platform, with blocking buffer containing 2% FBS (Life Technologies, USA) and 0.1% Tween 20 (Sigma-Aldrich, USA) in PBS (2 mL). Samples were kept in the dark during incubations and washes following the addition of fluorescently conjugated primary or secondary antibodies. Incubation with primary antibodies was carried out (Table 2.4) (1 h, RT) on a rocking platform and samples were washed with PBS to remove excess antibody. Cells were then incubated (1 h, RT on a rocking platform) with Alexa Fluor (AF)-488 conjugated and AF568 conjugated secondary antibodies (Molecular Probes/Life Technologies, USA) (Table 2.4) (2 μg/mL) and then samples were washed with PBS. Where stated, cells were also stained with Phalloidin (Life Technologies, USA) for F-actin filaments (30 min, 2.6 Units/mL) and/or 4'6-diamidino-2-phenylindole (DAPI) (15 min, 300 nmol, Life Technologies, USA) for nuclei (Table 2.4). Samples were stored in PBS until imaged.

2.7.2 FLUORESCENCE LABELLING OF FHCL1

To determine the localisation of FhCL1 within primary human macrophages using confocal microscopy (Section 2.7.5), FhCL1 was conjugated to FITC (Life Technologies, USA) following the manufacturer's instructions. Briefly, this involved incubating FITC conjugate (20 μL per mL of protein) with FhCL1 O/N at 4 °C on a rotating wheel. Following FITC conjugation, excess unconjugated FITC was removed using the Vivaspin 20 mL Concentrator (Viva Science, Germany) (5,000 molecular weight cut off polyether sulfone). Prior to adding the sample to the column, the integrity of the membrane was assessed by centrifugation of 1xPBS (3220 x g, 5 min, RT, Eppendorf 5810R). FITC-conjugated FhCL1 (1 mL) was added into the upper chamber and made up to a volume of 10 mL with 1xPBS. Centrifugation (3220 x g, 30 min, RT, Eppendorf 5810R) was carried out until the upper chamber had 1 mL remaining. After removing the flow-through following centrifugation, the upper

Table 2.4: Antibodies and stains used for confocal microscopy experiments.

	Ig Species	Clone name	Concentration or Dilution [1]	Supplier
Primary antibodies				
TLR4	Mouse mAb	76B357.1	1.25 μg/mL	Abcam
TLR3	Mouse mAb	40C1285.6	1.25 μg/mL	Abcam
EEA-1	Rabbit polyclonal	-	200 ng/mL	Abcam
CD14 Pacific Blue	Mouse mAb	TüK4	5 μL per 10^6 cells	Life Technologies
α-tubulin	Mouse mAb	B-5-1-2	500 ng/mL	Life Technologies
α-tubulin	Rabbit mAb	EP1332Y	1:100	Abcam
IgG1	Mouse mAb	MopC-21	250 ng/mL	Sigma
Dynamin 1	Mouse mAb	D5	5 μg/mL	Abcam
Clathrin	Mouse mAb	X22	12 μg/mL	Abcam
Secondary antibodies				
AF488 anti-Mouse IgG	Goat		2 μg/mL	Life Technologies
AF568 anti-Rabbit IgG	Goat		2 μg/mL	Life Technologies
Stains and Probes				
Lysotracker Red DND-99			100nM	Life Technologies
AF568 Phalloidin			2.6 Units/mL	Life Technologies
AF647 Phalloidin			2.6 Units/mL	Life Technologies
DAPI			300 nmol	Life Technologies

[1] Concentrations provided where available, dilutions given where concentration was not defined for the product

chamber was topped up to 10 mL with 1x PBS and the process was repeated a total of 4 times to ensure 99.99% buffer exchange. Following the final wash, the sample in the upper chamber was reduced to between 0.75-1 mL depending on the desired final concentration.

To determine the concentration of the protein, the absorbance of an aliquot of the sample was measured at 280 nm, the absorbance maxima of protein; and 494 nm, the maximum absorbance of FITC (A_{max}). Based on the absorbance (A) values, the concentration of protein was calculated as follows:

$A_{protein}=A_{280}-A_{max}$ (CF) where the correction factor (CF) = 0.3

Assuming $1.4xA_{protein}$ units = 1 mg/mL

Concentration of protein (mg/mL) = $1.4xA_{protein}$

The degree of labelling can be determined as follows:

Degree of labelling= A_{max} x MW/[Protein] x ε

Where MW is the molecular weight of FhCL1 (24 kilo Daltons (kDa)) and ε is the extinction co-efficient of FITC (68,000 $Lmol^{-1}$ cm^{-1}).

2.7.3 FLUORESCENCE LABELLING OF LPS

To track the movement of LPS within macrophages, LPS (Sigma-Aldrich, USA) was conjugated to Cyano 5 (Cy5) Maleimide Mono-Reactive dye (GE Healthcare, Sweden) following the manufacturer's instructions. Briefly, this involved adding 50 μL of anhydrous dimethylformamide to one pack of dye. Dye solution (50 μL) was then added to LPS (1 mL) and mixed thoroughly. The mixture was incubated at RT for 2 h, with additional mixing every 30 min. The reaction was then left O/N at 4 °C. Following Cy5 conjugation, excess unconjugated Cy5 was removed using the Vivaspin 20 mL Concentrator (Viva Science, Germany) (5,000 molecular weight cut off), as per the method used for FITC-labelled FhCL1 (Section 2.7.2).

2.7.4 LYSOTRACKER STAINING

To determine if FhCL1 localised to lysosomes, cells were labelled with an acidic organelle-selective probe, LysoTracker Red DND-99 (Life Technologies, USA). Primary human macrophages, cultured in fluorodishes (Section 2.7.1), were washed and then stained with media (1 mL) containing LysoTracker DND-99 diluted to a 100 nM concentration (1 h, 37 °C), prior to fixation.

2.7.5 CONFOCAL IMAGING OF PRIMARY CELLS

Following staining with antibodies, fluorescent stains, probes or labelled proteins, cells were examined using a Nikon A1 confocal scanning laser microscope and camera with a Nikon Plan APO VC 100x 1.4 numerical aperture oil objective. Kohler illumination was established prior to imaging and settings depended on the fluorophores used. Cells were mounted in Fluorodish cell culture dishes (World Precision Instruments Inc, USA) with p-phenylenediamine (1 μg/mL; Sigma-Aldrich, USA) diluted in glycerol (90%; Amresco, USA). The samples were excited using combinations of up to four solid state lasers: 405 nm, 488 nm, 561 nm and 640 nm. Images were pseudo coloured and

analysed using NIS Elements software version 3.22.11 (Nikon). Area densitometry and measurements were performed using Image J software version 1.6.0_20 (NIH).

2.7.5.1 LIVE CELL IMAGING

In order to track the movement of fluorescently labelled proteins within macrophages over time, live cell imaging was performed. The sample chamber and the stage of the Nikon A1 confocal microscope were heated to 37 °C to produce optimal conditions for live cell imaging. Culture media was removed and replaced with PBS. Once the fluorodish was positioned correctly, the position focusing system was engaged to prevent focus drift during imaging. 200 ng/mL Cy5 labelled LPS (Section 2.7.3) was added to the culture and imaging initiated. Single images were taken every 2 min, for a period of 2 h, which allowed the movement of fluorescently conjugated proteins to be tracked within cells.

2.7.5.2 HIGH RESOLUTION IMAGING USING THE DELTAVISION OMX MICROSCOPE

In order to achieve a greater level of detail of the localisation of intracellular structures following staining with antibodies, macrophages were examined using a DeltaVision OMX (optical microscope experimental) 3D-SIM deconvolution microscope (Applied Precision, Inc, USA.). Cells were mounted in VectaShield anti-fade mounting medium. The samples were excited using solid state 488 nm and 598 nm lasers providing wide-field illumination. All data capture used emission filters of 500 to 550 nm and 608 to 648 nm, with a 100x 1.4-numerical aperture oil objective and multichannel simultaneous-imaging capability using two Photometrics Cascade (Photometrics, USA) back illuminated cameras (electron-multiplying charge-coupled device cameras; >90% quantum efficiency; 512 by 512 pixels). 3D-SIM images were sectioned using a 125 nm Z-step size. Imaging was performed by Lynne Turnbull (i3 Institute, UTS). All images were analysed using IMARIS software version 7.0.0 (Bitplane Scientific, Switzerland).

2.7.5.3 QUANTITATIVE DETERMINATION OF INTRACELLULAR PROTEIN EXPRESSION

After staining fixed human monocyte-derived macrophages with fluorescently labelled antibodies to CD14, TLR4, TLR3 and early endosome antigen (EEA)-1 or incubating

macrophages with Cy5 labelled LPS, cells were imaged by confocal microscopy (Section 2.7.5). Quantitative determination of fluorescence intensity levels was performed using Image J software (NIH) on images produced by confocal microscopy. For the analysis of intracellular CD14 levels, regions of interest within the images were defined for analysis of cells bodies by freehand tracing of every complete cell body in every field of view imaged (ranging from 4-6 fields of view for each treatment group). The averaged mean fluorescence intensity (MFI) was calculated for the AF408 channel to measure CD14 intensity within cell bodies. The MFI was averaged for all cell bodies in each treatment group and compared by a Wilcoxin matched pairs non-parametric t-test using GraphPad Prism version 5.02 for Windows (GraphPad software, San Diego California, USA) (Section 2.9).

Quantitative determination of the uptake of LPS by PBS-treated and FhCL1-treated macrophages over a 2 h period was determined using Image J software (NIH), by defining regions of interest encompassing the entire macrophage cell body. The MFI was calculated for the Cy5 channel to measure the intensity of Cy5 fluorescence at each time point. This was repeated for all cells within the field of view for three independent experiments. The MFI for each cell was then averaged at each time point to compare the uptake of LPS between treatments.

For the comparison of TLR4, TLR3 and EEA-1 levels in nanotubes and cell bodies of primary human macrophages, regions of interest within the images were defined by freehand tracing of every nanotube with at least one connected cell body in every field of view imaged (ranging from 5-10 fields of view for each treatment group). The MFI was calculated for the AF488 channel to measure TLR4 or TLR3 intensity in separate images and the AF568 channel to measure EEA-1 intensity in the defined nanotube regions. The MFI was then calculated in the defined regions of the corresponding cell body of macrophages. The localisation of each molecule in nanotubes versus the corresponding cell body was then compared by dividing the MFI in nanotubes by the MFI in the cell body to produce a ratio. A ratio of one indicated that there was no difference in localisation of the molecule of interest between the nanotubes and the cell body (i.e. equally distributed in cell bodies and nanotubes) and a ratio above 1 indicated the molecule was localised preferentially to the nanotubes, while a ratio below one indicated the molecule was localised preferentially to the cell body. This analysis was

performed for all pairs of nanotubes and corresponding cell bodies in untreated samples and FhCL1-treated samples, as well as LPS-stimulated cells over a time course (5 min, 15 min, 30 min, 1 h and 6 h) with and without FhCL1 pre-treatment. The ratio of MFI calculated for TLR4, TLR3 and EEA-1 for each nanotube and cell body pair was then averaged for each treatment group to produce an averaged ratio.

2.7.5.4 CALCULATION OF CO-LOCALISATION BY MANDER'S COEFFICIENT

Following confocal imaging, the co-localisation of proteins was analysed using the Coloc tool using IMARIS software version 7.0.0 (Bitplane Scientific, Switzerland). Threshold levels were set for individual fluorescence channels, ensuring that the thresholds were set at a level for which background fluorescence was excluded. Having selected the two channels in which co-localisation were to be assessed, a co-localisation channel was created and channel statistics were calculated. The Mander's coefficient was used to compare co-localisation, with a value of 0 indicating no co-localisation, and a value of 1.0 complete co-localisation. Mander's coefficient A indicates the amount of material A co-localised with material B and Mander's coefficient B indicates the amount of material B co-localised with A.

2.8 PROTEIN ISOLATION AND WESTERN ANALYSIS

2.8.1 ISOLATION OF PROTEIN FOR WESTERN ANALYSIS

Following the treatment of 1 mL cultures of $1x10^6$ primary human macrophages with 20 μg/mL FhCL1, 20 μg/mL FhCL1 with E64 and PBS both with and without 50 ng/mL LPS-stimulation, macrophages were collected by scraping 24 well plates. Cells from multiple individual wells were pooled to increase the yield of protein. Cells were collected by centrifugation (400 x g, 7 min, RT, Eppendorf 5702) and washed twice with ice cold PBS (1 mL) and re-centrifuged (400 x g, 7 min, RT, Eppendorf 5702). The cell pellets were resuspended in 100 μL Radio-immunoprecipitation assay (RIPA) buffer (Sigma-Aldrich, USA) and stored at -80 °C until required. Prior to sodium dodecyl sulphate-polyacrylamide gel electrophoresis (SDS-PAGE), samples were thawed on ice and centrifuged (16,100 x g, 3 min, RT, Eppendorf 5415D) to pellet cell membrane proteins.

2.8.2 ELECTROPHORESIS OF PROTEINS

Protein isolated from cell lysates was combined with 4 µl of 4x NuPAGE LDS (lithium dodecyl sulphate) Sample Buffer and 1 µL 10x NuPAGE Reducing Agent (Life Technologies, USA). Samples were heated at 100 ºC for five minutes to denature proteins, before loading onto NuPAGE 4-12% Bis-Tris Gels (Life Technologies, USA) with 1xNuPAGE MES (2-(*N*-morpholino)ethanesulfonic acid) SDS Running Buffer (Life Technologies, USA). Samples were electrophoresed with 10 µl of Novex Sharp Pre-stained Protein Standards (Life Technologies, USA). Proteins were separated by electrophoresis at 200V for 40 min at RT.

2.8.3 TRANSFER OF PROTEINS TO NITROCELLULOSE MEMBRANE

Following electrophoresis, transfer of separated proteins from the gel to nitrocellulose membrane (Life Technologies, USA) was performed using the iBlot Gel Transfer system (Life Technologies, USA), according to the manufacturer's instructions. After transfer, the membrane was stained for the presence of protein with Ponceau S (Ponceau S 0.1g, trichloroacetic acid 1 g/mL) for 5 min. Staining also confirmed that the transfer of proteins had been successful. Protein bands were visualised and scanned. The membrane was then rinsed with water to clear the background, before being used for western analysis.

2.8.4 WESTERN ANALYSIS

For western analysis, the membrane was initially placed in blocking buffer (Tris buffered saline (TBS) with Tween 20 (Sigma-Aldrich, USA) (1x TBS, 0.01% Tween-20) with 3% BSA (Research Organics, USA)). Membrane blocking was carried out for 1 h at RT (with agitation). Dilutions of primary antibodies were prepared using blocking buffer (Table 2.5) and the membrane was incubated with the appropriate primary antibody O/N at 4 °C. The membrane was then washed in TBS with Tween 20 (3x, 5 min) before the addition of the secondary antibody, goat-anti-rabbit IgG or horse-anti-mouse IgG horseradish peroxidise (HRP)-linked antibodies (Cell Signaling Technology, USA) (1 in 2000 dilution, made up in blocking solution). Binding of the secondary antibodies was carried out for 1 h at RT. The membrane was then washed in TBS with Tween 20 (4x, 5 min). Chemiluminescence detection reagent, Supersignal West Femto maximum sensitivity substrate (1:1) (Thermo Scientific, USA) was added to the

Table 2.5: Antibodies used for western analysis.

Antibody Target	Ig Species	Clone name	Target Protein Size (kDa)	Concentration or Dilution [3]	Supplier
Primary Antibody					
β-Actin	Rabbit mAb	13E5	45	1:1000	Cell Signaling
MyD88	Mouse mAb	1B4	33	290 ng/mL	Abcam
TRAF6	Rabbit mAb	EP591Y	58	1:5000	Abcam
TRIF	Rabbit polyclonal	-	76	400 ng/mL	Abcam
TRAF3	Mouse mAb	-	39	1 μg/mL	Abcam
IkBα	Rabbit mAb	44D4	39	1:1000	Cell Signaling
Phospho-IKBα	Rabbit mAb	14D4	40	1:1000	Cell Signaling
p44/42 MAPK Erk 1/2	Mouse mAb	3A7	42, 44	1:2000	Cell Signaling
Phospho-p44/42 MAPK Erk 1/2	Mouse mAb	E10	42, 44	1:2000	Cell Signaling
Dynamin 1	Mouse mAb	D5	104	5 μg/mL	Abcam
Clathrin	Mouse mAb	X22	180	12 μg/mL	Abcam
α-tubulin	Rabbit mAb	EP1332Y	50.5	1:2000	Abcam
Secondary Antibody					
Mouse IgG, HRP [1]-linked	Horse		-	1:2000	Cell Signaling
Rabbit IgG, HRP-linked	Goat		-	1:2000	Cell Signaling
Mouse IgG, AP [2]-linked	Rabbit		-	1:2000	Sigma-Aldrich

[1] Horseradish peroxidase
[2] Alkaline phosphatase
[3] Concentrations provided where available, dilutions given where concentration was not defined for the product

membrane and the results visualised using the Chemidoc Illumination System (Bio-Rad, USA) using Quantity One software version 4.6.9 (Bio-Rad, USA). Visualisation was conducted for a total of 3 min with a total of 10 images being captured with exposure time beginning at 10 s. β-actin was used as a protein loading control and β-actin blots were probed with rabbit anti-mouse IgG alkaline phosphatase-linked secondary antibodies (Sigma-Aldrich, USA) (1 in 2000 dilution, made up in blocking solution) (1 h, RT). The signal was developed using Sigmafast BCIP/NBT (5-bromo-4-chloro-1H-indol-3-yl dihydrogen phosphate/nitroblue tetrazolium chloride) tablets (Sigma-Aldrich, USA), with one tablet being dissolved in 10 mL deionised water. Once colour developed, blots were washed in deionised water to stop the reaction.

Densitometry was carried out on the developed images using Image J software (NIH) and the methodology of McLean (2011). The density of each protein band was determined by creating rectangles wide enough to cover the largest band within a lane, but not overlapping with a band in the next lane, and with the maximum height possible that did not include any other bands. After selecting this area in the first lane, the same rectangle was used in the next lane and selected, until all lanes were chosen (Figure 2.1). Lane profiles were plotted and a straight horizontal line drawn, using the line tool, to exclude gel background. A vertical line was then drawn from the top of the curve down to the horizontal line (Figure 2.1). The area under the curve was then calculated by clicking inside the left or right side of the curve using the wand tool. The same side of the curve was selected for all bands on the one gel taking into account whether the bands were symmetrical or whether one side better represented the band intensity (Figure 2.1). The area under the curve for β-actin was examined to determine whether there were loading differences. A ratio of the area under the curve for all proteins of interest was then created by dividing the area under the curve for each treatment group by the area under the curve for PBS-treated cells. Therefore, expression of proteins in PBS-treated macrophages had a baseline fold change of 1.0 and the expression of the same proteins in all other treatment groups were expressed as a fold change relative to PBS-treated macrophages.

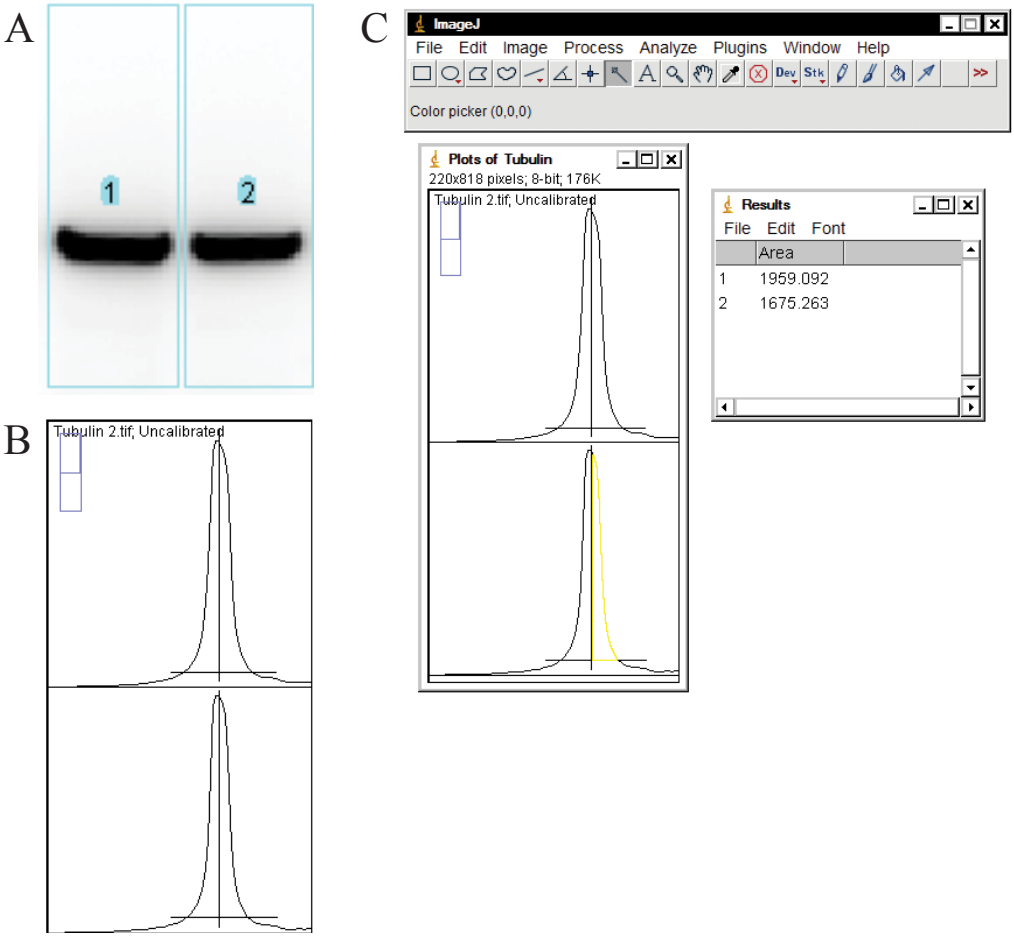

Figure 2.1: Performing densitometry to estimate protein expression changes using Image J.
Densitometry was performed on nitrocellulose membranes visualised by chemiluminescence or colourimetric detection using Image J software (NIH). A) Rectangles were drawn around bands. B) Lane profiles were plotted and a straight horizontal line was drawn above the background fluorescence and a vertical line from the top of the curve was drawn to cut the peak in half. C) The area under the curve was calculated on the left or right side of the peak using the wand tool, keeping the side of the peak consistent for all lanes within the gel.

2.9 STATISTICAL ANALYSIS

When comparing 2 treatments, statistical significance was determined using a Wilcoxin matched pairs non-parametric t-test, where a p value ≤ 0.05 indicated statistical significance. When comparing a single treatment group to a theoretical mean of 1.0, statistical significance was determined using a Wilcoxin one-sampled t test where a p value of ≤ 0.05 indicated statistical significance. The Wilcoxin t-test is a non-parametric test used to compare two related samples to compare whether their population mean ranks differ. When comparing a single group to a theoretical mean of 1.0 in the case of unrelated samples, such as the localisation of molecules within pairs of nanotubes and cell bodies, statistical significance was determined using a one-sampled t test where a p value of ≤ 0.05 indicated statistical significance. Statistical analysis was carried out using GraphPad Prism version 5.02 for Windows (GraphPad software, USA).

CHAPTER 3:

IMMUNE MODULATION BY FHCL1 IN HUMAN MACROPHAGES

3.1 INTRODUCTION

The excretory/secretory products of *F. hepatica* (FhES) has been shown to mimic the effects of parasite infection, with induction of alternative macrophage activation and Th2/regulatory T cell responses (Okano *et al.* 1999; Holland *et al.* 2000; O'Neill *et al.* 2000; Donnelly *et al.* 2005). The FhES therefore represents an alternative to active helminth infection therapy as a potential treatment for inflammatory and autoimmune diseases. In order for helminth products to be considered for any kind of therapeutic use, the precise immune-modulatory effect of individual FhES products, and combinations thereof, requires elucidation. Fractionation of FhES by SDS-PAGE has revealed that, compared to the ES products of other helminth species, such as *S. mansoni* (Everts *et al.* 2009), FhES is a relatively simple mixture of components (Figure 1.6). Furthermore, high performance liquid chromatography separated the FhES mixture into two major peaks (Donnelly *et al.* 2008). Mass spectrometry revealed that the first peak was composed predominately of peroxiredoxin (Prx) (Donnelly *et al.* 2005) and a defensin-like molecule termed helminth defence molecule (HDM)-1 (Robinson *et al.* 2011b), while the second peak contained mainly cathepsin L1 (FhCL1) (Collins *et al.* 2004). To determine whether parasite-secreted molecules have therapeutic potential, specific immune-modulatory molecule(s) must be identified and their mechanisms of action defined within human cells. Recombinant forms of the excreted molecules from *F. hepatica* have been prepared for study in our laboratory. The immune-modulatory effects of these key molecules have been investigated in antigen presenting cells (APCs), with Prx inducing alternative activation of murine macrophages (Donnelly *et al.* 2005) and HDM-1 inhibiting antigen processing and presentation in human macrophages by inhibiting the acidification of endolysosomes (Robinson *et al.* 2012). In contrast, studies examining the effect of FhCL1 on murine macrophages, found that FhCL1 did not induce alternative macrophage activation (Donnelly *et al.* 2008). Instead, degradation of Toll-like receptor (TLR)-3 was observed, which was associated with down-regulation of inflammatory mediators such as nitric oxide (NO), IL-6, TNF and IL-12 in response to LPS stimulation (Donnelly *et al.* 2010). FhCL1 also provided protection against the development of septic shock in response to a lethal dose of LPS in mice (Donnelly *et al.* 2010).

Given that FhCL1 modulated Toll-interleukin-1 receptor (TIR)-domain-containing adaptor-inducing interferon-β (TRIF)-dependent, TLR3 signalling in response to LPS-stimulation in murine macrophages, the effect of FhCL1 on TLR signalling in human monocyte-derived macrophages was investigated. LPS complexes with LPS binding protein (LBP), which associates with CD14 and TLR4 at the surface of cells to initiate cell signalling. Beneath the cell surface TLR4 signalling is mediated by the Myeloid differentiation primary response gene 88 (MyD88)-dependent pathway and associated with Toll-interleukin 1 receptor-domain containing adaptor protein (TIRAP) (MyD88 adaptor-like protein) (Kagan *et al.* 2006; Kagan *et al.* 2008). Tumour necrosis factor receptor-associated factor (TRAF)-6 (Gohda *et al.* 2004) and interleukin 1 receptor-associated kinase (IRAK)-1, -2 and -4 are then activated (Hacker *et al.* 2006), and initiate signalling through transforming-growth factor-β-activated kinase (TAK1) (Takaesu *et al.* 2003), resulting in the early activation of transcription factors nuclear factor-κB (NF-κB) and activating protein (AP)-1, resulting in the production of pro-inflammatory cytokines, IL-1β, IL-6, IL-12 and TNF (for a review see Akira *et al.* 2004) (summarised in Figure 3.1).

Once the TLR4/LPS complex is endocytosed, intracellular signalling occurs through recruitment of TRIF and TRIF-related adaptor molecule (TRAM) (Kagan *et al.* 2008; Watts 2008; Chaturvedi *et al.* 2009). This complex further recruits TRAF3 and ultimately results in activation of the transcription factor interferon regulatory factor (IRF)-3, stimulating production of type 1 interferons (IFN), such as IFN-β and the anti-inflammatory cytokine IL-10 (Sato *et al.* 2003; Yamamoto *et al.* 2003; Akira *et al.* 2004; Chang *et al.* 2007; Iyer *et al.* 2010) (summarised in Figure 3.1). MyD88-independent, TRIF-dependent signalling also initiates late activation of NF-κB and thus expression of pro-inflammatory cytokines through the recruitment of TRAF6 (Kawai *et al.* 2007). The maturation of endosomes into lysosomes results in degradation of the TRIF/myeloid differentiation protein-2 (MD-2) complex, causing cessation of TLR cell signalling (Saitoh 2009). Unlike TLR4, TLR3 does not utilise the MyD88-dependent signalling pathway. Instead the endosomally located TLR3 only signals through the TRIF-dependent pathway (Akira *et al.* 2004).

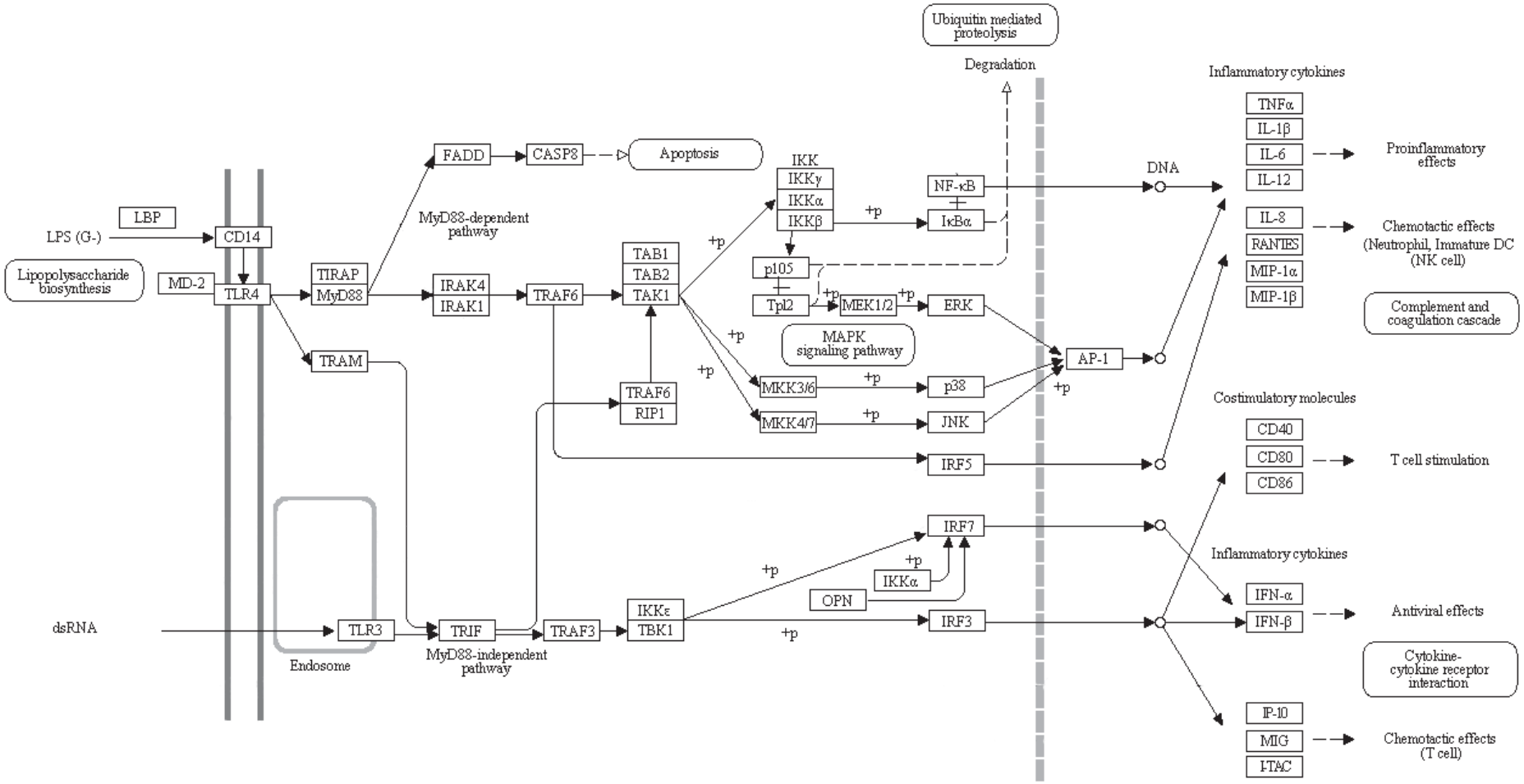

Figure 3.1: Toll-like receptor signalling pathways.
Bacterial LPS binds to LPS-binding protein (LBP) which binds to CD14. The CD14/LPS complex binds to TLR4, resulting in recruitment of Toll-interleukin-1 receptor domain containing adaptor protein (TIRAP) and signals through the MyD88-dependent pathway, initiating the expression of pro-inflammatory cytokines. Once endocytosed, TLR3 and TLR4 recruit TRIF and signal through the MyD88-independent pathway, initiating expression of co-stimulatory molecules and inflammatory cytokines, including IFN-β. (Adapted from KEGG pathway 2010).

The effect of FhCL1 on human innate immune cells was investigated concurrently on human monocyte-derived DCs (M. Lund, unpublished). Treatment with FhCL1 had been found to induce partial maturation of monocyte-derived DCs, with no changes in expression of CD80, CD83, CD86 and human leukocyte antigen-D receptor (HLA-DR) (M. Lund, unpublished). Similar results were observed in bone marrow-derived murine DCs, with up-regulation of CD40, but no change in CD80, CD86 or major histocompatibility complex (MHC)-II (Dowling *et al.* 2010). Therefore, results to date indicated that FhCL1 treatment did not alter the maturation of DCs with respect to antigen presenting and T cell co-stimulatory molecules. Furthermore, cytokine protein expression profiles of *in vitro* FhCL1-treated human monocyte-derived DCs showed that there was no change in the expression of IL-1β, IL-12, IL-8, IL-6, TNF and IL-10 (M. Lund, unpublished). However, it is known that FhCL1 treatment alters the cytokine profile of murine DCs, reducing the production of IL-17 and IL-23, while increasing the expression of IL-6, IL-12 and macrophage inflammatory protein 1 and 2 in a TLR4-dependent manner (Dowling *et al.* 2010). This suggests that the effects of FhCL1 on DCs is potentially species-specific or differs between different types of DCs, and highlights the possibility that the effect of FhCL1 on human monocyte-derived macrophages may differ to that observed in murine peritoneal macrophages.

3.1.1 SPECIFIC AIM

Collectively, the ES products of *F. hepatica* induce an alternatively activated macrophage phenotype and drive Th2/regulatory T cell responses in mice (Donnelly *et al.* 2008). However, murine studies have shown that recombinant FhCL1 does not induce an ‘alternative macrophage activation’ phenotype (Donnelly *et al.* 2008), but instead it modulates the TRIF-dependent signalling pathway through degradation of TLR3, and down-regulates expression of IL-6, IL-12, TNF and NO when stimulated with LPS (Donnelly *et al.* 2010). This study therefore aims to determine the effect of FhCL1 on primary human monocyte-derived macrophages with respect to TLR signalling, cell phenotype and inflammatory cytokine responses.

3.2 RESULTS

3.2.1 ISOLATION OF MONOCYTES FROM WHOLE HUMAN BLOOD

F. hepatica ES protein FhCL1 has previously been shown to modulate cell signalling in murine peritoneal macrophages (Donnelly *et al.* 2010). This led to the question as to whether FhCL1 modulated immune responses in human monocyte-derived macrophages by a similar mechanism. To address this possibility, human peripheral blood was obtained and cultured as a source of *in vitro*-derived monocyte-derived human macrophages. For this, peripheral blood mononuclear cells were purified by Ficoll density gradient centrifugation from whole human blood, followed by 'positive selection' with anti-$CD14^+$ magnetic beads. To confirm the extent of monocyte enrichment, cell populations were analysed by flow cytometry, pre- and post- $CD14^+$ enrichment (Figure 3.2). Following $CD14^+$ enrichment, FACS analysis showed a cell population with increased size and granularity (increased forward (FSC-A) and side scatter (SSC-A)), indicative of a monocytic population. Gating on monocytes (events), demonstrated an increased percentage of $CD14^+$ cells (89%) with increased size and granularity, compared to only 9% from the pre-enriched cell population (Figure 3.2). This represents a nearly 10-fold enrichment of $CD14^+$ monocytes. $CD14^+$ monocytes were cultured for a period of 5-6 days to allow for maturation of monocytes into macrophages. During this process, the cell phenotype changed from a non-adherent to an adherent cell phenotype, allowing selection of the macrophage population. Monocytes do not express CD206 (Pilling *et al.* 2009), however CD206 is expressed on the surface of a subset of macrophages identified as alternatively activated (Porcheray *et al.* 2005). Therefore, to confirm maturation of the $CD14^+$ cell population, differentiated cells were stained with anti-CD206 after 6 days, and were analysed by flow cytometry together with undifferentiated monocytes cultured for 6 days in RPMI media in the absence of human serum. FACS analysis indicated an increase in CD206 expression in differentiated cells compared to undifferentiated cells, which had similar levels of fluorescence to unstained cells (Figure 3.3). Thus, the increased surface expression of CD206 in 6 day-differentiated cells is indicative of maturation of monocyte-derived macrophages.

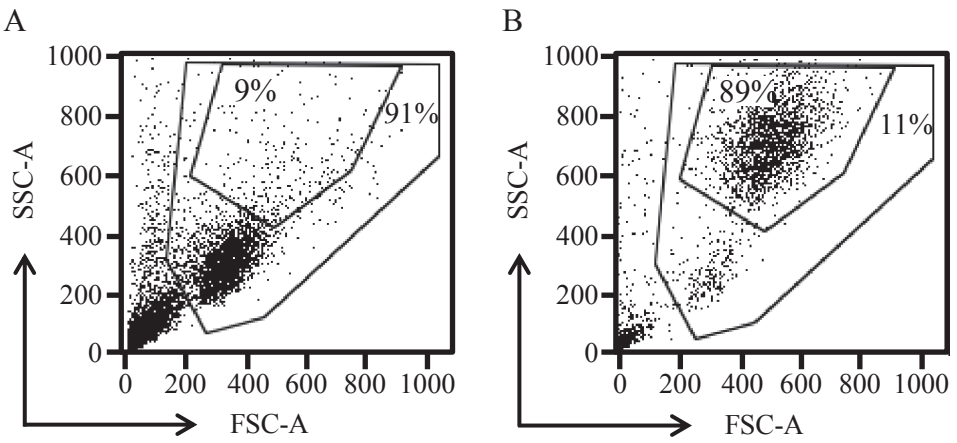

Figure 3.2: Isolation and enrichment of monocytes from peripheral blood mononuclear cells pre- and post- CD14$^+$ selection.
Flow cytometry analyses of monocytes isolated from human peripheral blood mononuclear cells, A) before and B) after CD14$^+$ magnetic bead selection. Data shown are FACS dot plots, gated to determine the relative purity.

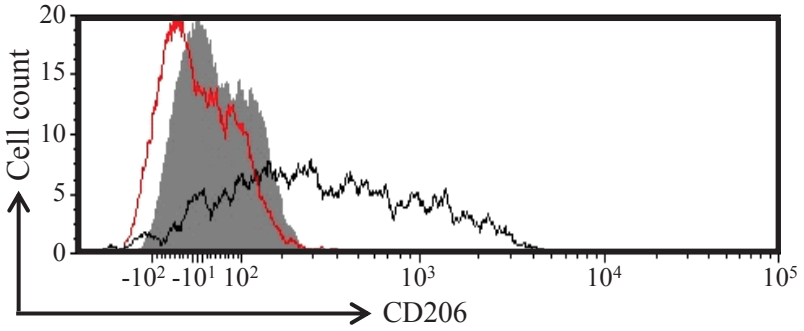

Figure 3.3: Flow cytometry analysis for CD206 surface expression on primary human CD14$^+$ monocyte-derived macrophages.
Data shown are histogram overlays (biexponential scale) for unstained (grey filled histogram) and undifferentiated CD14$^+$ monocytes (red unfilled histogram), compared to day 6, fully differentiated monocyte-derived macrophages (black unfilled histogram).

3.2.2 EFFECT OF FHCL1 TREATMENT ON CYTOKINE EXPRESSION BY PRIMARY HUMAN MACROPHAGES

Generally, helminth parasites modulate the host immune response through the induction of a Th2/regulatory T cell dominated immune response (reviewed in Maizels *et al.* 2004; reviewed in Allen *et al.* 2011). This is accompanied by down-regulation of Th1/Th17 responses. For example, infection with *F. hepatica* results in the rapid induction of a Th2 response, and suppression of Th1 responses, with induction of alternative macrophage activation as early as 4 days post infection (Donnelly *et al.* 2005). In murine studies, FhCL1 was observed to prevent the release of inflammatory mediators, including NO, IL-6, TNF and IL-12, by down-regulating TRIF-dependent cell signalling in macrophages, without inducing alternative activation (Donnelly *et al.* 2010). It was therefore hypothesised that FhCL1 may be able to modulate the expression of inflammatory cytokines in human macrophages. To address this possibility, the effect of FhCL1 on the production of Th1 pro-inflammatory and Th2/regulatory cytokines by primary human macrophages was investigated at both the mRNA and protein levels. To first assess changes in cytokine expression at the mRNA level, oligonucleotide primers were designed to amplify regions of IFN-β, a pro-inflammatory cytokine induced by the TRIF-dependent signalling pathway, and three cytokines which are induced by both the MyD88 and TRIF-dependent signalling pathways, IL-1β, IL-10 and IL-12. The expression of these genes was compared to that of reference or 'housekeeping' gene RPL36AL. Although not a frequently used reference gene, RPL36AL is a reported housekeeping gene (Eisenberg *et al.* 2003) and is expressed in a diverse array of tissues (Su *et al.* 2002).

As these were newly designed primers, RT-qPCRs required optimisation and validation. The annealing temperature of primer pairs was tested and optimised for PCR product yield, and all primers including the reference gene RPL36AL amplified optimally at 61˚C (data not shown). Primer concentration was also optimised to determine the optimal forward and reverse primer concentrations for maximal amplification of each specific cDNA, while limiting the formation of primer dimer. Thus, optimal primer concentrations were those which produced the highest end fluorescence and the lowest threshold cycle (C_t) value. The primer concentrations included a matrix of varying combinations of forward and reverse primer concentrations (9.0, 6.0, 3.0 and 0.5 μM).

Representative results of primer concentration optimisation reaction are shown (Figure 3.4A). Amplification optimisation reactions with varying forward and reverse primer concentrations indicated that the 9.0 μM, 6.0 μM and 3.0 μM concentrations all produced consistent PCR amplification of cDNA. The concentration of primers (forward and reverse) for all sets of primers was therefore selected to be 6.0 μM. Melt curve analysis was also assessed, to confirm single product amplification and the absence of primer dimer (Figure 3.4B). To determine whether amplification was quantitative, RT-PCR was performed on serial 2-fold dilutions of cDNA template, ranging from 5-40ng per reaction. In each case, amplification (amount of PCR product) was reduced with serially-diluted cDNA template concentrations (Figure 3.4C). As expected, there was no amplification in the no cDNA template control. Therefore, primer pairs successfully and quantitatively amplified a single product with no primer dimer for RPL36AL, IL-1β, IL-10 and IFN-β cDNA (Figure 3.4). The amplification of IL-12, however, was not quantitative and failed to amplify cDNA template reproducibly (Figure 3.4). Therefore, IL-12 expression was quantitated only at the protein level.

Macrophages from eight human donors were treated with PBS, 10 μg/mL FhCL1, 10 μg/mL FhCL1 with 10 μM E64 protease inhibitor, or 10 μM E64 alone for 18 h. Following RNA isolation and cDNA synthesis, the expression of IL-1β, IL-10 and IFN-β was quantitated by RT-qPCR. As expected, the no cDNA template did not amplify product. Results showed that treatment with FhCL1 had no significant effect on the levels of IL-1β, IL-10 or IFN-β mRNAs compared to PBS-treated macrophages (Figure 3.5). The protease inhibitor, E64, which reduces the enzymatic activity of FhCL1 (Section 2.2) was included as a control. The presence of 10 μM E64 in the presence or absence of FhCL1 had no significant effect on cytokine mRNA expression (Figure 3.5). In murine macrophages, differences in NO and IL-12 mRNA expression were induced following stimulation with LPS (Donnelly *et al.* 2010). Therefore, FhCL1 pre-treated macrophages were stimulated with 50 ng/mL LPS for 6 h prior to RNA isolation and cDNA synthesis. Stimulation with 50 ng/mL LPS resulted in significant up-regulation of IL-1β, IL-10, and IFN-β mRNA as expected ($p=<0.05$, not shown), albeit to varying degrees for each donor that was tested (Figure 3.5). While the cytokine expression for all three genes was investigated in all (eight) human donors, some donors samples expressed undetectable levels of cytokine mRNA by 40 cycles, and therefore,

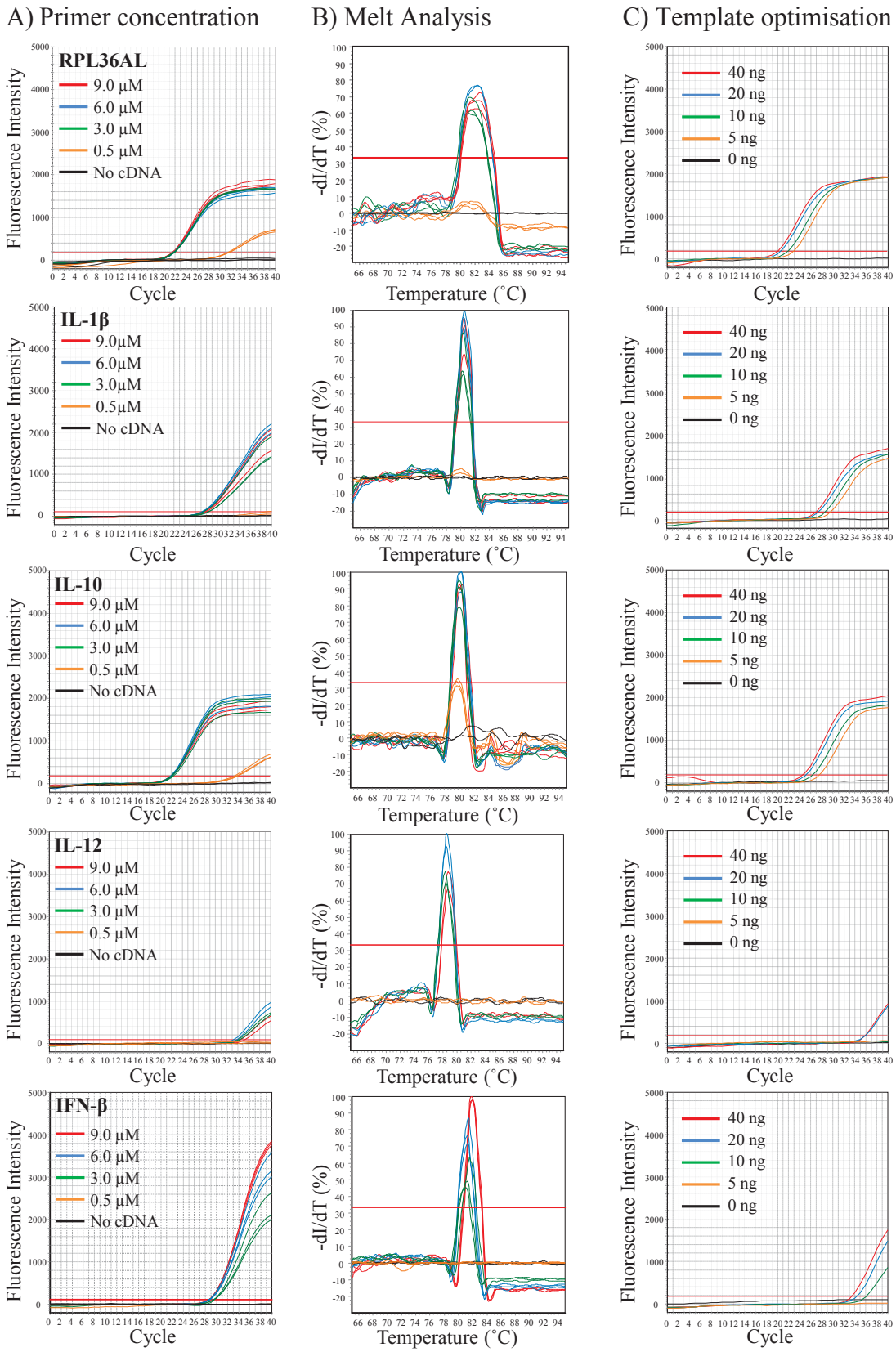

Figure 3.4: Optimisation of RT-qPCR analysis.
A) Optimisation of primer concentration for amplification of reference gene RPL36AL, and cytokines IL-1β, IL-10, IL-12B, and IFN-β cDNAs. The primer combinations included 9.0, 6.0, 3.0 and 0.5 µM for both primers. Data shown are only equal concentrations of forward and reverse primers, in triplicate reactions. B) Melt curve analysis illustrating single PCR product amplification. C) Real time RT-PCR, showing serial 2-fold cDNA template dilution, demonstrating quantitative amplification.

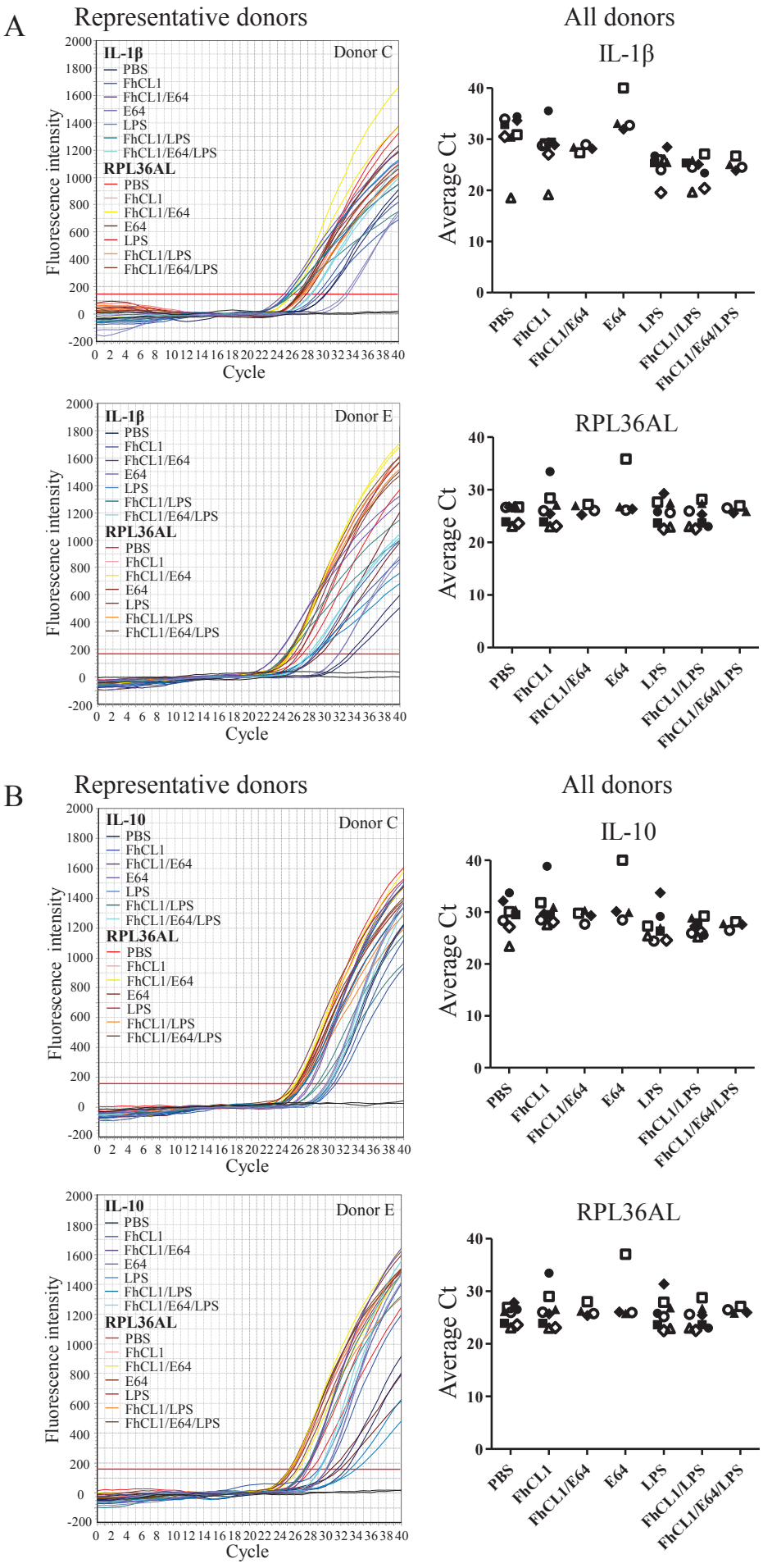
A
Representative donors
All donors
IL-1β
Donor C
IL-1β
PBS
FhCL1
FhCL1/E64
E64
LPS
FhCL1/LPS
FhCL1/E64/LPS
RPL36AL
Fluorescence intensity
Cycle
Average Ct
RPL36AL
Donor E
B
Representative donors
All donors
IL-10
Donor C
IL-10
Donor E

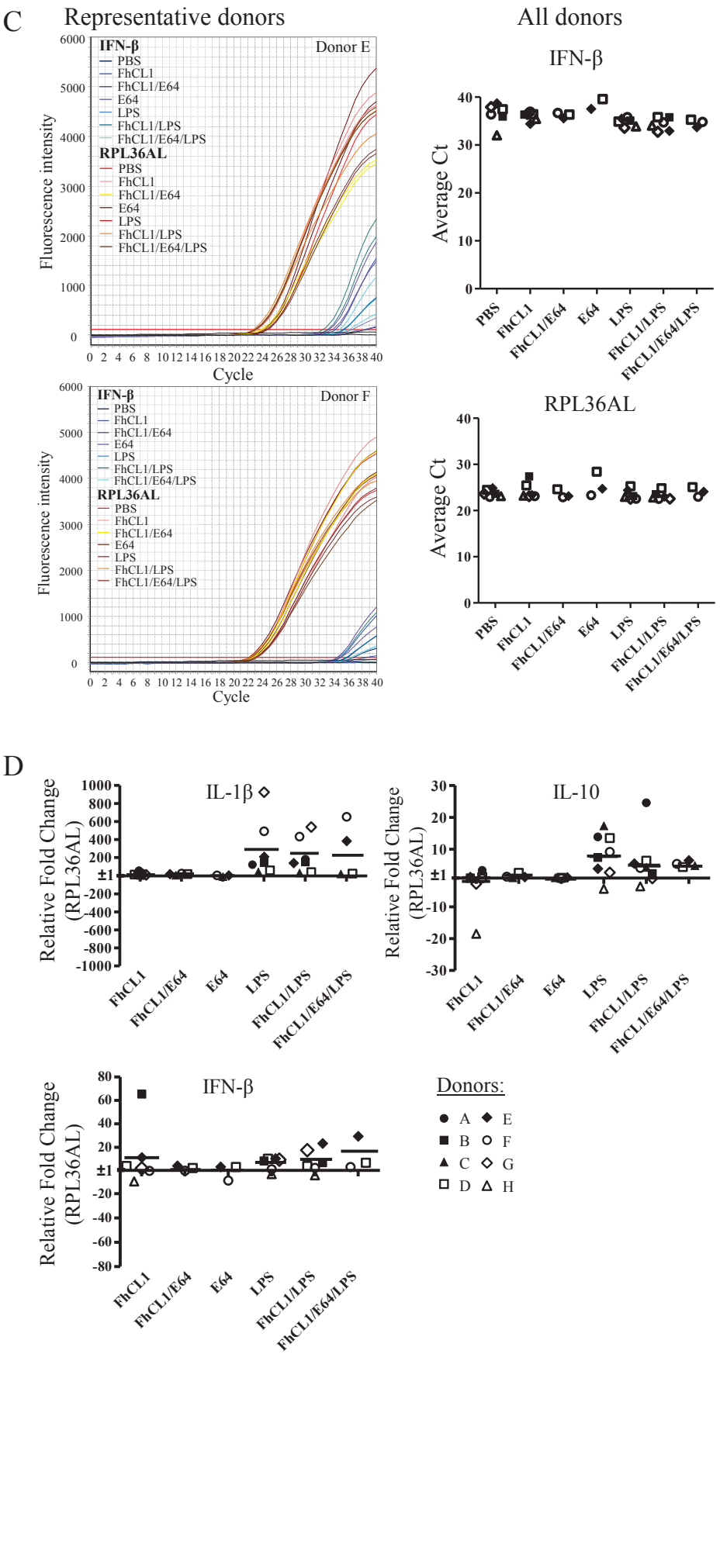
C
Representative donors
All donors
IFN-β
Donor E
Donor F
RPL36AL
PBS
FhCL1
FhCL1/E64
E64
LPS
FhCL1/LPS
FhCL1/E64/LPS
Fluorescence intensity
Cycle
Average Ct
D
IL-1β
IL-10
IFN-β
Relative Fold Change (RPL36AL)
Donors:
A
B
C
D
E
F
G
H

Figure 3.5: Cytokine mRNA expression in primary human macrophages cultured with FhCL1.

Primary human macrophages were cultured with PBS, 10 μg/mL FhCL1, 10 μg/mL FhCL1 with 10 μM protease inhibitor E64, or 10 μM E64, for 18 h, with or without 50 ng/mL LPS for 6 h. Data shown are representative fluorescence intensity RT-qPCR profiles for A) IL-1β, B) IL-10, C) IFN-β and RPL36AL mRNA expression for two representative individual donors. Also shown are the average Ct values for up to eight donors. D) Scatter graphs depict the fold change in cytokine expression relative to the reference gene RPL36AL and compared to the expression in PBS-treated macrophages. Horizontal bars are means from up to 8 donors. Data pairs, LPS to FhCL1/LPS, LPS to FhCL1/E64/LPS and FhCL1/LPS to FhCL1/E64/LPS, were analysed by Wilcoxin matched pairs t-test. Individual treatments, LPS, FhCL1, FhCL1/E64 and E64, were tested by a one sample Wilcoxin t-test to a hypothetical median of 1.0 (representative of PBS-treated samples). No statistically significant differences were observed between any of the data pairs.

these results could not be graphed. Nevertheless, FhCL1 pre-treatment had no significant effect on the mRNA levels of IL-1β, IL-10, and IFN-β following LPS stimulation (Figure 3.5). Thus, while FhCL1 modulated the expression of pro-inflammatory cytokines in response to LPS in murine peritoneal macrophages (Donnelly *et al.* 2010), FhCL1 had no statistically significant effect on pro-inflammatory or anti-inflammatory cytokine mRNA expression in human monocyte-derived macrophages.

Treatment with FhCL1 alone did not alter the level of cytokine expression at the mRNA level in human monocyte-derived macrophages, however, at the protein level, FhCL1 down-regulated NO, IL-6, IL-12 and TNF expression in response to 1 μg/mL bacterial LPS in murine peritoneal macrophages (Donnelly *et al.* 2010). This led to the question as to whether FhCL1 had a similar effect on cytokine expression in human macrophages. To address this possibility, monocyte-derived macrophages from eight human donors were tested. For this, monocyte-derived macrophages were cultured with PBS or 10 μg/mL FhCL1 for 18 h with or without stimulation with 50 ng/mL LPS. Cell supernatants from eight donors were collected 24 h post stimulation and assayed using a cytokine bead array, which included analysis of the pro-inflammatory cytokines, IL-1β, IL-12, IL-6, IL-8 and TNF, and the anti-inflammatory/regulatory cytokine, IL-10. The CBA assay was reported by BD Biosciences to be able to detect cytokine expression above 7.2 pg/mL for IL-1β, 1.9 pg/mL for IL-12, 2.5 pg/mL for IL-6, 3.6 pg/mL for IL-8, 3.7 pg/mL for TNF and 3.3 pg/mL for IL-10. However, as the lowest cytokine standard included in this assay was 20 pg/mL, and hence to be able to determine the concentration of cytokine with confidence, the limit of detection was considered to be 20 pg/mL (Figure 3.6, dotted line). In order to quantitatively determine cytokine expression, a serial dilution of recombinant human cytokine standards was performed for all cytokines assayed, ranging from 20 pg/mL to 5000 pg/mL, and standard curves produced (Appendix 2). In human monocyte-derived macrophages, treatment with PBS or FhCL1 alone resulted in no significant change in expression for any of the cytokines examined (Figure 3.6). As expected, LPS treatment resulted in statistically significant up-regulation of IL-6, IL-8, TNF and IL-10 production (Figure 3.6). Production of IL-12 remained low and relatively unchanged by all treatments (Figure 3.6). In contrast, LPS stimulation led to a significant increase in IL-6 ($p=0.0156$) and IL-8 ($p=0.0391$) in

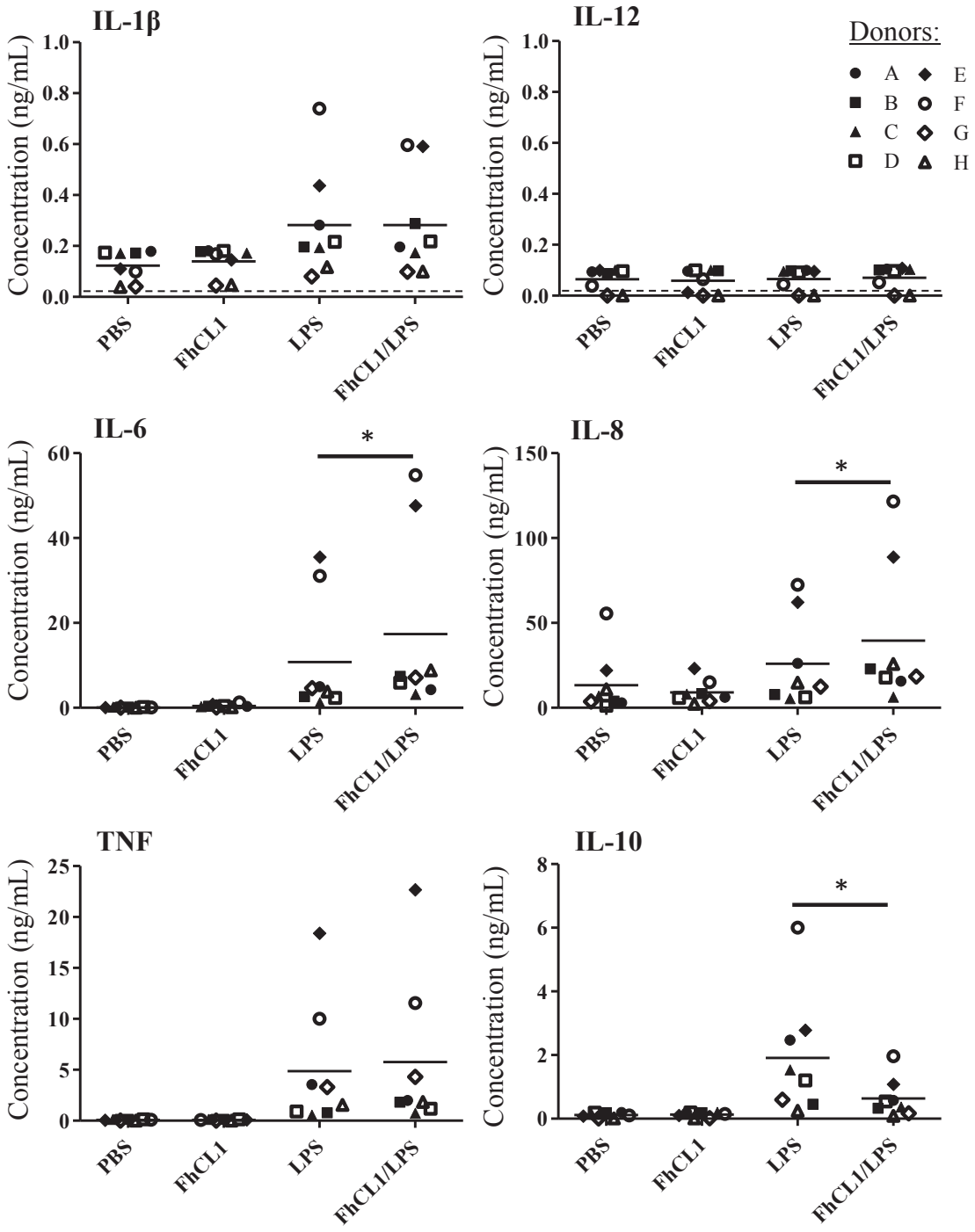

Figure 3.6: Cytokine production from primary human monocyte-derived macrophages treated with FhCL1.

Primary human monocyte-derived macrophages were incubated with PBS or 10 μg/mL FhCL1 for 18 h, and stimulated with 50 ng/mL LPS for 24 h. Production of IL-1β, IL-12, IL-6, IL-8, TNF and IL-10 was assessed by cytometric bead array. Data shown are from eight individual donors, the limit of detection for all cytokines is approximately 20 pg/mL (dashed line). Mean cytokine levels form the eight donors (horizontal lines) are also shown. Data were analysed by Wilcoxin matched pair T-test, and significant differences ($p<0.05$) in cytokine expression between LPS stimulated macrophages in the presence or absence of FhCL1 are as indicated (*).

FhCL1-treated monocyte-derived macrophages compared to LPS stimulated macrophages in the absence of FhCL1 (Figure 3.6). However, pre-treatment with FhCL1 had no significant effect on the production of IL-1β or TNF in response to LPS stimulation (Figure 3.6). Furthermore, results indicated that pre-treatment with FhCL1 resulted in a significant decrease in IL-10 production in macrophages in response to LPS stimulation ($p=0.0078$) (Figure 3.6). Thus, while FhCL1 down-regulated pro-inflammatory cytokines in response to LPS in murine peritoneal macrophages (Donnelly *et al.* 2010), FhCL1 enhanced the production of pro-inflammatory cytokines in human monocyte-derived macrophages, while IL-10 expression was down-regulated by FhCL1 pre-treatment.

3.2.3 EFFECT OF FHCL1 ON CELL SURFACE MARKER EXPRESSION IN PRIMARY HUMAN MACROPHAGES

Treatment with FhCL1 modulates the function of murine macrophages, specifically inhibiting their ability to respond to Th1 stimuli, such as LPS or dsRNA (Donnelly *et al.* 2010). However, analysis of the cytokine profile of human macrophages following FhCL1 treatment showed that FhCL1 increased the production of pro-inflammatory cytokines, while down-regulating production of the anti-inflammatory cytokine IL-10 (Figure 3.6). Given that APCs play an important role in determining the nature of adaptive immune responses, through cell surface receptors, antigen presentation and cytokine secretion (reviewed in Martinez *et al.* 2009), it was hypothesised that, modulation of cell surface marker expression might contribute to FhCL1 modulation of immune responses to a pro-inflammatory stimulus in human macrophages. To investigate this possibility, cell surface proteins associated with macrophage maturation, activation and antigen presentation were investigated by flow cytometry. Monocyte-derived macrophages derived from four human donors were cultured with PBS, 10 μg/mL FhCL1, 10 μg/mL FhCL1 with 10 μM E64 inhibitor or 10 μM E64 alone, for 18 h, to determine the effect of FhCL1 on the phenotype of macrophages. Macrophages were then incubated with fluorescence-conjugated antibodies specific to typical macrophage markers including, markers of alternative activation: mannose receptor CD206 (Stein *et al.* 1992) and haemoglobin scavenger receptor CD163 (Kristiansen *et al.* 2001), T cell activation co-stimulatory marker CD86 (Chen *et al.* 1994), antigen presentation molecule, HLA-DR (Pinet *et al.* 1995), and the co-receptor of LPS, CD14 (Wright *et al.* 1990). However, treatment with FhCL1 had no significant effect on the

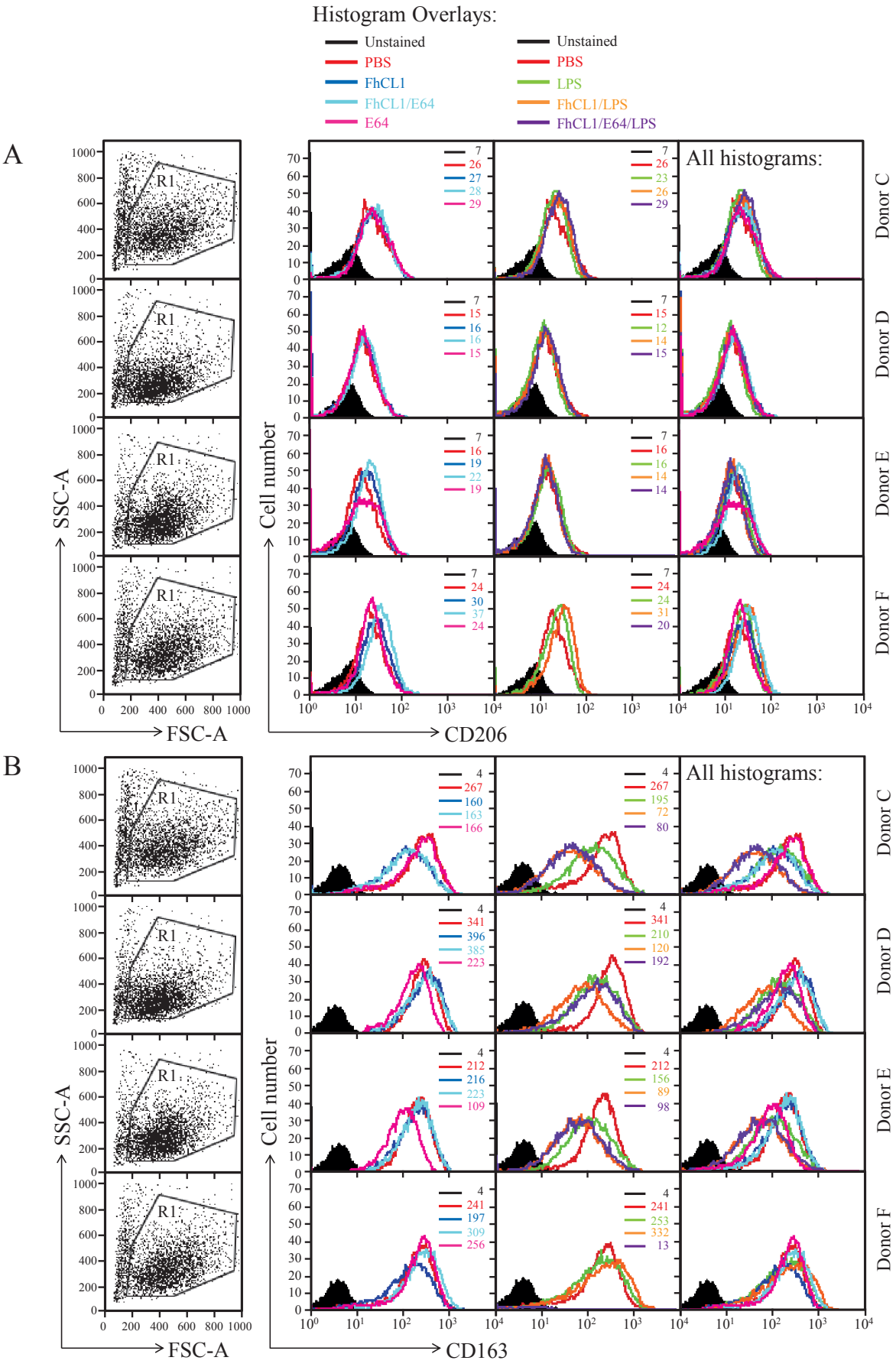
Histogram Overlays:
Unstained
PBS
FhCL1
FhCL1/E64
E64
Unstained
PBS
LPS
FhCL1/LPS
FhCL1/E64/LPS
A
B
R1
SSC-A
FSC-A
Cell number
CD206
CD163
All histograms:
Donor C
Donor D
Donor E
Donor F

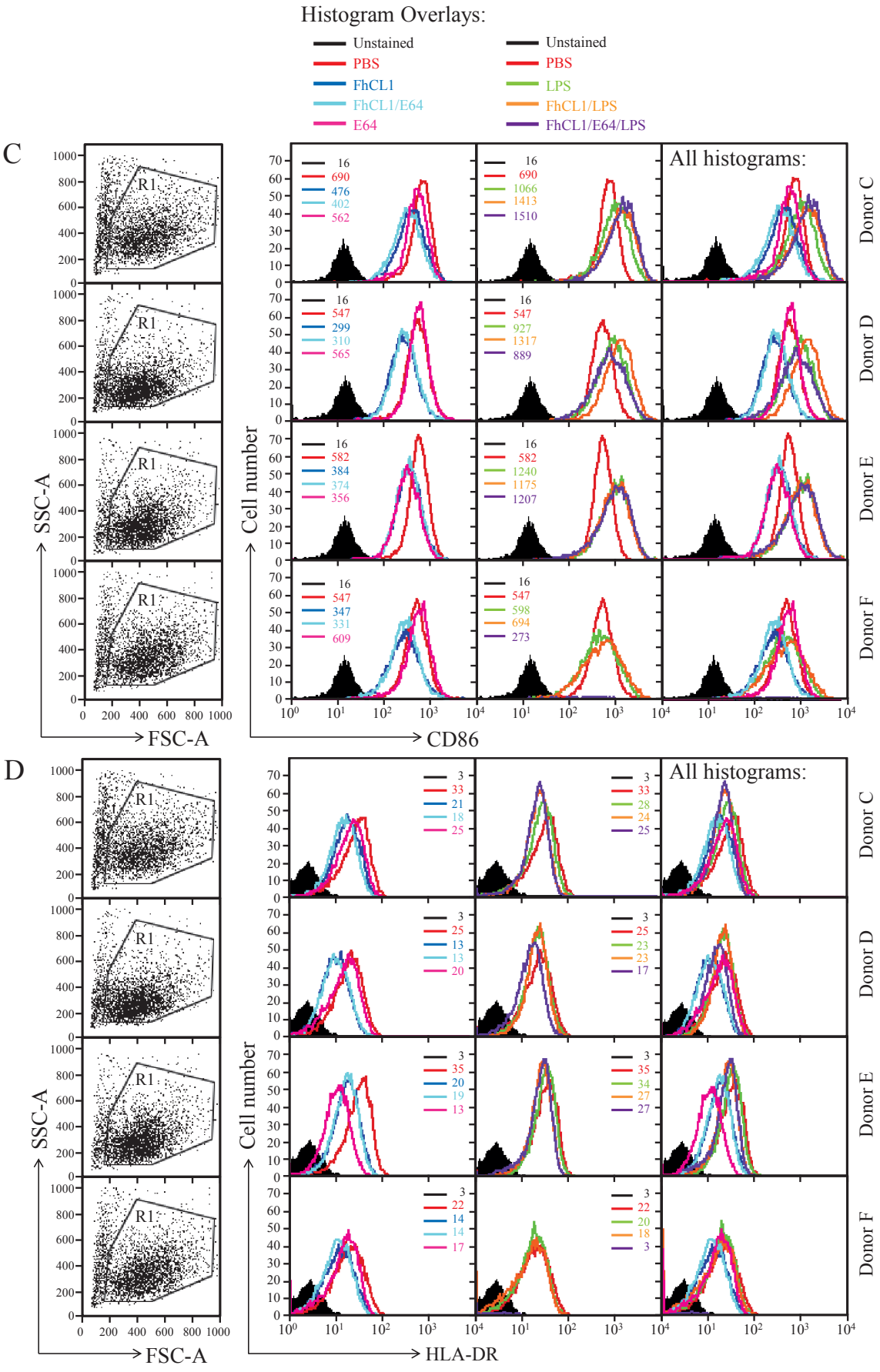
Histogram Overlays:
Unstained
PBS
FhCL1
FhCL1/E64
E64
Unstained
PBS
LPS
FhCL1/LPS
FhCL1/E64/LPS
C
D
R1
SSC-A
FSC-A
Cell number
CD86
HLA-DR
All histograms:
Donor C
Donor D
Donor E
Donor F

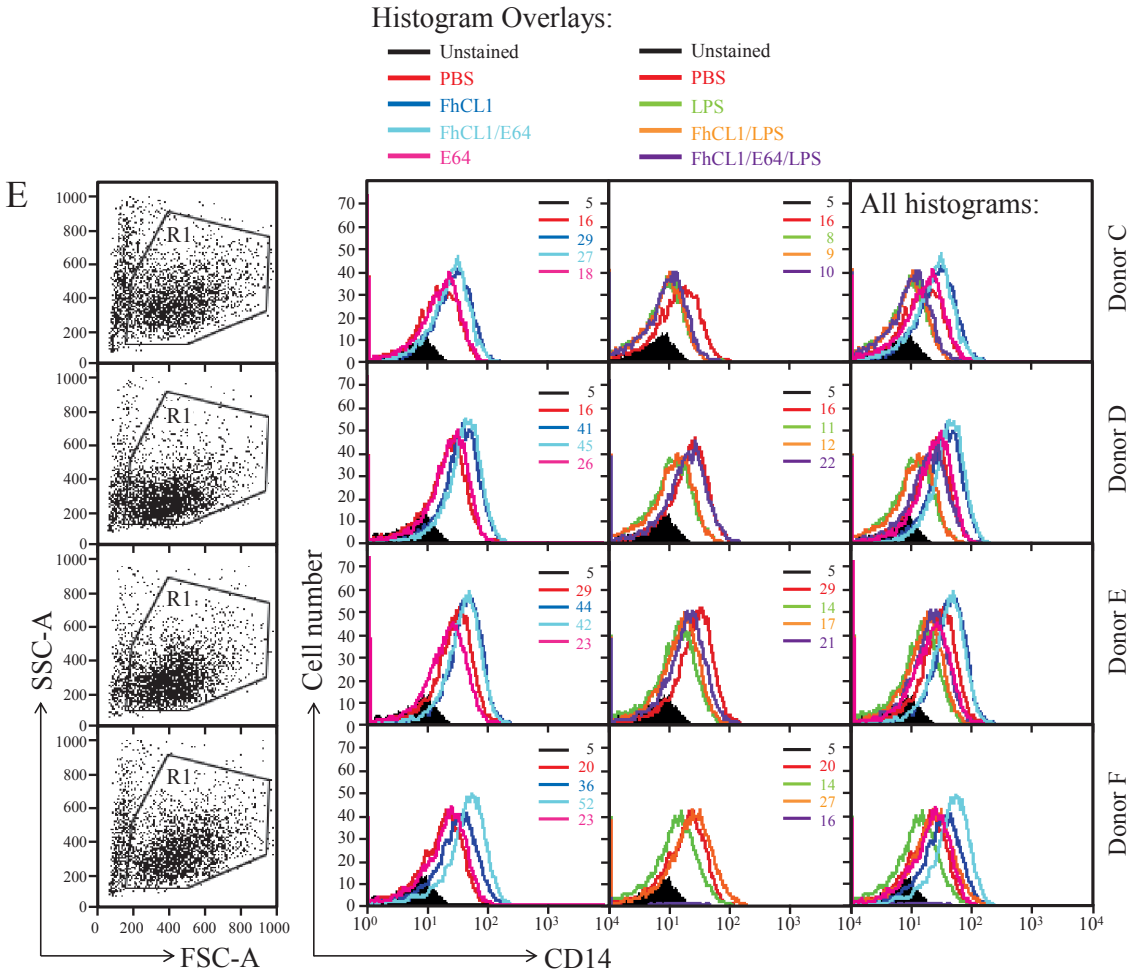

Figure 3.7: Analysis of cell surface marker expression in FhCL1-treated primary human macrophages.

Macrophages were treated with PBS, 10 µg/mL FhCL1, 10 µg/mL FhCL1 with 10 µM E64 or 10 µM E64 for 18 h and were subsequently stimulated with 50 ng/mL LPS. Surface expression of A) CD206, B) CD163, C) CD86, D) HLA-DR and E) CD14 was determined by flow cytometry. Data shown are histogram overlays with MFI values as indicated (top right hand panel numbers), determined from single cells (FSC-A versus SSC-A dot plot; R1). Data are separated to show relevant comparisons, ie PBS versus FhCL1 with and without protease inhibitor E64, or FhCL1 with and without LPS (coloured unfilled histograms). Unstained cells are also shown (black filled histogram).

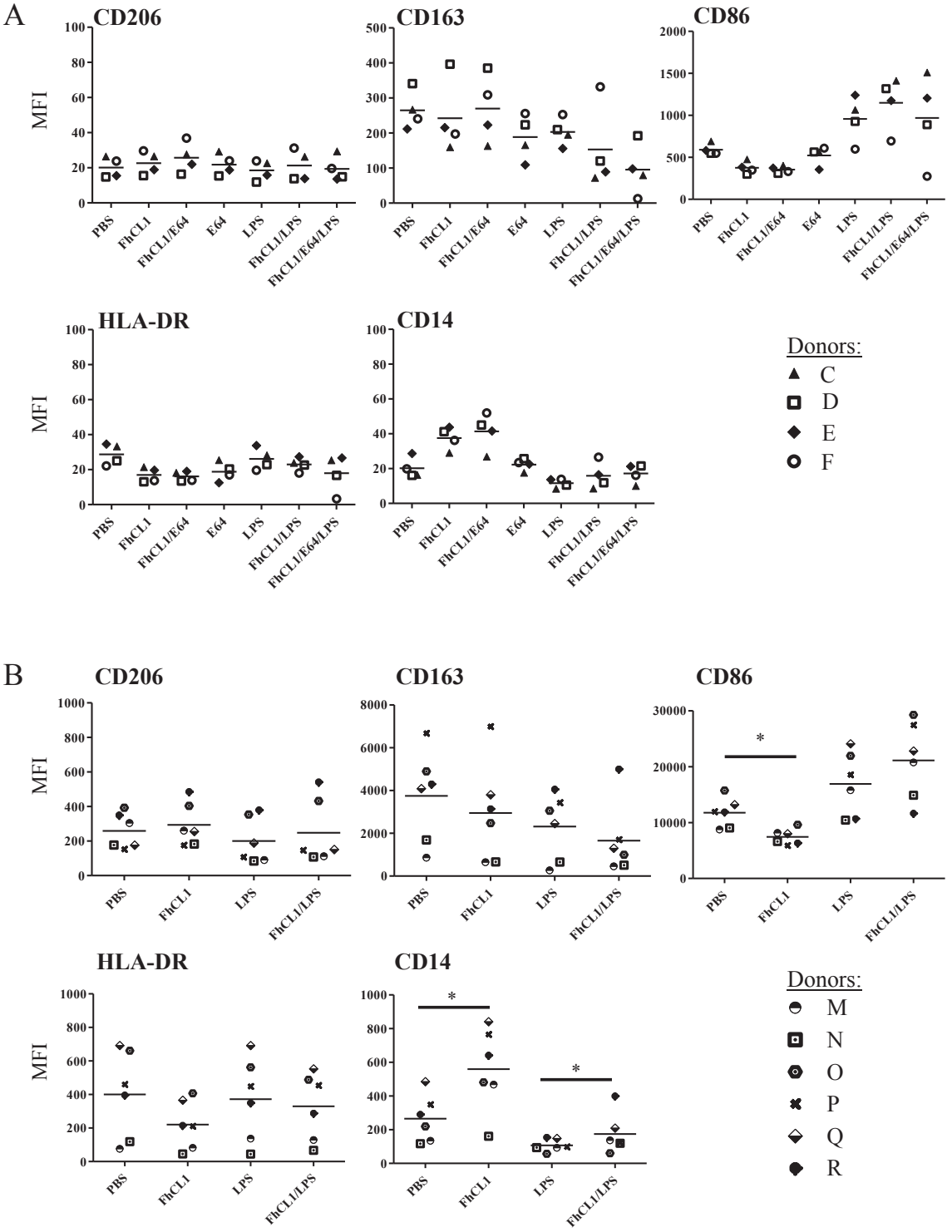

Figure 3.8: Analysis of cell surface marker expression in FhCL1-treated primary human macrophages.

Monocyte-derived macrophages were treated with PBS, 10 μg/mL FhCL1, 10 μg/mL FhCL1 with 10 μM E64 or 10 μM E64 for 18 h and were subsequently stimulated with 50 ng/mL LPS. A) Data shown are MFI values from histogram plots (Figure 3.7), for the surface expression of CD206, CD163, CD86, HLA-DR and CD14 on macrophages from four donors. B) Surface marker expression was also assessed in a six donor cohort. MFI data were analysed by Wilcoxin matched pairs t-test, and significant differences ($p < 0.05$) between data pairs (PBS and FhCL1, LPS and FhCL1/LPS) are as indicated (*).

surface expression levels of alternative activation markers CD206 and CD163 (Figure 3.7A, B and Figure 3.8). Likewise, treatment with FhCL1 with E64 or E64 alone had no effect on the expression of CD206 or CD163 (Figure 3.7A, B and Figure 3.8A). Treatment with FhCL1, in the presence and absence of E64, showed a trend towards decreased surface expression of CD86 and HLA-DR. In contrast, treatment with FhCL1, either in the presence or absence of E64, showed a trend towards up-regulated surface expression of CD14 (Figure 3.7 and Figure 3.8B). Therefore, to further investigate and confirm (or not) the effect of FhCL1 on the expression of cell surface markers, a second independent experiment was performed. Due to macrophage isolation occurring on different days, flow cytometer settings differed for each experiment, thus, MFI values are shown separately for the 2 independent analyses of different donor cohorts. In both cohorts, treatment with FhCL1 had no significant effect on the expression of CD206 or CD163 (Figure 3.7A, B and Figure 3.8). However, FhCL1 showed a trend towards down-regulated CD86 expression and up-regulated CD14 expression in the four donor cohort, and this reached statistical significance in the second, larger donor cohort, with expression of CD86 being significantly down-regulated ($p=0.028$), and expression of CD14 significantly up-regulated ($p=0.028$) in the six donor cohort (Figure 3.8B).

Surface expression of CD206, CD163, CD86, HLA-DR and CD14 was also examined in macrophages following LPS stimulation, with and without pre-treatment with 10 μg/mL FhCL1 or 10 μg/mL FhCL1 with E64. There was no significant difference in CD206, CD163, CD86 and HLA-DR expression in either the four donor cohort (Figure 3.7 and Figure 3.8A), or a second six donor cohort (Figure 3.8B). In contrast, although up-regulation of surface expression of CD14 was not significant in the four donor cohort, the second six donor cohort showed that CD14 expression was significantly up-regulated by FhCL1 following LPS stimulation ($p=0.028$) (Figure 3.8B). In summary, FhCL1 treatment modulated cell surface marker expression in human macrophages, noticeably decreasing CD86 surface expression in unstimulated macrophages and up-regulating CD14 surface expression with and without LPS stimulation.

3.2.4 EFFECT OF FHCL1 TREATMENT ON INTRACELLULAR CD14 LOCALISATION

As the cell surface co-receptor for LPS, CD14 can enhance signalling through the MyD88-dependent TLR4 pathway (Haziot *et al.* 1996). Furthermore, up-regulation of CD14 has been associated with enhanced expression of pro-inflammatory cytokines (Sugawara *et al.* 1998; Tamai *et al.* 2002), and thus the up-regulation of CD14 on the cell surface following FhCL1 treatment (Figure 3.7 and Figure 3.8) appears to correlate with the observed increased expression of IL-6 and IL-8 by FhCL1 (Figure 3.6). Also, expression of IL-10 is induced by both the MyD88-dependent and TRIF-dependent TLR4 signalling pathways (Boonstra *et al.* 2006; Shen *et al.* 2008) and TRIF-dependent IL-10 expression is induced following endocytosis of the CD14/TLR4 complex (Tanimura *et al.* 2008). Therefore, given that IL-10 expression was down-regulated by FhCL1 treatment, this presented the possibility that FhCL1 treatment may be modulating intracellular expression or localisation of CD14 in human macrophages. To address this possibility, primary human macrophages were cultured with PBS or 10 μg/mL FhCL1 for 18 h, and then stimulated with 50 ng/mL LPS over a time course up to 6 h. Cells were fixed at various time points and stained with anti-CD14 antibody and phalloidin which binds to F-actin. When the localisation of CD14 was examined in individual cells by confocal microscopy, results indicated that there was little difference in the localisation of intracellular CD14 in primary human monocyte-derived macrophages treated with FhCL1 compared to PBS-treated control cells, with CD14 consistently distributed throughout the cell (Figure 3.9). Similarly, FhCL1 pre-treated LPS-stimulated cells exhibited no difference in CD14 localisation compared to untreated LPS-stimulated cells (Figure 3.9). This suggests that FhCL1 treatment had no effect on the intracellular localisation of CD14, even though cell surface levels were previously shown to be increased in flow cytometry analysis (Figure 3.7E and Figure 3.8A, B).

To investigate the total intracellular expression levels of CD14 following FhCL1 treatment, the MFI of individual permeabilised cells was calculated for each time point for all cells in each field of view (Table 3.1). Statistical analysis of CD14 fluorescence intensity demonstrated that there was no significant difference in CD14 in FhCL1 treated cells compared to control cells ($p=0.3547$). Likewise, comparing LPS stimulated

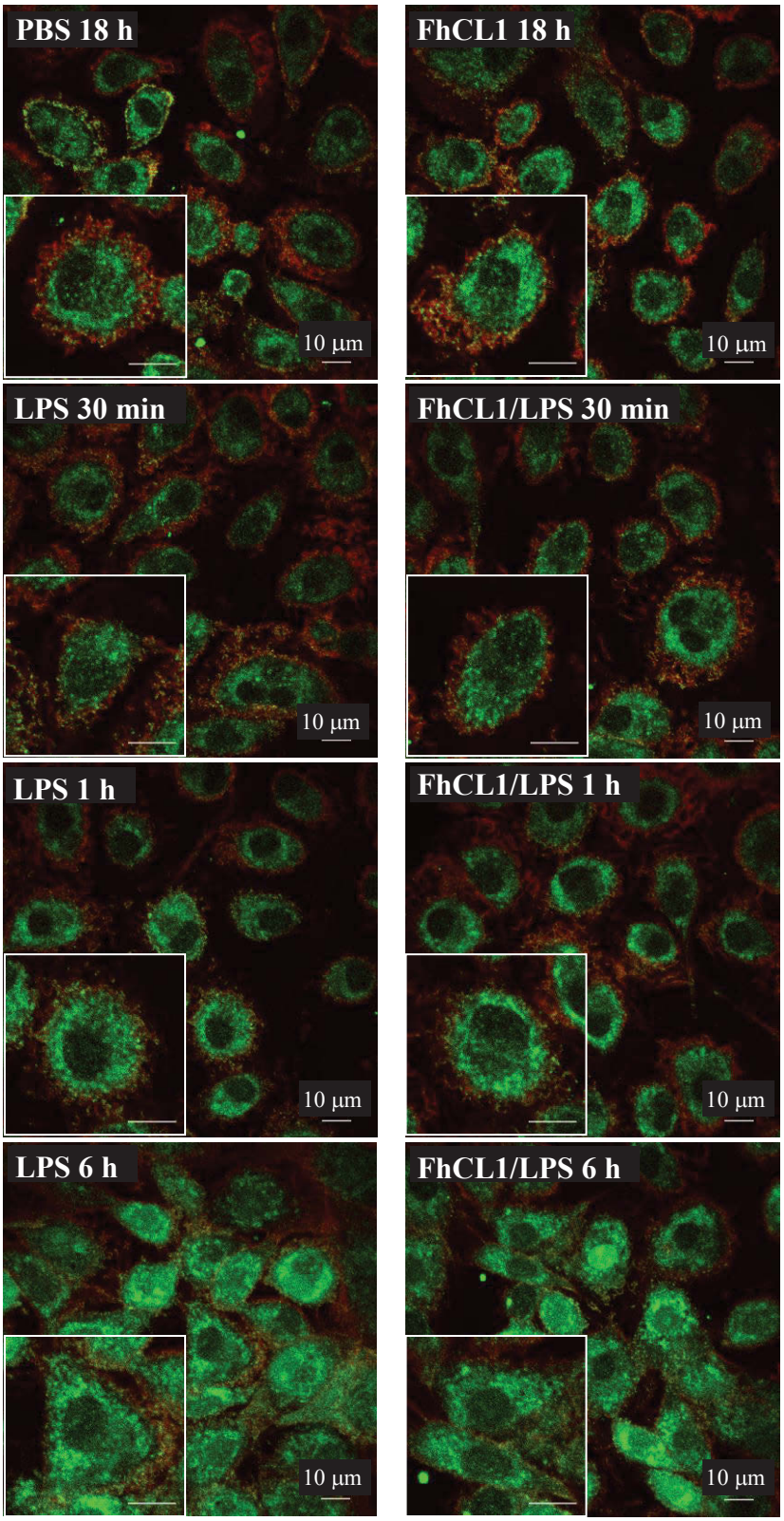

Figure 3.9: Localisation of CD14 within FhCL1-treated primary human macrophages with and without LPS stimulation.

Pooled primary human macrophages were treated with PBS or 20 µg/mL FhCL1 (18 h) prior to stimulation with 50 ng/mL LPS for up to 6 h. Macrophages were stained with anti-CD14 Pacific Blue antibody (green) and phalloidin (red) to detect F-actin. Imaging was performed using the Nikon A1 Confocal Scanning Laser Microscope. Data are representative of two independent experiments, with a minimum of four images acquired for each time point and a minimum of 40 cells examined at each time point. Inset shows magnified image of CD14 localisation in a subset of cells.

Table 3.1: Mean fluorescence intensity of intracellular CD14 in FhCL1-treated primary human monocyte-derived macrophages with and without LPS stimulation.

	Control	FhCL1	FhCL1/ LPS 30 min	LPS 30 min	FhCL1/ LPS 1 h	LPS 1 h	FhCL1/ LPS 6 h	LPS 6 h
Number of cells	51	45	40	45	43	45	48	58
MFI	766	789	726	710	841	734	997	999
Standard deviation	121	107	110	94	115	111	216	217
P-value	0.3547		0.1993		<0.0001 *		0.9468	

* Statistically significant

cells with FhCL1 pre-treated cells showed no significant difference at the 30 min (p=0.1993) or 6 h (p=0.9468) time points. However, at the 1 h LPS stimulation time point, there was a significant increase in CD14 in FhCL1 pre-treated cells (mean: 841, SD (standard deviation): 115) compared to untreated, LPS stimulated cells (mean: 734, SD: 111; p= <0.0001) (Table 3.1). This suggested that, intracellular CD14 expression is up-regulated following LPS-stimulation in FhCL1-treated macrophages consistent with previous reports (Saitoh *et al.* 2004; Kobayashi *et al.* 2006). Therefore, FhCL1 treatment modulated intracellular CD14 expression in primary human monocyte-derived macrophages.

3.2.5 EFFECT OF FHCL1 TREATMENT ON EXPRESSION OF KEY MOLECULES WITHIN THE MYD88-DEPENDENT AND TRIF-DEPENDENT SIGNALLING PATHWAYS

Treatment of murine peritoneal macrophages with FhCL1 resulted in down-regulated expression of NO, IL-6, IL-12 and TNF in response to LPS stimulation (Donnelly *et al.* 2010). In contrast, treatment of primary human monocyte-derived macrophages with FhCL1 resulted in significant up-regulation of IL-6 and IL-8 post-LPS-stimulation (Figure 3.6). In response to LPS, pro-inflammatory cytokine expression is induced by TLR4-mediated MyD88-dependent and TRIF-dependent signalling (Akira *et al.* 2004) (Figure 3.1). However, in FhCL1-treated murine peritoneal macrophages, the down-regulation of pro-inflammatory cytokines in response to LPS induced inhibition of TRIF-dependent signalling (Donnelly *et al.* 2010). Thus, while FhCL1 had an opposing effect on human macrophages, it was hypothesised that within human monocyte-derived macrophages, FhCL1 might modulate TLR signalling pathways. To address this possibility, western blot analysis was used to investigate the expression of key proteins involved in both the MyD88 and TRIF-dependent signalling pathways. To examine the early part of the MyD88 signalling pathway, MyD88 and TRAF6 were selected as MyD88 is the first protein recruited to the CD14/TLR4 complex following the binding of LPS and both the MyD88 and TRIF signalling pathways require TRAF6 (Medzhitov *et al.* 1998). In the MyD88-dependent signalling pathway, MyD88 signalling through TRAF6 induces early NF-κB activation of pro-inflammatory cytokines, while in the TRIF-dependent pathway, TRIF recruits TRAF6 for late NF-κB signalling (Figure 3.1) (Sato *et al.* 2003; Jiang *et al.* 2004; Hacker *et al.* 2006; reviewed in Kawai *et al.* 2007).

Three further candidates were chosen to examine the later part of the pathway shared by both the MyD88 and TRIF-dependent pathways. Phosphorylation and degradation of nuclear factor of kappa light polypeptide gene enhancer in B-cells inhibitor, alpha (IκBα) activates NF-κB to induce cytokine expression (Beg *et al.* 1993; Sun *et al.* 1994) and thus expression and phosphorylation of IκBα was examined. Extracellular signal-regulated kinase (ERK)-1, and ERK2 were also selected based on their association with AP-1 to induce cytokine expression (Macian *et al.* 2001). The selection of these signalling molecules allowed for an examination of the effect of FhCL1 on different stages of the MyD88-dependent pathway and the TRIF-dependent pathway. MyD88 and TRAF6 were examined following pre-treatment with FhCL1 but without LPS, to examine whether FhCL1 alone altered protein expression of these candidates. The expression and phosphorylation of IκBα, ERK1 and ERK2 were examined both with and without LPS stimulation, as phosphorylation of these molecules following stimulation induces downstream cytokine expression (Beg *et al.* 1993; Sun *et al.* 1994; Macian *et al.* 2001).

To examine the effect of FhCL1-treatment on MyD88 and TRAF6 expression, primary human macrophages from four donors were pooled and cultured with PBS, 20 μg/mL FhCL1, 20 μg/mL FhCL1 with 20 μM protease inhibitor E64 or 20 μM E64 alone for 18 h. Following treatment, protein was isolated and separated by SDS-PAGE prior to transfer onto nitrocellulose membranes. Membranes were probed with anti-MyD88, anti-TRAF6 and anti-β-actin -specific antibodies (see Table 2.5 for antibody clone details). Antibody to β-actin was used as an indication of equal total protein loading, with densitometry results confirming that consistent amounts of protein were loaded into each lane (Figure 3.10). Antibodies specific to MyD88 and TRAF6 had varying degrees of non-specific binding, and while the main band detected by anti-TRAF6 antibody corresponded to the reported size of TRAF6 (58 kDa), the main bands when detected by anti-MyD88 antibody were larger than the reported size of MyD88 (33 kDa) (Figure 3.10). Nevertheless, visual assessment of the bands corresponding to MyD88 and TRAF6 suggested that treatment with FhCL1, FhCL1 with protease inhibitor E64 or E64 alone had no effect on the expression of either MyD88 or TRAF6 (Figure 3.10A).

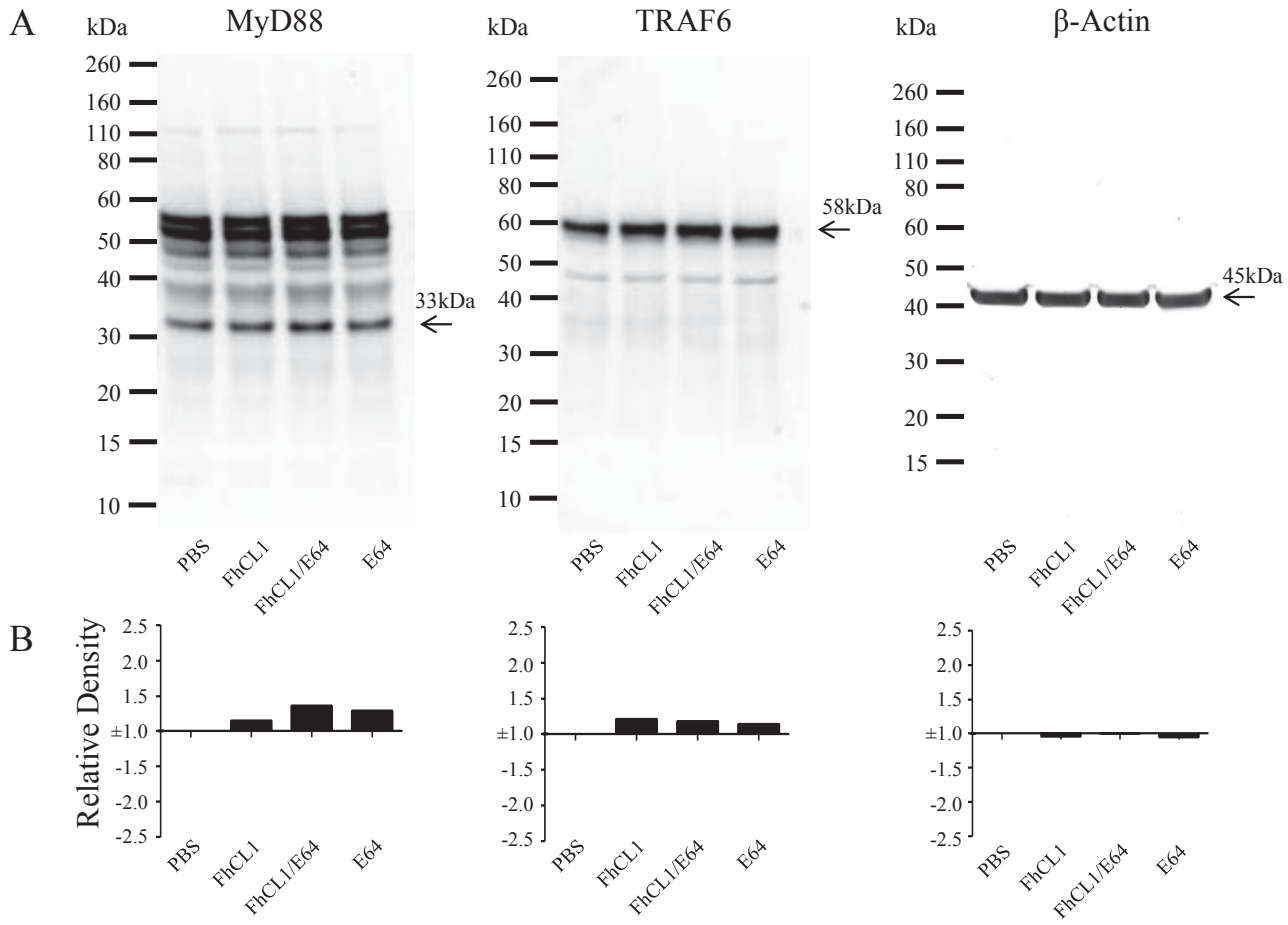

Figure 3.10: Western blot analysis of MyD88 and TRAF6 expression in primary human macrophages treated with FhCL1.
Macrophage cell lysates were prepared from four pooled donors treated with PBS, 20 μg/mL FhCL1, 20 μg/mL FhCL1 with 20 μM E64 and 20 μM E64. A) Western blot membranes were incubated with antibodies specific for MyD88, TRAF6 or β-actin. Protein size markers are as indicated. Specific proteins, MyD88, TRAF6 and β-actin, are detected at the expected size (arrow). B) Densitometry graphs showing the relative density of MyD88, TRAF6 and β-actin for each treatment. Data shown is representative of a single experiment.

Densitometry analysis was performed to better estimate any relative changes in protein expression, and this confirmed that there was essentially no difference in MyD88 or TRAF6 protein in FhCL1-treated macrophages (Figure 3.10B). This suggested that the mechanism by which FhCL1 modulated signalling was not through changes in MyD88 or TRAF6 protein expression.

Inactive NF-κB is complexed with inhibitory Iκ kinases including IκBα (Inoue *et al.* 1992; Hatada *et al.* 1993) and activation and translocation of NF-κB into the nucleus for cell signalling requires phosphorylation, ubiquination and degradation of IκBα (Beg *et al.* 1993; Finco *et al.* 1994; Miyamoto *et al.* 1994; Sun *et al.* 1994). Thus, the activation of this pathway was examined by determining the phosphorylation status and level of IκBα in FhCL1-treated macrophages. Primary human macrophages were treated with PBS or 20 μg/mL FhCL1 and stimulated with 50 ng/mL LPS for up to 3 h. Protein was isolated and separated by SDS-PAGE, prior to transfer to nitrocellulose membranes. Membranes were probed with anti-IκBα, anti-phosphorylated IκBα (pIκBα) and anti-β-actin antibodies (Figure 3.11). While some degree of non-specific binding was observed on membranes probed with both anti-IκBα and anti-pIκBα antibodies, the main band corresponded to the reported size of IκBα (39 kDa) and pIκBα (40 kDa) and was clearly evident. Detectable levels of IκBα were already present in unstimulated cells, with FhCL1 and PBS-treated control macrophages expressing similar levels of IκBα (Figure 3.11). However, IκBα levels declined after LPS stimulation, with marginally less IκBα in FhCL1-treated samples compared to PBS samples. In fact, densitometry analysis suggested a greater than 20-fold decrease in IκBα protein expression in FhCL1-treated LPS stimulated samples. However, levels were so low that they were difficult to quantitate by densitometry (Figure 3.11). At 30 min and 1 h post LPS-stimulation, levels of IκBα remained low, before increasing again at 3 h post LPS-stimulation, with similar levels of IκBα protein in PBS and FhCL1-treated macrophages (Figure 3.11). Therefore, at all time points post LPS stimulation, levels of IκBα were essentially similar in PBS and FhCL1-treated macrophages. This suggests that FhCL1-treatment did not modulate cytokine expression by altering IκBα expression.

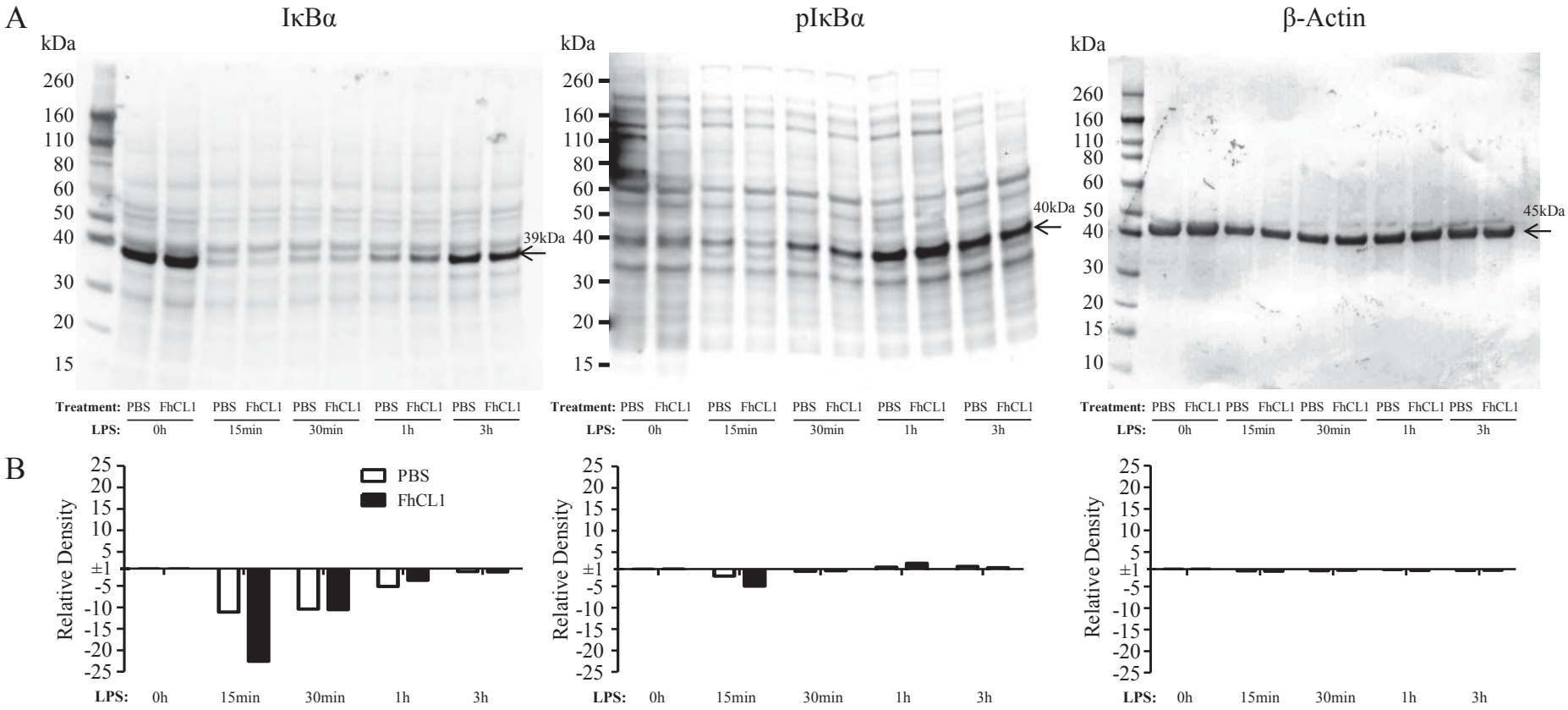

Figure 3.11: Western blot analysis of IκBα expression and phosphorylation in primary human macrophages cultured with FhCL1. Macrophage cell lysates were prepared from four pooled donors treated with PBS or 20 μg/mL FhCL1 and stimulated with 50 ng/mL LPS. A) Western blot membranes were incubated with antibodies specific for IκBα, phosphorylated (p) IκBα, or β-actin. Protein size markers are as indicated. Specific proteins, IκBα, pIκBα, or β-actin, are detected at the expected size (arrow). B) Densitometry graphs showing the relative density of IκBα, pIκBα, or β-actin for each treatment. Data shown is representative of a single experiment.

Phosphorylation of IκBα was also examined using phospho-specific antibodies, since it is the phosphorylated form that most contributes to NFκB signalling (Beg *et al.* 1993; Sun *et al.* 1994). Unstimulated macrophages had low levels of pIκBα, with FhCL1-treated macrophages showing similar levels of IκBα phosphorylation compared to PBS-treated control macrophages (Figure 3.11). Levels of pIκBα began to increase 30 min post LPS stimulation, with visually similar levels of pIκBα between PBS- and FhCL1-treated macrophages (Figure 3.11). Phosphorylation of IκBα continued to increase 1 h post LPS stimulation, with a visual difference between PBS and FhCL1-treated macrophages, with increased phosphorylation levels in FhCL1-treated macrophages compared to PBS-treated macrophages (Figure 3.11A). At 3 h post LPS-stimulation, phosphorylation of IκBα had begun to decrease in both PBS- and FhCL1-treated macrophages to a similar degree (Figure 3.11). These effects were confirmed by semi-quantitative densitometry analysis (Figure 3.11B). Thus, FhCL1 slightly enhanced phosphorylation of IκBα by 1 h post LPS stimulation. This slight increase in phosphorylation may enhance activation of NF-κB, and this suggests that FhCL1 may modulate the expression of pro-inflammatory cytokines through the IκBα/NFκB pathway.

The Mitogen-activated protein kinase (MAPK) pathways consists of three alternate pathways, the ERK pathway, the p38 MAP kinases and the c-Jun NH2-terminal kinases (JNK), which all transcriptionally regulate gene expression through the transcription factor AP-1 (Dong *et al.* 2002). Stimulation of cells with LPS activates all three MAPK pathways (Hambleton *et al.* 1996). To date, the effect of FhCL1 on the JNK, p38 or ERK MAPK pathways has not been investigated in primary human monocyte-derived macrophages. Therefore, as a representative of the MAPK pathways, the effect of FhCL1 on ERK1 and ERK2 was investigated. In inactive cells, ERK1 and ERK2 are generally distributed throughout the cells, however, following phosphorylation by MAP kinase kinases (MEK1/2) (Boulton *et al.* 1991a; Boulton *et al.* 1991b; Payne *et al.* 1991), ERK1 and ERK2 accumulate in the nucleus where they phosphorylate the transcription factor AP-1, initiating gene transcription (Chen *et al.* 1992; Gonzalez *et al.* 1993; Lenormand *et al.* 1993), including the expression of pro-inflammatory cytokines, such as IL-6 and IL-8 (Mukaida *et al.* 1989; Ray *et al.* 1989; Libermann *et al.* 1990). Therefore, since IL-6 and IL-8 expression were up-regulated following FhCL1-

treatment, the expression and phosphorylation of ERK1 and ERK2 were assessed in primary human monocyte-derived macrophages. Macrophages were cultured with PBS or 20 μg/mL FhCL1 for 18 h followed by stimulation with 50 ng/mL LPS for up to 3 h. Protein was isolated and analysed by western immunoblotting with antibodies specific to ERK1/2 and phosphorylated (p) ERK1/2. ERK1 and ERK2 were detected in all samples, with and without LPS stimulation, with albeit small differences in protein expression. For example, the levels of ERK1 and ERK2 were visually only slightly higher in FhCL1-treated macrophages compared to PBS-treated macrophages (Figure 3.12). Levels of pERK1/2 were low in both PBS and FhCL1-treated macrophages, with essentially no difference in expression between treatment groups (Figure 3.12). However, ERK1/2 phosphorylation was induced 15 min post LPS-stimulation (Figure 3.12), but the levels of phosphorylated ERK1 and ERK2 were increased in both PBS- and FhCL1- treated LPS stimulated macrophages. In addition, there was only a slight increase in pERK1 and pERK2 in FhCL1-treated macrophages compared to PBS control LPS-stimulated macrophages (Figure 3.12A). This was confirmed by densitometry which suggested FhCL1 induced 1.5-fold higher levels of pERK1/2. (Figure 3.12B). After 30 min LPS-stimulation, levels of pERK1 and pERK2 began to decline compared to the 15 min time point with similar levels in FhCL1-treated cells compared to PBS-treated macrophages (Figure 3.12). At both 1 h and 3 h post LPS stimulation, levels of pERK1 and pERK2 continued to decline in both PBS and FhCL1-treated macrophages, with little to no pERK1/2 detected 3 h post LPS stimulation (Figure 3.12). Given that LPS-induced phosphorylation of ERK1/2 contributes to the production of multiple cytokines, including IL-6 (Goral *et al.* 2004) and IL-8 (Bhattacharyya *et al.* 2002), the slightly enhanced phosphorylation of ERK1 and ERK2 at 15 min post LPS stimulation supports the potential activation of the MAPK signalling pathway by FhCL1.

To determine whether FhCL1 modulated mRNA expression of ERK1 and ERK2, human macrophages from six donors were treated with PBS, 20 μg/mL FhCL1, 20 μg/mL FhCL1 with 20 μM E64 or 20 μM E64 alone for 18 h, and analysed by RT-qPCR. As expected, the no cDNA template produced no amplification. Macrophages treated with FhCL1 showed no difference in expression of either ERK1 or ERK2 mRNA compared to PBS-treated cells, as expected, due to its phosphorylation being the

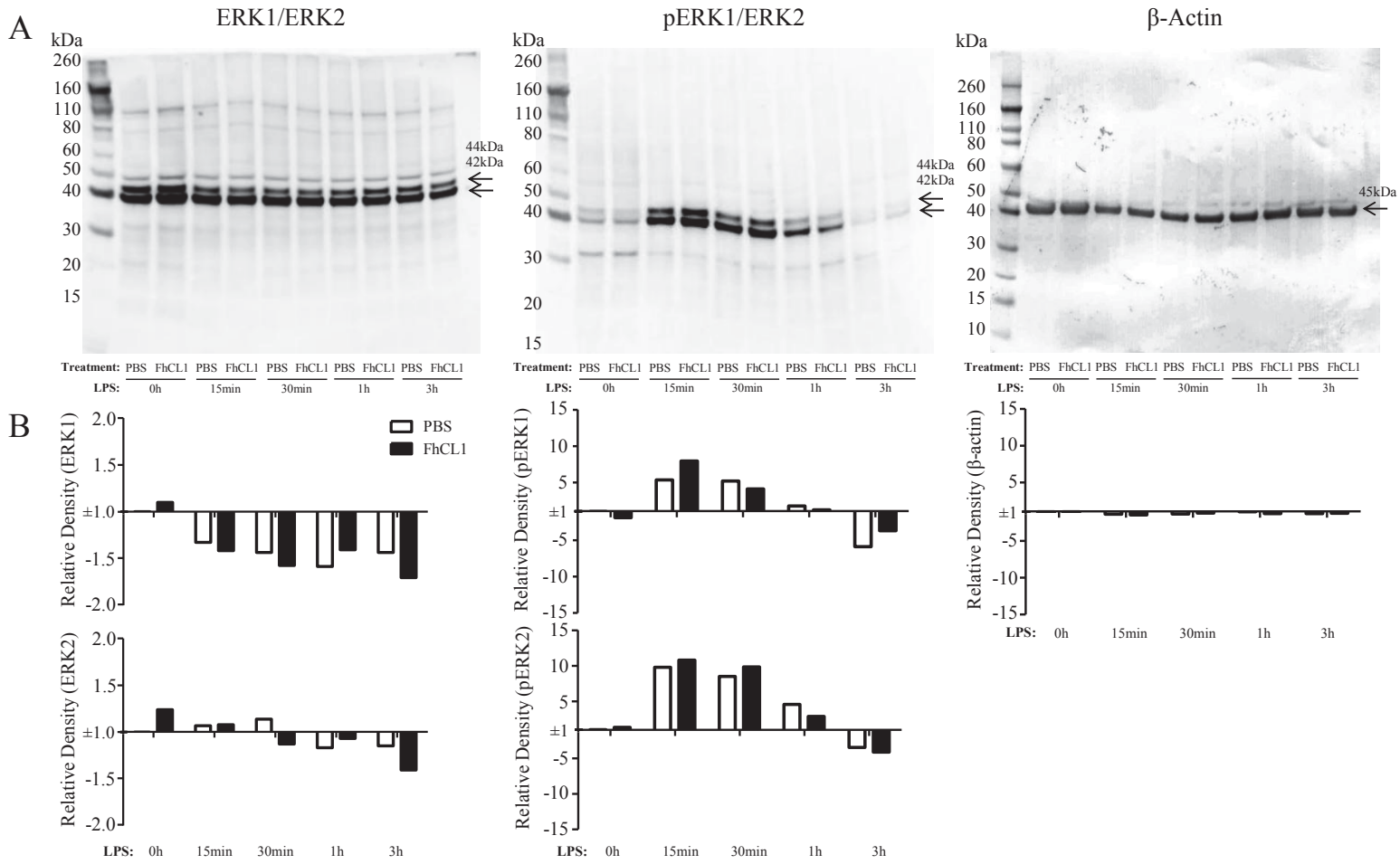

Figure 3.12: Western blot analysis of ERK1/2 expression and phosphorylation in primary human macrophages cultured with FhCL1. Macrophage cell lysates were prepared from four pooled donors treated with PBS or 20 μg/mL FhCL1 and stimulated with 50 ng/mL LPS. A) Western blot membranes were incubated with antibodies specific for ERK1 and ERK2, phosphorylated (p) ERK1 and ERK2, or β-actin. Protein size markers are as indicated. Specific proteins, ERK1, ERK2, pERK1, pERK2, or β-actin, are detected at the expected size (arrow). B) Densitometry graphs showing the relative density of ERK1, ERK2, pERK1, pERK2 or β-actin for each treatment. Data shown is representative of a single experiment.

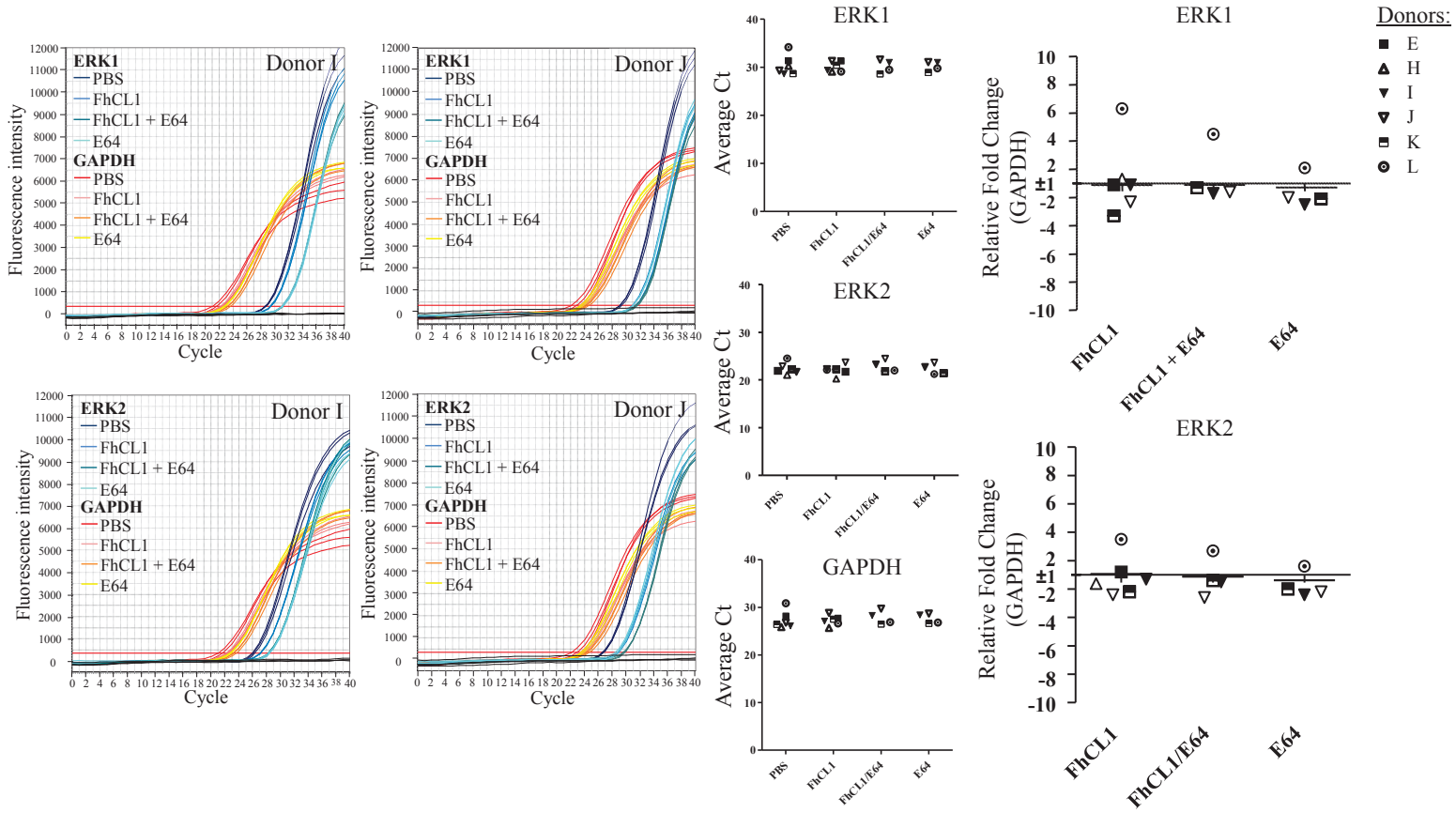

Figure 3.13: ERK1 and ERK2 mRNA expression in primary human macrophages cultured with FhCL1.
Primary human macrophages were incubated with PBS, 20 µg/mL FhCL1, 20 µg/mL FhCL1 with 20 µM E64, or 20 µM E64, for 18 h. Data shown are representative fluorescence intensity RT-qPCR profiles for ERK1, ERK2 and GAPDH mRNA expression for two individual donors. Also shown are the average Ct values for up to six donors. Scatter graphs depict the fold change in cytokine expression relative to the reference gene GAPDH and compared to the expression in PBS-treated macrophages. Means (horizontal bars) are also shown. Data were analysed by Wilcoxin matched pairs t-test, and no statistically significant differences were observed between any treatment groups.

biologically important factor (Figure 3.13). No significant detectable differences were also observed for both ERK1 and ERK2 mRNA in macrophages treated with FhCL1 and the E64 protease inhibitor or E64 alone (Figure 3.13). Thus, FhCL1 did not modulate ERK1/2 mRNA expression levels in unstimulated macrophages. Therefore, taken together, FhCL1 treatment did not appear to specifically target the MyD88-dependent signalling pathway, as FhCL1 did not alter the expression of MyD88. Likewise, expression of TRAF6, which is activated by either the MyD88-dependent or TRIF-dependent signalling pathway, was unchanged by FhCL1 treatment. However, FhCL1 treatment slightly enhanced the phosphorylation of IκBα at 1 h post LPS stimulation and ERK1/2 phosphorylation 15 min post LPS stimulation. This increased phosphorylation might indicate enhanced activation of cell signalling in the presence of FhCL1, which is corroborated by the increased expression of pro-inflammatory cytokines, IL-6 and IL-8 (Figure 3.6).

3.2.6 EFFECT OF FHCL1 TREATMENT ON EXPRESSION OF TRANSCRIPTION FACTORS OF THE TRIF SIGNALLING PATHWAY

Treatment of primary human monocyte-derived macrophages with FhCL1 down-regulated expression of IL-10 following LPS stimulation (Figure 3.6). Additionally, the surface marker CD86 was also shown to be down-regulated following FhCL1 treatment (Figure 3.8). Modulation of IL-10 secretion and CD86 surface expression in FhCL1-treated macrophages could be dependent on signalling from type 1 IFNs (Chang *et al.* 2007; Iyer *et al.* 2010), which, in turn, are induced by IRF3 (Sato *et al.* 2003; Yamamoto *et al.* 2003), with type 1 IFNs and IRF3 both being involved in the TRIF signalling pathway. It has previously been shown in murine macrophages that FhCL1 did not cause changes in the expression of transcription factors acting early in the TRIF-dependent pathway, namely TRIF and TRAF3, despite affecting TRIF-dependent signalling (Donnelly *et al.* 2010). However, it was important to determine if FhCL1 modulated this pathway in human monocyte-derived macrophages. Thus, to further elucidate the mechanism by which FhCL1 was modulating CD86 and IL-10 expression, the expression levels of TRIF, TRAF3 and IRF3 were examined in primary human monocyte-derived macrophages following FhCL1 treatment.

To investigate the expression of TRIF and TRAF3, human macrophages from four donors were pooled and treated with PBS, 20 μg/mL FhCL1, 20 μg/mL FhCL1 with 20 μM E64 protease inhibitor or 20 μM E64 alone for 18 h. Following treatment, protein was isolated and examined by western immunoblotting. Membranes were probed with antibodies specific to TRIF, TRAF3 and β-actin (loading control) and densitometry used to confirm relative protein amounts (Table 2.5, Section 2.8). Antibodies used to determine TRIF and TRAF3 expression had varying degrees of non-specific binding and the most prominant bands when probed with anti-TRIF or anti-TRAF3 antibodies did not correspond to the reported size of these proteins (Figure 3.14). Nevertheless, visual assessment of the 76 kDa band predicted to correspond to TRIF protein suggested that treatment with FhCL1, FhCL1 with E64, or E64 alone, had no effect on TRIF expression (Figure 3.14A). However, visual analysis of western blots for TRAF3 suggested a decrease in TRAF3 expression in FhCL1-treated macrophages, with FhCL1 with E64 having less of an effect on TRAF3 expression, while E64 appeared to have no effect on TRAF3 expression (Figure 3.14A), which was confirmed by densitometry analysis (Figure 3.14B). This suggested that while FhCL1 had no effect on TRIF expression, the TRIF-dependent pathway may be slightly suppressed by the down-regulation of TRAF3.

To determine whether TRAF3 was also down-regulated by FhCL1 at the level of transcription, the mRNA expression of TRAF3 was investigated by RT-qPCR. Human monocyte-derived macrophages were treated with PBS, 20 μg/mL FhCL1, 20 μg/mL FhCL1 with 20 μM E64 or 20 μM E64 for 18 h prior to RNA isolation and cDNA synthesis. As expected, the no cDNA template produced no amplification. Consistent with the protein expression analyses, macrophages treated with FhCL1, in the presence or absence of E64, showed no significant difference in TRAF3 mRNA compared to PBS-treated cells (Figure 3.15). Therefore, FhCL1 does not modulate TRAF3 mRNA, and only slightly altered TRAF3 protein expression.

Finally, to further investigate the activation of the TRIF-dependent pathway, the effect of FhCL1 on the expression of IRF3 was examined. IRF3 normally resides in the cytoplasm in unactivated cells along with IRF7 (reviewed in Taniguchi *et al.* 2001) (Figure 3.1). Following the activation of TRIF and TRAF3, IκB kinase related proteins,

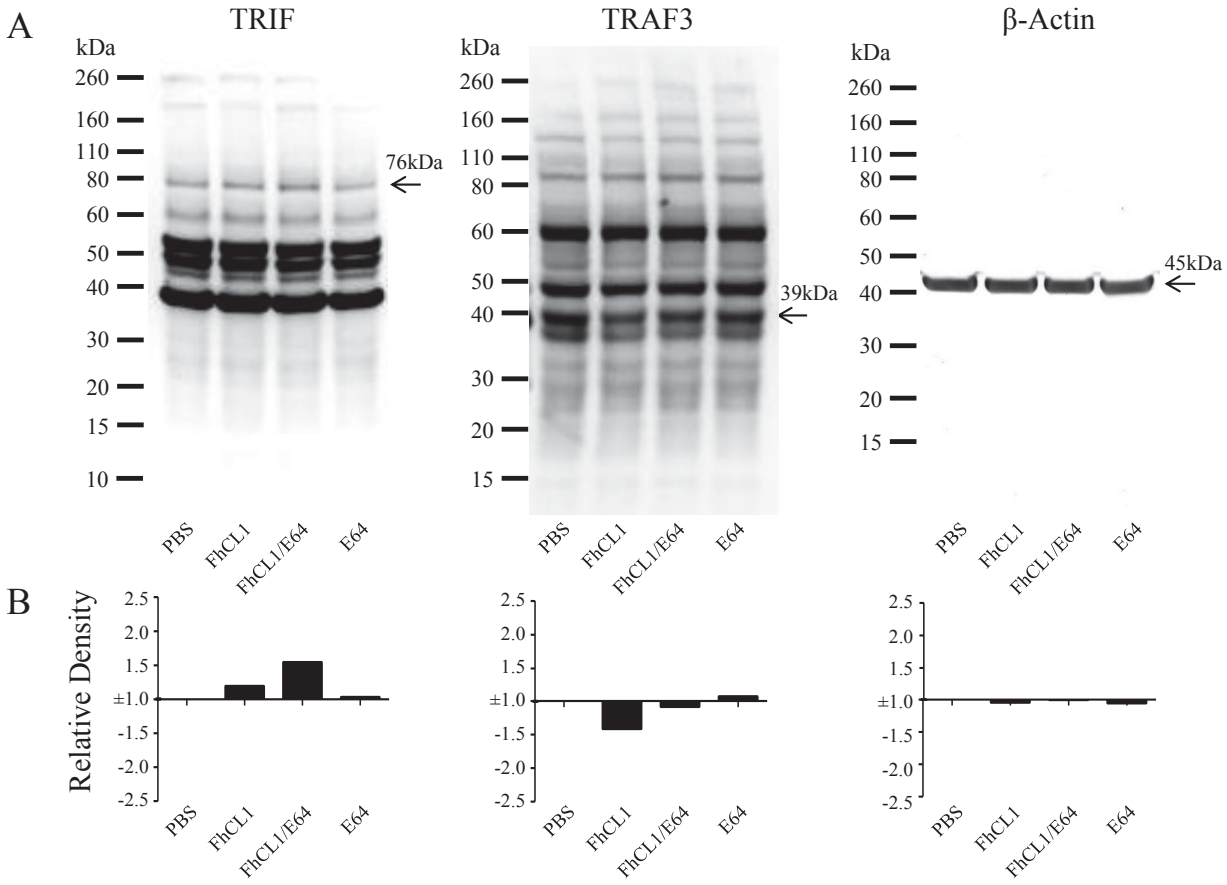

Figure 3.14: Western blot analysis of TRIF and TRAF3 expression in primary human macrophages treated with FhCL1.
Macrophage cell lysates were prepared from four pooled donors treated with PBS, 20 μg/mL FhCL1, 20 μg/mL FhCL1 with 20 μM E64 and 20 μM E64. A) Western blot membranes were incubated with anti-TRIF, anti-TRAF3 or anti-β-actin. Protein size markers are as indicated. Specific proteins, TRIF, TRAF3 and β-actin, are detected at the expected size (arrow). B) Densitometry graphs showing the relative density of TRIF, TRAF3 and β-actin for each treatment. Data shown is representative of a single experiment.

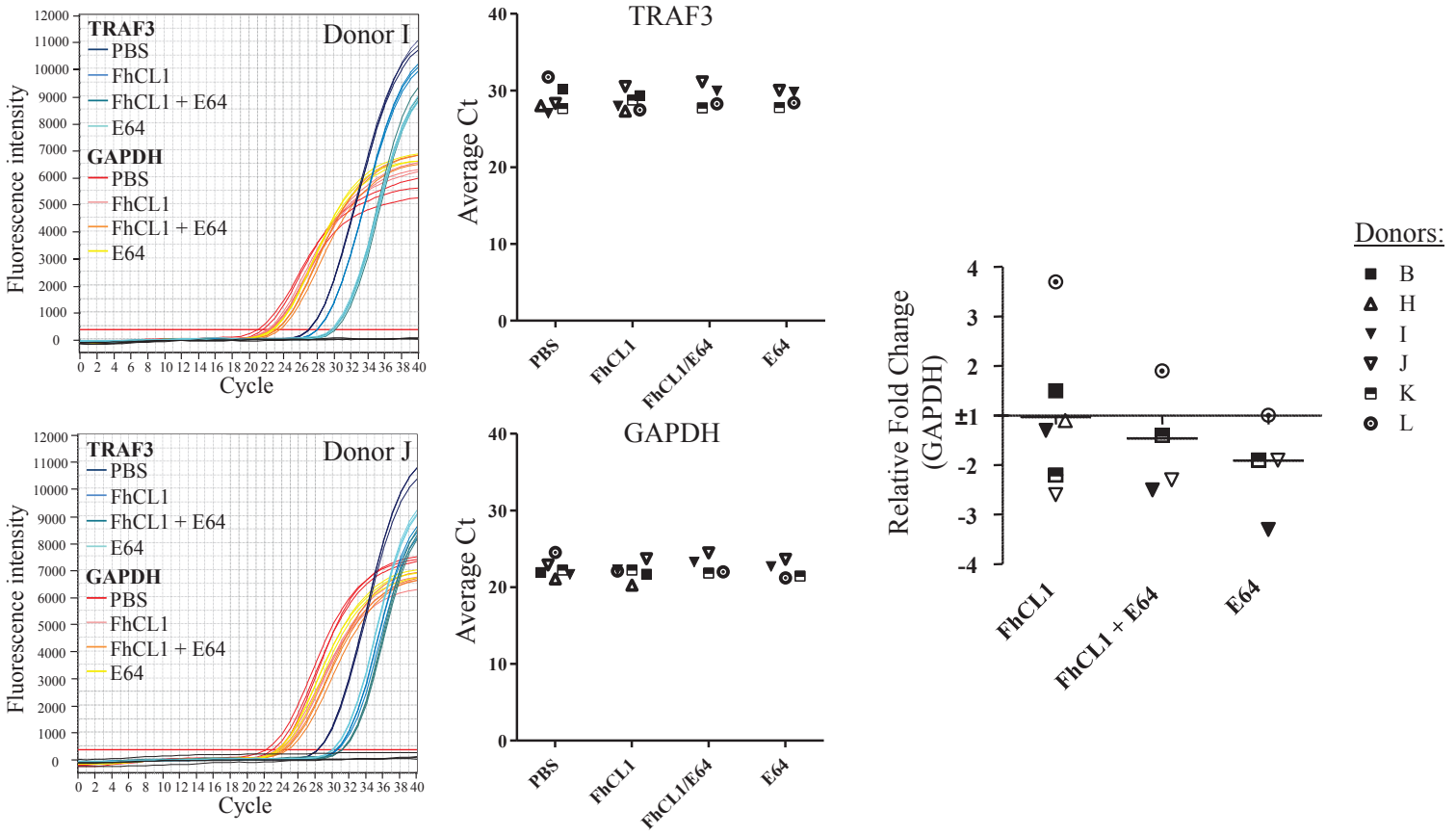

Figure 3.15: TRAF3 mRNA expression in primary human macrophages cultured with FhCL1.
Primary human macrophages were incubated with PBS, 20 µg/mL FhCL1, 20 µg/mL FhCL1 with 20 µM E64, or 20 µM E64, for 18 h. Data shown are representative fluorescence intensity RT-qPCR profiles for TRAF3 and GAPDH mRNA expression for two individual donors. Also shown are the average Ct values for up to six donors. Scatter graphs depict the fold change in cytokine expression relative to the reference gene GAPDH and compared to the expression in PBS-treated macrophages. Horizontal bars are means from up to six donors. Data were analysed by one sample Wilcoxin t-test, and no statistically significant differences were observed between any treatment groups.

IκKε and TRAF family member-associated NF-κB activator Binding Kinase (TBK1), phosphorylate IRF3 (Fitzgerald *et al.* 2003) (Figure 3.1) resulting in its translocation into the nucleus, where it activates promoters containing IRF3 binding sites (Hiscott *et al.* 1999). Thus phosphorylation of IRF3 indicates activation of the TRIF signalling pathway. Given that treatment of human macrophages with FhCL1 resulted in down-regulation of IL-10 and CD86, it was hypothesised that IRF3 phosphorylation may be altered, i.e. down-regulated following FhCL1 treatment. This is important because IRF3 phosphorylation induces IFN-β expression (Grandvaux *et al.* 2002) which through the JAK/STAT pathway induces IL-10 and CD86 expression (Rudick *et al.* 1996; Chang *et al.* 2007; Wiesemann *et al.* 2008). First, RT-qPCR was performed to determine IRF3 mRNA expression following FhCL1 treatment. Primers for the amplification of IRF3 (Izaguirre *et al.* 2003) were optimised for annealing temperature (data not shown), primer concentration and amplification, as previously described (Figure 3.16). IRF3 primers successfully and quantitatively amplified a single product with no primer dimer (Figure 3.16). As expected, the no cDNA template control showed no product amplification. Human macrophages were treated with PBS, 10 μg/mL FhCL1, 10 μg/mL FhCL1 with 10 μM E64 or 10 μM E64 and IRF3 mRNA expression was examined by RT-qPCR. However, monocyte-derived macrophages treated with FhCL1 showed no difference in IRF3 mRNA expression compared to PBS control cells (Figure 3.17) and treatment with FhCL1 with E64 inhibitor or E64 alone had no effect on IRF3 mRNA expression (Figure 3.17). Furthermore, LPS stimulation significantly down-regulated IRF3 mRNA expression, but FhCL1 pre-treatment had no significant effect on IRF3 mRNA expression (Figure 3.17). FhCL1 with E64 also had no effect on IRF3 expression. Therefore, FhCL1 does not modulate IRF3 at the mRNA level.

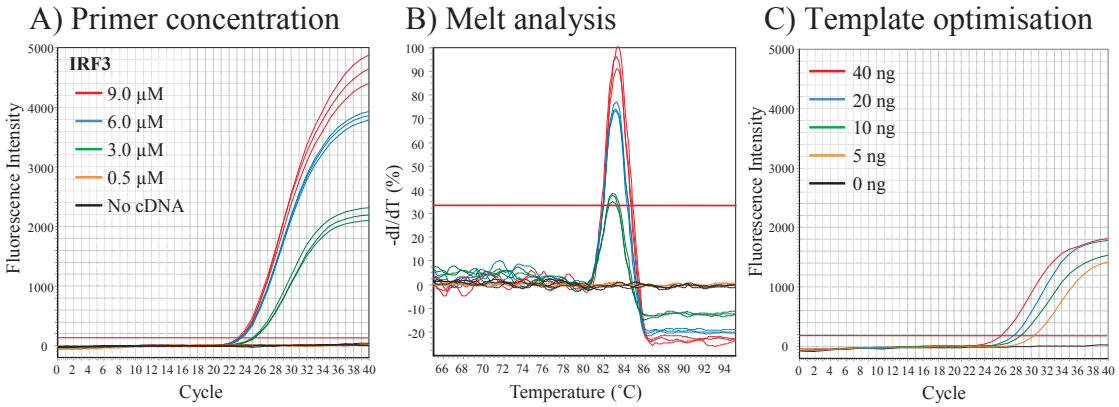

Figure 3.16: Optimisation of IRF3 primers for RT-qPCR analysis.
A) Optimisation of primer concentration for amplification of IRF3. The primer combinations included 9.0, 6.0, 3.0 and 0.5 µM for both primers. Data shown are only equal concentrations of forward and reverse primers. B) Melt curve analysis illustrating single PCR product amplification. C) Real time RT-PCR, showing serial 2-fold cDNA template dilution, demonstrating quantitative amplification.

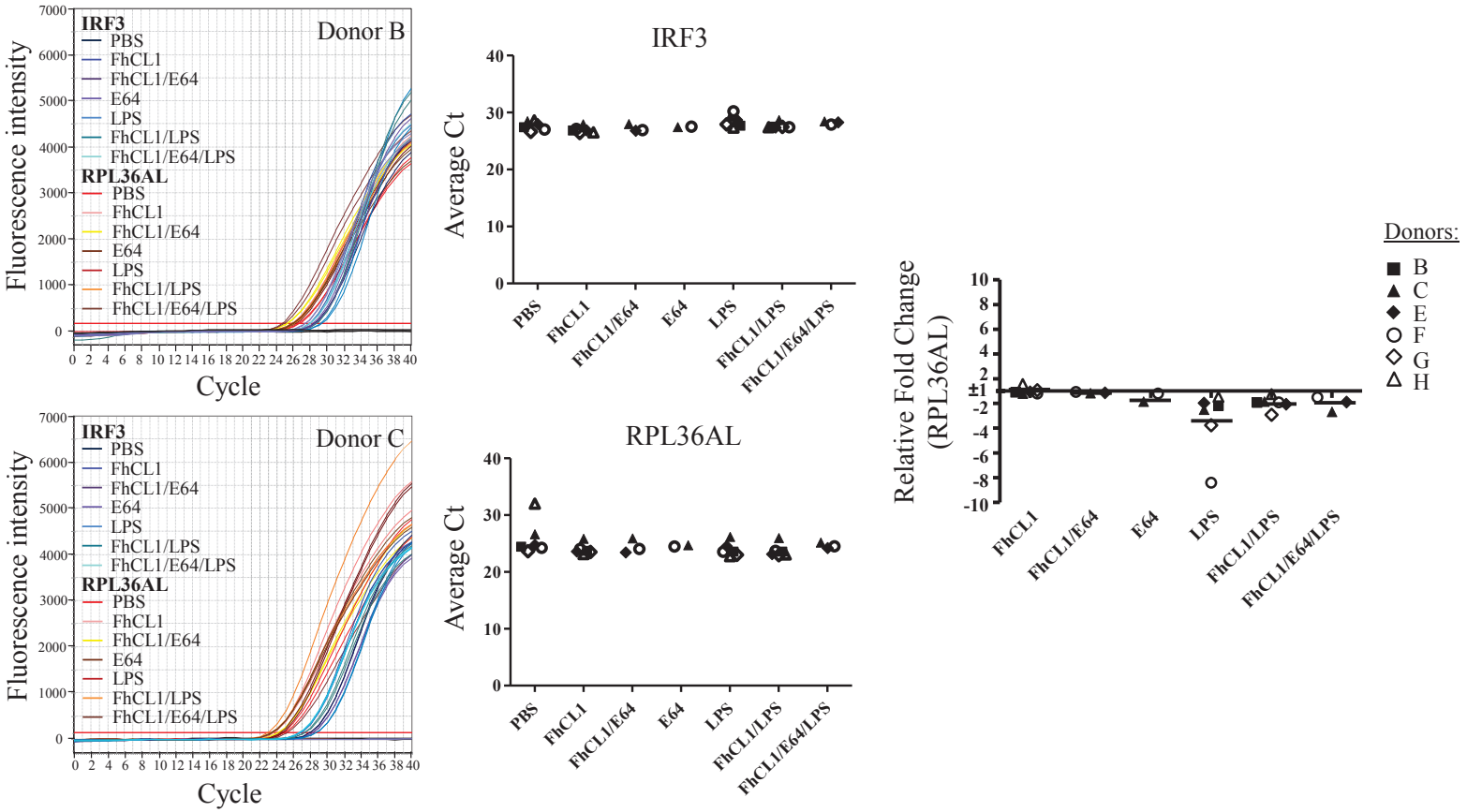

Figure 3.17: IRF3 mRNA expression in primary human macrophages cultured with FhCL1.
Primary human macrophages were incubated with PBS, 10 µg/mL FhCL1, 10 µg/mL FhCL1 with 10 µM E64, or 10 µM E64, for 18 h and with or without 50 ng/mL LPS for 6 h. Data shown are representative fluorescence intensity RT-qPCR profiles for IRF3 and RPL36AL mRNA expression for two individual donors. Also shown are the average Ct values for up to six donors. Scatter graphs depict the fold change in cytokine expression relative to the reference gene RPL36AL and compared to the expression in PBS-treated macrophages. Means (horizontal bars) are also shown. Data were analysed by Wilcoxin matched pairs t-test with no statistically significant differences observed between any data pairs.

To examine post translational changes in IRF3, investigation of IRF3 protein expression and phosphorylation was conducted by western blotting, as part of a parallel investigation performed by a colleague. This analysis indicated that FhCL1 treatment had no convincing effect on the expression of IRF3 when compared to macrophages cultured with PBS (A. Hutchinson, unpublished, data not shown). Similarly, LPS stimulation for up to 6 h demonstrated that FhCL1-treatment had no effect on the level of phosphorylated IRF3 (A. Hutchinson, unpublished, data not shown). Therefore, taken together, the RT-qPCR and western analysis indicated that FhCL1 had no significant effect on IRF3 phosphorylation or expression.

3.3 DISCUSSION

This thesis has described, for the first time, the immune-modulatory effect of FhCL1 on human monocyte-derived macrophages. It was observed that FhCL1 treatment down-regulates expression of the cell surface marker CD86, and down-regulates IL-10 and TRAF3 expression. Furthermore, FhCL1-treatment increased the surface and intracellular expression of the LPS co-receptor, CD14 in response to LPS stimulation and enhanced cell activation through increased phosphorylation of ERK1, ERK2 and IκBα, and up-regulation of pro-inflammatory cytokines IL-6 and IL-8 following LPS stimulation.

During the completion of these studies, two concentrations of FhCL1 were investigated, 10 μg/mL and 20 μg/mL. Within experiments, the concentration was kept consistent, ensuring that the observed effects of FhCL1 were not affected by this variable. However, investigations into the effect of FhCL1 on human macrophages could be enhanced by performing a dose response curve at the protein level. With regard to controls, the cysteine protease inhibitor E64 was included in the majority of experiments. In the presence of E64, FhCL1 had approximately only 20% residual activity (J. To, data not shown), and where results differed between FhCL1-treated and FhCL1 with E64-treated macrophages, this suggested that enzymatic activity may have been mediating these effects. Although, in most cases FhCL1 with E64 had the same effect as FhCL1 alone, suggesting that either 20% activity is sufficient to mediate the effects of FhCL1, or that enzymatic activity is not required for each effect being examined. Unfortunately, during the completion of the cytokine bead array studies, the cysteine protease inhibitor E64 had not yet been included in the study. Previous studies have established that the immune-modulatory mechanism of FhCL1 is dependent upon its enzymatic activity (Donnelly *et al.* 2010; Dowling *et al.* 2010). This means that conclusions cannot be drawn based on the requirement for the enzymatic activity of FhCL1 in the modulation of cytokine expression in human macrophages. Interpretation of this data may be further enhanced by the inclusion of additional controls. Potential candidates include an enzymatically inactive 'kinase dead' mutant of FhCL1 in which amino acids which are essential to enzymatic activity are replaced, or heat-inactivated FhCL1. Both of which would establish that the FhCL1-mediated effects were dependent upon enzymatic activity. However, a heat inactivated control may also cause spurious

results as cells may handle a denatured protein differently compared to an intact protein. Alternatively, an irrelevant protein such as BSA might be useful as this would confirm that the effects seen were specific to FhCL1. Comparison to human recombinant cathepsin L would also be of value, as this would allow for comparison between protease substrate activities between human and *F. hepatica* encoded enzymes, however this reagent was not available.

Achieving statistical significance within the data set was hampered by difficulties in working with human donor monocyte-derived macrophages. For example, the donors included in this study were obtained over a period of approximately three years with different donors each time. This was confounded by experimental variables such as baseline differences in instruments such as the LSRII flow cytometer over the three years. As a consequence, MFI values should not be directly compared across individual experiments. Therefore, different donor cohorts were plotted individually to assess trends in the effects of FhCL1 on surface and intracellular proteins. In the case of western blot analyses, pooled macrophages from multiple donors were used in order to obtain sufficient protein to perform the analyses. Therefore, the results indicate a general trend and have been interpreted as such. Furthermore, western blots need to be repeated in independently acquired cohorts of individual donors. Secondly, for ethical reasons no identifying information was attached to the individual donor. However, this meant that there was no patient history and information regarding previous infection status for each donor and hence basal activation status. Furthermore, human donors had the likely potential to be heterogenous in genotypes for genes known to alter the extent of responses including those to LPS. For example, polymorphisms in the TNF gene are known to alter its gene expression level (Pociot *et al.* 1995; Wilson *et al.* 1997), just as polymorphisms in the SLC11A1 gene can result in differences in macrophage activation status and cytokine expression (Searle *et al.* 1999; Awomoyi *et al.* 2002; Zaahl *et al.* 2004).

Investigation into the effect of FhCL1-treatment on cytokine expression in monocyte-derived macrophages at both the mRNA and protein level highlighted a discrepancy in the differences in expression, with FhCL1 having no significant effect on IL-10 mRNA expression post LPS stimulation, while significantly down-regulating IL-10 protein secretion post LPS stimulation. However, mRNA was analysed at 6 h post LPS

stimulation and protein expression analysed at 24 h post LPS stimulation. These time points were chosen so as to investigate initial changes in cytokine mRNA expression, versus the accumulated cytokine secretion over time, respectively. Therefore, the differences in cytokine expression are most likely due to assaying different time points. Thus, a time course investigation into changes in cytokine mRNA expression may have been informative. However, such analysis is expensive and difficult given the limited human donor monocyte-derived macrophage sample material available for each experiment. Furthermore, this study examined changes in cytokine expression in primary human macrophages pre-treated with FhCL1 for 18 h and stimulated with LPS for 6 h. Although not assessed as part of this study, it should be considered that a different experimental outcome may have resulted from simultaneous treatment of primary human macrophages with FhCL1 and LPS or alternatively stimulation of macrophages with LPS followed by FhCL1-treatment. Both alternatives could be investigated as part of future studies.

It should also be noted that not all cytokines that showed a change in secretion were investigated at the mRNA level. For example, secretion of IL-6 and IL-8 proteins were up-regulated by FhCL1 treatment following LPS stimulation, however, these cytokines were not investigated at the mRNA level. Within this context, investigation into the effect of FhCL1 on cytokine secretion was considered more important. This is because changes at the cytokine mRNA level are not always indicative of changes at the protein level, as many cytokines are known to undergo post-transcriptional regulation. For example, the mRNA stability of TNF, IL-6, IL-8, IL-1β and IL-10 is regulated via 3'-AU-rich mRNA motifs (Neininger *et al.* 2002; Zhang *et al.* 2002; Garnon *et al.* 2005; Chen *et al.* 2006; Lu *et al.* 2006; Paschoud *et al.* 2006; Winzen *et al.* 2007; Stoecklin *et al.* 2008), and as such, mRNA expression of these cytokines is frequently not indicative of cytokine secretion (Schook *et al.* 1994). Traditionally this is interpreted as tristetraproline and other 3'UTR proteins affecting mRNA half-life and thereby translation, but it is also now appreciated that microRNAs may similarly play a role in regulating protein expression levels of these cytokines (Jing *et al.* 2005). Furthermore, the increase in ERK1 and ERK2 protein expression following FhCL1 treatment was not associated with differences at the mRNA level. The reasons for this are currently unclear, but post-transcriptional regulation of ERK expression may also in part explain this difference. In fact, post-transcriptional regulation of ERK has been observed in

invertebrates and has recently been investigated in humans, with RNA binding proteins and microRNAs playing a role in post-transcriptional regulation of the MAPK pathway (Whelan *et al.* 2012). Having said this, not all changes in protein levels reflect translation or transcription per se, and other post-transcriptional regulation mechanisms may be involved. For example, total IκBα was decreased after LPS stimulation, and although this was unrelated to the amount and timing of its phosphorylation, it is likely to be due to its ubiquitination and degradation. This is because the inhibitor protein needs to be removed to allow for NF-κB activation.

In the context of *F. hepatica* infection, migration of the parasite out of the microflora populated gastrointestinal tract towards the liver is likely always associated with the exposure of internal tissues to parasite products, as well as bacteria and their products (Ogunrinade *et al.* 1982; Dalton 2006; Valero *et al.* 2006). Typically the release of bacteria would be expected to induce pro-inflammatory cytokines through TLR4-dependent cell signalling, even sometimes resulting in septic shock (Ferluga *et al.* 1979). However, helminth infection is often almost completely asymptomatic, suggesting that immune modulation by helminth parasites generally suppress the response to bacteria (Maizels *et al.* 2004). For this reason, it is relevant to examine the effect of parasite-derived molecules on innate immune cells in combination with bacterial products such as LPS.

One of the findings of this chapter was that treatment with FhCL1 modulated CD14 protein expression in human monocyte-derived macrophages. CD14 is required for the binding of LPS by TLR4 (Wright *et al.* 1990; Kitchens 2000) and following the ligation of the LPS-LBP complex, CD14 subsequently presents LPS to the TLR4/MD-2 complex (Kitchens *et al.* 1998; Aderem *et al.* 2000; Triantafilou *et al.* 2002). In this study, treatment with FhCL1 up-regulated surface CD14, both with and without LPS stimulation. Up-regulated surface CD14 is known to be associated with increased expression of pro-inflammatory cytokines in human fibroblasts (Sugawara *et al.* 1998; Tamai *et al.* 2002), just as was evident in monocyte-derived macrophages. In addition to the up-regulation of surface CD14, FhCL1 up-regulated intracellular CD14 1 h post LPS stimulation, although there was no detectable effect on the localisation of CD14 within monocyte-derived macrophages. This indicated that FhCL1 was not up-regulating surface CD14 by preventing the internalisation of CD14, meaning increased

surface CD14 was not simply due to its surface accumulation. Given CD14 plays a role in the recognition of bacterial LPS and the induction of pro-inflammatory cytokines (Sugawara *et al.* 1998; Tamai *et al.* 2002), up-regulation of CD14 by FhCL1 seems counter-intuitive to host survival and as a consequence, the longevity of the helminth within the host. Therefore, the biological significance of increased CD14 cannot be explained within the context of the current published literature. Investigation into CD14 mRNA levels would resolve whether FhCL1 transcriptionally induced CD14, or alternatively, whether these changes reflect protein turnover and recycling.

The effect of FhCL1 on cytokine secretion and phenotype in response to LPS stimulation was investigated in human monocyte-derived DCs (M. Lund, unpublished). LPS stimulation of FhCL1-treated DCs had no significant effect on the secretion of IL-1β, IL-12, IL-6, IL-8, TNF or IL-10 (M. Lund, unpublished). This was in contrast to the effect of FhCL1 on human monocyte-derived macrophages as shown here, in which FhCL1 up-regulated IL-6 and IL-8 secretion and down-regulated IL-10 secretion in response to LPS stimulation. These contrasting results suggest that FhCL1 might be interacting with a molecule(s) specific to macrophages. Surface CD14 in FhCL1-treated macrophages represents a potential candidate, as human monocyte-derived DCs are CD14 negative (O'Doherty *et al.* 1994). Together, this suggests that the modulation of CD14 is integral to the effects of FhCL1 on monocyte-derived macrophages.

FhCL1-treatment also down-regulated surface expression of CD86 in monocyte-derived macrophages. CD86 is a T cell co-stimulatory factor that is required for T cell activation (Hathcock *et al.* 1994). One possible mechanism by which FhCL1 may down-regulate surface CD86 is by enzymatically cleaving it. The substrate specificity of FhCL1 has not been completely characterised, and it is reported to be a promiscuous enzyme with broad substrate specificity (Robinson *et al.* 2011a). Nevertheless, substrates of FhCL1 include matrix proteins such as fibronectin, laminen and collagen (Berasain *et al.* 1997; Robinson *et al.* 2011a) and immunoglobulin (Smith *et al.* 1993a). In addition to degrading matrix proteins (Barrett *et al.* 1981), the substrate of human cathepsin L is also quite varied and includes the endocytosis protein dynamin (Sever *et al.* 2007), IL-8 precursor (Ohashi *et al.* 2003), the histone protein H3 histone proteins (Duncan *et al.* 2008). However, taking into account the fact that CD86 expression was also down-regulated by a similar degree in monocyte-derived macrophages treated with FhCL1 in

the presence of the cysteine protease inhibitor E64, it is unlikely that FhCL1 cleaves CD86. In fact, E64 was found to reduce FhCL1 activity by approximately 80% (J. To, data not shown), and thus, given that the reduction of enzymatic activity resulted in a similar down-regulation of CD86, it can be concluded either that enzymatic activity is not necessary for the modulation of CD86 expression, or that 20% activity is sufficient to degrade surface CD86.

An alternative explanation is that FhCL1 may be altering a cell signalling pathway(s) that induces/regulates the expression of CD86. Modulation of TLR signalling is a mechanism of immune modulation commonly observed after exposure of APCs to helminth molecules (van der Kleij *et al.* 2004; Goodridge *et al.* 2005; Semnani *et al.* 2008). Surface CD86 expression is induced by TLR4 cell signalling following LPS stimulation, as confirmed by studies using TLR4-knockout mouse DCs, in which the expression of CD86 was not induced following LPS stimulation (Kaisho *et al.* 2001; Yamamoto *et al.* 2002; Shen *et al.* 2008). Following recognition and binding of LPS by TLR4 and CD14, TLR4 signals through two pathways, the MyD88-dependent pathway which is initiated beneath the cell surface and is common to all TLRs except TLR3, and the TRIF-dependent pathway, which is initiated within endosomes and is utilised by only TLR4 and TLR3 (for reviews see Takeda *et al.* 2004; and Chaturvedi *et al.* 2009 and shown in Figure 3.18). Expression of CD86 is regulated by both the MyD88-dependent and TRIF-dependent signalling pathways, as evidenced by studies investigating CD86 expression in murine DCs from TIRAP-knockout, MyD88 and TIRAP-double knockout, MyD88-knockout and TRIF-knockout mice (Yamamoto *et al.* 2002; Shen *et al.* 2008). All of these knockout models have shown up-regulation of CD86 surface expression in response to LPS, indicating that CD86 expression is mediated by the remaining non-defective pathway. In unstimulated macrophages, FhCL1 down-regulates the expression of surface CD86, however, in response to LPS stimulation, FhCL1 had no significant effect on CD86 expression. Since LPS stimulation can up-regulate the expression of CD86 through either the MyD88- or TRIF- dependent pathways, it was possible that FhCL1 may have been modulating cell signalling via either of these pathways. However, in response to LPS, the unaffected pathway may compensate for CD86 expression and thus, mask the effect of FhCL1.

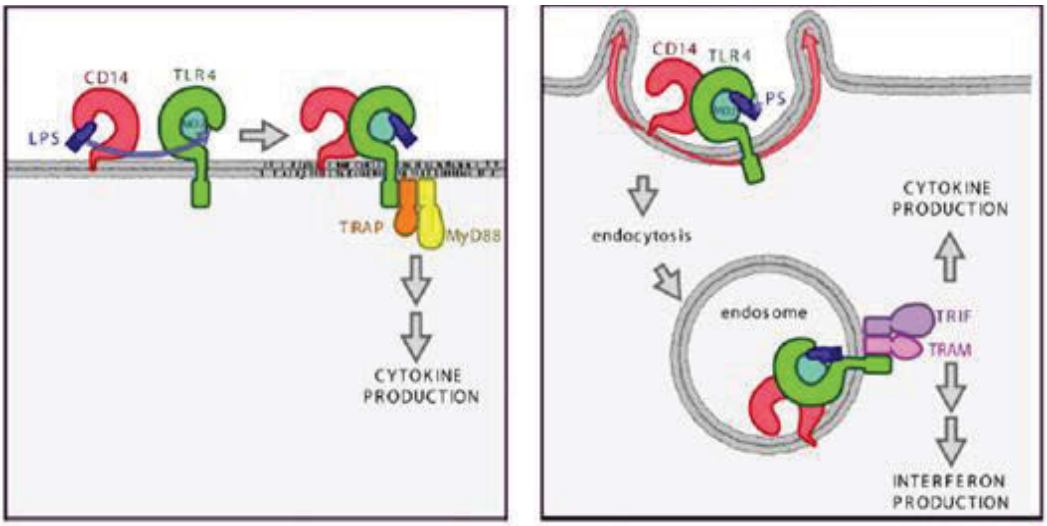

Figure 3.18: The location of the CD14/TLR4 complex determines cell signalling. Following recognition of LPS by CD14, CD14 and TLR4 complex and cell signalling is initiated at the cell surface via MyD88, resulting in expression of pro-inflammatory cytokines. The CD14/TLR4 complex is subsequently internalised where signalling occurs via the TRIF-dependent pathway, resulting in cytokine expression and interferon production. (Adapted from Zanoni *et al.* 2011).

Modulation of TLR signalling is also supported by the cytokine secretion profile of FhCL1-treated macrophages. Pro-inflammatory cytokines are induced by either the MyD88-dependent pathway through activation of NF-κB and AP-1 (reviewed in Medzhitov *et al.* 1998; Akira *et al.* 2004) or via the TRIF-dependent pathway through late NF-κB activation (Hoebe *et al.* 2003; Yamamoto *et al.* 2003; Kagan *et al.* 2008). In response to LPS stimulation, FhCL1-treated monocyte-derived macrophages up-regulate the secretion of pro-inflammatory cytokines IL-6 and IL-8. Therefore, as IL-6 and IL-8 are induced by NF-κB and AP-1 (Mukaida *et al.* 1989; Ray *et al.* 1989; Libermann *et al.* 1990), FhCL1 may have been modulating cell signalling via either the MyD88-dependent and/or TRIF-dependent pathways. Activation of NF-κB requires phosphorylation and degradation of IκBα (Beg *et al.* 1993; Sun *et al.* 1994), while activation of AP-1 requires phosphorylation of MAPK proteins, such as ERK1 and ERK2 (reviewed in Karin 1995; and Waskiewicz *et al.* 1995). Preliminary western blot experiments indicate that FhCL1 had no effect on protein expression levels of MyD88, TRIF or TRAF6 which are utilised early in the signalling pathway, but phosphorylation of IκBα, ERK1 and ERK2 was minimally enhanced in FhCL1-treated macrophages following LPS stimulation. Nevertheless, this suggests FhCL1 enhances the activation of cell signalling pathways shared by both MyD88 and TRIF, summarised in Figure 3.19.

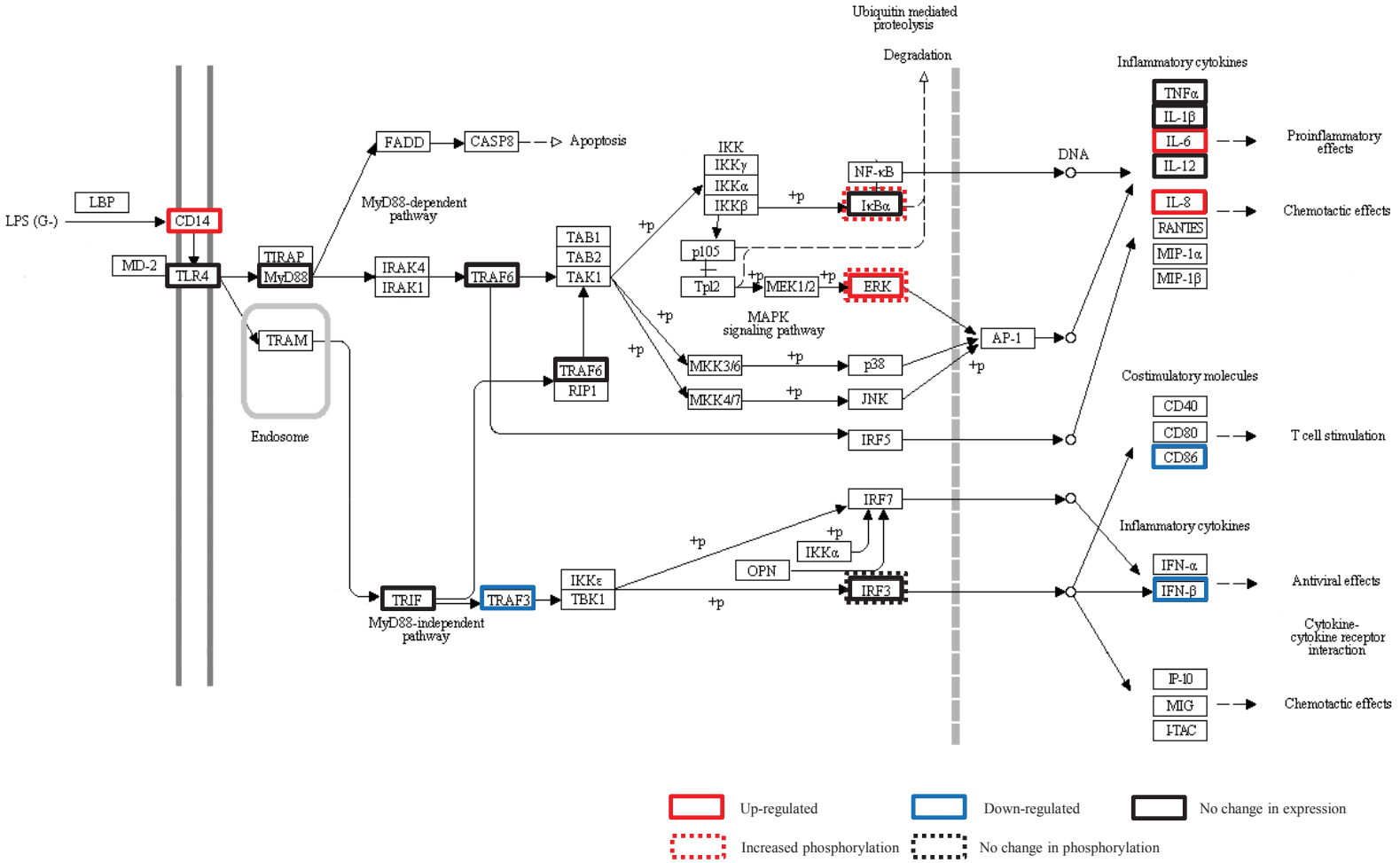

Figure 3.19: FhCL1 modulates the toll-like receptor signalling pathway.
Treatment of human macrophages up-regulates expression of surface CD14, which results in increased expression of ERK1/2 and enhanced phosphorylation of IκBα and ERK1/2. The activation of these pathways results in increased expression of pro-inflammatory cytokines, IL-6 and IL-8. However, FhCL1 treatment also modulates endosomal TRIF-dependent signalling, with down-regulation of TRAF3. This results in down-regulation of TRIF-dependent cytokine, IFN-β (M. Lund, unpublished) and down-regulation of co-stimulatory molecules CD86. (Adapted from KEGG pathway 2010).

The anti-inflammatory cytokine, IL-10 is also induced by both the MyD88-dependent and TRIF- dependent pathways. Indeed both murine DCs and macrophages from MyD88-knockout and TRIF-knockout mice demonstrate that both pathways control LPS-induced IL-10 expression (Boonstra *et al.* 2006; Shen *et al.* 2008). Thus, as FhCL1 enhanced both the MyD88- and TRIF- dependent pathways, the down-regulation of IL-10 in FhCL1-treated macrophages must have been due to a different mechanism to that of IL-6 and IL-8. It was proposed that FhCL1 may modulate cell signalling via the MyD88-independent, TRIF-dependent pathway. Signalling through the MyD88-independent, TRIF-dependent pathway is mediated by TRAF3, which is known to recruit IκB kinase ε (IKKε) and TBK1 and is essential for the expression of IFN-β and IL-10 (Hacker *et al.* 2006) (summarised in Figure 3.19). In fact TRAF3-deficient cells overproduce pro-inflammatory cytokines due to the lack of IL-10 expression (Hacker *et al.* 2006). Western blot analysis of TRAF3 demonstrated that FhCL1 slightly down-regulated TRAF3 expression, with FhCL1 with E64 having less of an effect. This may therefore explain the suppression of IL-10 secretion and CD86 expression by FhCL1 in human monocyte-derived macrophages. However, it is important to note that the western blot for TRAF3 had high levels of non-specific binding, which diminishes the confidence in this result. It is an important result nonetheless and its potential significance cannot be overlooked. Moreover, as the protease inhibitor E64 reduced the FhCL1-induced decrease in TRAF3, this additionally suggests that FhCL1 enzymatically acts on TRAF3 in human macrophages. More precise characterisation of the proteolytic specificity of FhCL1 would likely shed light on how this might occur. The decrease in TRAF3 expression differed to the effect of FhCL1 on murine peritoneal macrophages, where TRAF3 was unaffected by FhCL1 treatment (Donnelly *et al.* 2010). The reason for this difference is at this point unclear and may be due to differences in *ex vivo* peritoneal macrophages and human blood monocyte-derived macrophages, as it is unlikely that FhCL1 would cleave human but not murine TRAF3. Further experiments, for example potentially using different TRAF3 specific antibodies, may help to reconcile these results, especially given the high degree of background evident in the western blots with the current antibody.

The mRNA expression of TRIF-dependent cytokine IFN-β was also investigated in human monocyte-derived macrophages, with this study demonstrating that FhCL1

treatment had no effect on IFN-β mRNA expression either alone or at 6 h post LPS stimulation. However, a parallel study investigated IFN-β mRNA expression in FhCL1-treated human macrophages at 1 h and 3 h post LPS stimulation and demonstrated down-regulation of IFN-β mRNA in response to LPS stimulation at the 1 h time point (M. Lund, unpublished). Type 1 interferons have previously been reported to induce IL-10 in response to LPS, as C57BL/6 mice macrophages treated with a neutralising antibody specific to IFN-β resulted in decreased IL-10 expression (Chang *et al.* 2007; Iyer *et al.* 2010). Furthermore, human peripheral blood mononuclear cells cultured with IFN-β up-regulate IL-10 expression (Rudick *et al.* 1996). Therefore, this provided further support for the model that FhCL1 suppresses the TRIF-dependent signalling pathway and correlates with the down-regulation of IL-10. The suppression of IFN-β mRNA expression at 1 h post LPS stimulation in FhCL1-treated human monocyte-derived macrophages is supported by studies using peritoneal macrophages from BALB/c mice, with reduced mRNA expression of IFN-β in FhCL1-treated macrophages 6 h post LPS-stimulation (Donnelly *et al.* 2010). Taken together, there was no obvious explanation for the fact that in this study, recombinant FhCL1 had no effect on IFN-β expression at 6 h post LPS stimulation compared to murine macrophages. Investigation of IFN-β protein expression in FhCL1-treated human monocyte-derived macrophages would also add value to the study to examine whether the differences observed at 1 h post LPS stimulation by RT-qPCR equated to differences at the protein level. The mechanism by which IFN-β expression is suppressed in human monocyte-derived macrophages is yet to be elucidated and attempts to identify this mechanism by investigating the phosphorylation of IRF3 indicated that FhCL1 had no significant effect on IRF3 phosphorylation (A. Hutchinson, unpublished).

Collectively, the FhES products of *F. hepatica* facilitate immune modulation in mice through a variety of mechanisms, namely, alternative activation of macrophages, suppression of pro-inflammatory Th1 responses and induction of anti-inflammatory Th2/regulatory T cell responses (Donnelly *et al.* 2008; Carranza *et al.* 2012). Treatment of human monocyte-derived macrophages with FhCL1 did not induce alternative macrophage activation, as FhCL1 did not up-regulate markers of alternative activation, i.e. mannose receptor (CD206) and haemoglobin scavenger receptor (CD163).

Furthermore, analysis of cytokine levels indicated that treatment of human macrophages with FhCL1 did not increase expression of the Th2/regulatory T cell cytokine IL-10 in response to LPS or down-regulate expression of Th1 cytokines, IL-1β, IL-12, IL-6, IL-8 and TNF, commonly associated with helminth infection, such as *F. hepatica* (O'Neill *et al.* 2000; Allen *et al.* 2011). Ultimately, this demonstrates that the immune modulation induced by FhES is not induced by FhCL1 alone, and it is therefore more likely that FhCL1 modulates immune responses in human macrophages by an alternative mechanism(s), such as altered TLR signalling.

Within BALB/c peritoneal macrophages, FhCL1 was also demonstrated to modulate TLR signalling, inhibiting the TRIF-dependent pathway (Donnelly *et al.* 2010). FhCL1 treatment down-regulated TRIF-dependent IFN-β mRNA expression (Donnelly *et al.* 2010). This was associated with down-regulation of iNOS and IL-12 in response to LPS (Donnelly *et al.* 2010), both of which are induced by IFN-β (Kawai *et al.* 2001; Thomas *et al.* 2006). Pro-inflammatory cytokines, IL-6 and TNF, were also down-regulated in response to LPS, which was attributed to modulation of TRIF-dependent, late NF-κB activation (Donnelly *et al.* 2010). However, the cytokine profile of FhCL1-treated primary human monocyte-derived macrophages indicated that analogous changes were not induced in human monocyte-derived macrophages as in murine peritoneal macrophages (summarised in Figure 3.20). Instead, secretion of pro-inflammatory cytokines, namely IL-6 and IL-8, was enhanced by FhCL1 treatment in response to LPS, with no change in TNF or IL-12 secretion. Interestingly, FhCL1 treatment of murine DCs was shown to up-regulate pro-inflammatory cytokine expression, including IL-6 and IL-12, by a TLR4-dependent mechanism, although this was not in response to LPS stimulation (Dowling *et al.* 2010). Thus this provides further support for potential FhCL1 modulation of TLR signalling in human monocyte-derived macrophages and also demonstrates precedence for FhCL1 up-regulation of pro-inflammatory cytokines.

There are a number of potential reasons for the differences in FhCL1-mediated immune modulation between the murine and human studies. Firstly, the current study was completed in an *in vitro* model using monocyte-derived macrophages isolated from peripheral blood, while the murine study utilised peritoneal macrophages isolated from mice that were intraperitoneally injected with FhCL1, prior to *ex vivo* stimulation with

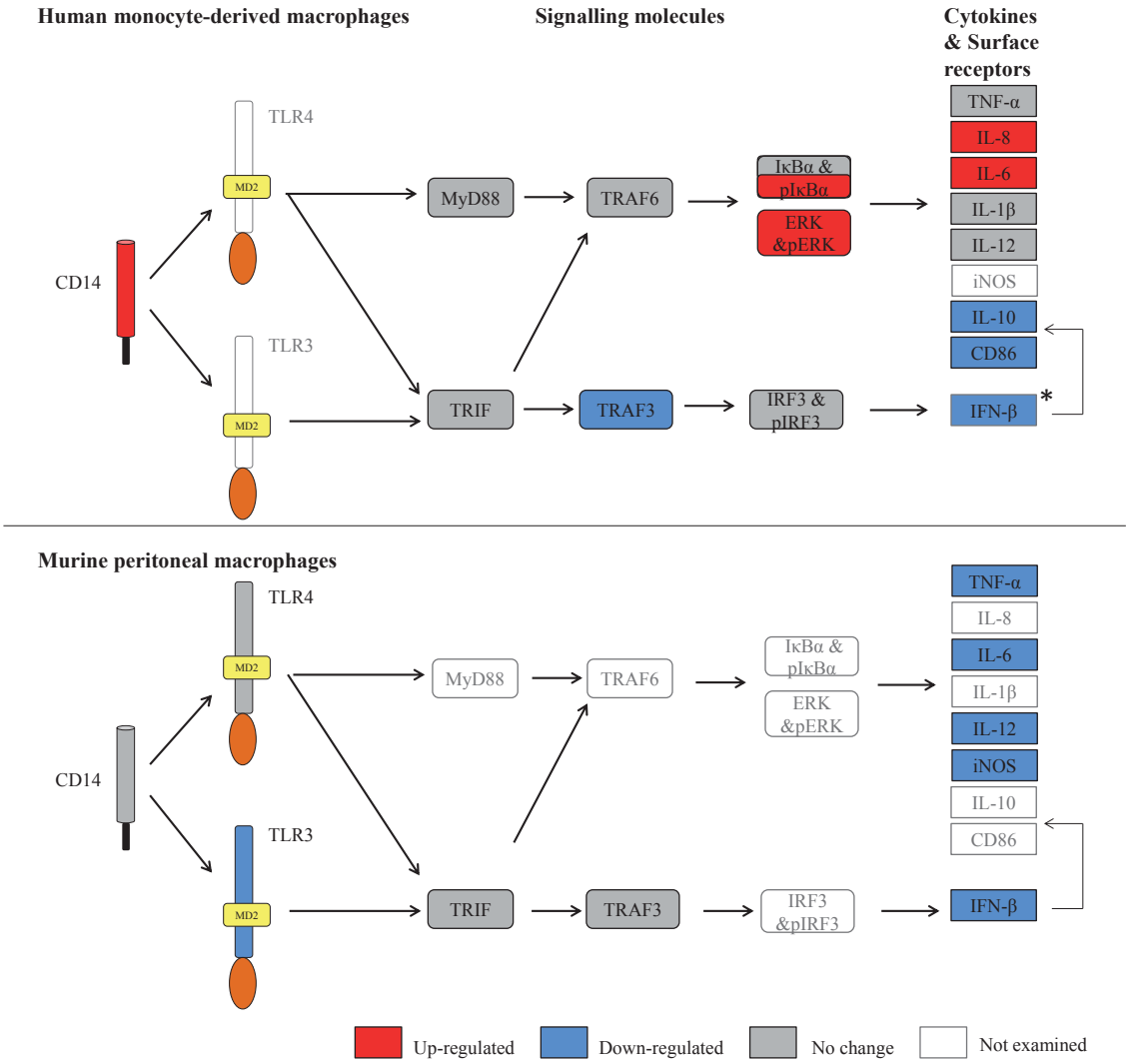

Figure 3.20: Immune-modulatory effects of FhCL1 on macrophages are species- or cell type- specific.

The immune-modulatory effect of FhCL1 on macrophages differs depending on the species or cell type. Both human and murine macrophages showed suppression of the TRIF-dependent signalling pathway. In human monocyte-derived macrophages this was associated with down-regulation of TRAF3, while in murine peritoneal macrophages this was associated with cleavage of endosomal TLR3 (Donnelly *et al.* 2010). The effect of FhCL1 on the expression of pro-inflammatory cytokines in human and murine macrophages also differed, with FhCL1 increasing surface CD14, resulting in enhanced expression of pro-inflammatory cytokines IL-6 and IL-8. Contrastingly, FhCL1 had no effect on CD14 expression in murine macrophages and pro-inflammatory cytokines TNF, IL-6, IL-12 and iNOS were down-regulated (Donnelly *et al.* 2010), which was associated with suppression of TRIF-dependent, late NF-κB activation. * M. Lund, unpublished.

LPS *in vitro* (Donnelly *et al.* 2010). Due to the treatment of mice with FhCL1 taking place *in vivo*, it is likely that other factors contributed to the activation of murine macrophages. For example, it is likely that peritoneal neutrophils produce IL-8 to influence murine macrophage maturation and activation, and hence function or immune molecule expression. Secondly, investigations into the immune modulatory effect of FhCL1 in BALB/c mice had the advantage that mice were genetically identical, removing the potential effect of differing genotypes on the response of individual mice to FhCL1. Furthermore, mice were housed under specific pathogen free conditions, ensuring naïve baselines and similar responses. Investigations in murine models must also take into account the genetic background of the mice that experiments were performed in, with well reported differences in disease susceptibility and immune responses between strains. For example, during *Leishmania major* infection, C57BL/6J mice are predisposed to produce a predominately Th1 immune response, while BALB/c mice have a more Th2 dominated immune response (Locksley *et al.* 1987; Gessner *et al.* 1993). The dichotomous immune responses between strains results in difference in susceptibility to infection, with BALB/c mice susceptible to *L. major* infection and C57BL/6 mice resistant to infection (Locksley *et al.* 1987; Gessner *et al.* 1993). Likewise, during LPS stimulation, C56BL/6J mice produce significantly higher levels of TNF and IL-12 compared to BALB/c mice, with relatively no difference in IL-10 secretion (Watanabe *et al.* 2004). Therefore, the down-regulation of pro-inflammatory responses in FhCL1-treated peritoneal macrophages from BALB/c mice in response to LPS stimulation (Donnelly *et al.* 2010), may be influenced by the predominant Th2 response in the BALB/c mouse strain.

CHAPTER 4:

THE EFFECT OF FHCL1 ON TOLL-LIKE RECEPTORS AND INTRACELLULAR TRAFFICKING IN HUMAN MACROPHAGES

4.1 INTRODUCTION

The ES products of helminth parasites are able to modulate immune responses in a number of ways, including the induction of alternative macrophage activation or tolerogenic DCs, the induction of T cell anergy and modulation of TLR signalling. The immune-modulatory effects of FhCL1 have been investigated in murine macrophages, where FhCL1 was shown to localise within the endosomes of murine macrophages, where it modulates TLR signalling by degrading TLR3, which signals exclusively through the TRIF-dependent pathway. The degradation of TLR3 was associated within decreased expression of TRIF-dependent inflammatory mediators in response to LPS stimulation, namely, nitric oxide (NO), IL-6, IL-12 and TNF (Donnelly *et al.* 2010). This chapter investigates the effects of FhCL1 on TLR signalling in primary human monocyte-derived macrophages to determine whether similar effects occur in human macrophages as documented in murine peritoneal macrophages.

The culture of primary human monocyte-derived macrophages in the presence of FhCL1 led to an increase in the expression of pro-inflammatory, MyD88 and TRIF-dependent cytokines and a decrease in the expression of MyD88-independent, TRIF-dependent cytokines (Chapter 3). TLR4 signalling through the MyD88-dependent pathway is initiated following formation of the TLR4/LPS/CD14 complex at the cell surface (Kagan *et al.* 2008), while TRIF-dependent signalling takes place following the endocytosis of the TLR4/LPS/CD14 complex (Kagan *et al.* 2008; Watts 2008; Chaturvedi *et al.* 2009). Further investigation identified an up-regulation of surface CD14 in human macrophages following FhCL1 treatment, which was suggested to be responsible for the up-regulated expression of MyD88-dependent cytokines (Figure 3.7 and Figure 3.8). However, as CD14 is essential for the endocytosis of the TLR4/LPS complex required for TRIF-dependent signalling (Jiang *et al.* 2005; Tanimura *et al.* 2008), the up-regulation of surface CD14 itself was unlikely to be the cause of the inhibition of TRIF-dependent signalling observed.

Data collected thus far suggested two possible mechanism of potential immune-modulation induced by FhCL1. Firstly, in murine macrophages, FhCL1 modulated TRIF-dependent signalling by cleavage of TLR3 (Donnelly *et al.* 2010). Thus, it is possible that, in human macrophages, FhCL1 may degrade TLRs, or an associated

molecule, thus preventing TRIF-dependent signalling. Given that only TLR3 and TLR4 signal through the TRIF-dependent pathway, both represent potential targets for modulation by FhCL1 in primary human macrophages. Therefore, this chapter comprises a study of the expression and localisation of TLR3 and TLR4 within human macrophages to further investigate the mechanism of immune modulation by FhCL1.

The second potential mechanism is that FhCL1 may possibly be involved in the modulation of trafficking of the TLR4/LPS/CD14 complex into endosomes, and thereby influence TRIF-dependent signalling (Husebye *et al.* 2006; Saitoh 2009). If FhCL1 inhibits endosomal trafficking, signalling via the MyD88-dependent pathway which takes place beneath the cell membrane may be enhanced, while endosome-based TRIF-dependent signalling would be suppressed. Therefore, this chapter also investigates LPS uptake and trafficking protein expression and localisation in FhCL1-treated human macrophages.

4.1.1 SPECIFIC AIM

Studies in murine macrophages have shown that, FhCL1 co-localises with endolysosomes (Donnelly *et al.* 2010). To further investigate the immune-modulatory effects of FhCL1 in human macrophages, the uptake and localisation of FhCL1 will be examined. Furthermore, FhCL1 has been observed to influence TLR signalling by enhancing the expression of pro-inflammatory cytokines and by suppressing TRIF-dependent signalling. Therefore, the effect of FhCL1 on the expression and localisation of key cellular proteins associated with TLR signalling and endosome trafficking will be investigated.

4.2 RESULTS

4.2.1 INTERNALISATION OF FHCL1 BY PRIMARY HUMAN MACROPHAGES

In primary human macrophages, treatment with FhCL1 significantly increased the expression of surface and intracellular CD14 in response to LPS stimulation (Figure 3.8 and Figure 3.9), which was correlated with increased expression of IL-6 and IL-8 (Figure 3.6), and increased phosphorylation of IκBα, ERK1 and ERK2 (Figure 3.11 and Figure 3.12). Thus FhCL1 treatment resulted in the expression of pro-inflammatory cytokines, likely by involving both the MyD88- and TRIF-dependent signalling pathways. Treatment with FhCL1 also down-regulated the expression of TRAF3, an intermediate in the TRIF signalling pathway, and down-regulated expression of CD86 (Figure 3.8B) and IL-10 (Figure 3.6). However, the precise mechanism by which FhCL1 was mediating these observed changes was yet to be elucidated. In murine macrophages, FhCL1 was rapidly internalised and found to co-localise with early endosomes, and lysosomes at 2 h post treatment (Donnelly *et al.* 2010). It was therefore hypothesised that FhCL1 was also internalised by human macrophages and acted intracellularly to mediate these effects. To investigate this hypothesis, the uptake and localisation of FhCL1 within human macrophages was examined by flow cytometry and confocal microscopy.

First, recombinant FhCL1 was conjugated to FITC (FhCL1-FITC) and primary human monocyte-derived macrophages were then cultured with 20 μg/mL FhCL1-FITC over an 18 h time course. Flow cytometry analysis demonstrated that increased fluorescence over unstained control cells was detectable as early as 5 min post FhCL1-FITC incubation (Figure 4.1). This indicated rapid uptake of FhCL1-FITC, or binding of FhCL1-FITC to the surface of macrophages. The uptake and/or binding of FhCL1-FITC continued to increase up to 2 h post incubation, and by 18 h there was a substantial increase in surface or internalised fluorescence (Figure 4.1). Thus, while FhCL1 surface binding or uptake occurred as early as 5 min post incubation, maximal FhCL1-FITC surface binding or uptake occurred over 18 h.

To determine if the increase in fluorescence observed in primary human macrophages cultured with FhCL1-FITC was indicative of uptake and internalisation of FhCL1,

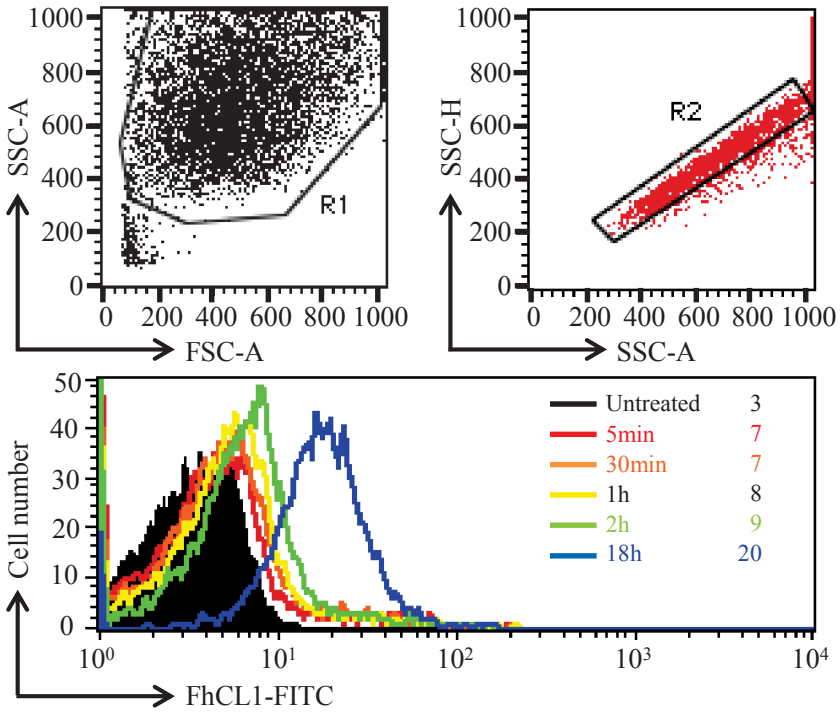

Figure 4.1: Flow cytometry analysis of FhCL1 uptake or binding by primary human macrophages.

Primary human macrophages were cultured with 20 µg/mL FITC-conjugated FhCL1 over a time course up to 18 h. The uptake/binding of FhCL1 was determined by flow cytometry after gating on the single cell macrophage population (SSC-A versus SSC-H dot plot; R2). Data shown are histogram overlays with MFI values as indicated, for unstained (black filled histogram) and FITC-conjugated FhCL1 (coloured unfilled histograms).

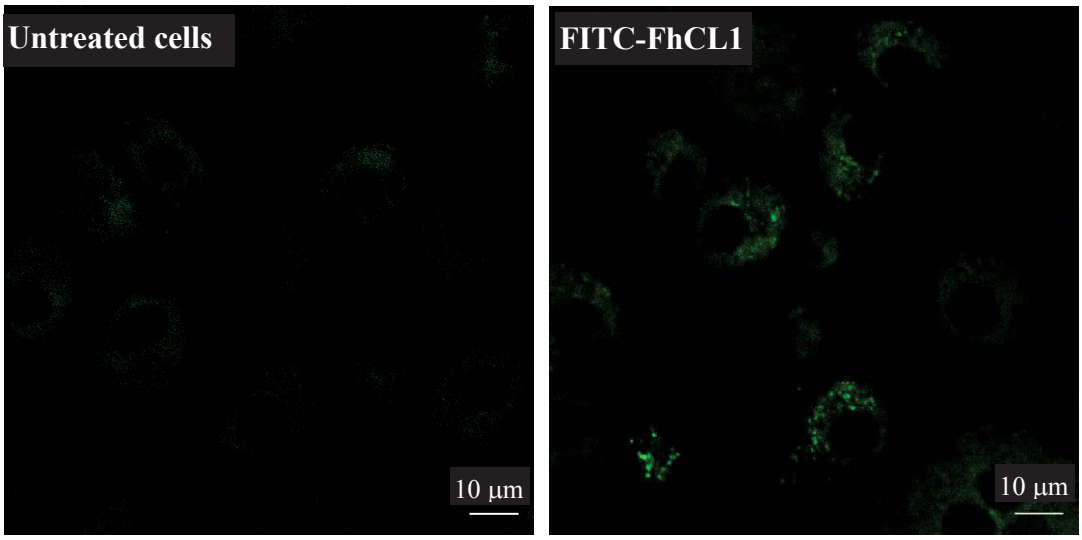

Figure 4.2: Confocal microscopy analysis of FhCL1 uptake by primary human macrophages.

Primary human macrophages were cultured with 20 µg/mL FITC-conjugated FhCL1 for 18 h and compared to untreated control cells. Imaging was performed following fixation, using the Nikon A1 Confocal Scanning Laser Microscope. Data shown are representative of two independent experiments, each with a minimum of 10 images acquired per treatment with a minimum of 110 cells examined in total.

immunofluorescence microscopy was utilised to examine the subcellular levels and localisation of FhCL1 within macrophages. Confocal microscopy analysis indicated that macrophages incubated with 20 μg/mL FhCL1-FITC for 18 h resulted in high levels of fluorescence in punctate clusters within the cytoplasm (Figure 4.2).

In murine peritoneal macrophages, FhCL1 uptake resulted in FhCL1 localised within endolysosomal compartments (Donnelly *et al.* 2010). Therefore, it was hypothesised that FhCL1 might similarly be localised within endolysosomal compartments within human macrophages. Lysotracker-Alexa Fluor (AF)568, a fluorescent probe which localises to the acidic lysosomal compartments of live cells, was therefore used to visualise and detect lysosome formation within macrophages. Compared to untreated (PBS) macrophages, cells cultured with 20 μg/mL unlabelled (non-FITC conjugated) FhCL1 for 18 h displayed a substantial increase in Lysotracker-AF568 fluorescence, indicative of increased lysosome vesicles (Figure 4.3). Additionally, levels of Lysotracker-AF568 were also examined in macrophages incubated with 20 μg/mL FhCL1 with 10 μM E64 protease inhibitor, with these macrophages also demonstrating a similar increase in Lysotracker-AF568 fluorescence (Figure 4.3).

The subcellular localisation of FhCL1-FITC itself within human macrophages was also examined. Macrophages were cultured with 20 μg/mL FhCL1-FITC for 18 h and then incubated with Lysotracker-AF568. FhCL1-FITC appeared to be localised primarily to the same areas within the cells as Lysotracker-AF568 (Figure 4.4), this was seen in greater than 120 cells examined. To more analytically confirm co-localisation, the Mander's coefficient was calculated using IMARIS software (Bitplane Scientific, Switzerland). After threshold levels were set to exclude background signal (threshold set to 200 for both FhCL1-FITC and Lysotracker-AF568), image analysis determined that 34% of FhCL1-FITC co-localised with Lysotracker-AF568 (Mander's coefficient A = 0.34), and 64% of Lysotracker-AF568 co-localised with FhCL1-FITC (Mander's coefficient B = 0.64) (Table 4.1), within what appeared morphologically to be endolysosomal compartments.

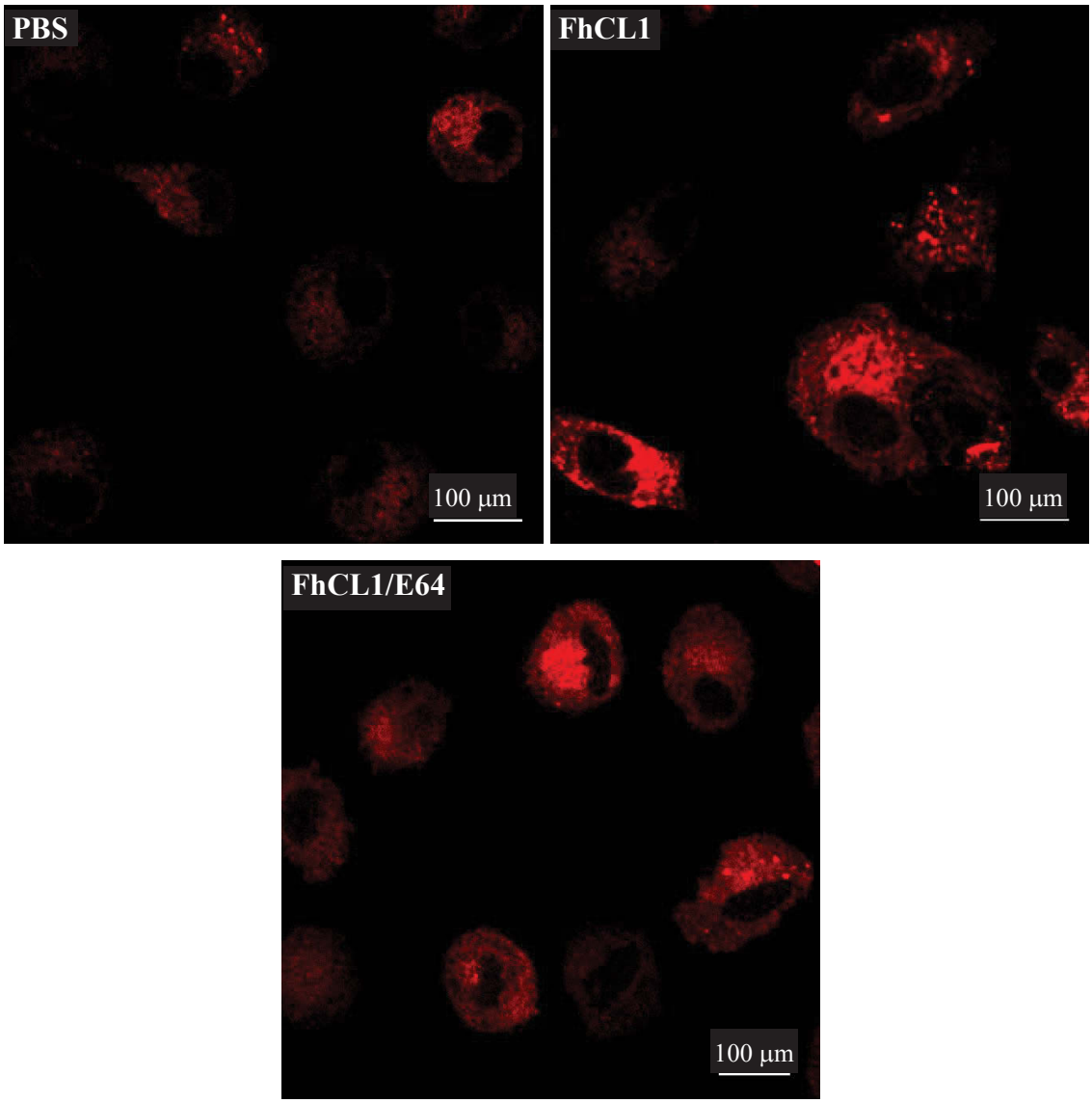

Figure 4.3: Modulation of lysosome formation within FhCL1-treated primary human macrophages.
Macrophages were cultured with PBS, 20 µg/mL FhCL1 or 20 µg/mL FhCL1 with 10 µM E64 for 18 h prior to incubation with 100 nM Lysotracker-AF568 (red) for 1 h. Imaging was performed following fixation using the Nikon A1 Confocal Scanning Laser Microscope. Data are representative of a minimum of six images analysed with greater than 80 cells in total for each treatment.

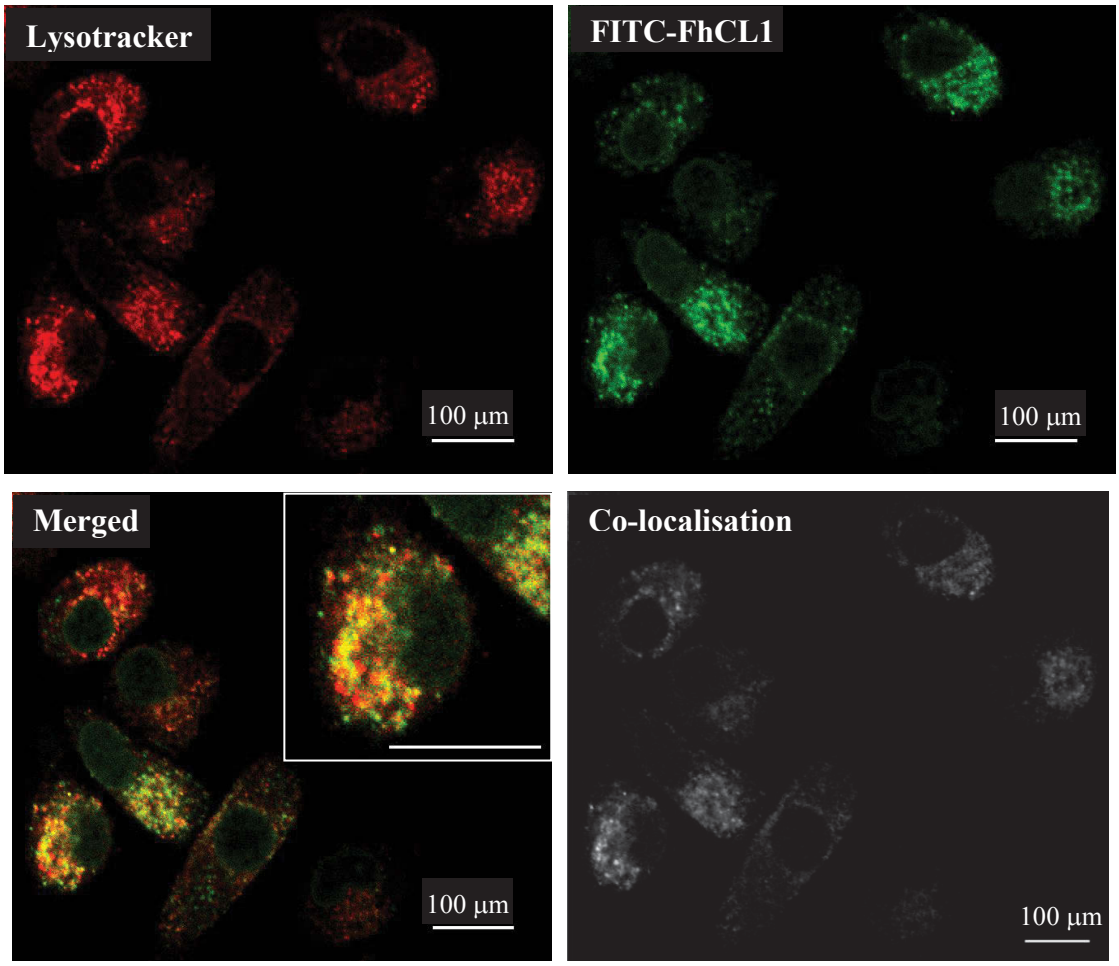

Figure 4.4: Localisation of FhCL1 and lysosomes within primary human macrophages.
Macrophages were cultured with 20 µg/mL FITC-labelled FhCL1 (green) for 18 h prior to incubation with 100 nM Lysotracker (red) for 1 h. The merged and co-localisation images show co-localisation of FhCL1 to lysosomal compartments (yellow and white respectively). Imaging was performed following fixation using the Nikon A1 Confocal Scanning Laser Microscope. Inset shows magnified image of co-localisation. Data are representative of nine images analysed with 119 cells examined in total.

Table 4.1: Mander's co-localisation coefficient analysis for FhCL1-FITC and Lysotracker-AF568 localisation within primary human macrophages.

Image	Number of co-localised pixels	% of data co-localised	% of FhCL1-FITC above threshold co-localised	% of Lysotracker-AF568 above threshold co-localised	Thresholded Mander's coefficient A	Thresholded Mander's coefficient B
1	93522	8.9	51.0	82.9	0.38	0.60
2	78947	7.5	45.3	81.9	0.33	0.59
3	72221	6.9	43.2	85.8	0.34	0.66
4	41912	10.8	58.1	93.1	0.49	0.77
5	49879	4.8	40.9	84.2	0.30	0.60
6	61318	5.9	41.8	85.6	0.33	0.65
7	62403	6.0	40.9	82.0	0.31	0.61
8	77523	7.4	35.5	78.3	0.28	0.60
9	48619	4.6	40.1	87.8	0.31	0.67
Total number of cells = 119				**Average**	**0.34**	**0.64**

4.2.2 EFFECT OF FHCL1 TREATMENT ON TLR3 EXPRESSION OR LOCALISATION IN PRIMARY HUMAN MACROPHAGES

Following LPS stimulation, FhCL1-treated human macrophages down-regulated the expression of IL-10 (Figure 3.6). This was likely attributable to modulation of the TRIF-signalling pathway, with FhCL1 treatment also down-regulating TRAF3 expression (Figure 3.14). Thus, it was hypothesised that FhCL1 may be modulating TRIF-dependent signalling in primary human macrophages through a similar mechanism to that in murine macrophages (Donnelly *et al.* 2010). Therefore, TLR3 mRNA expression was investigated by RT-qPCR. In addition TLR3 protein expression and subcellular localisation within human macrophages was investigated by confocal microscopy. To assess TLR3 mRNA expression, primers were designed to specifically amplify TLR3 cDNA. As these primers were newly designed, RT-qPCR required optimisation and validation. The primer pair amplified optimally with an annealing temperature of 57˚C (data not shown). The concentration of primer (forward and reverse) for TLR3 was performed as previously described, with the optimal concentration of primer determined to be 6.0 μM (Figure 4.5A). Melt curve analysis was also assessed which confirmed a single product amplification and the absence of primer dimer (Figure 4.5B). Finally, to determine whether PCR amplification was quantitative, RT-PCR was performed on serial 2-fold dilutions of cDNA template, ranging from 5-40 ng per reaction, and cDNA amplification (amount of PCR product) was reduced with serial 2-fold dilutions of cDNA template (Figure 4.5C). As expected, the no cDNA template control did not amplify product. Therefore, TLR3 primers successfully and quantitatively amplified a single product without forming primer dimers. Human macrophages were treated with PBS, 10 μg/mL FhCL1 or 10 μg/mL FhCL1 with 10 μM E64 protease inhibitor. Following RNA isolation and cDNA synthesis, RT-qPCR was performed for the amplification of TLR3 cDNA. In all reactions, the no cDNA template control did not amplify product. FhCL1 treatment had no effect on TLR3 mRNA expression in human macrophages as assessed in macrophages obtained from six donors, compared to TLR3 expression in PBS control cultured cells (Figure 4.6). This suggested that treatment with FhCL1 did not modulate TLR3 mRNA generation or half-life.

In murine macrophages, Donnelly *et al.* (2010) reported degradation of TLR3 at the protein level using both western blot and confocal microscopy. Therefore, protein expression of TLR3 in primary human macrophages treated with PBS or 10 μg/mL FhCL1 were assessed by confocal microscopy (Figure 4.7). However, TLR3 protein levels were low and bordered on being undetectable in both PBS and FhCL1-treated macrophages. FhCL1 treatment did not affect TLR3 protein expression, as there was no detectable difference in fluorescence intensity or subcellular localisation between the two treatment groups (n=26 cells for each treatment) (Figure 4.7 and data not shown). While the secondary antibody control (omission of primary antibody) confirmed that FhCL1 staining was not a result of non-specific binding of the secondary antibody, TLR3 expression and localisation was similar to the isotype control (Figure 4.7). In summary, while FhCL1 was observed to degrade TLR3 protein in murine macrophages (Donnelly *et al.* 2010), the low levels of TLR3 expression make it difficult to assess the effect of FhCL1 on TLR3 in human monocyte-derived macrophages.

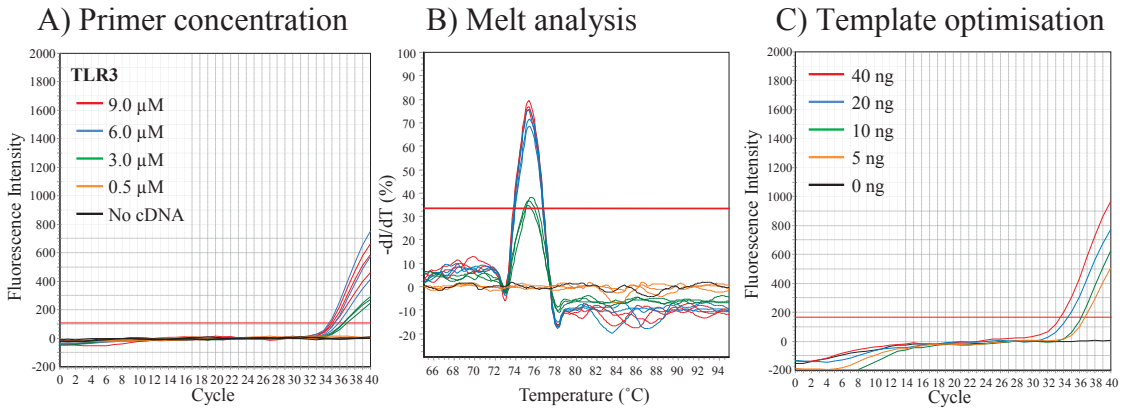

Figure 4.5: Optimisation of TLR3 primers for RT-qPCR analysis.
A) Optimisation of primer concentration for amplification of TLR3. The primer combinations included 9.0, 6.0, 3.0 and 0.5 μM for both primers. Data shown are only equal concentrations of forward and reverse primers. B) Melt curve analysis illustrating single PCR product amplification. C) Real time RT-PCR, showing serial 2-fold cDNA template dilution, demonstrating quantitative amplification of TLR3 cDNA.

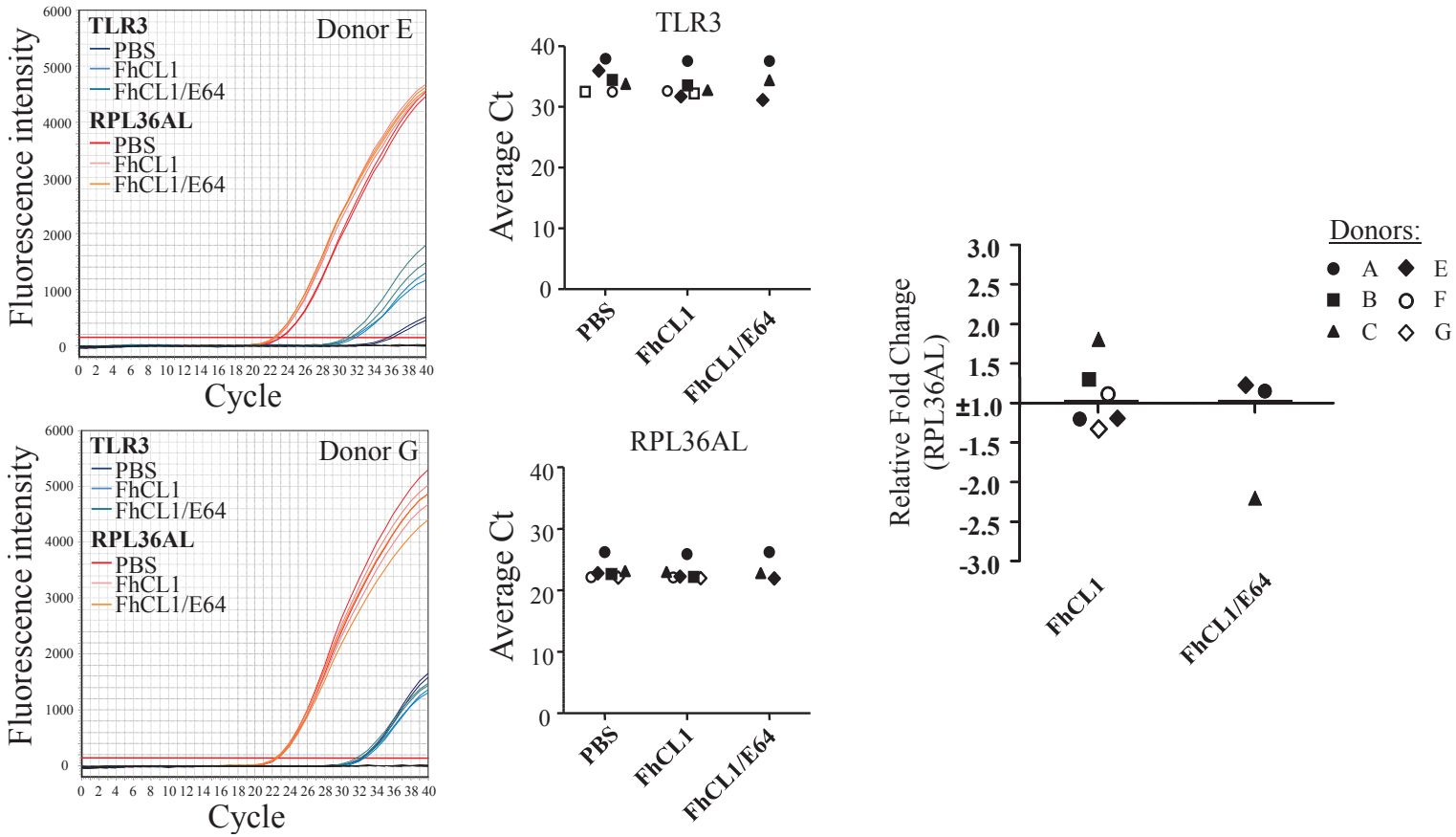

Figure 4.6: TLR3 mRNA expression in primary human macrophages cultured with FhCL1.
Primary human macrophages were incubated with PBS, 10 µg/mL FhCL1, 10 µg/mL FhCL1 with 10 µM E64, for 18 h. Data shown are representative fluorescence intensity RT-qPCR profiles for TLR3 and RPL36AL mRNA expression for two individual donors. Also shown are the average Ct values for up to six donors. Scatter graphs depict the fold change in cytokine expression relative to the reference gene RPL36AL and compared to the expression in PBS-treated macrophages. Horizontal bars are means from up to six donors. Data were analysed by one sample Wilcoxin t-test against a value of 1.0 (representative of expression in PBS treated control macrophages), with no statistically significant differences observed.

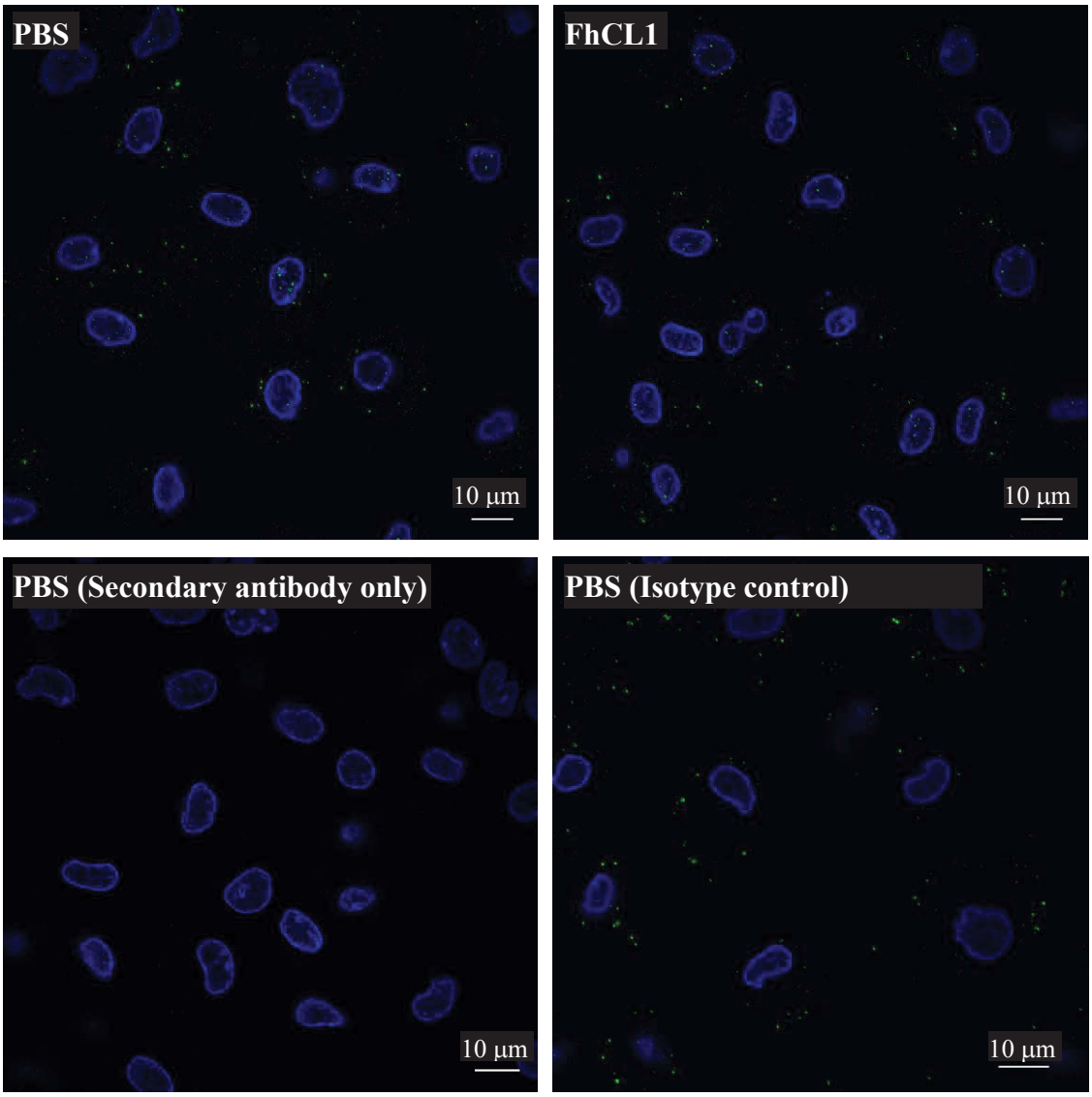

Figure 4.7: Localisation of TLR3 in primary human macrophages cultured with FhCL1.
Pooled primary human monocyte-derived macrophages were treated with PBS or 10 μg/mL FhCL1 for 18 h. Macrophages were incubated with anti-TLR3 antibody or IgG1-κ isotype control antibody and goat anti-mouse-AF488 secondary antibody (green), together with DAPI (blue) to detect nuclei. Imaging was performed using the Nikon A1 Confocal Scanning Laser Microscope. Images shown are representative of a minimum of two fields of view analysed for each time point with a minimum of 26 cells for each treatment.

4.2.3 EFFECT OF FHCL1 TREATMENT ON TLR4 EXPRESSION AND LOCALISATION IN PRIMARY HUMAN MACROPHAGES

Although TLR3 levels were extremely low, they were not detectably altered by FhCL1 treatment (Figure 4.7). However, FhCL1 did inhibit TRIF-dependent signalling following LPS-stimulation (as indicated by decreased TRAF3 expression; Figure 3.14, decreased IFN-β mRNA expression 1 h post LPS stimulation (M. Lund, unpublished), and subsequently decreased IL-10 in response to LPS; Figure 3.6). Given that TLR4 is the only other TLR to signal through a TRIF-dependent pathway (reviewed in Takeda *et al.* 2004), TLR4 was a likely candidate for immune modulation by FhCL1 in human monocyte-derived macrophages. To examine this possibility, TLR4 mRNA expression, as well as surface and intracellular expression and subcellular localisation were examined. To first assess changes in TLR4 mRNA expression, primers were designed to amplify TLR4 cDNA. As these were newly designed primers, once again the RT-qPCR assay required optimisation and validation. The primer pair amplified TLR4 optimally with an annealing temperature of 61˚C (data not shown) and the optimal primer concentration for both forward and reverse primers produced a single PCR product as indicated by the melt curve analysis (Figure 4.8A, B). Moreover, the PCR was determined to be quantitative, judged from amplification of serial 2-fold dilutions of cDNA template (Figure 4.8C). As expected, the no cDNA template control showed no product amplification. Macrophages from eight human donors were treated with PBS, 10 μg/mL FhCL1 or 10 μg/mL FhCL1 with 10 μM E64 protease inhibitor, for 18 h and RNA was isolated for cDNA synthesis. In all reactions, the no cDNA template control had no amplification. Results indicated that treatment with FhCL1, in the presence or absence of E64, had no significant effect on the levels of TLR4 mRNA compared to PBS-treated macrophages (Figure 4.9). This suggested that treatment with FhCL1 did not modulate expression of TLR4 mRNA.

To assess levels of surface and intracellular TLR4 protein, primary human monocyte-derived macrophages were cultured with PBS or 10 μg/mL FhCL1 for 18 h, with or without stimulation with 50 ng/mL LPS. Macrophages were surface stained with anti-TLR4 antibody with AF488 goat anti-mouse secondary antibody and examined by flow cytometry. After gating on large granular (high FSC and SSC) single cells, flow cytometric results showed that surface expression of TLR4 was low, but increased after

LPS stimulation (Figure 4.10). This is consistent with previous observations of TLR4 expression in LPS stimulated cells (Juarez *et al.* 2010). Furthermore, treatment with FhCL1 had no convincing effect on surface expression of TLR4 pre- or post-LPS stimulation when compared with PBS control macrophages (Figure 4.10). Similarly, staining following permeabilisation demonstrated intracellular TLR4 expression clearly detectable above isotype control staining, although there was again no difference in intracellular TLR4 expression levels between FhCL1 and PBS-treated control cells (Figure 4.10). Therefore, taken together, these results show that the modulation of IL-6, IL-8 and IL-10 cytokine expression and CD86 surface receptor expression does not correlate with, and is therefore not dependent on, modulation of surface or intracellular TLR4.

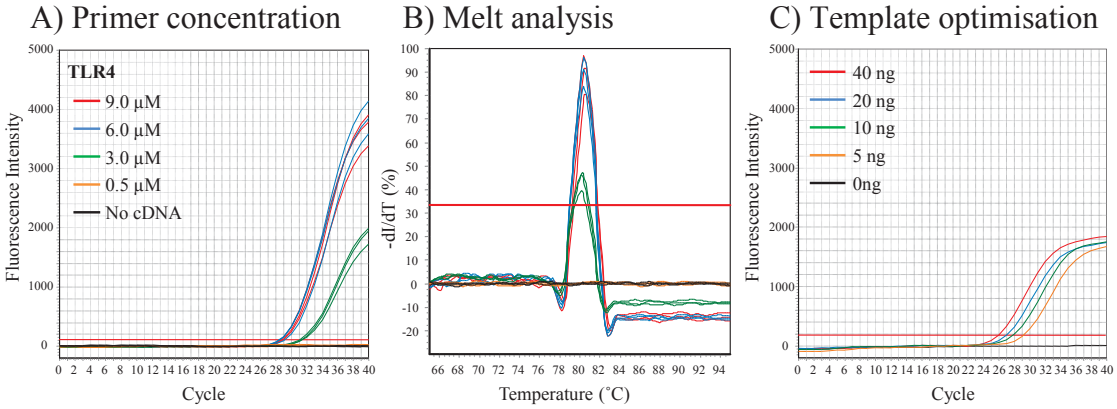

Figure 4.8: Optimisation of TLR4 primers for RT-qPCR analysis.
A) Optimisation of primer concentration for amplification of TLR4. The primer combinations included 9.0, 6.0, 3.0 and 0.5 µM for both primers. Data shown are only equal concentrations of forward and reverse primers. B) Melt curve analysis illustrating single PCR product amplification. C) Real time RT-PCR, showing serial 2-fold cDNA template dilution, demonstrating quantitative amplification.

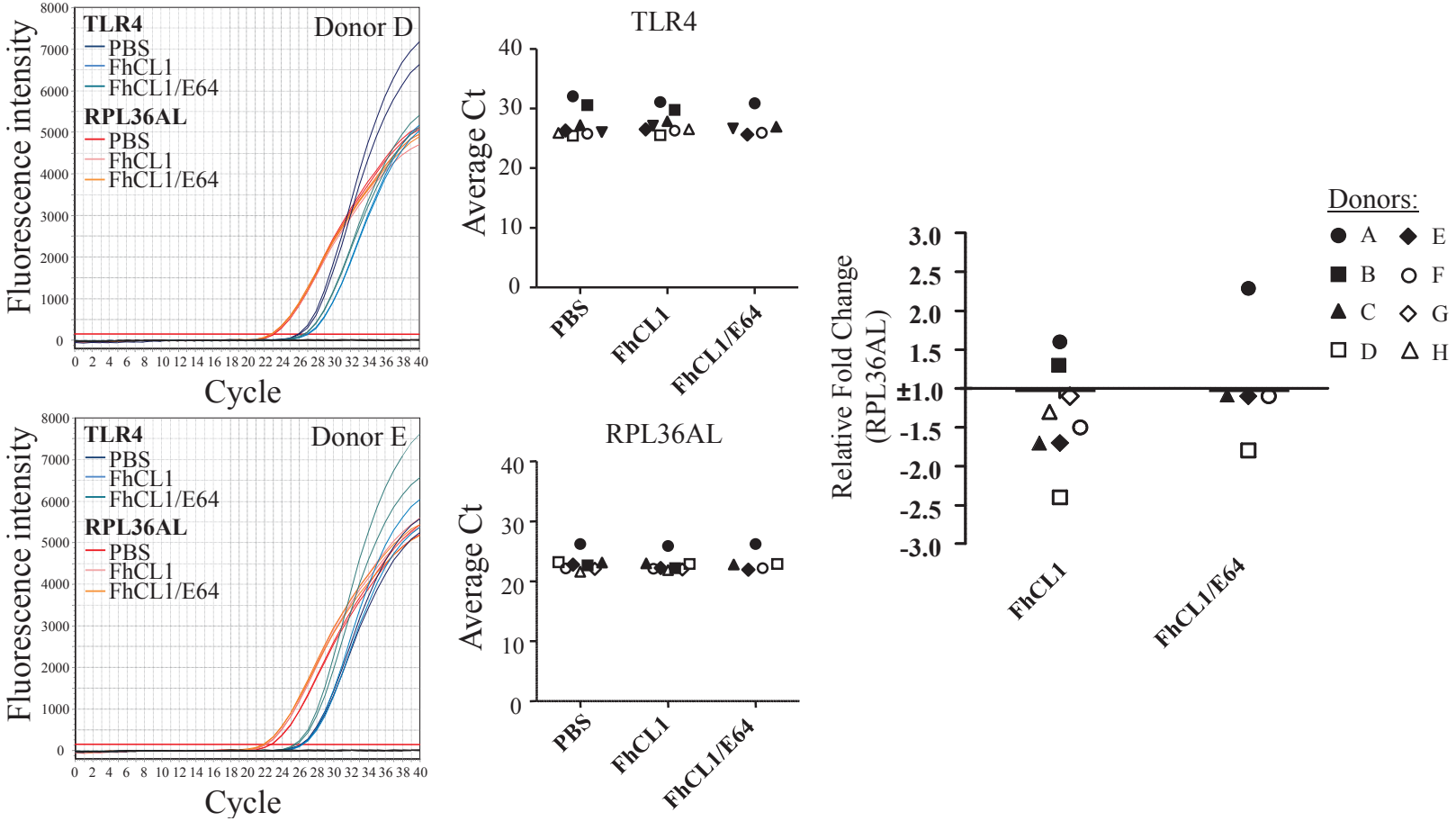

Figure 4.9: TLR4 mRNA expression in primary human macrophages cultured with FhCL1.
Primary human macrophages were incubated with PBS, 10 µg/mL FhCL1 or 10 µg/mL FhCL1 with 10 µM E64, for 18 h. Data shown are representative fluorescence intensity RT-qPCR profiles for TLR4 and RPL36AL mRNA expression for two individual donors. Also shown are the average Ct values for up to eight donors. Scatter graphs depict the fold change in cytokine expression relative to the reference gene RPL36AL and compared to the expression in PBS-treated macrophages. Means (horizontal bars) are also shown. Data were analysed by one sample Wilcoxin t-test, and no statistically significant differences were observed between treatment groups.

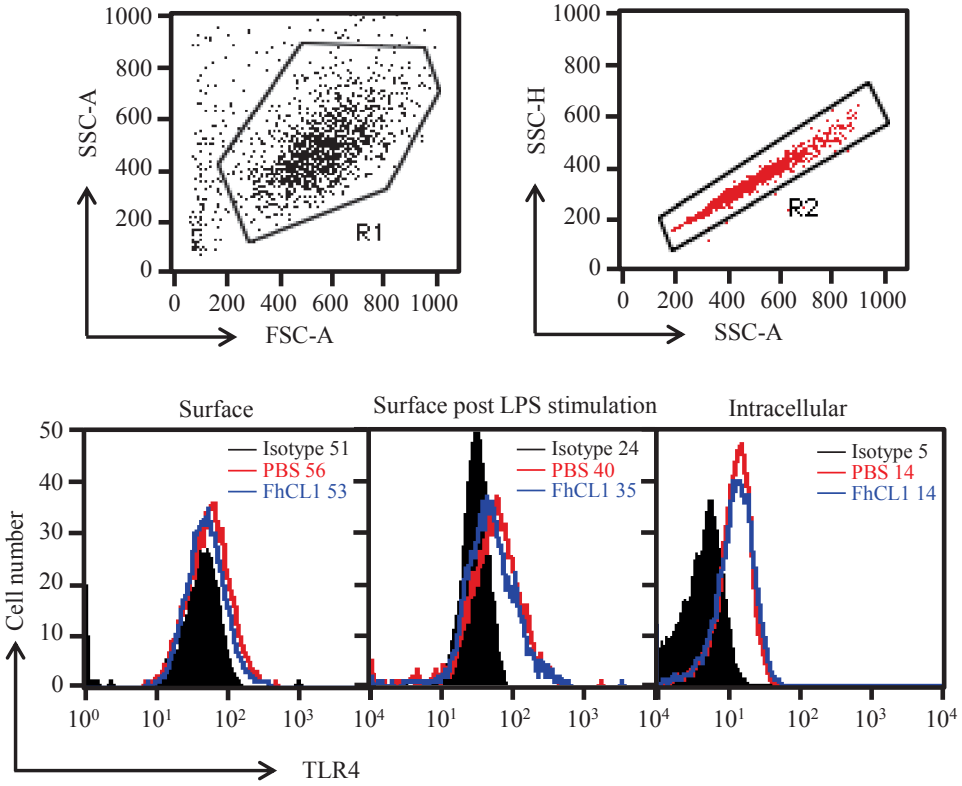

Figure 4.10: Flow cytometry analysis of surface and intracellular TLR4 expression in primary human macrophages treated with FhCL1.
Macrophages were treated with PBS or 10 µg/mL FhCL1 for 18 h and subsequently stimulated with 50 ng/mL LPS. Surface and intracellular expression of TLR4 was determined by flow cytometry after gating on single cells (SSC-A versus SSC-H dot plot; R2). Data shown are histogram overlays of anti-TLR4 antibody with goat anti-mouse-AF488 secondary antibody (coloured unfilled histograms), overlayed with isotype controls (black filled histogram). MFI values are indicated by numbers in the key. Data shown are representative of two donors examined.

The MyD88- and TRIF-dependent signalling pathways induced by TLR4 engagement occur beneath the cell surface and within endosomes, respectively (Kagan *et al.* 2008). Having established that FhCL1 had no effect on the surface or intracellular expression of TLR4 (Figure 4.10), this did not exclude the possibility that FhCL1 may be modulating the distribution and/or localisation of TLR4, thereby affecting TLR signalling. Therefore, the effect of FhCL1 on the localisation of TLR4 in human macrophages was examined by confocal microscopy. Macrophages were treated with PBS, 10 µg/mL FhCL1 or 10 µg/mL FhCL1 with 10 µM E64 protease inhibitor for 18 h, then fixed, permeabilised and stained with anti-TLR4 primary antibody and goat anti-mouse-AF488 secondary antibody. Results showed that in PBS-treated macrophages, TLR4 had a uniform distribution through the cytoplasm (Figure 4.11A) but treatment with FhCL1, or FhCL1 with E64 protease inhibitor, caused no observable difference in TLR4 localisation compared to PBS control cells (Figure 4.11A, B).

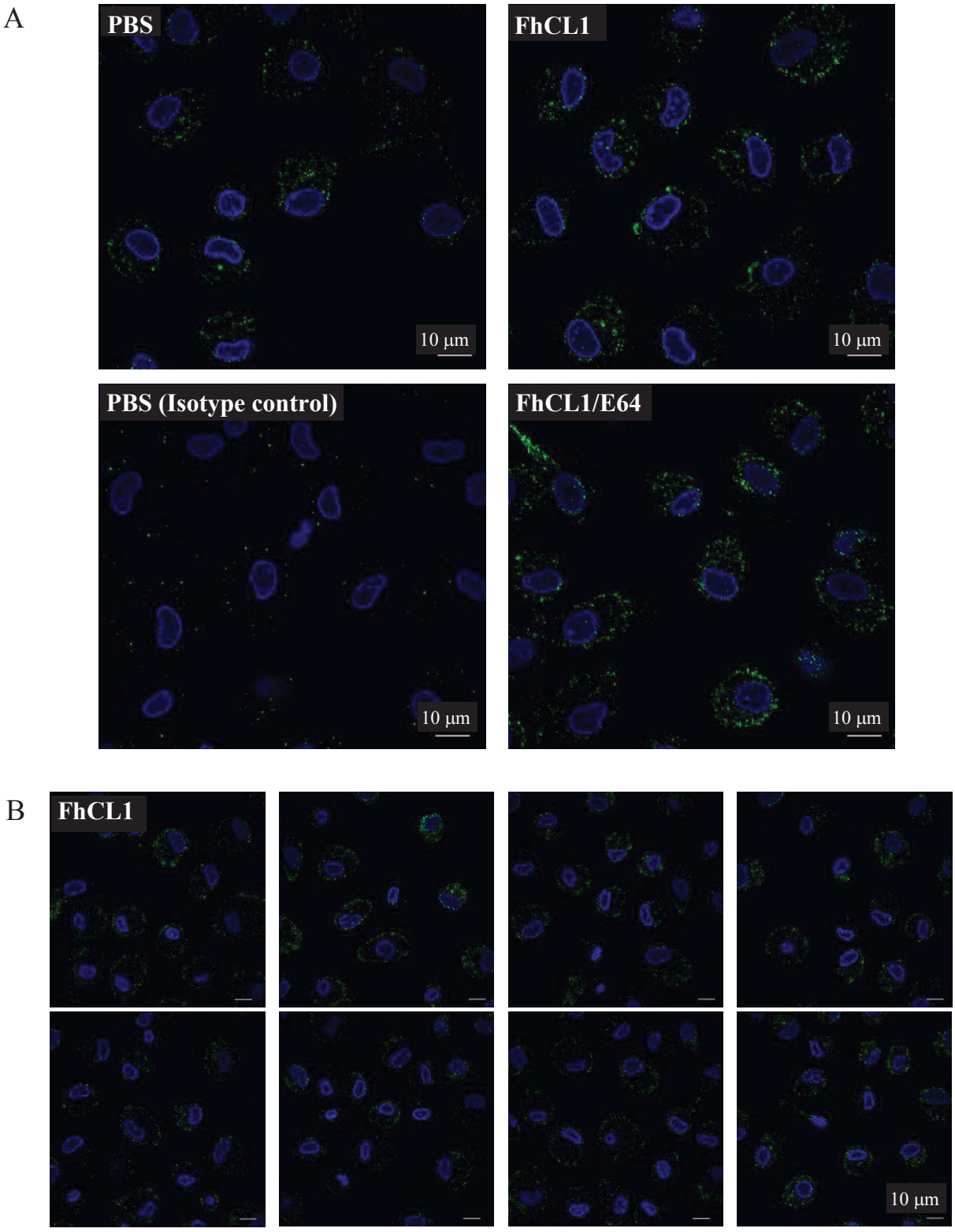

Figure 4.11: Localisation of TLR4 in human macrophages cultured with FhCL1. Pooled primary human macrophages were incubated with PBS, 10 μg/mL FhCL1 or 10 μg/mL FhCL1 with 10 μM E64 for 18 h. Macrophages were stained with anti-TLR4 antibody or IgG1-κ isotype control antibody with goat anti-mouse-AF488 secondary antibody (green) together with DAPI (blue) to detect nuclei. A) Data shown are representative images for each treatment and representative of four independent experiments, each with a minimum of 6 images acquired per treatment with a minimum of 72 cells in total. B) Data shown are additional examples of TLR4 in macrophages cultured with FhCL1. Imaging was performed using the Nikon A1 Confocal Scanning Laser Microscope.

4.2.4 EFFECT OF FHCL1 ON LPS TRAFFICKING IN HUMAN MACROPHAGES

It was possible that FhCL1 modulated cytokine expression by altering the internalisation of LPS, thus promoting MyD88-dependent signalling, initiated beneath the cell surface, while inhibiting endosomal TRIF-dependent signalling. Therefore, the uptake of LPS was investigated in FhCL1-treated human macrophages by confocal microscopy. Macrophages were incubated with PBS or 10 μg/mL FhCL1 for 18 h, and then stimulated with 200 ng/mL Cy5-labelled LPS prior to examination by live cell imaging. Control macrophages endocytosed significantly more LPS-Cy5 compared to FhCL1-treated macrophages (Figure 4.12). At 15 min post LPS stimulation, there was a significant decrease in LPS uptake by FhCL1-treated macrophages compared to PBS-control macrophages ($p=0.0002$) (Figure 4.12A). This trend continued at 30 min post LPS stimulation ($p <0.0001$) and continued until the experimental endpoint (2 h post LPS stimulation, $p=0.0041$), with PBS-treated macrophages taking up significantly more LPS compared to FhCL1-treated macrophages ($p=0.0015$) (Figure 4.12A, B) (Note: Data shown are mean ± SD, and of note, SD does not indicate statistical significance as such, but the distribution of fluorescence intensity and the variation in uptake of LPS-Cy5, as expected, in individual cells). These results suggest that FhCL1 treatment suppresses the ability of macrophages to internalise LPS. It is unknown however whether the decreased uptake of LPS is associated with the decreased expression of TRIF-dependent CD86 and IL-10.

4.2.5 EFFECT OF FHCL1 TREATMENT ON ENDOSOME TRAFFICKING PROTEINS IN PRIMARY HUMAN MACROPHAGES

FhCL1 is internalised into endolysosomal compartments of primary human macrophages (Figure 4.4), where it appeared to modulate TLR4 cell signalling (Chapter 3), as indicated by up-regulated CD14, enhanced phosphorylation of IκBα, ERK1 and ERK2, and up-regulated IL-6 and IL-8, as well as down-regulated TRAF3 and IFN-β mRNA expression (M. Lund, unpublished), and decreased CD86 surface expression and IL-10 secretion. While, FhCL1 treatment had no effect on the expression or localisation of TLR4 itself (Figure 4.11), treatment of human macrophages with FhCL1 was associated with suppression of LPS internalisation (Figure 4.12). Thus, it was proposed that FhCL1 affected LPS internalisation and TLR4 signalling by modulating

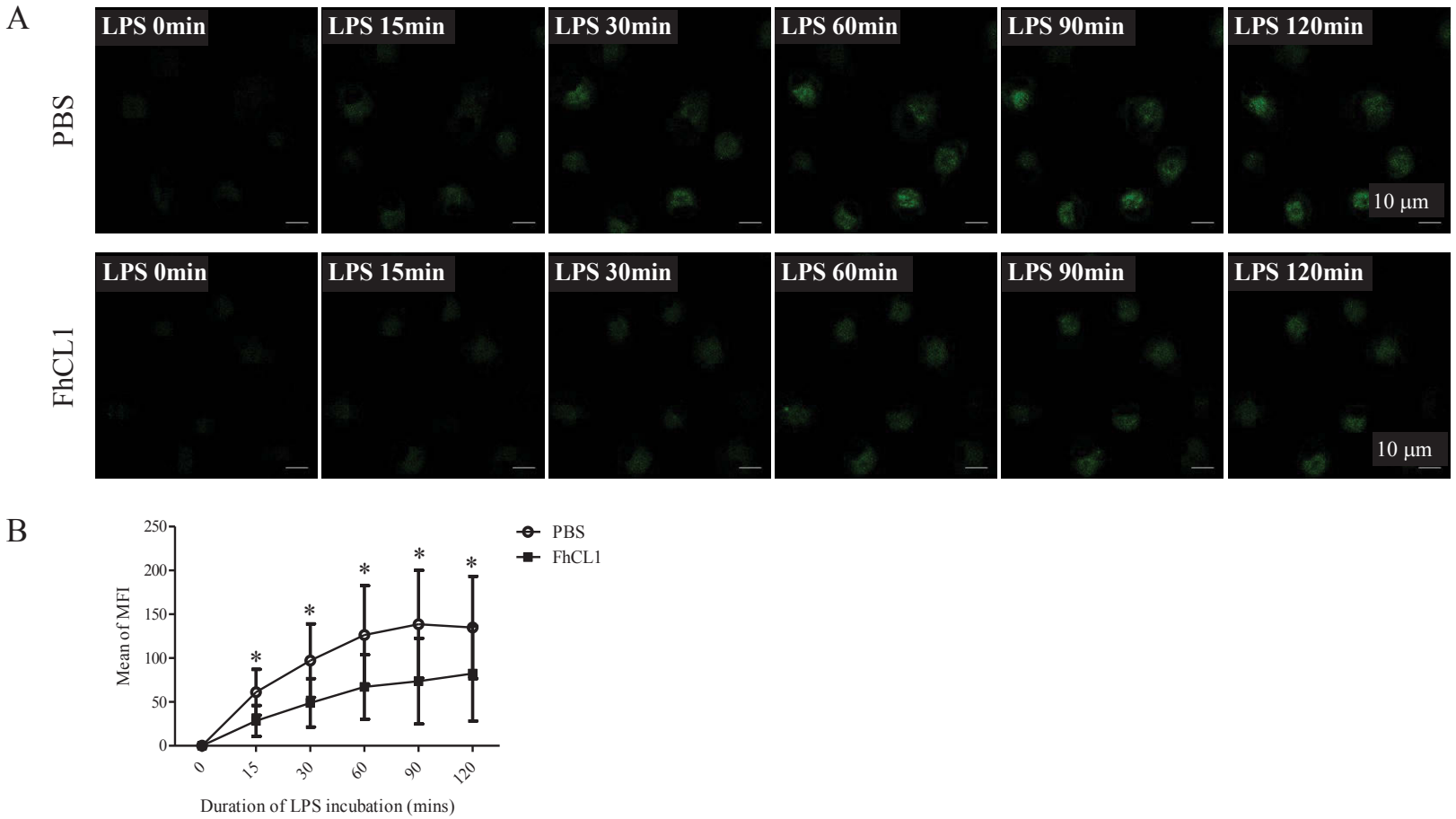

Figure 4.12: Uptake of LPS by primary human macrophages following FhCL1 treatment.
Pooled primary human macrophages were incubated with PBS or 10 μg/mL FhCL1 for 18 h and subsequently stimulated with 200 ng/mL LPS. Cells were imaged every two minutes. A) Data shown are images of live cells at selected time points following the addition of Cy5-labelled LPS (green) for 2 h. B) The uptake of LPS was quantified by averaging the mean fluorescence intensity of 23 cells for PBS (circle) and 23 cells for FhCL1-treated macrophages (square). Error bars indicate the standard deviation of the means. Data were analysed by Wilcoxin paired t-test, and significant differences ($p<0.05$) between PBS and FhCL1-treated macrophages are indicated (*). Data shown are representative of three independent experiments.

intracellular trafficking proteins, such as clathrin (Husebye *et al.* 2006), dynamin (Schmid *et al.* 1998), and tubulin (Matteoni *et al.* 1987; Gruenberg *et al.* 1989), which are involved in LPS internalisation (Figure 4.13). Indeed, dynamin is a known substrate of human cathepsin L (Sever *et al.* 2007), and thus it was a particularly important candidate to assess. To investigate this possibility, pooled primary human macrophages were cultured with PBS, 20 μg/mL FhCL1, 20 μg/mL FhCL1 with 20 μM E64 protease inhibitor, or 20 μM E64 and intracellular trafficking proteins examined by western blot. Cell lysates were harvested and separated by SDS-PAGE prior to transfer onto nitrocellulose membranes. Membranes were probed with anti-clathrin, anti-α-tubulin, and anti-β-actin antibodies. Western blotting indicated that while the main band when probed with anti-α-tubulin corresponded to the reported size of α-tubulin (50.5 kDa), the main bands when probed with anti-clathrin antibody were smaller (approximately 38 and 50 kDa) than the reported size of the heavy chain of clathrin (180 kDa). Nevertheless, visual assessment of the band corresponding to clathrin suggested that treatment with FhCL1, FhCL1 with E64 or E64 alone arguably had a small but minimal effect on clathrin expression (Figure 3.10A). As an attempt to semi-quantify relative changes in protein expression, densitometry analysis was performed comparing clathrin expression in macrophages treated with FhCL1, FhCL1 with E64 and E64 alone to PBS-treated control macrophages. However, densitometry indicated that there was a small detectable differences between treatments (Figure 3.10B). In contrast, FhCL1 in the presence and absence of E64, and E64 alone slightly down-regulated α-tubulin expression (Figure 4.14A). Densitometry analysis also suggested down-regulation (Figure 4.14B). Disappointingly, quantitation of dynamin was unsuccessful by both western analysis and confocal microscopy due to extensive non-specific binding of the antibody (data not shown). Taken together, these results indicate that FhCL1 may modulate trafficking by altering clathrin and/or α-tubulin expression.

The subcellular localisation of clathrin and tubulin within primary human macrophages was also examined by confocal microscopy to identify whether FhCL1-induced changes in the localisation of these proteins. Macrophages were cultured with PBS, 20 μg/mL FhCL1 or 20 μg/mL FhCL1 with E64 inhibitor for 18 h, prior to fixation, permeabilisation and staining with anti-clathrin and anti-α-tubulin antibodies. There was no obvious discernible difference in clathrin subcellular localisation between

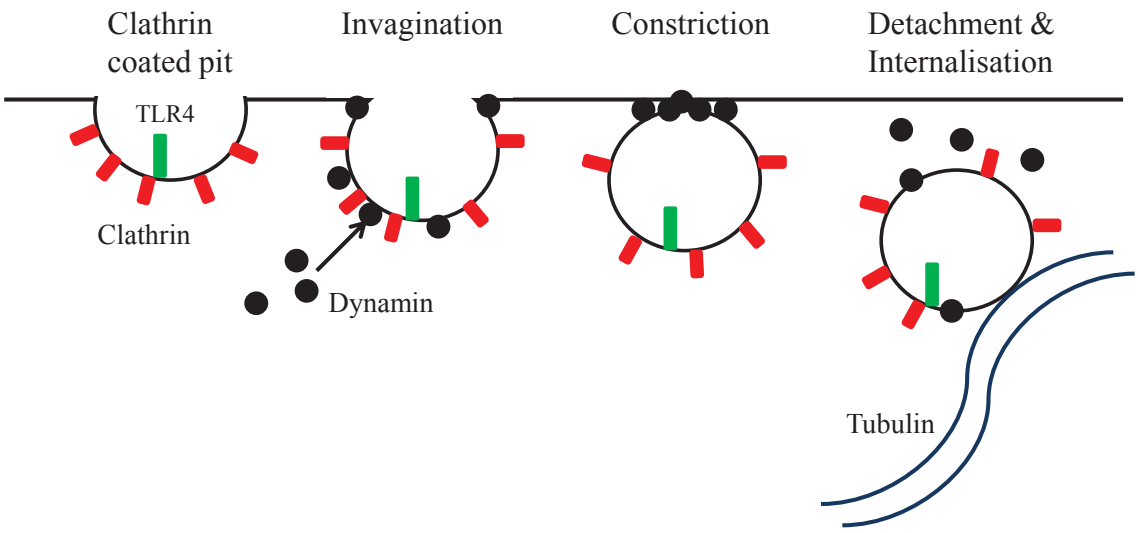

Figure 4.13: The role of dynamin, clathrin and tubulin in surface protein internalisation.
Internalisation of surface proteins, such as TLR4, requires the formation of a clathrin coated pit, where clathrin is recruited to the cell membrane. Dynamin is targeted to coated pits and guanosine-5'-triphosphate (GTP) triggers dynamin to form 'spiral collars' at the cell membrane, first initiating invagination and later causing constriction of the membrane to release the vesicle into the cytoplasm. Once released, the vesicle traffics via the tubulin network. (Adapted from Schmid *et al.* 1998).

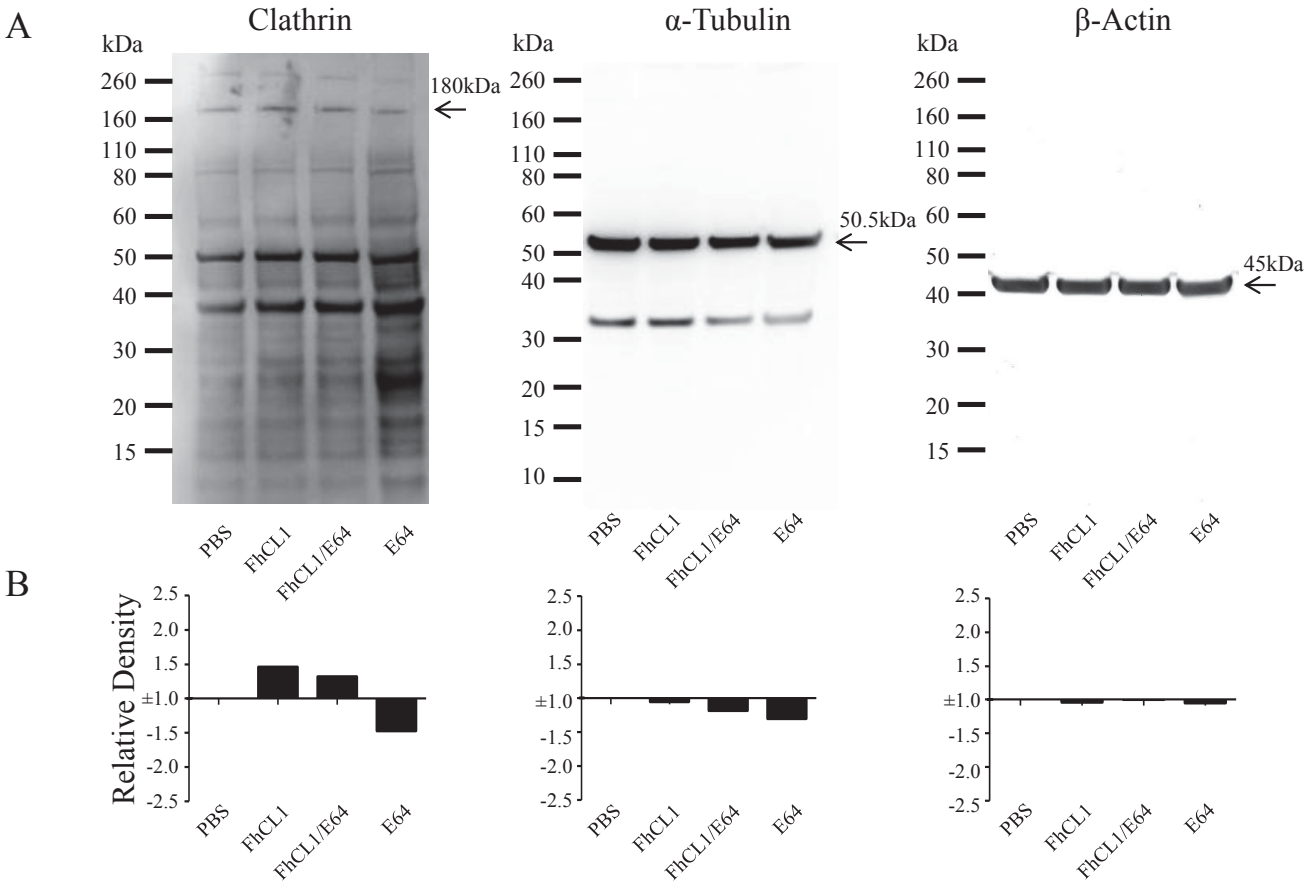

Figure 4.14: Western blot analysis of clathrin and α-tubulin expression in primary human macrophages cultured with FhCL1.
Macrophage cell lysates were prepared from four pooled donors treated with PBS, 20 μg/mL FhCL1, 20 μg/mL FhCL1 with 20 μM E64 and 20 μM E64. A) Western blot membranes were incubated with anti-clathrin, anti-α-tubulin or anti-β-actin. Protein size markers are as indicated. Specific proteins, clathrin, α-tubulin, and β-actin, are detected at the expected size (arrow). B) Densitometry graphs showing the relative density of clathrin, α-tubulin, and β-actin for each treatment. Data shown is representative of a single experiment.

FhCL1-treated and PBS-treated macrophages (Figure 4.15). Therefore, FhCL1 did not alter LPS internalisation by altering clathrin localisation. It should be noted however, that these results are potentially diminished by extensive non-specific staining from the 'clathrin-specific' antibody.

Investigation into the localisation of α-tubulin in primary human macrophages showed that within PBS-control macrophages, α-tubulin was highly branched and distributed throughout the cell (Figure 4.16). However, localisation of α-tubulin differed between FhCL1 and PBS-treated macrophages, with three distinct localisation patterns visible within FhCL1-treated macrophage populations. Some FhCL1-treated macrophages appeared similar to the PBS and FhCL1 with E64 samples, with highly branched and brightly staining α-tubulin creating an intracellular network (Figure 4.16B). Alternatively, some cells within the FhCL1-treated sample showed reduced intensity of α-tubulin, with fluorescence restricted to an area just beneath the cell membrane (Figure 4.16A, B). A third sub-population of macrophages showed a lack of α-tubulin beneath the cell membrane, with α-tubulin branching within the centre of the cell, but with less intensity than PBS-treated macrophages (Figure 4.16B). On the other hand, macrophages treated with FhCL1 with E64 showed no difference in α-tubulin localisation compared to PBS-treated macrophages (Figure 4.16A). These results suggested that FhCL1 modulated the localisation of α-tubulin within human macrophages and that this modulation was dependent upon its enzymatic activity. Furthermore, for control purposes, human macrophages were also treated with nocodazole. Nocodazole is a tubulin inhibitor (Samson *et al.* 1979), and its presence resulted in cells with similar appearance to the FhCL1-treated cells, that is, with a decrease in the fluorescence of α-tubulin with accumulation beneath the plasma membrane (Figure 4.16A). The disruption of α-tubulin may explain the inhibition of LPS uptake by FhCL1-treated primary human macrophages. However, this result was disappointingly not convincingly reproducible in an independently performed experiment. However it should be noted that this experiment utilised pooled monocyte-derived macrophages obtained from different donors, and repeated experiments did not examine any of the same individual donors.

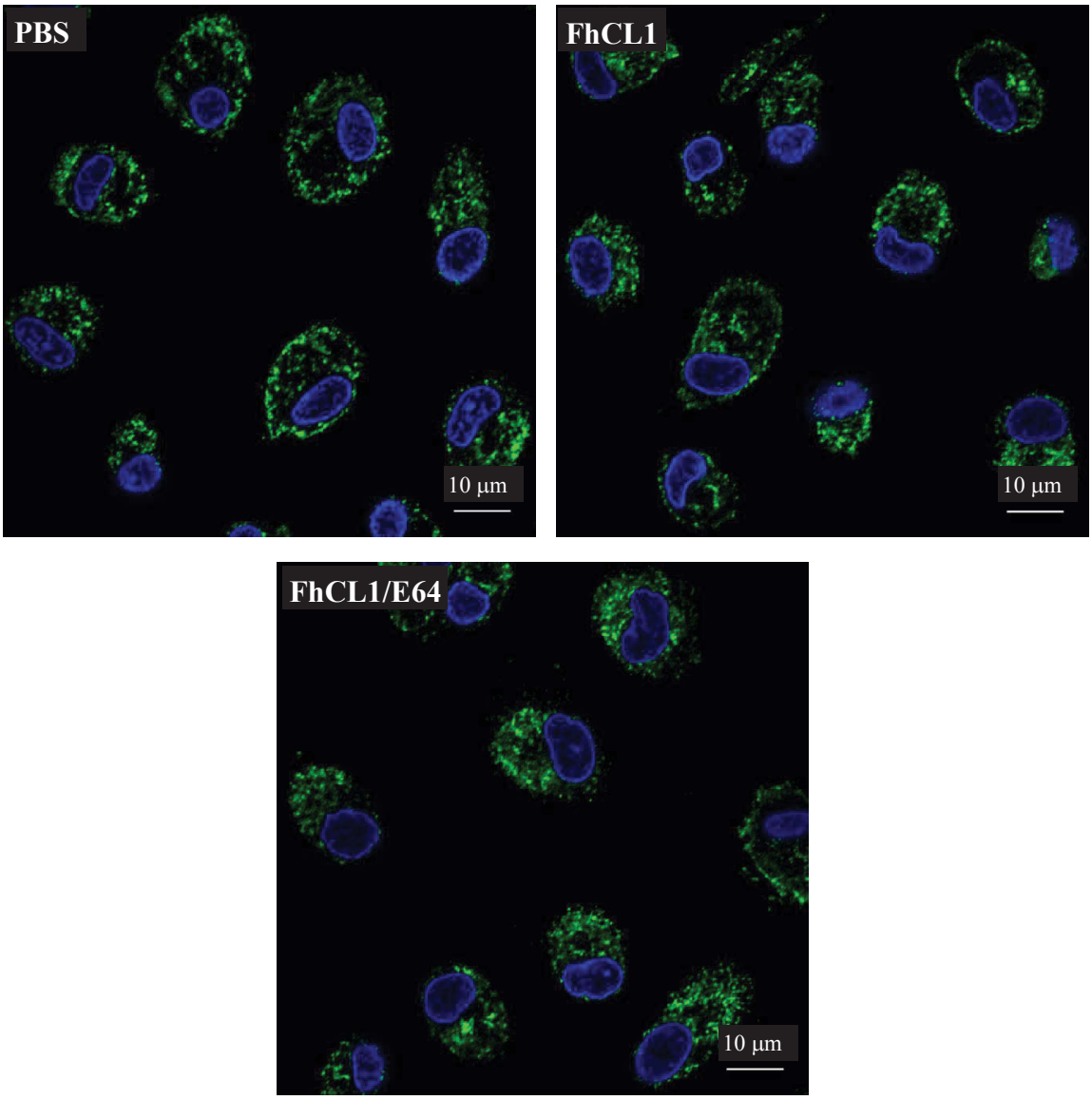

Figure 4.15: Localisation of clathrin in primary human macrophages cultured with FhCL1.

Pooled primary human macrophages were incubated with PBS, 20 μg/mL FhCL1 or 20 μg/mL FhCL1 with 20 μM E64 for 18 h. Macrophages were stained with anti-clathrin antibody and goat anti-mouse-AF488 secondary antibody (green) together with DAPI to detect nuclei (blue). Data shown are representative images for each treatment. Imaging was performed using the Nikon A1 Confocal Scanning Laser Microscope. Representative of a minimum of eight images and 50 cells acquired per treatment.

A

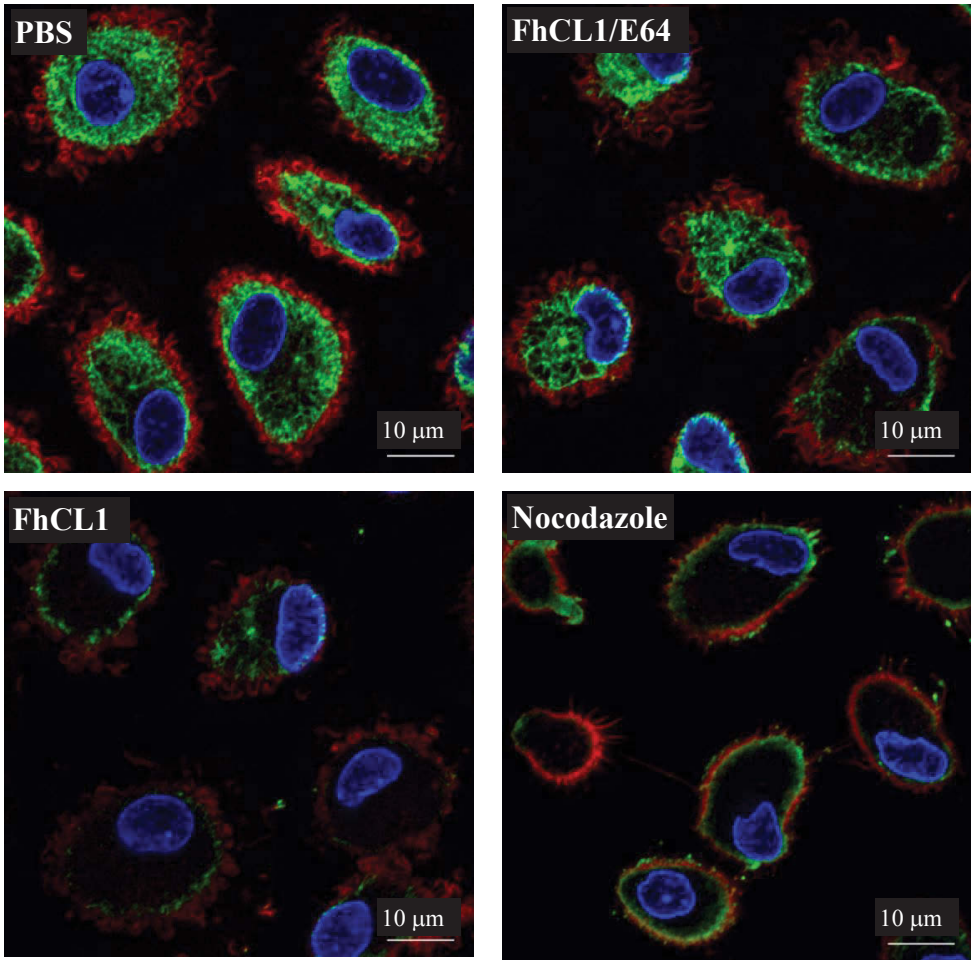

B

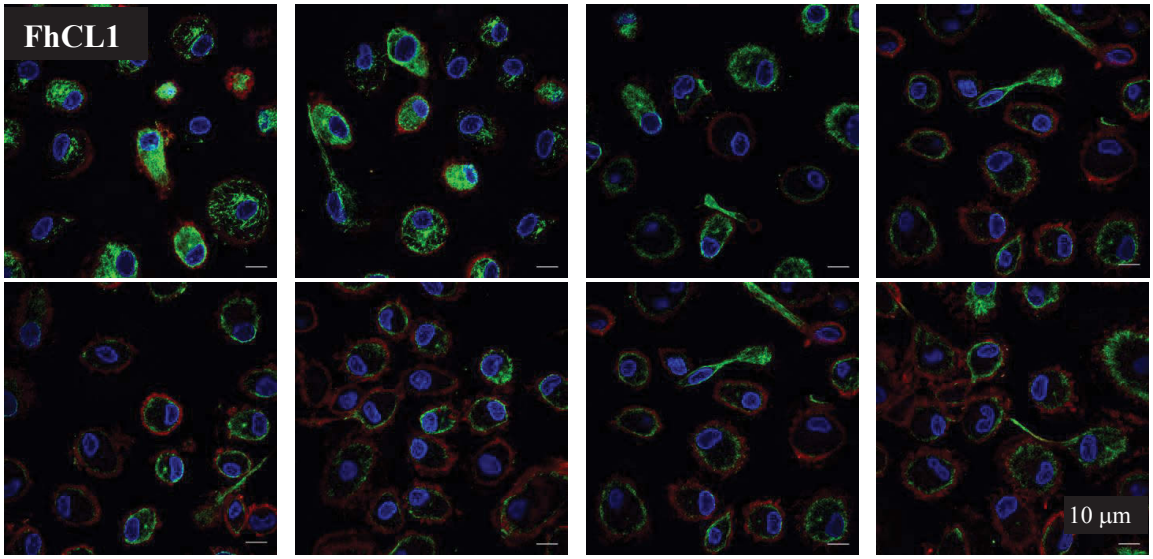

Figure 4.16: Localisation of α-tubulin in primary human macrophages cultured with FhCL1.

Pooled primary human macrophages were incubated with PBS, 20 µg/mL FhCL1 with 20 µM E64, or 20 µg/mL FhCL1 for 18 h, or 2 µg/mL tubulin inhibitor, Nocodazole for 30 min. Macrophages were stained with anti-α-tubulin antibody and goat anti-rabbit-AF488 secondary antibody (green), phalloidin to detect F-actin (red), and DAPI to detect nuclei (blue). A) Data shown are representative images for each treatment, each with a minimum of eight images and 60 cells acquired per treatment. B) Data shown are additional images for macrophages cultured with FhCL1. Imaging was performed using the Nikon A1 Confocal Scanning Laser Microscope.

4.3 DISCUSSION

This chapter examined the internalisation and localisation of FhCL1 within human macrophages, along with the localisation of TLRs, namely TLR3 and TLR4, the uptake of LPS and associated trafficking proteins. Results showed that FhCL1 was internalised and localised within lysosomes, but had no effect on TLR expression or localisation. The localisation of FhCL1 within lysosomes correlated with suppression of LPS uptake by primary human macrophages. This also appeared to be associated with the altered localisation of α-tubulin in primary human monocyte-derived macrophages. This study has therefore provided insight into the immune-modulatory role of FhCL1 in primary human monocyte-derived macrophages, which has been found to be considerably different to that observed in murine peritoneal macrophages.

Little is known about the mechanism by which FhCL1 is internalised. Extracellular material can be internalised by cells via three main pathways: (1) surface receptor-mediated endocytosis, which involves a coated pit (either clathrin-mediated or caveolae/lipid raft-mediated) (Le Roy *et al.* 2005), (2) non-surface receptor-mediated internalisation, which is the internalisation of small scale non-specific extracellular material, usually fluids and solutes (pinocytosis or macropinocytosis) (for a review see Lamaze *et al.* 1995), and (3) phagocytosis, which is the internalisation of larger scale material such as bacteria, and can be enhanced by opsonisation of the material (for a review see Aderem *et al.* 1999). How material is internalised can influence how the material mediates effects on host proteins. For example, when the TGF-β surface receptor is internalised within clathrin-coated vesicles, cell signalling is induced, whereas internalisation of TGF-β into caveolae targets the receptor for degradation (Di Guglielmo *et al.* 2003). Therefore, in order to investigate the mechanism by which FhCL1 is internalised and modulates immune responses, one approach might have been to examine markers of each of these pathways. Instead, having shown in the previous chapter that TLR signalling was modulated by FhCL1, the pathway by which TLRs are internalised was examined, that is, the clathrin-mediated pathway (Husebye *et al.* 2006). Therefore, the localisation of FhCL1 within cells was examined, as well as its effect on TLR3 and TLR4 expression and localisation and the internalisation of these molecules.

The study of the localisation of FhCL1 within murine peritoneal macrophages utilised an antibody specific to the 6xHis tag of recombinant FhCL1, and showed that FhCL1 co-localised with early endosomes and lysosomes of murine macrophages (Donnelly *et al.* 2010). This required fixed and permeabilised cells to enable two step antibody staining. In the current study, the localisation of FhCL1 within human macrophages utilised a fluorescently conjugated FhCL1 and Lysotracker-AF568 as a marker of lysosomes. Therefore, this was performed using fixed cells, but without permeabilisation. This latter approach similarly showed that FhCL1 was internalised by macrophages where it also appeared to reside in lysosomes. One difference between these studies is that in murine macrophages, FhCL1 is predominately localised in endosomes at 2 h post incubation whereas this study did not include an endosome marker, and 34% of FhCL1 co-localised with Lysotracker-AF568. It is therefore possible that the remaining FhCL1 is localised in endosomes. Moreover, the human macrophages were examined at 18 h, not 2 h as per the murine macrophages. In other words, the human and murine macrophages were studied in a similar, but not identical manner, and yet results are consistent with endosomal/lysosomal localisation of FhCL1.

The enzymatic activity of FhCL1 has been established to be maximal at pH 4.5 (Dalton *et al.* 2003), and this is similar to the pH that exists within endosomes (Geisow *et al.* 1984). More recently, FhCL1 was shown to be very stable with the capacity to cleave substrates over a wide pH range (3.0-9.0) (Lowther *et al.* 2009). Thus, given that FhCL1 is still expected to be active at the acidic pH of the endosome, this may represent the site of modulation of TRIF-dependent signalling, especially considering that TRIF signalling occurs following endocytosis of the TLR4/LPS complex (Kagan *et al.* 2008; Watts 2008; Chaturvedi *et al.* 2009).

Considering FhCL1 modulated expression of TRIF-dependent surface receptors, cytokines and signalling molecules in human monocyte-derived macrophages, the TLRs which signal through the TRIF-dependent pathway, that is TLR3 and TLR4, were potential targets of FhCL1. However, there was no significant difference in TLR3 mRNA or protein expression in human monocyte-derived macrophages after FhCL1 treatment, and there were only very low levels of TLR3 mRNA and protein detectable in these cells. This is consistent with previous findings that compare the mRNA expression of TLR3 in human macrophages to DCs, where RT-qPCR demonstrated that

the expression of TLR3 was very low in human macrophages but higher in human DCs (Heinz *et al.* 2003). In this regard, the addition of further PCR cycles may have been useful for improving the detection of TLR3 mRNA. In contrast, TLR3 is strongly expressed in murine macrophages, and expression is enhanced following IFN-β or LPS stimulation (Alexopoulou *et al.* 2001; Heinz *et al.* 2003). However, surface and intracellular TLR3 has also been reported in primary human monocyte-derived macrophages by flow cytometry (Lundberg *et al.* 2007). Comparison of these studies to the current study demonstrated that different methods of maturation were used to produce monocyte-derived macrophage. This study used human serum and IMDM to induce differentiation of monocytes, while Lundberg *et al.* (2007) cultured primary human monocytes in recombinant macrophage colony stimulating factor to induce maturation. Furthermore, TLR3 mRNA RT-qPCR analysis used PMA-differentiated THP-1 cells as a model of macrophages (Heinz *et al.* 2003), and while this induces a macrophage-like phenotype, there are significant differences between monocyte-derived macrophages and differentiated cell lines (Daigneault *et al.* 2010). Thus, the low levels of TLR3 detected in this study may reflect differences in the method of macrophage maturation or the actual cell types examined in each study.

Previous work conducted by Donnelly *et al.* (2010) observed modulation of the TRIF-dependent signalling pathway by FhCL1 in BALB/c peritoneal macrophages following stimulation with LPS – the ligand for TLR4; and poly (I·C) – an immunostimulant of TLR3 and this was attributed to degradation of TLR3 at the protein level (Donnelly *et al.* 2010). Unfortunately, it was difficult to determine the effect of FhCL1 on TLR3 protein expression in human monocyte-derived macrophages due to the low TLR3 protein expression levels found to be present in these cells. The expression and localisation of TLR4, the ligand of LPS, was also examined in human macrophages. TLR4 signals through the MyD88-dependent pathway, as well as being the only other TLR to signal through the TRIF-dependent pathway (Akira *et al.* 2004; Kagan *et al.* 2008; Watts 2008; Chaturvedi *et al.* 2009). There was no change in TLR4 mRNA or protein expression in macrophages treated with FhCL1, thus the up-regulation of pro-inflammatory cytokines and the suppression of the TRIF-dependent signalling pathway by FhCL1 cannot be attributed to altered expression of surface or internal TLR4. This appeared to be analogous to murine peritoneal macrophages, where FhCL1 also had no effect on TLR4 mRNA or surface protein TLR4 (Donnelly *et al.* 2010).

Macrophages pre-treated with FhCL1 and stimulated with LPS showed a decrease in LPS uptake over a 2 h time course, suggesting that FhCL1 treatment inhibited the ability of macrophages to internalise LPS. The subcellular location of TLR4 dictates which signalling pathway is induced, that is MyD88-dependent pathway signals beneath the cell surface, while the TRIF-dependent pathway signals from within endosomes (reviewed in Chaturvedi *et al.* 2009). Therefore, the suppressed uptake of LPS is a potential explanation of the decrease in TRIF-dependent TRAF3, IFN-β (M. Lund, unpublished) and IL-10 expression in human monocyte-derived macrophages.

Trafficking of the LPS/TLR4 complex utilises dynamin and clathrin, with the early phase (first 40 min) of LPS trafficking being predominantly a clathrin-dependent event (Husebye *et al.* 2006). Furthermore, inhibition of either clathrin or dynamin prevents the internalisation of the TLR4/LPS complex in murine RAW 264.7 macrophages (Wang *et al.* 2012). Inhibition of clathrin and dynamin results in the subsequent accumulation of the TLR4/LPS complex near the inner surface of the cell membrane (Wang *et al.* 2012). This accumulation is associated with inhibited signalling through the TRIF-dependent, late NF-κB pathway, indicated by decreased IL-6 (which is induced through either the MyD88- or TRIF- dependent pathways) (Wang *et al.* 2012). While the localisation of TLR4 beneath the plasma membrane of human macrophages did not appear to be altered by FhCL1, the TRIF-dependent pathway was suppressed as demonstrated by decreased TRAF3, decreased IFN-β mRNA (M. Lund, unpublished) and decreased IL-10 secretion. Clathrin and dynamin, therefore, represented potential candidates by which FhCL1 modulated TLR signalling. Treatment of human macrophages with FhCL1 in the presence or absence of protease inhibitor E64 had no visible effect on the expression or localisation of clathrin. However, densitometry analysis suggested that there were differences between FhCL1-treated and PBS control macrophages, in the magnitude of 1.5 fold. In this instance, limited weight should be given to the densitometry result as low abundance proteins, such as that observed for the heavy chains of clathrin, are difficult to quantitate by this method. Furthermore, the presence of numerous non-specific bands and high background in the western blot clouds the interpretation and reliability of this data. Moreover, results also suggested that despite this antibody being specific for the heavy chain of clathrin (~180 kDa), this antibody may also recognise light chains of clathrin (~25-29 kDa) which migrate at between 30-36 kDa due to high negative charge (Brodsky 1988). This may have been

responsible for part of the so called 'non-specific binding' observed. The use of this antibody has been published, both for western blot (Butler *et al.* 2012) and immunofluorescence (Puri 2009; Kuo *et al.* 2010; Shieh *et al.* 2011). In this study, detection of clathrin was conducted under reducing conditions on cell lysates prepared in RIPA buffer in the presence of complete protease inhibitor. At this stage it is unknown if the antibody works best under non-denatured conditions, in which circumstance, detection by immunofluorescence is still valid. Further experiments are required to characterise the reactivity of the antibody. Taken together, the internalisation of FhCL1 into macrophage endolysosomes did not appear to be associated with altered expression or localisation of clathrin.

Preliminary investigations into the effect of FhCL1 on the expression and localisation of dynamin were unsuccessful. Dynamin is a reported substrate of human cathepsin L (Sever *et al.* 2007), and thus, depending on the differences in substrate specificities between parasite and mammalian cathepsin L, modulation of dynamin remains a potential explanation for the immune modulation induced by FhCL1. Therefore, further investigation, for example through the use of a different antibody, is required to ascertain the effect of FhCL1 on dynamin expression and subcellular localisation. Additionally, biochemical analysis investigating whether FhCL1 could proteolytically cleave dynamin *in vitro* would strengthen the study. For example, immunoprecipitation of dynamin from lysates of untreated and FhCL1-treated macrophages could be analysed by western blot to compare the effect of FhCL1 on dynamin *in vitro*, however this too is dependent upon good quality dynamin-specific antibodies, and the epitopes on dynamin to which they bind.

Treatment of human macrophages with FhCL1 did, however, result in differences in the expression (albeit slight), and localisation of α-tubulin, a globular intracellular structural protein, that in conjunction with β-tubulin is associated with the formation of microtubules (reviewed in Downing *et al.* 1998). Microtubules are a component of the cytoskeleton that establishes and maintains cell shape and structure (for a review see de Forges *et al.* 2012). Furthermore, in association with motor proteins, microtubules are associated with the late stages of endocytosis, in the trafficking between early and late endosomes (Matteoni *et al.* 1987; Gruenberg *et al.* 1989). Treatment of human

macrophages with FhCL1 resulted in different α-tubulin localisation patterns observed with approximately equal frequency. The localisation patterns observed after culturing with FhCL1 were not visualised in macrophages cultured with FhCL1 with E64, which suggested that α-tubulin modulation was dependent upon the enzymatic activity of FhCL1. A previous study in human monocyte-derived DCs demonstrated that the depolymerisation of microtubules resulted in inhibited intracellular TLR4 expression, which was associated with suppression of cytokine expression (Uronen-Hansson *et al.* 2004). Thus, modulation of α-tubulin localisation by FhCL1 might inhibit intracellular transport and thus the movement of vesicles away from the cell surface and this could be responsible for the observed suppression of TRIF-dependent signalling by FhCL1. However, just how FhCL1 mediates this modulation in α-tubulin is unknown at this point, particularly as it is internalised within endolysosomal compartments and therefore may not have been in prolonged direct contact with α-tubulin. This requires further investigation, for example, this study could be enhanced by additional *in vitro* time course experiments with live cell imaging, to observe the effect of FhCL1 on α-tubulin over time.

While FhCL1 is known to degrade matrix and trafficking proteins, such as collagen, fibronectin, laminin and dynamin (Berasain *et al.* 1997; Sever *et al.* 2007; Robinson *et al.* 2011a), it has not previously been demonstrated to degrade or modulate the subcellular localisation of α-tubulin. However, bovine cathepsin L has been observed to degrade murine β-tubulin (Kim *et al.* 2006). A dose-dependent degradation of β-tubulin has been observed in murine striatal X57 cells treated with bovine cathepsin L, as detected by western blotting (Kim *et al.* 2006). Thus, β-tubulin is in fact a likely candidate for the modulation of intracellular trafficking by FhCL1, depending on the protease substrate specificities of parasite and mammalian cathepsin L. Therefore, while FhCL1 treatment of human monocyte-derived macrophages had little effect on α-tubulin as observed by western blot, the levels of β-tubulin should be examined by both western blot and confocal microscopy.

The heterogeneity of α-tubulin localisation within FhCL1-treated samples might be explained by a number of factors. First, microscopy was performed on pooled macrophage donors and thus it is most likely that the differences are a result of the

effect of FhCL1 on individual donor's cells. However, tubulin is often used as a loading control during western blot analysis (Mendoza-Villanueva *et al.* 2010; Groenendijk *et al.* 2011; Bachetti *et al.* 2012) or a housekeeping gene in real-time RT-PCR assay (Eisenberg *et al.* 2003) and as such heterogeneity in α-tubulin responses are unexpected, and cannot be easily explained at present. Nevertheless, this highlights the limitations of the use of primary human monocyte-derived macrophages due to potential differences between individual donors. It remains possible that individual donors might have different inherent capacity to internalise FhCL1, and without knowing the precise mechanism by which FhCL1 is internalised it is difficult to speculate with regard to potential causes for these differences. Repetition of these experiments with individual donors, rather than pooled cells from different donors, would confirm whether the effect was donor dependent, nontheless it is also possible that the heterogenous results are due to problems with the stability of FhCL1 (see next paragraph).

Unfortunately, this study has been hampered by certain results not easily being found to be reproducible. This led to questioning whether the stocks of recombinant *P. pastoris*-derived FhCL1 were unstable, despite storage of individual aliquots at -20˚C and thawing on ice to minimise potential protein degradation. For this reason, historical protein gels which examined the integrity of FhCL1 protein were re-analysed to assess the quality and stability of different batches of recombinant protein over time. This re-analysis revealed that FhCL1 had indeed become partially degraded over time (Figure 4.17), and this likely explains difficulties in reproducing some of the later experimental results. Indeed, Coomassie stained gels performed to check the purity of FhCL1 post-preparation showed significant degradation of FhCL1, and that this degradation was prevented when FhCL1 was incubated with E64 protease inhibitor (Figure 4.17, Batch 3). Furthermore, faint additional bands are also present in published figures of Coomassie stained gels from *P. pastoris*-derived FhCL1 (Collins *et al.* 2004), which could similarly represent degradation products. It is known that human procathepsin L is autocatalytically cleaved to produce a propeptide and mature enzymatically active cathepsin L (Menard *et al.* 1998), and it is thought that FhCL1 undergoes a similar process (Collins *et al.* 2004). Further autocatalytic degradation of FhCL1 has not been reported, but FhCL1 is considered a promiscuous enzyme with broad substrate specificity (Robinson *et al.* 2011a), and thus this degradation may occur as a result of long term storage of recombinant FhCL1. In this regard, it is possible that

storage without a substrate may lead to its autocatalysis, i.e. in the absence of any other substrate. Yet the presence of an exogenous substrate implicitly prevents its activity in treated cells. This further highlights the instability of FhCL1 and thus, the difficulties of storing and working with a proteolytic enzyme. If FhCL1 is in fact autocatalytic, the storage of autocatalytic enzymes is sometimes achieved by making use of the pH range over which the enzyme is active, that is storing the protein at a pH at which the enzyme is inactive, or by storing in the enzyme in the absence of co-factors required for enzymatic activity. FhCL1 is known to be enzymatically active over a broad pH range (Lowther *et al.* 2009), and thus better characterisation of FhCL1 is required to determine the optimal conditions for its storage. The degradation of FhCL1 was identified at the same time as the western blot experiments were performed for this thesis and attempts to create fresh stocks of undegraded FhCL1 were unsuccessful. Unfortunately this prevented the completion of additional repeats of the western blot experiments shown in Figure 3.10, Figure 3.11, Figure 3.12, Figure 3.14 and Figure 4.14.

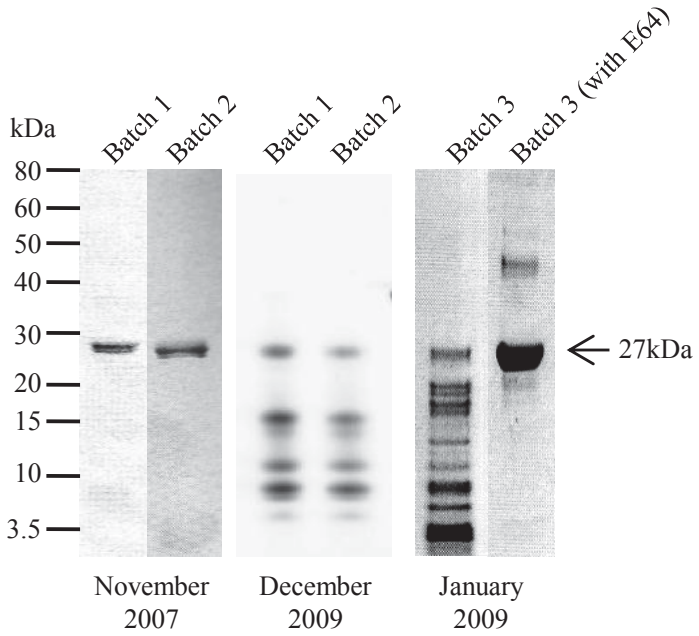

Figure 4.17: Protein analysis of FhCL1.
Western blot analysis of three batches of FhCL1 (27 kDa) examined under reducing conditions. The purity/degradation of the original two batches of FhCL1 was tested at two time points, first after production in November 2007 using Coomassie stain and two years later in December 2009 using Flamingo stain. A third batch of FhCL1 was produced in January 2009 and examined by SDS-PAGE with Coomassie staining, however this batch of FhCL1 was rapidly degraded and E64 protease inhibitor was required to prevent this degradation. Protein gels performed by J. To and D. Xu (UTS).

CHAPTER 5:

THE EFFECT OF BACTERIAL AND HELMINTH STIMULI ON MACROPHAGE-ASSOCIATED NANOTUBES

5.1 INTRODUCTION

5.1.1 TOLL-LIKE RECEPTORS AND NANOTUBES

Surface receptors and antigen/receptor complexes have been shown to be transported through nanotubes between connected cells (Watkins *et al.* 2005; Chinnery *et al.* 2008). Likewise, bacterial and viral proteins are transported between connected cells via nanotubes (Watkins *et al.* 2005; Onfelt *et al.* 2006; Sherer *et al.* 2007; Sowinski *et al.* 2008). Given the role of TLRs in antigen recognition and the initiation of cell signalling in response to bacterial and viral ligands, the transport of TLRs between cells via nanotubes has been proposed (Chinnery *et al.* 2008). However, the transport of TLRs between cells via nanotubes has not been established to date.

TLR4 localises to the plasma membrane of both the cell surface and intracellular compartments, where it recognises LPS, as well as several other proteins including helminth products (reviewed in Thomas *et al.* 2003; Akira *et al.* 2004; Goodridge *et al.* 2005). Produced in the endoplasmic reticulum, TLR4 is trafficked to the cell surface by the golgi apparatus, likely in association with microtubulin (Uronen-Hansson *et al.* 2004). Following recognition of LPS, TLR4 initiates cell signalling through one of two pathways, inducing the expression of pro-inflammatory cytokines and co-stimulatory molecules (Saitoh 2009), resulting in activation.

TLR3 is a receptor located on the membrane of intracellular compartments, such as endosomal vesicles (Matsumoto *et al.* 2003; Nishiya *et al.* 2004; Lee *et al.* 2006), and recognises dsRNA (Alexopoulou *et al.* 2001), playing a role in the detection of viruses (reviewed in Schroder *et al.* 2005). Following the detection of dsRNA, the expression of pro-inflammatory cytokines and type 1 interferons is initiated through the TRIF signalling pathway resulting in activation of cells (Yamamoto *et al.* 2003; Kawai *et al.* 2006).

5.1.2 SPECIFIC AIM

Cell activation following recognition of bacterial, viral and helminth antigens by TLRs occurs through the initiation of cell signalling pathways which ultimately up-regulate the expression of cytokines and co-stimulatory factors. Following the recognition of

antigen, and activation of the cell, it is essential that surrounding cells are rapidly activated to mount a response against the pathogen (Takeuchi *et al.* 2010). Nanotubes are a means by which cells can share cellular resources and rapidly activate surrounding cells. During microscopy investigations, macrophage nanotubes were observed to connect cells. Therefore, the localisation of endosomes and TLRs within nanotubes and the effects of bacterial and helminth products, namely LPS and FhCL1, on the localisation of TLRs within macrophage nanotubes are investigated.

5.2 RESULTS

5.2.1 CYTOSKELETAL STRUCTURE OF NANOTUBES CONNECTING PRIMARY HUMAN MACROPHAGES

A feature of macrophage cultures consistently observed by confocal microscopy analysis of TLR4 localisation, was the presence of nanotubes. These structures were repeatedly observed to connect human monocyte-derived macrophages, in both FhCL1-treated and PBS control cells. The cytoskeletal components of primary human macrophage-associated nanotubes were previously shown to include F-actin, either with, or without, microtubulin (Onfelt *et al.* 2006). Nanotubes can be classified as either 'thick' or 'thin', according to their diameter and cytoskeletal components, with 'thin' nanotubes being <0.7 μm, and containing only F-actin, and thick nanotubes being ≥0.7 μm and composed of both F-actin and microtubulin (Onfelt *et al.* 2006). To investigate whether the observed nanotubes connecting primary human macrophages in this study had a similar composition to those previously described, macrophages were stained with anti-α-tubulin antibody and/or phalloidin (to detect F-actin) and were analysed by confocal microscopy. The macrophage-associated nanotubes observed in this study, were predominantly of the 'thick' type with greater than 97% (101/104) of nanotubes being ≥0.7 μm in diameter (Figure 5.1). These nanotubes were composed of both α-tubulin and F-actin (Figure 5.1), consistent with previous reports describing 'thick' nanotubes (Onfelt *et al.* 2006).

5.2.2 LOCALISATION OF TLR4, TLR3 AND EARLY ENDOSOMES IN NANOTUBES OF PRIMARY HUMAN MACROPHAGES

Viruses, such as murine leukaemia virus, have been observed to traffic between combinations of cells such as human embryonic kidney 293 cells, Cos-1 fibroblast cells and XC muscle cells through nanotubes (Sherer *et al.* 2007), and stimulation with soluble bacterial components, such as *E. coli* supernatant, induces activation of the distal connected cells via cell signalling that occurs through the nanotube (Watkins *et al.* 2005). TLRs are important in the recognition and binding of bacterial and viral antigens and initiate TLR cell signalling at the cell surface and/or within endosomes (Akira *et al.* 2004). Furthermore, the transport of endosome-related organelles, lysosomes and MHC molecules (HLA-C) has been observed to occur through

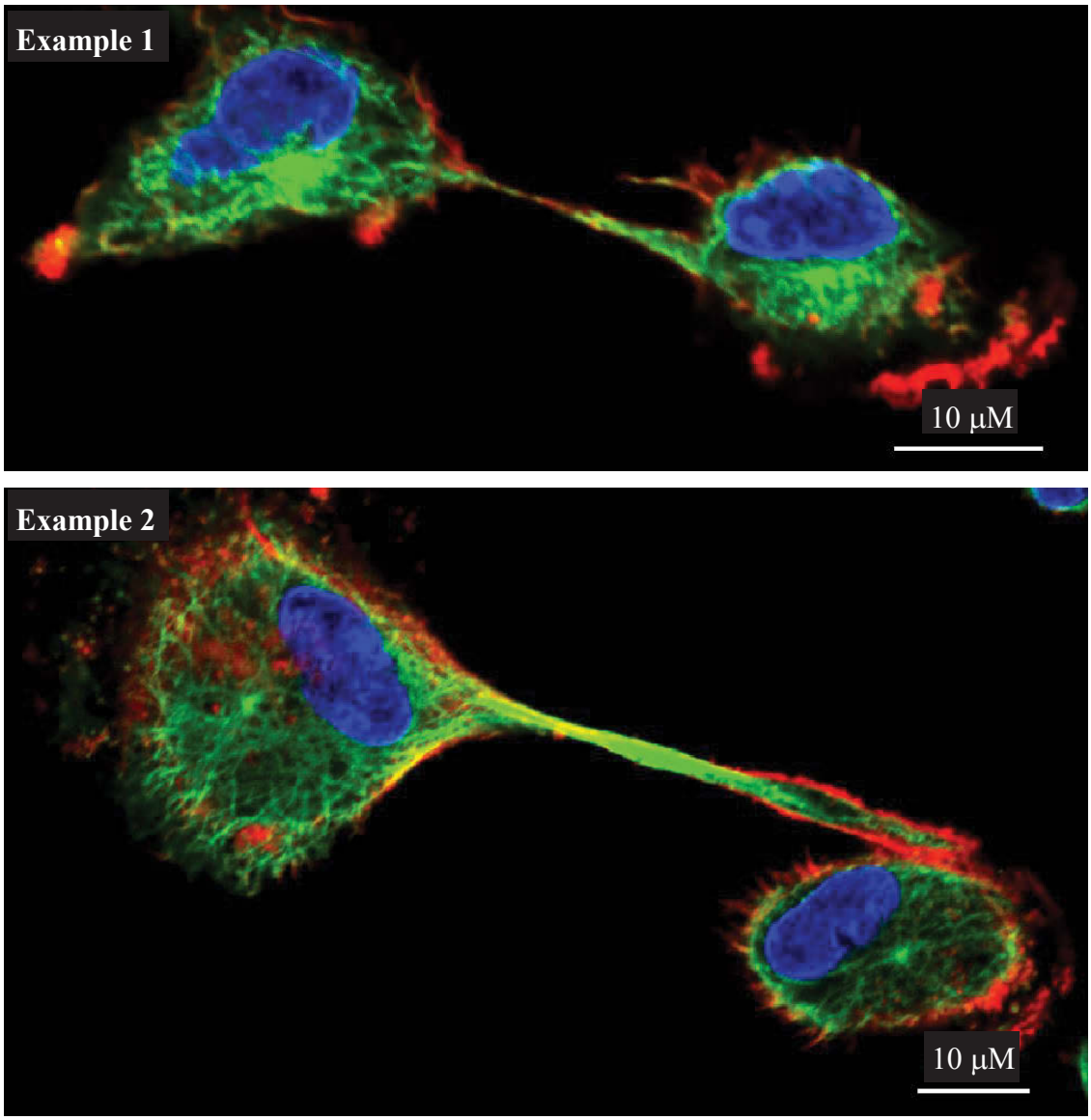

Figure 5.1: Cytoskeletal structure of nanotubes connecting primary human macrophages.
Macrophages were stained with anti-α-tubulin antibody and goat anti-mouse-AF488 secondary antibody (green), together with phalloidin (red) for detection of F-actin and DAPI (blue) for nuclei. Data shown are representative images of thick nanotubes with a diameter of ≥0.7 μm. Imaging was performed using a Nikon A1 Confocal scanning laser microscope. Representative of twelve individual images acquired.

macrophage-associated nanotubes (Watkins *et al.* 2005; Onfelt *et al.* 2006). Therefore, given the important role of TLRs in antigen recognition and the initiation of cell signalling, it was proposed that TLRs might traffic through nanotubes. To address this possibility, primary human macrophages were incubated with anti-EEA-1 antibody, EEA-1 being a marker of early endosomes (Mu *et al.* 1995), together with anti-TLR4 antibody, or anti-TLR3 antibody. Confocal microscopy analyses showed that EEA-1 was present in nanotubes (Figure 5.2). However, when visually comparing the distribution of EEA-1 between the cell bodies of macrophages and their associated nanotubes, EEA-1 appeared to be present in a higher concentration within the cell body compared to the nanotubes. (Please note: for this study the 'cell body' refers to the main body of the cell excluding any protrusions). To further investigate this difference in localisation, quantitative determination of EEA-1 fluorescence intensity levels was performed in PBS control cultured macrophage cells. The cell bodies and their associated nanotubes were defined for analysis and levels of fluorescence were measured. The mean fluorescence intensity (MFI) was calculated separately for EEA-1 molecules in the nanotubes and the corresponding cell bodies of macrophages. A ratio of the MFI was calculated for EEA-1 within nanotubes versus the MFI of EEA-1 in the cell body and the ratios of all nanotube/cell body pairs were averaged (for details see Section 2.7.5.3). Using this averaged ratio of MFI, the relative localisation of each molecule within the macrophage cell body could be compared to the levels of the same molecule within the associated nanotubes, with a ratio of 1.0 indicating no difference in localisation, i.e. equal distribution in cell body and nanotubes, >1.0 indicating an increase in localisation within nanotubes, and <1.0 indicating increased localisation in the cell body. Despite nanotubes being shown to traffic EEA-1, the early endosome protein EEA-1 localised preferentially to the cell body (ratio: 0.4, p=<0.0001) (Table 5.1; see Appendix 3 for raw MFI values).

Similarly, TLR4 and TLR3 were also observed within macrophage-associated nanotubes (Figure 5.2). Although, in contrast to EEA-1, both TLR4 and TLR3 were observed to localise equally within both the cell body and associated nanotubes of PBS-treated macrophages (Figure 5.2) (TLR4 ratio: 1.1, p=0.6293, TLR3 ratio: 1.1, p=0.8030) (Table 5.1; see Appendix 4 and 5 for raw MFI values). However, as previously discussed, the expression of TLR3 in human monocyte-derived macrophages was low and difficult to detect above isotype control staining and thus no further

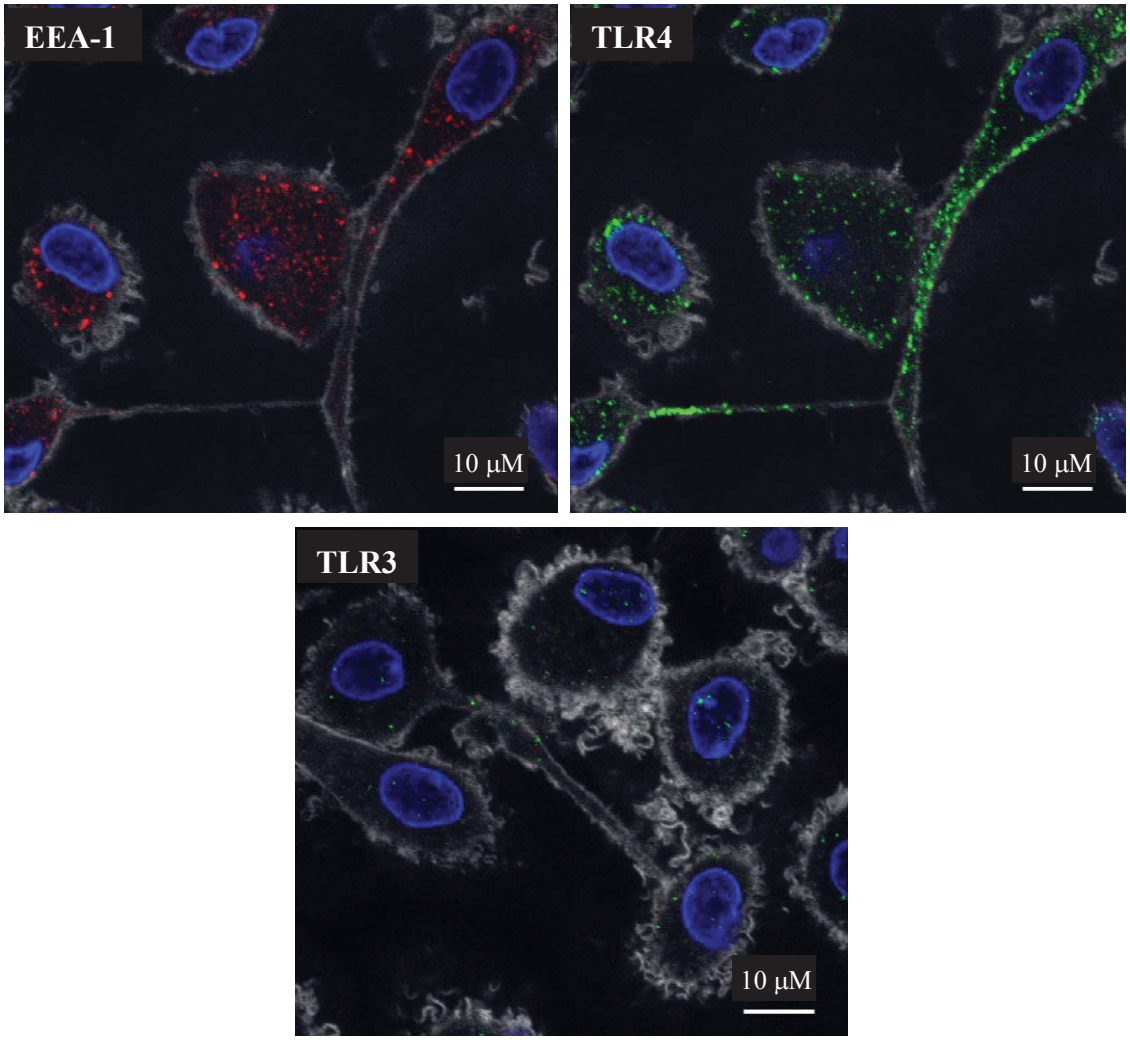

Figure 5.2: Localisation of EEA-1, TLR4 and TLR3 within nanotubes of primary human macrophages.
Macrophages were stained with anti-EEA-1 antibody and goat anti-rabbit-AF568 secondary antibody (red), anti-TLR4 antibody and goat anti-mouse-AF488 secondary antibody (green), or anti-TLR3 antibody and goat anti-mouse-AF488 secondary antibody (green), phalloidin (white) for F-actin and DAPI (blue) to detect nuclei. Data shown are representative images of 14 nanotubes for EEA-1 and TLR4 and 3 nanotubes for TLR3. Samples were imaged using a Nikon A1 Confocal scanning laser microscope.

Table 5.1: Ratio of localisation of early endosome antigen (EEA-1), TLR4 and TLR3 in nanotubes versus the cell body in PBS treated human macrophages.

Molecule	Number of nanotube-cell body pairs analysed	Averaged ratio of MFI ± SD	P-value of ratio compared to 1.0
EEA-1	14	0.4 ± 0.3	<0.0001 *
TLR4	14	1.1 ± 0.8	0.6293
TLR3	3	1.1 ± 0.8	0.8030

* Statistically significant.

investigations into the localisation of TLR3 within macrophage associated nanotubes were conducted. For this reason, only a small number of nanotubes-cell body pairs were examined for TLR3. Therefore, as well as containing EEA-1, macrophage-associated nanotubes also contain TLR4 and potentially TLR3.

5.2.3 LOCALISATION OF EEA-1 AND TLR4 WITHIN MACROPHAGE-ASSOCIATED NANOTUBES FOLLOWING LPS STIMULATION

Following recognition of LPS by TLR4, cell signalling is induced and the TLR4/LPS complex is rapidly internalised (reviewed in Akira *et al.* 2004; Kagan *et al.* 2008). It was therefore hypothesised that LPS stimulation may alter the localisation of TLR4 within macrophage-associated nanotubes. Therefore, confocal analysis was performed to investigate the localisation of EEA-1 and TLR4 within macrophage cell bodies and their associated nanotubes following stimulation with 50 ng/mL LPS over a time course up to 6 h (Table 5.2). When the localisation of EEA-1 was compared between cell bodies and their associated nanotubes following LPS stimulation, results showed that EEA-1 was found to predominately localise within the cell body (ratio: 0.5, p=<0.0001), similar to unstimulated macrophages (ratio: 0.4, p=<0.0001) (Table 5.2; see Appendix 3 for raw MFI values). Furthermore, EEA-1 was predominately localised within the cell body when the cell body-nanotube pairs were analysed at individual time points, with all time points, except 1 h, being statistically significant (Table 5.2, Figure 5.3 and Figure 5.4A). These results suggest that LPS stimulation has no effect on the localisation of EEA-1 within macrophage nanotubes.

When the localisation of TLR4 was compared between pairs of cell bodies and their associated nanotubes following stimulation with 50ng/mL LPS, it was evident that, collectively, LPS stimulation significantly increased the localisation of TLR4 within nanotubes (p=0.0077) (Table 5.3; see Appendix 4 for raw MFI values). However, when the cell body-nanotube pairs were analysed at individual time points post-LPS stimulation, there were no statistically significant differences in the localisation of TLR4, with the average MFI suggesting that there were fluctuations in TLR4 localisation over time (Table 5.3, Figure 5.3 and Figure 5.4A). Overall, these results suggest that LPS stimulation increased the localisation of TLR4 within macrophage-associated nanotubes.

Despite EEA-1 being a marker of early endosomes (Mu *et al.* 1995) and TLR4 being endocytosed into early endosomes (Husebye *et al.* 2006), an incidental finding of this work was that TLR4 and EEA-1 visually did not appear to co-localise (Figure 5.4B). To more analytically investigate the localisation of TLR4 and EEA-1, the Mander's coefficient was calculated after setting threshold levels to exclude background signal (threshold set to 700 for both TLR4 and EEA-1). Image analysis determined that on average between 1 and 3% of TLR4 and EEA-1 co-localised at all time points post LPS stimulation (Table 5.4). Thus, this result suggests that EEA-1 and TLR4 do not co-localise in human monocyte-derived macrophages.

Table 5.2: Ratio of localisation of EEA-1 within nanotubes and corresponding cell bodies of primary human macrophages following LPS stimulation.

Timepoint	Number of nanotube-cell body pairs analysed	Averaged ratio of MFI ± SD [1]	P-value of ratio compared to 1.0
PBS	14	0.4 ± 0.3	<0.0001 *
LPS 5 min	4	0.5 ± 0.2	0.0190 *
LPS 15 min	6	0.4 ± 0.1	<0.0001 *
LPS 30 min	6	0.5 ± 0.3	0.0080 *
LPS 1 h	3	0.6 ± 0.4	0.2567
LPS 6 h	10	0.6 ± 0.2	0.0005 *
Average LPS	**29**	0.5± 0.2	<0.0001 *

[1] Presented graphically in Figure 5.3 and individual image examples presented in Figure 5.4. *Significant.

Table 5.3: Ratio of localisation of TLR4 within nanotubes and corresponding cell bodies of primary human macrophages following LPS stimulation.

Timepoint	Number of nanotube-cell body pairs analysed	Averaged ratio of MFI ± SD [1]	P-value of ratio compared to 1.0
PBS	14	1.1 ± 0.8	0.6293
LPS 5 min	4	1.7 ± 0.9	0.2257
LPS 15 min	6	0.8 ± 0.4	0.2856
LPS 30 min	6	1.3 ± 0.7	0.2888
LPS 1 h	6	1.5 ± 0.9	0.1062
LPS 6 h	10	1.5 ± 0.7	0.0757
Average LPS	**32**	1.3 ± 0.7	0.0077 *

[1] Presented graphically in Figure 5.3 and individual image examples presented in Figure 5.4. * Significant.

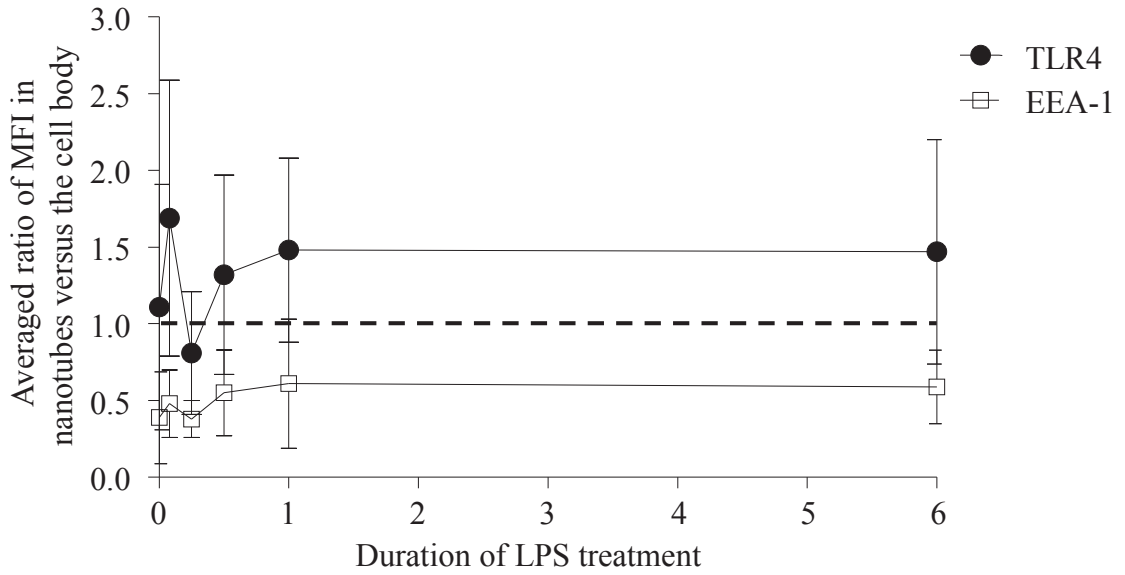

Figure 5.3: Graphical representation of the relative localisation of EEA-1 and TLR4 within macrophages and their associated nanotubes following LPS treatment.

Data shown are the averaged ratio of EEA-1 (open square) and TLR4 (closed circle) in nanotubes compared to corresponding cell bodies for all nanotubes/cell body pairs following LPS stimulation for up to 6 h. Equal localisation in cell body and nanotubes is indicated by a dashed line. The error bars represent the standard deviation.

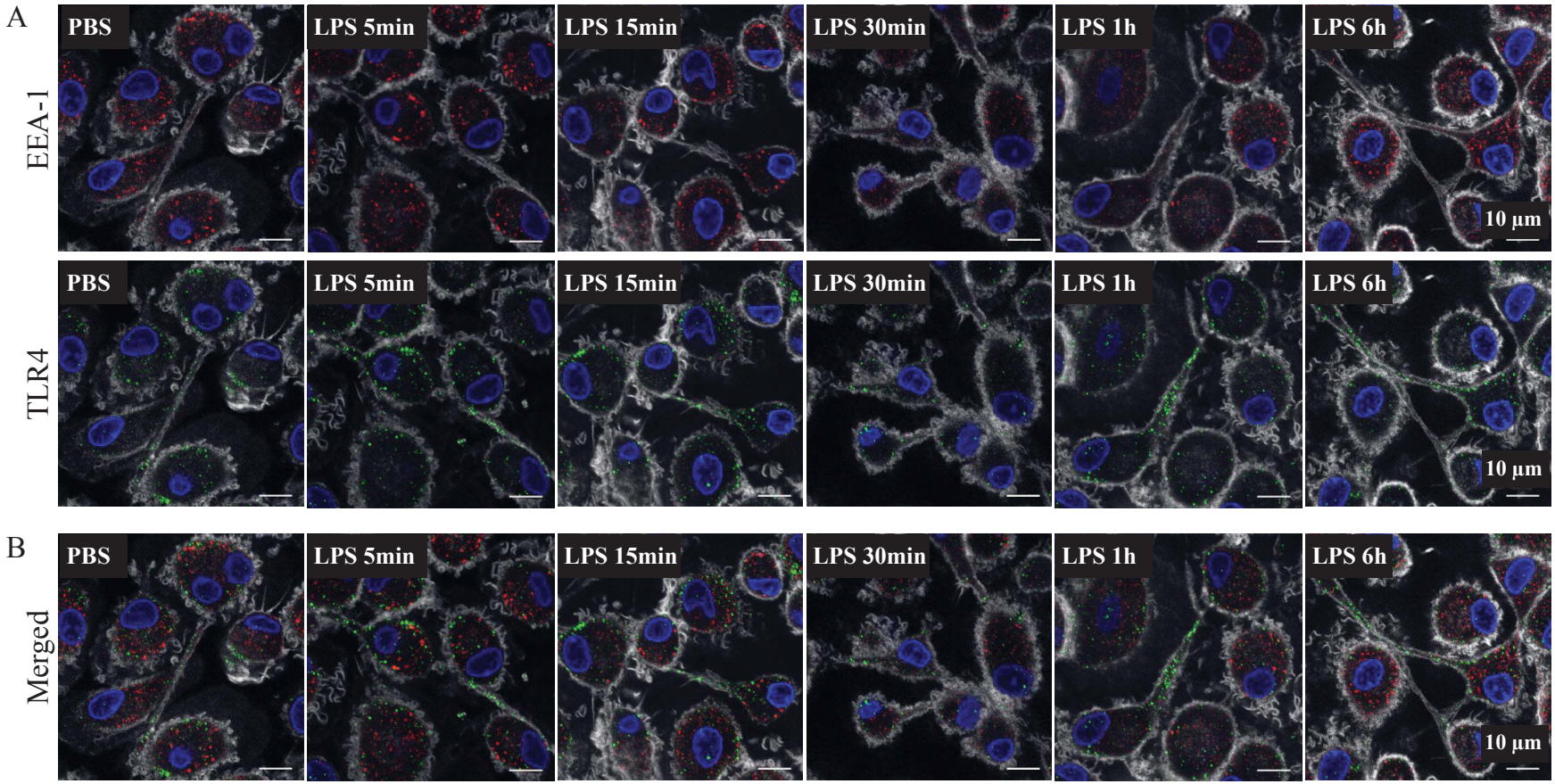

Figure 5.4: Localisation of EEA-1 and TLR4 within nanotubes of primary human macrophages following LPS stimulation.
A) Macrophages were stained with anti-EEA-1 antibody (top panel) and then with goat anti-rabbit-AF568 secondary antibody (red) and anti-TLR4 antibody (bottom panel) and goat anti-mouse-AF488 secondary antibody (green), together with phalloidin (white) for F-actin and DAPI (blue) to detect nuclei. B) Merged images of TLR4 and EEA-1 localisation in monocyte-derived macrophages. Data shown are representative images of the localisation of EEA-1 and TLR4 in macrophage nanotubes compared to corresponding cell bodies following LPS stimulation for up to 6 h. Samples were imaged using a Nikon A1 Confocal scanning laser microscope. Representative of a minimum of three nanotubes for each time point.

Table 5.4: Mander's co-localisation coefficient analysis for TLR4 and EEA-1 localisation within primary human macrophages.

Image	Number of co-localised voxels	% of dataset co-localised	% of TLR4 above threshold co-localised	% of EEA-1 above threshold co-localised	Thresholded Mander's coefficient A	Thresholded Mander's coefficient B
Control						
1	311	0.0	2.7	2.7	0.03	0.02
2	154	0.0	2.5	1.5	0.02	0.01
3	234	0.0	2.7	2.1	0.03	0.02
4	161	0.0	1.3	3.4	0.01	0.03
5	256	0.0	2.9	2.7	0.03	0.02
6	210	0.0	2.2	2.1	0.02	0.02
7	390	0.0	3.8	4.0	0.03	0.03
8	361	0.0	2.8	3.7	0.03	0.04
Total number of cells = 116				**Average**	**0.03**	**0.02**
LPS 5 min						
1	302	0.0	2.5	2.7	0.02	0.02
2	150	0.0	3.0	1.9	0.02	0.02
3	288	0.0	2.8	4.3	0.02	0.04
4	162	0.0	3.3	2.0	0.03	0.02
5	275	0.0	3.3	2.7	0.03	0.03
6	316	0.0	2.9	3.3	0.03	0.03
Total number of cells = 86				**Average**	**0.03**	**0.03**
LPS 15 min						
1	500	0.1	5.1	3.1	0.04	0.02
2	528	0.1	4.8	3.5	0.04	0.03
3	438	0.0	3.6	2.6	0.04	0.02
4	354	0.0	3.4	2.4	0.03	0.02
5	538	0.1	4.5	3.9	0.04	0.03
6	497	0.1	4.3	3.1	0.04	0.03
Total number of cells = 97				**Average**	**0.04**	**0.03**
LPS 30 min						
1	36	0.0	1.0	1.4	0.01	0.01
2	34	0.0	0.7	1.3	0.01	0.01
3	23	0.0	0.6	1.1	0.00	0.01
4	14	0.0	0.2	0.9	0.00	0.01
5	109	0.0	2.6	2.4	0.01	0.02
6	63	0.0	1.2	1.9	0.01	0.01
7	131	0.0	0.8	1.4	0.01	0.01
Total number of cells = 127				**Average**	**0.01**	**0.01**
LPS 1 h						
1	305	0.0	3.8	2.9	0.03	0.02
2	294	0.0	3.8	2.4	0.03	0.02
3	374	0.0	4.8	3.2	0.04	0.03
4	305	0.0	3.1	2.6	0.02	0.02
5	444	0.0	6.1	4.0	0.04	0.03
6	339	0.0	4.0	3.0	0.03	0.03
Total number of cells = 109				**Average**	**0.03**	**0.03**
LPS 6 h						
1	444	0.0	3.5	2.3	0.03	0.02
2	379	0.0	3.6	2.0	0.03	0.02
3	314	0.0	4.2	1.7	0.03	0.02
4	331	0.0	4.0	1.7	0.03	0.02
5	389	0.0	5.0	2.5	0.04	0.02
6	553	0.1	4.1	2.9	0.04	0.03
7	344	0.0	4.6	2.4	0.04	0.02
8	383	0.0	4.5	2.1	0.03	0.02
Total number of cells = 135				**Average**	**0.03**	**0.03**

5.2.4 LOCALISATION OF TLR4 WITHIN NANOTUBES

Levels of surface TLR4 expression are low on primary human macrophages prior to LPS stimulation (Figure 4.10), but confocal imaging indicated that TLR4 was localised within macrophage-associated nanotubes (Figure 5.2). It was therefore hypothesised that TLR4 was trafficked via endosomes through nanotubes, rather than being localised predominately to the cell surface. To investigate this hypothesis, macrophages were incubated with anti-TLR4 antibody with azide (1 h, 4 ˚C) to prevent phagocytosis and internalisation of the TLR4 specific antibody (Oda *et al.* 1986). Macrophages were subsequently fixed and permeabilised prior to incubation with goat anti-mouse-AF488 secondary antibody which aimed to stain surface TLR4, as well as any internalised antibody. As a positive control, one sample was stained with anti-TLR4 primary antibody following fixation and permeabilisation (Figure 5.5). Results demonstrated virtually no TLR4 on both the surface of the cell body and the surface of nanotubes (Figure 5.5). This confirmed that there were only very low levels of surface TLR4 expression prior to LPS stimulation. However, as macrophages are known to express some, albeit low, levels of surface TLR4 (Juarez *et al.* 2010) as confirmed by flow cytometry (Figure 4.10), it was concluded that surface TLR4 was so low that it was difficult to detect by confocal microscopy. As such, due to the complete lack of detectable surface TLR4 on both the cell body and nanotubes, it could not be convincingly determined whether TLR4 was localised to the cell surface of nanotubes of primary human monocyte-derived macrophages.

5.2.5 LOCALISATION OF TLR4 AND CYTOSKELETAL PROTEINS IN NANOTUBES

The cell cytoskeleton is composed of a number of proteins which mediate migration and intracellular transport (reviewed in Doherty *et al.* 2008). For example, F-actin is responsible for maintaining cell structure by providing support for the cell membrane, mediates migration, and is associated with membrane invagination during phagocytosis and endocytosis, while endosome transport is mediated via microtubules (for reviews see Doherty *et al.* 2008; and de Forges *et al.* 2012). Therefore, to further investigate the localisation of TLR4 within nanotubes, its localisation with respect to α-tubulin (a component of microtubules) and F-actin was investigated. Primary human macrophages were stained with anti-TLR4 antibody, anti-α-tubulin antibody and phalloidin to

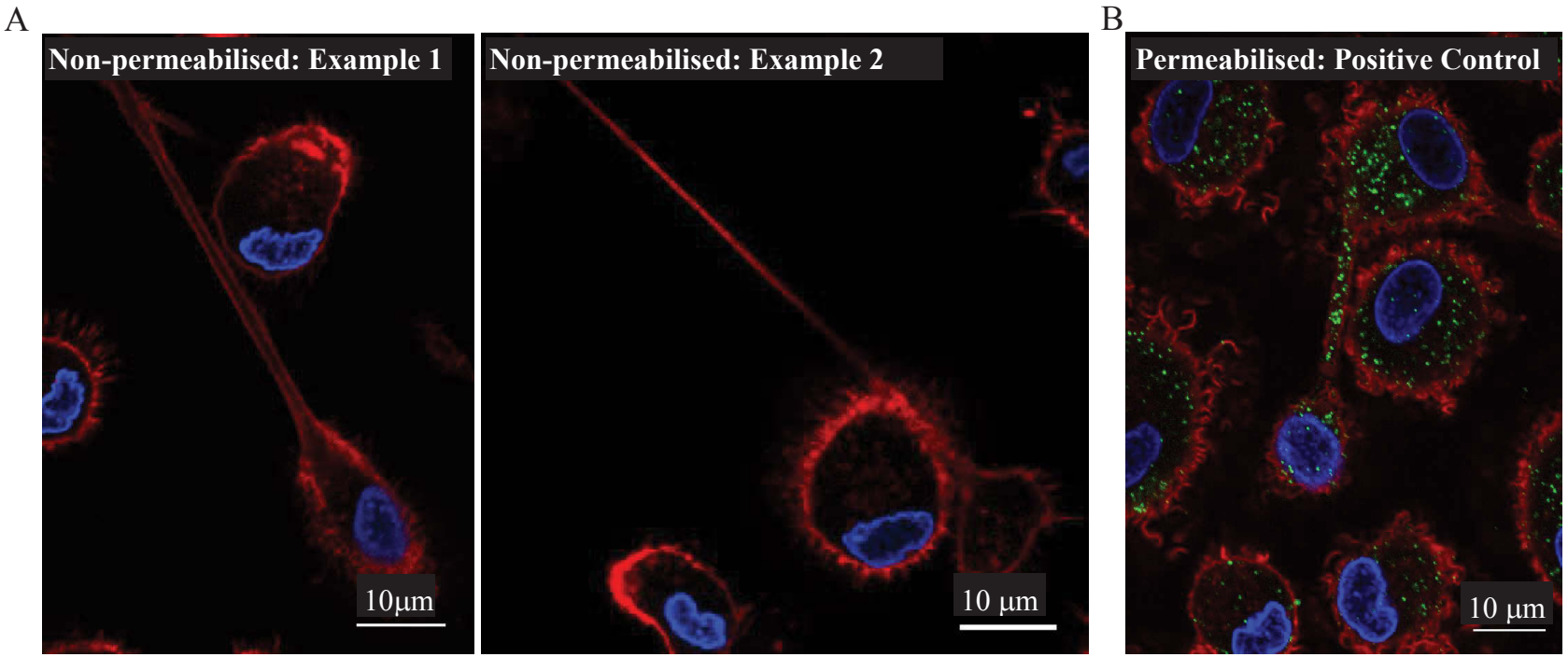

Figure 5.5: Localisation of TLR4 on the cell surface of macrophage nanotubes.
A) Macrophages were incubated (1 h, 4 °C) with anti-TLR4 antibody prior to fixation and permeabilisation. Following fixation, cells were permeabilised and stained with goat anti-mouse-AF488 secondary antibody (green), together with phalloidin (red) for F-actin and DAPI (blue) for nuclei. Data shown are representative images of thick nanotubes imaged using a Nikon A1 Confocal scanning laser microscope. Data shown are representative of 40 cells and 5 nanotubes. B) As a positive control, macrophages were fixed and permeabilised prior to staining with anti-TLR4 antibody with goat anti-mouse-AF488 secondary antibody (green).

detect F-actin, and analysed by confocal microscopy. Results showed that TLR4 was associated with α-tubulin beneath the plasma membrane and within nanotubes (Figure 5.6), and this suggested that there was less co-localisation of TLR4 with F-actin filaments (Figure 5.6). To calculate co-localisation within both nanotubes and the cell body, Mander's coefficient was calculated using IMARIS software (Bitplane Scientific, Switzerland). After threshold levels were set to exclude background signal (threshold set to 1200 for TLR4 and 900 for α-tubulin), image analysis determined that, on average, 52% of TLR4 co-localised with α-tubulin (Mander's coefficient A = 0.52), and 22% of α-tubulin co-localised with TLR4 (Mander's coefficient B = 0.22) (Table 5.5). When comparing the co-localisation of TLR4 and F-actin (threshold set to 1200 for TLR4 and 1000 for F-actin), image analysis determined that, on average 28% of TLR4 co-localised with F-actin (Mander's coefficient A = 0.28), while only 8% of F-actin co-localised with TLR4 (Mander's coefficient B = 0.08) (Table 5.6). Therefore, within both the macrophage cell body and associated nanotubes, TLR4 co-localised with both α-tubulin and F-actin, with a higher degree of co-localisation with α-tubulin.

In order to confirm that there was limited co-localisation of TLR4 with F-actin within nanotubes, the ultrafine structure of F-actin and TLR4 was investigated using high resolution fluorescence deconvolution microscopy. F-actin filaments were visible with greater resolution, as were TLR4 molecules and even at this resolution F-actin and TLR4 did not appear to co-localise. Therefore either by confocal microscopy or high resolution OMX microscopy, TLR4 and F-actin showed limited co-localisation either within the cell body or within the nanotubes (Figure 5.7). Taken together, TLR4 is more likely to be transported by α-tubulin within nanotubes.

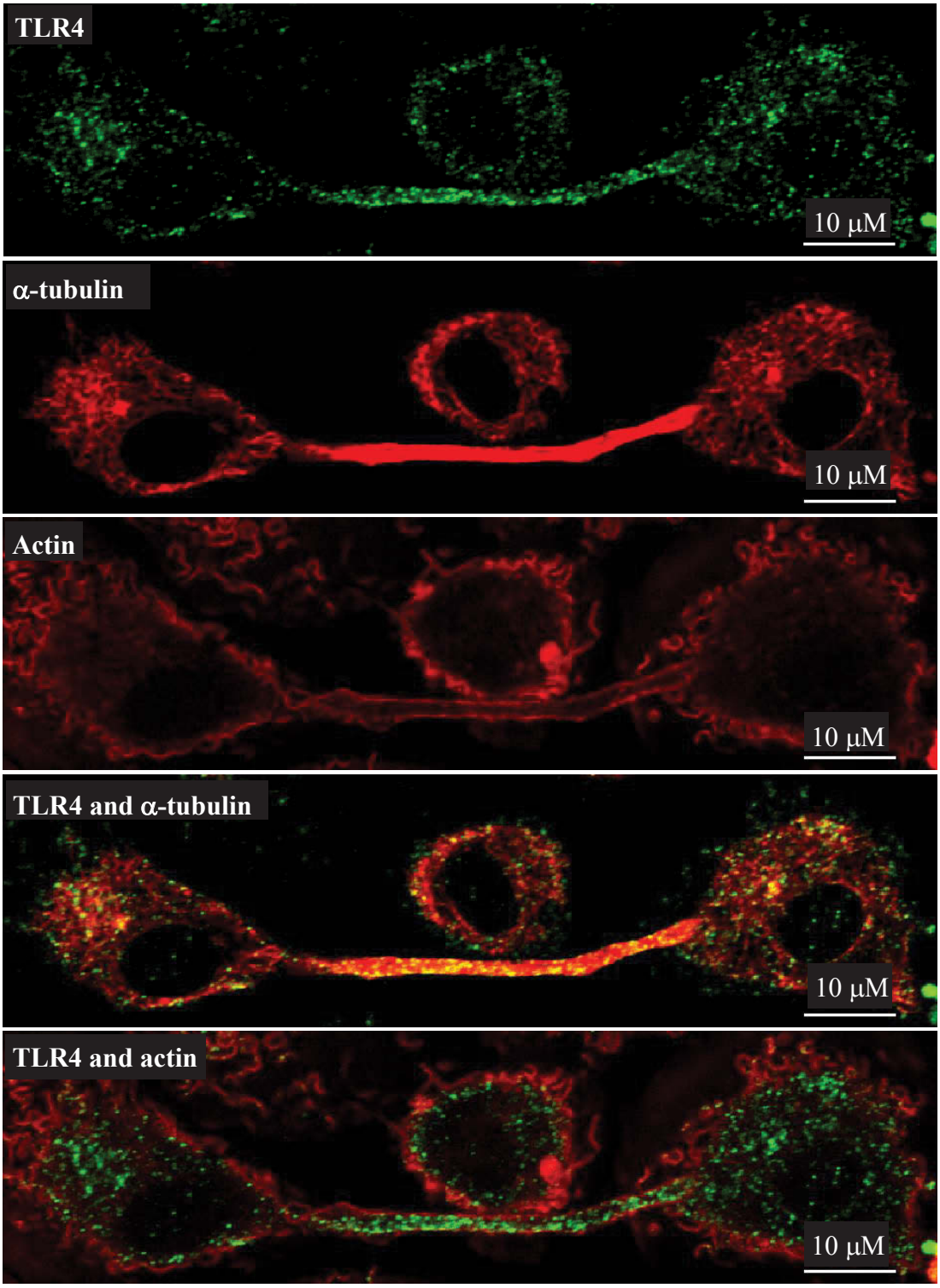

Figure 5.6: Localisation of TLR4, α-tubulin and F-actin within nanotubes connecting primary human macrophages.
Macrophages were stained with anti-TLR4 antibody and goat anti-mouse-AF488 secondary antibody (green), anti-α-tubulin antibody and goat anti-rabbit-AF568 secondary antibody (red), together with phalloidin (red) for F-actin. Imaging was performed using the Nikon A1 Confocal scanning laser microscope. Images show the localisation of TLR4 within nanotubes with regard to α-tubulin and F-actin. Co-localisation is indicated by a yellow colour (overlay of pseudo coloured red and green images). Data shown are representative images of 11 nanotubes.

Table 5.5: Mander's co-localisation coefficient analysis for TLR4 and α-tubulin localisation within primary human macrophages.

Image	Number of co-localised voxels	% of dataset co-localised	% of TLR4 above threshold co-localised	% of α-tubulin above threshold co-localised	Thresholded Mander's coefficient A	Thresholded Mander's coefficient B
1	42198	4.0	71.6	26.3	0.50	0.22
2	57519	5.5	72.8	28.0	0.50	0.22
3	34742	3.3	78.9	26.7	0.52	0.21
4	43373	4.1	83.1	31.5	0.59	0.26
5	44889	4.3	74.9	25.9	0.50	0.20
6	41951	4.0	75.3	29.5	0.52	0.24
7	33829	3.2	77.9	27.9	0.53	0.22
8	15809	1.5	80.5	22.5	0.51	0.18
Total number of cells = 102				**Average**	**0.52**	**0.22**

Table 5.6: Mander's co-localisation coefficient analysis for TLR4 and F-actin localisation within primary human macrophages.

Image	Number of co-localised voxels	% of dataset co-localised	% of TLR4 above threshold co-localised	% of F-actin above threshold co-localised	Thresholded Mander's coefficient A	Thresholded Mander's coefficient B
1	27433	2.6	45.0	15.0	0.38	0.10
2	33503	3.2	41.0	14.9	0.33	0.12
3	9498	0.9	20.6	9.9	0.20	0.07
4	13486	1.3	25.1	13.4	0.24	0.08
5	18397	1.8	29.4	13.8	0.25	0.09
6	18860	1.8	33.5	17.0	0.27	0.09
7	12201	1.2	26.7	10.8	0.27	0.07
8	5985	0.6	28.8	8.5	0.27	0.04
Total number of cells = 102				**Average**	**0.28**	**0.08**

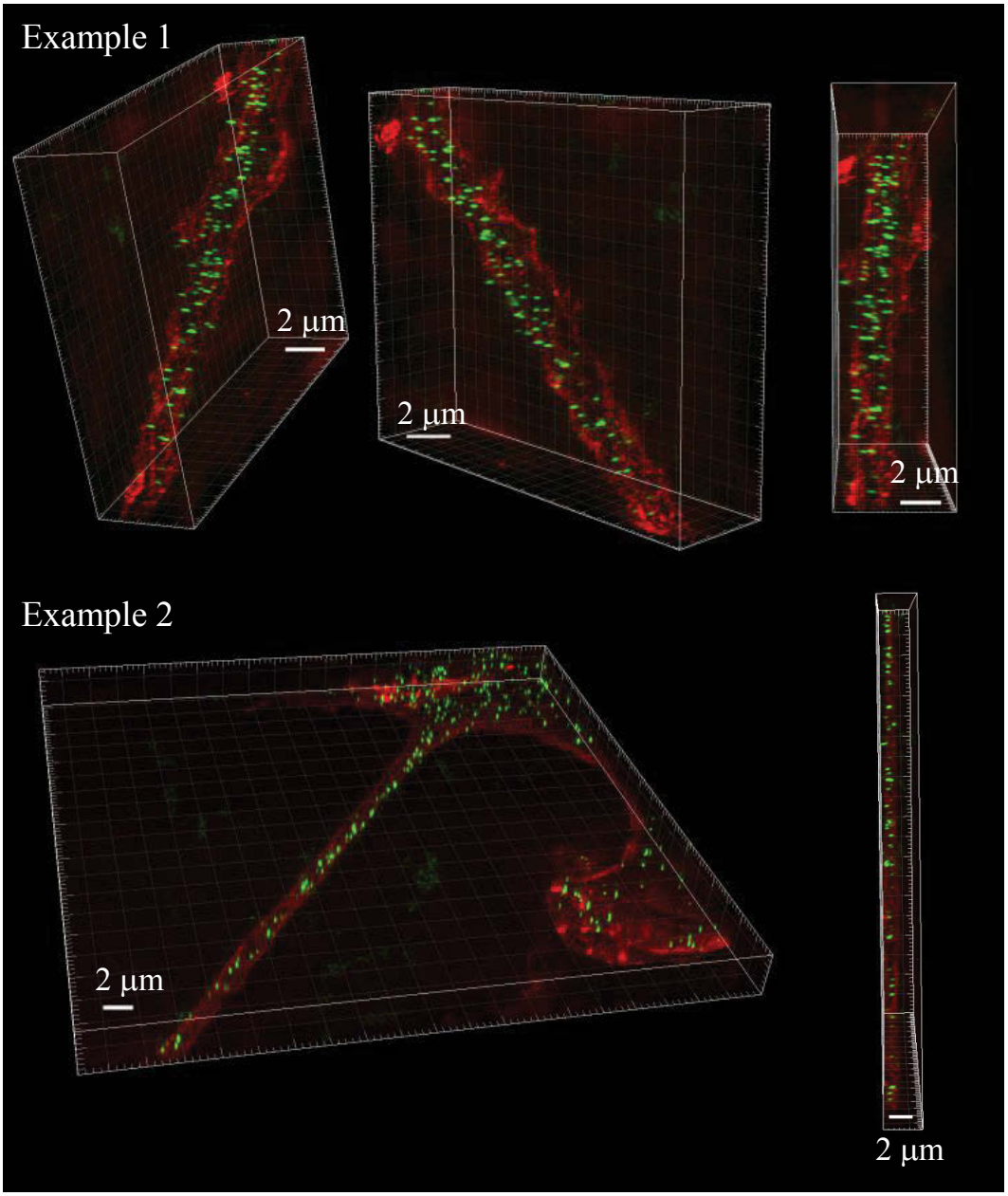

Figure 5.7: High resolution imaging and localisation of TLR4 in nanotubes of primary human macrophages.
Macrophages were stained with anti-TLR4 antibody and goat anti-mouse-AF488 secondary antibody (green) and phalloidin (red) for the detection of F-actin. Data shown are representative images of the localisation of TLR4 within thick nanotubes (Example 1 and 2). Samples were imaged using a DeltaVision deconvolution microscope. Data shown are representative of 20 nanotubes.

5.2.6 EFFECT OF FHCL1 TREATMENT ON TLR4 LOCALISATION IN NANOTUBES OF PRIMARY HUMAN MACROPHAGES

As discussed in Chapter 4, treatment of primary human macrophages with FhCL1 for 18 h resulted in no significant change in cell surface or intracellular TLR4 levels or localisation, being evenly distributed throughout the cytoplasm (Section 4.2.3). Having established that LPS stimulation increased the localisation of TLR4 within nanotubes compared to corresponding cell bodies (Section 5.2.3), and given FhCL1 was observed to suppress LPS uptake (Figure 4.12), the localisation of TLR4 within nanotubes formed between FhCL1-treated macrophages was investigated. Macrophages were treated with PBS or 20 μg/mL FhCL1 (from a previous batch) for 18 h, prior to staining with anti-TLR4 antibody with goat anti-mouse-AF488 secondary antibody. Microscopy analysis indicated that both PBS-treated (ratio: 1.1, p=0.6293) and FhCL1-treated macrophages (ratio: 1.1, p=0.4697) exhibited similar levels of TLR4 within nanotubes and the cell body (Table 5.7, see Appendix 4 and 6 for raw MFI values). Thus treatment with FhCL1 alone did not significantly alter the localisation of TLR4 within nanotubes. However, while stimulation with LPS significantly increased the localisation of TLR4 within nanotubes (ratio: 1.3, p=0.0077) (Table 5.7, see Appendix 4 for raw MFI values), FhCL1 treatment prior to LPS stimulation resulted in no significant change in TLR4 localisation between nanotubes and corresponding cell bodies (ratio: 1.1, p=0.5246) (Table 5.7 and Figure 5.8, see Appendix 6 for raw MFI values). Therefore, FhCL1 treatment inhibits the LPS-mediated transport of TLR4 into macrophage-associated nanotubes.

Table 5.7: Ratio of TLR4 localisation in human macrophages and associated nanotubes following FhCL1-treatment and LPS stimulation.

Treatment	No. of nanotube-cell body pairs analysed	Averaged ratio of MFI ± SD	P-value of ratio compared to 1.0	
PBS	14	1.1 ± 0.8	0.6293	
FhCL1	8	1.1 ± 0.4	0.4697	
LPS	32	1.3 ± 0.7	0.0077	*
FhCL1/LPS	23	1.1 ± 0.1	0.5246	

* Significant.

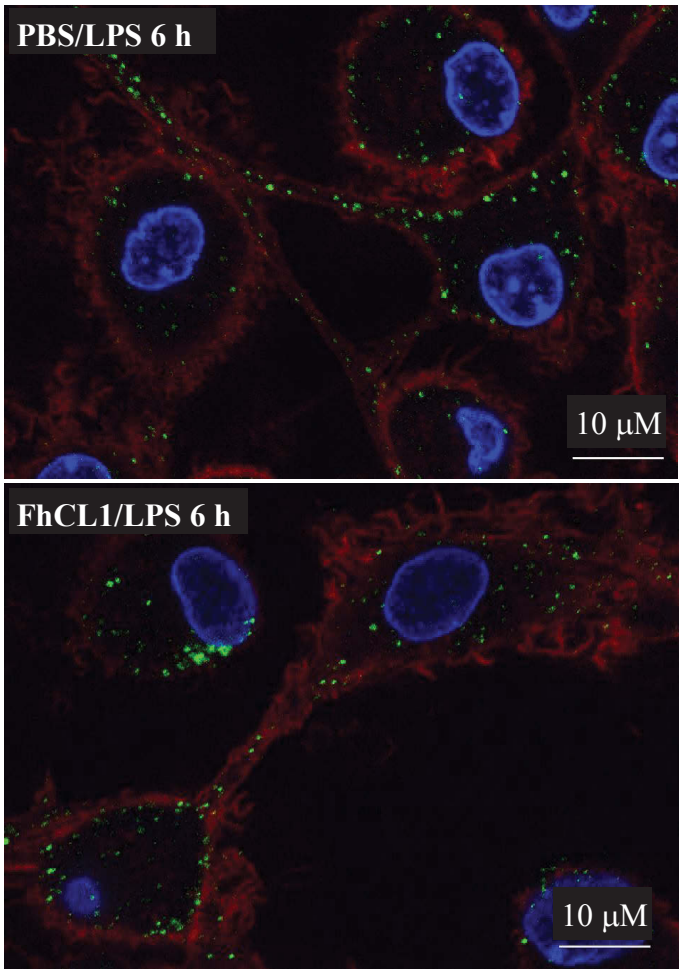

Figure 5.8: Localisation of TLR4 within nanotubes of LPS-stimulated, FhCL1-treated primary human macrophages.
Macrophages were stained with anti-TLR4 antibody and goat anti-mouse-AF488 secondary antibody (green), phalloidin (red) for F-actin and DAPI (blue) to detect nuclei. Data shown are representative images of the localisation of TLR4 in nanotubes connecting macrophages cultured with PBS or FhCL1 with subsequent stimulation with 50 ng/mL LPS for up to 6 h. Samples were imaged using a Nikon A1 Confocal scanning laser microscope. Representative of a minimum of six nanotubes for each treatment.

5.3 DISCUSSION

This study aimed to determine the localisation of TLR4, TLR3 and early endosomes within the cell bodies of macrophages and their associated nanotubes. While TLR4 was found to be distributed evenly throughout the cell body and nanotubes in untreated macrophages, more TLR4 translocated to the nanotubes compared to the cell body in response to LPS stimulation. Treatment of primary human macrophages with the helminth-derived molecule, FhCL1, showed no effect on the localisation of TLR4 within nanotubes and cell bodies; however, following LPS stimulation, FhCL1 treatment suppressed the LPS-mediated localisation of TLR4 in nanotubes. Furthermore, investigation into the localisation of TLR4 within nanotubes demonstrated that TLR4 was likely co-localised with α-tubulin within nanotubes. Additionally, while EEA-1, a marker of early endosomes (Mu *et al.* 1995), was observed to localise within macrophage-associated nanotubes, higher levels of EEA-1 were observed in the cell body, with LPS stimulation having no effect on the cellular localisation of EEA-1. The localisation of TLR3 in cell bodies and nanotubes of primary human macrophages was also investigated, however, due to the low expression levels, limited conclusions could be drawn about its localisation within cells.

Nanotubes of human macrophages have been characterised according to size and cytoskeletal composition, into ‘thin’ and ‘thick’ types (Onfelt *et al.* 2006). Almost all of the macrophage-associated nanotubes observed in this study (101/104) were characterised as thick nanotubes. Studies have shown that nanotubes, particularly ‘thin’ nanotubes are highly sensitive to light exposure, agitation of the culture dish and some fixation methods which are known to disrupt nanotube structure (Rustom *et al.* 2004; Koyanagi *et al.* 2005). Thus, the bias towards thick nanotubes observed in this study may in part be due to these factors. However, within human macrophages, thick nanotubes are capable of transferring organelles and vesicles and were thus of more relevance to this project than thin nanotubes, which have not been observed to play a role in organelle transfer in human macrophages (Onfelt *et al.* 2006).

This study observed the presence of EEA-1 within nanotubes connecting primary human monocyte-derived macrophages and is the first instance in which EEA-1 was reported within macrophage nanotubes. When comparing the localisation of EEA-1

within macrophage nanotubes and their associated cell bodies, with and without LPS stimulation, EEA-1 was localised predominantly within the macrophage cell body. This may be due to maturation of the early endosome during endocytosis and the changes in endosome receptors/markers that takes place during this process. Following endocytosis, early sorting endosomes are formed, which are characterised by molecules such as Rab5 and EEA-1. These molecules enable early endosomes to merge with other early endosomes and it is the recruitment of other Rab molecules that determines the ultimate function of the endosome (for a review see Spang 2009). For example, as demonstrated in HeLa cells, the recruitment of Rab11 to the early endosome results in formation of a recycling endosomes, and the return of material to the plasma membrane (Peden *et al.* 2004). In contrast, Rab7 replaces Rab5 and EEA-1 during the formation of late endosomes and ultimately mediates fusion with lysosomes, and the destruction of endosome cargo (Rink *et al.* 2005). Therefore, the change in endosome receptors during the formation of recycling endosomes or late endosomes is one explanation for the low levels of EEA-1 observed within nanotubes. Indeed, it may be that a different type of endosome or lysosome is trafficked between cells with higher preference. While this was not assessed as part of this study, the presence of late endosomes/lysosomes within human macrophage-associated nanotubes, as identified by antibodies specific for the marker LAMP-1, has previously been reported (Onfelt *et al.* 2006). The published staining of LAMP-1 is similar to that observed with EEA-1, with relatively low levels of LAMP-1 within the nanotubes compared to the associated cell body (Onfelt *et al.* 2006). Therefore, the low levels of EEA-1 'early endosome' marker within nanotubes may be due to endosome maturation. It may also simply be a feature of the endosomes and/or lysosomes that exist and traffic within nanotubes, which have not yet been well characterised.

To date, the purpose of endosome transfer between cells is just beginning to be investigated. Endocytosis is essential for regulating the availability of surface receptors, and can contribute to the initiation of cell signalling (reviewed in Sadowski *et al.* 2009). Thus, it can be hypothesised that the transport of endosomes between cells via nanotubes may initiate cell signalling and activation in connected cells. However, the use of fixed cells to examine the localisation of endosomes within nanotubes can only give information on endosome localisation at a single point in time. Thus, elucidating the purpose of endosome transport would require live cell imaging experiments.

Investigations into the localisation of TLR4 within primary human monocyte-derived macrophages demonstrated that TLR4 was clearly visible within macrophage-associated nanotubes. Although this study was the first to report the localisation of TLR4 within nanotubes, this is consistent with the reports of receptor transport via nanotubes. For example, green fluorescent protein (GFP)-tagged MHC class 1 (HLA-C) receptor has been observed to traffic through nanotubes connecting natural killer cells and 721.221 B cells (Onfelt *et al.* 2004). MHC class I (HLA-A, B, C) was also used as a means of more sensitively detecting nanotubes connecting THP-1 macrophage-like cells and DCs (Watkins *et al.* 2005). Furthermore, the transfer of B cell immunoglobulin receptors between adjacent B cells of different clonality has been reported to occur via 'short' nanotubes (Quah *et al.* 2008). This occurs by a process of membrane transfer, and is postulated to be a second mechanism by which antigen-specific immune responses are rapidly amplified (the first being division of antigen-specific cells) (Quah *et al.* 2008). Sharing of T cell receptors via membrane transfer has also been observed, though not specifically attributed to nanotube formation (Chaudhri *et al.* 2009). Thus, the localisation of toll-like receptors within nanotubes is not entirely unexpected.

Stimulation with LPS is reported to increase endocytosis of TLR4-containing endosomes within the first 40 min of LPS stimulation and is mainly attributed to clathrin-associated internalisation (Husebye *et al.* 2006). This study observed that collectively LPS stimulation was associated with increased localisation of TLR4 within macrophage-associated nanotubes. However, results showed that at individual time points there was no significant difference in TLR4 localisation between the macrophage cell body and their connected nanotubes, and that fluctuations in TLR4 localisation were observed. This is likely due to small sample sizes, but this may also indicate that the localisation of TLR4 within nanotubes is a dynamic process. A larger scale study and/or time lapse live cell imaging would provide more information regarding the kinetics of TLR4 transport between cells.

Given that TLR4 recognises bacterial LPS (reviewed in Ulevitch *et al.* 1995; Beutler 2000), and that soluble bacterial factors such as *E. coli* supernatant are capable of activating connected cells through the movement of calcium ions (Watkins *et al.* 2005), it is possible that TLR4 localised within nanotubes serves to induce immune responses in connected cells, and that this is enhanced by LPS stimulation. In murine corneal

stromal tissue, stimulation with LPS enhances the formation of nanotubes connecting DCs *in vivo* (Chinnery *et al.* 2008). This suggests that nanotubes play a role in intercellular communication during inflammation (Chinnery *et al.* 2008). While this study focused not on nanotube number, but on TLR4 localisation within nanotubes, future studies could determine the number of nanotubes in culture with or without LPS stimulation and in the presence or absence of FhCL1.

During the internalisation of LPS, the TLR4/LPS complex is endocytosed into early endosomes (Husebye *et al.* 2006). As a marker of early endosomes, EEA-1 has previously been reported to co-localise with TLR4 within Human Embryonic Kidney 293 cells where co-localisation of cyan fluorescent protein-tagged EEA-1 together with yellow fluorescent protein-tagged TLR4 was observed (Husebye *et al.* 2006). This was also investigated in human monocytes with antibodies specific to both EEA-1 and TLR4, but was only reported as 'data not shown' (Husebye *et al.* 2006). Co-localisation of EEA-1 and TLR4 has also been demonstrated in human monocyte-derived macrophages using antibodies specific to EEA-1 or TLR4 (Bruscia *et al.* 2011). Despite these reports, the experiment presented in this chapter clearly and reproducibly demonstrated no co-localisation of EEA-1 and TLR4. This might be explained by differences in the specificity and reactivity of different antibodies used; previous reports used monoclonal antibodies, whereas this study used a polyclonal antibody. As such, further investigation into the localisation of early endosomes and their co-localisation with TLR4 within monocyte-derived macrophage-associated nanotubes requires repetition with a monoclonal antibody specific for EEA-1. In addition, assessing alternative markers of early endosomes such as Rab5 should be considered in future experiments. Finally, further characterisation of the antibody used in this study, i.e. its specificity (or not) to react only with EEA-1, would significantly enhance the interpretation of these results.

The helminth-derived molecule FhCL1 had no effect on TLR4 localisation within macrophage-associated nanotubes. However, FhCL1 was observed to inhibit the LPS-mediated localisation of TLR4 within nanotubes. As FhCL1 was demonstrated to suppress the uptake of LPS by human monocyte-derived macrophages (Chapter 4), this suggests that decreased LPS uptake may be responsible for the reduced localisation of TLR4 within nanotubes. Although the purpose of TLR4 within nanotubes is currently

unclear, this may ultimately have ramifications for the activation of connected macrophages in response to bacterial LPS, as described in the introduction of this thesis.

It was considered that TLR4 may be localised to the surface of nanotubes in human monocyte-derived macrophages, similar to the localisation observed with MHC class I (HLA-C) on nanotubes connecting NK cells and 721.221 B cells (Onfelt *et al.* 2004), or that TLR4 may be localised within nanotubes. To investigate this possibility, macrophages were stained with TLR4 prior to fixation, permeabilisation and staining with fluorescently-conjugated secondary antibody. TLR4 was not detected on the surface of macrophages by confocal microscopy, and this contradicted the detection of TLR4 surface expression by flow cytometry. However, during investigation into the localisation of TLR4 expression in permeabilised macrophages, some TLR4 was observed to visually co-localise with phalloidin, suggestive of *bona fide* low level 'surface' expression of TLR4 (Figure 5.9). This result explains and confirms the detection of TLR4 by both confocal microscopy and flow cytometry, as confocal microscopy demonstrated that expression of surface TLR4 was low and as such is not visible on every cell for a single frame. Similarly, flow cytometry analyses indicated very low levels of expression compared to isotype control staining. Collectively, these results point to the primary location of TLR4 beneath the cell membrane and in cell bodies and nanotubes, rather than being at the cell surface.

Investigations into the cytoskeletal composition of nanotubes demonstrated that macrophage-associated nanotubes were composed of F-actin and α-tubulin. The majority of TLR4 within macrophage nanotubes was observed to co-localise with α-tubulin, with very little co-localisation of TLR4 and F-actin. Nanotubes stained heavily for α-tubulin, such that when setting laser levels for confocal microscopy in order to view α-tubulin within the cell body, α-tubulin within nanotubes often appeared 'saturated'. While pixel saturation should be avoided when investigating co-localisation (Zinchuk *et al.* 2007), these images demonstrate the extent of α-tubulin localised within the nanotube, compared to the cell body. It was therefore not surprising that TLR4 co-localised with α-tubulin within macrophage nanotubes. In fact, within human DCs,

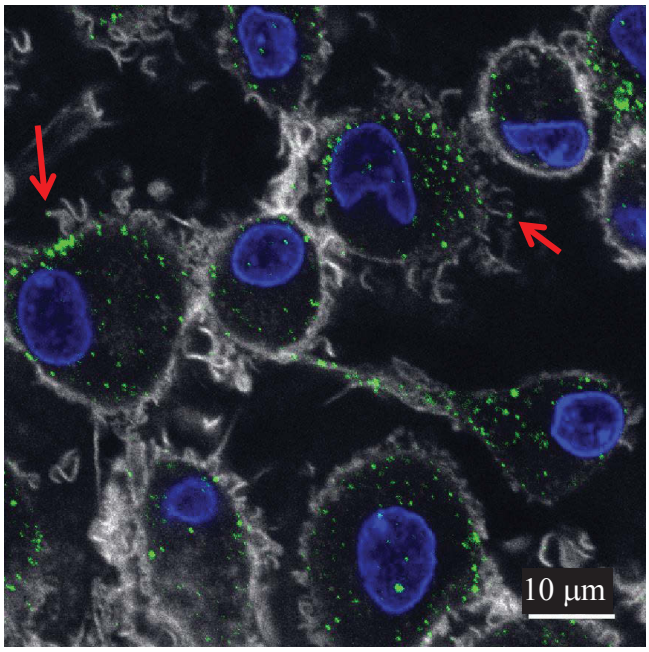

Figure 5.9: Localisation of TLR4 in permeabilised primary human macrophages. Macrophages were stained with anti-TLR4 antibody with goat anti-mouse-AF488 secondary (green), together with phalloidin (white) for F-actin and DAPI (blue) to detect nuclei. Data shown is an example of the localisation of TLR4 molecules visually co-localising with phalloidin at surface of macrophages (arrows), compared to the more extensive intracellular localisation of TLR4. Samples were imaged using a Nikon A1 Confocal scanning laser microscope.

TLR vesicles have also been reported to co-localise with α-tubulin (Uronen-Hansson *et al.* 2004) and thus it was highly likely that TLR4 is trafficked into nanotubes via microtubulin.

Most studies examining the structure of nanotubes have been performed using wide-field or confocal microscopy with limited resolution (Onfelt *et al.* 2004; Rustom *et al.* 2004; Koyanagi *et al.* 2005; Watkins *et al.* 2005; Zhu *et al.* 2005; Onfelt *et al.* 2006; Sherer *et al.* 2007; Quah *et al.* 2008). Nanotubes have also been examined using electron microscopy (Rustom *et al.* 2004; Sherer *et al.* 2007; Sowinski *et al.* 2008), but while this represents a significant improvement on resolution, investigation of the localisation of molecules within nanotubes using electron microscopy is limited to an older technology, such as immunogold labelling (Faulk *et al.* 1971). This is dependent upon the ability to conjugate antibodies to differently sized gold particles, and can only really be successfully undertaken with two simultaneous antibody-gold particles (of different particle size). Newer technologies enable multi-colour fluorescence and although not on the same resolution as electron microscopy, arguably it offers more

versatility in detecting different molecules, and often more than two molecules simultaneously. Therefore, the ultrafine structure of cytoskeleton proteins and TLR4 molecules are arguably better examined using high resolution fluorescence microscopes, such as with the DeltaVision OMX microscope (Applied Precision, Inc.). This microscope has a high resolving power and can separate individual molecules down to 90 nm in X and Y plane, and 220 nm in Z plane. This is compared to 80 nm in X, 192 nm in Y and 320 nm in Z for the Nikon A1 confocal microscope. Thus, high resolution microscopy allowed for better visualisation of TLR4 molecules and F-actin filaments. While TLR4 clearly co-localised with tubulin, even high resolution microscopy indicated that it did not co-localise with F-actin. Further microscopy experiments are required to determine whether TLR4 is associated with other molecules within nanotubes, i.e. in addition to α-microtubulin.

In conclusion, this study observed 'early endosome marker EEA-1' and TLR4 to be localised within nanotubes connecting primary human monocyte-derived macrophages. TLR4 preferentially localised to nanotubes following LPS stimulation. It is proposed that the localisation of TLR4 within nanotubes may play an important role in the activation of distant, but connected cells, potentially inducing a pro-inflammatory response across a network of connected cells without the need for direct interaction of bacteria or their products with all cells. Interestingly, treatment with FhCL1 impeded the movement of TLR4 into nanotubes following LPS stimulation and thereby potentially diminishes activation of the connected adjacent cells. Macrophage-associated nanotubes appear to be a means by which cells share antigen-specific receptors with other connected cells, potentially enhancing immune surveillance and responses and it would be beneficial for a parasite to prevent or diminish the amplification of the host response to infection.

CHAPTER 6:

GENERAL DISCUSSION

The ES products of helminths exert potent immune-modulatory effects, which influence both innate and adaptive immune cells to establish an anti-inflammatory/regulatory environment within the host (for a review see Allen *et al.* 2011). This is believed to promote the longevity of the helminth within the host while concomitantly preventing tissue damage. This is achieved in part through the induction of alternative macrophage activation (Herbert *et al.* 2004; Donnelly *et al.* 2005; Donnelly *et al.* 2008) and tolerogenic DCs (Jankovic *et al.* 2004; Hamilton *et al.* 2009), which promote differentiation of Th2 (O'Neill *et al.* 2000; Jankovic *et al.* 2004), regulatory T cells (Taylor *et al.* 2005; Taylor *et al.* 2009b) and regulatory B cells (Adjobimey *et al.* 2010). The ES products of *F. hepatica* (FhES) have been demonstrated to prevent the onset of type 1 diabetes within the NOD mouse model, inducing an anti-inflammatory environment through the suppression of pro-inflammatory cytokine release by autoreactive T cells, the alternative activation of macrophages, as well as the activation of regulatory B cells and a switch in antibody isotype from IgG2a to IgG1 (Lund *et al.* in preparation). Fractionation of ES products has facilitated the identification of the immune-modulatory effect(s) of individual components to identify which ES components are responsible for the induction of the anti-inflammatory/regulatory milieu. Fractionation of the FhES revealed that it is predominately composed of peroxiredoxin (Prx) (Donnelly *et al.* 2005), helminth defence molecule (HDM)-1 (Robinson *et al.* 2011b) and cysteine proteases (O'Neill *et al.* 2001; Donnelly *et al.* 2010).

This study aimed to investigate the effect of *F. hepatica*-derived cysteine protease FhCL1 on human macrophages. In setting up this study, a number of factors were considered. Firstly, during infection, the adult *F. hepatica* lives within the liver where it feeds on host haemoglobin (reviewed in Dalton 2006). Therefore, a physiological approach to the investigation of the effect of parasite products within the human host would be to examine the effect of these products on Kupffer cells, the resident tissue macrophage of the liver. Indeed, the role of immune cells residing within the liver cannot be underestimated when considering the host response to hepatic parasitic infections. As an example of this, *S. mansoni* infection is typically associated with a pro-inflammatory response during the initial stages of infection, characterised by the expression of IFN-γ, TNF and IL-2 (Lambertucci 2010), which coincides with migration of the parasite through the gut (Doenhoff 1997; reviewed in Gause *et al.*

2003), and it is only once the helminth matures and egg production begins that the immune response switches to a Th2 response (Jankovic *et al.* 2004; Pearce 2005). However, within the liver, hepatic T cells demonstrate a Th2 immune response, even during the early stages of infection (Hayashi *et al.* 1999). This is attributed to Kupffer cells driving increased IL-4 and IL-13 in hepatic T cell populations (Hayashi *et al.* 1999). Thus, the effect of helminths and their products differs depending on the cells examined. However, sources of human Kupffer cells are essentially not available, and as the aim was to examine the effect of FhCL1 on human macrophages, the use of murine Kupffer cells was not considered. Therefore this study investigated the effect of FhCL1 on human monocyte-derived macrophages which are easily obtained from peripheral blood.

While this study has taken a reductionist approach and investigated the effect of FhCL1 on human monocyte-derived macrophages, ultimately, the excretory/secretory helminth-derived products have the potential to interact with a large number of host immune cells, including, but not limited to different macrophage populations. In general, tissue macrophages are associated with the clearance of senescent cells as well as the repair and remodelling of tissue after inflammation, however, resident tissue macrophages often have highly specialised roles (reviewed in Gordon *et al.* 2005). For example, within the lung, alveolar macrophages are focused on the recognition and clearance of viruses, bacteria and miscellaneous particles and as a result have high expression of pattern recognition receptors (McCusker *et al.* 1989; Taylor *et al.* 2002). In contrast, macrophages within the gastrointestinal tract have low levels of pattern recognition molecules and do not produce pro-inflammatory cytokines in response to inflammatory stimuli presumably in order to prevent aberrant inflammation in this heavily microflora populated organ (Smythies *et al.* 2005). These are just two examples of the many different tissue macrophages that arise from mesencyhymal stem cells and due to cell type-specific protein expression and function, macrophages present at different sites might be expected to respond differently, or be modulated differently by helminth-derived molecules.

Additionally, helminth molecules modulate immune responses by interacting with other immune cells, such as DCs. In fact, there is a wealth of literature regarding the effect of helminth products on DCs and their ability to modulate adaptive immune responses. For

example, the *H. polygyrus* ES products induce tolerogenic DCs with reduced CD40, CD86 and MHC-II expression on the surface of murine DCs (Segura *et al.* 2007). Furthermore, *H. polygyrus* ES products also suppress cytokine production, suggesting that cells were not activated by the ES products (Segura *et al.* 2007). Tolerogenic DCs are also associated with the induction of regulatory T cells. For example, the soluble egg antigen of *S. mansoni* requires DCs to induce TGF-β-dependent $Foxp3^+$ regulatory T cells (Zaccone *et al.* 2009). Therefore, the effects of a helminth-derived product on humans cannot be elucidated based on its effects on a single cell type and instead its effects need to be considered as a whole. Our group has extended this study of human monocyte-derived macrophages to investigate the effect of FhCL1 on human monocyte-derived DCs and although there was no discernable effect on DCs (M. Lund, unpublished), it is essential that the effects of helminth-derived molecules in individual cell populations are examined before effects are investigated on a larger scale.

Comparisons between the effect of FhCL1 on human monocyte-derived macrophages (this study) and murine peritoneal macrophages (Donnelly *et al.* 2010), in response to LPS, demonstrated that FhCL1 had a vastly different effect on the macrophage populations from the two different species and reasons for the differences in responses were discussed in Chapter 3. It is worth noting that in order to truly be able to compare these two studies, despite their differences, macrophages from both species should be examined within the same assays – this would enable one to determine the precise differences between cell types and the relative magnitude of the response in each macrophage type. Nevertheless, interpretation of the data as a whole indicates that FhCL1 modulates TLR signalling in both species. Inflammation is generally triggered by recognition of foreign or stimulatory agents via pattern recognition receptors, including TLRs (for a review see Takeuchi *et al.* 2010). Inappropriate activation of TLR signalling pathways frequently leads to inflammation and in the case of nucleic acid sensing TLRs (such as TLR7 and TLR9) can even be involved in the pathogenesis of autoimmune diseases (reviewed in Takeuchi *et al.* 2010). In assessing the potential of FhCL1 as a therapeutic candidate for the treatment or amelioration of autoimmune and inflammatory disease, the increased pro-inflammatory response in human monocyte-derived macrophages suggests that FhCL1 is unlikely to have therapeutic value. In fact, within the diabetes-prone NOD mouse, administration of FhCL1 at four weeks of age exacerbated, rather than ameliorated, diabetes development (personal communication

S. Donnelly and B. O'Brien). This indicates that FhCL1 is not the component responsible for the prevention of diabetes observed following the administration of the FhES products. Investigation of potential therapeutic candidates is a continued research focus for our laboratory and based on current knowledge, recombinant FhCL1 may not be of obvious therapeutic value to humans.

FhCL1 did however protect BALB/c mice from a lethal dose of LPS, suggesting that it played a role in the prevention of septic shock (Donnelly *et al.* 2010), which is a systemic pro-inflammatory reaction induced following the engagement of TLRs during severe bacterial infection (for reviews see Beutler 2004; Nguyen *et al.* 2006). Septic shock was prevented by suppressing TRIF-dependent signalling in murine macrophages, due to the cleavage of TLR3 (Donnelly *et al.* 2010). This prevented the activation of downstream signalling of pro-inflammatory cytokines, IL-12, IL-6, TNF and iNOS, as well as inhibiting IFN-β mRNA expression (Donnelly *et al.* 2010), with the expression of type 1 interferons being essential for the induction of septic shock (Karaghiosoff *et al.* 2003; Mahieu *et al.* 2006; Mahieu *et al.* 2007; Kim *et al.* 2009). While, this study showed that FhCL1 suppressed the uptake of LPS-Cy5 and suppressed TRIF-dependent signalling, and given that IFN-β expression has been observed to be suppressed by FhCL1 in human monocyte-derived macrophages (M. Lund, unpublished), the expression of pro-inflammatory cytokines was enhanced. Thus, unlike in murine macrophages, suppression of pro-inflammatory responses to LPS is not a mechanism of action of FhCL1 in human monocyte-derived macrophages. Whilst there is a benefit of undertaking experiments in mice, such as the examination of *in vivo* responses, i.e. in live organisms, there is also benefit in examining responses in human cells. Although human cells are more frequently examined in isolation and *in vitro*, it is still desirable to have knowledge of the human/cell response, as ultimately one would like to have agreement in biological activity in both murine models and human cells before moving to pre-clinical development.

While it is generally accepted that helminths promote an anti-inflammatory/regulatory response within the host, the migration of helminths through tissues is pro-inflammatory in its own right, i.e. simply due to the resultant tissue damage, such as in the case of *S. mansoni* (Lambertucci 2010). While collectively, the helminth ES products induce an anti-inflammatory environment, the main purpose of some products is to mediate the

destruction of host tissues for feeding and migration. FhCL1 is one such product, and during *F. hepatica* infection, FhCL1 plays a role in the breakdown of extracellular matrix proteins such as collagen, laminen and fibrinogen (Berasain *et al.* 1997). In fact, using RNA interference to knockdown parasite cathepsin L prevents the migration of *F. hepatica* through tissues (McGonigle *et al.* 2008). While the pro-inflammatory response associated with tissue migration may simply be a result of lysis and degradation of extracellular matrix and the presence of necrotic cells, the work shown here indicates that human macrophages in their own right induce the expression of pro-inflammatory cytokines in response to FhCL1. This is corroborated by the pro-inflammatory response induced by dsRNA associated with egg production by *S. mansoni*, which induces the expression of pro-inflammatory cytokines and interferon-stimulated genes by signalling through TLR3 (Aksoy *et al.* 2005; Vanhoutte *et al.* 2007). Therefore, the inflammatory response is mediated, at least in part, by parasite products.

One aspect which was not investigated within this study was the effect of FhCL1 on phagocytosis and antigen processing/presentation in human monocyte-derived macrophages. Microtubules are essential for the transport of MHC-II (HLA-DMA) molecules and thus antigen presentation (Wubbolts *et al.* 1999), that is, while material may be taken up by macrophages, its processing and surface presentation may be hindered by microtubule depolymerisation. In primary murine DCs, transport of MHC-II to the cell surface is dependent upon microtubules, as microtubule destabilisation causes collapse of MHC-II^{+} tubular endosomes (Vyas *et al.* 2007). Furthermore Vyas *et al.* (2007) proposed that disruption of the cytoskeleton by pathogens and the subsequent prevention of endosomal protein translocation to the cell surface may subvert immune responses. Interestingly, HDM-1, a second component of the FhES has been associated with defects in antigen processing and presentation, by inhibiting acidification of the endolysosome (Robinson *et al.* 2012). FhCL1 was observed to modulate the localisation of α-tubulin within monocyte-derived macrophages, but only in some macrophages within the culture. This was interpreted as potentially due to heterogeneity within macrophage donors, nevertheless, it could be a significant result. Thus it is possible that the altered localisation of α-tubulin following FhCL1 treatment may impact phagocytosis and/or antigen presentation, and interestingly despite FhCL1 having no significant effect on HLA-DR surface expression, there was a trend towards down-regulated HLA-DR. Furthermore, murine cysteine proteases, such as cathepsin L are

required for antigen presentation, playing a role in breaking down antigen and processing the invariant chain of MHC-II (Hsieh *et al.* 2002), which is required prior to the loading of peptide onto the MHC-II receptor for antigen presentation (reviewed in Obermajer *et al.* 2006). Cathepsin L homologues from vertebrates and invertebrates may have different substrates and cleavage sites and without knowing the specificity of FhCL1, it makes it impossible to know how the enzyme works and whether it impacts on peptide cleavage and thus alters how many peptides are generated and loaded onto HLA molecules. Nevertheless, this is a possible mechanism by which FhCL1 may act. Therefore, investigating the effect of FhCL1 on antigen processing and presentation, which is an important role of macrophages, remains a potential avenue for study. This could be examined by investigating antigen-specific T cell proliferation following co-incubation of FhCL1-treated macrophages with naïve T cells in the presence of antigen. This would enable elucidation of the effect of FhCL1 on antigen processing and presentation when compared with proliferation induced by control macrophages. However, this is not as straight forward and easily examined as in murine systems, where genetically identical strains of mice and syngeneic target or responder cells of known MHC-II allotype can be used to investigate antigen processing and presentation and target cell proliferation or killing.

One interesting finding was that FhCL1 treatment suppressed the transport of TLR4 through macrophage nanotubes. The purpose for the localisation of TLR4 within macrophage nanotubes is currently unknown. The formation of tunnelling nanotubes between cells has been observed to induce macrophage activation through the propagation of activation signals to connected cells (Watkins *et al.* 2005). As TLR4 induces cell signalling in response to bacterial LPS (Hoshino *et al.* 1999), it is suggested that the LPS-mediated localisation of TLR4 within macrophage-associated nanotubes may result in the initiation of cell signalling in connected macrophages, thus amplifying the response to include connected cells. The decrease in TLR4 localised within FhCL1-treated macrophage nanotubes correlates with the FhCL1-mediated suppression of LPS uptake. Therefore, this could be hypothesised to prevent the LPS-mediated activation of connected cells and thus may be associated with the control and containment of the host and connected cell responses. In order to truly be able to comment on the physiological purpose of the localisation of TLR4 within nanotubes and the effect of LPS and FhCL1 treatment, live cell imaging is required. Through the use of cells transfected with green

fluorescent protein (GFP)-tagged TLR4 and Resorufin arsenical hairpin binder (ReAsH)-tagged (fluorescent) IFN-β, the potential for TLR4 to activate TLR specific cell signalling in connected cells via nanotubes could be investigated. This would allow the set up of a LPS micro-injection system, whereby only one of two cells connected by a nanotube is stimulated with LPS, and activated through endosomal TLR4. The movement of GFP-tagged TLR4 between cells within nanotubes would allow visualisation of intercellular TLR4 trafficking. In addition, the use of cells stably transfected with ReAsH tagged-IFN-β controlled by its endogenous promoter would demonstrate TLR4-induced IFN-β expression. Furthermore the use of syngeneic mixed cultures (IFN-β ReAsH expressing and not expressing cells) would be particularly beneficial and it would allow for easy discrimination of the connected versus LPS-stimulated cell. In any case, further investigation is required to elucidate the biological significance of the transport of TLR4 through nanotubes.

In conclusion, this study has shown that the *F. hepatica* cysteine protease, FhCL1 modulated immune responses in human macrophages, enhancing the expression of pro-inflammatory cytokines in response to LPS, which was associated with up-regulation of surface CD14. FhCL1 also suppressed the uptake of LPS, down-regulating endosome based TRIF-dependent signalling and down-regulating CD86 surface expression, potentially by altering the distribution of α-tubulin within macrophages. The induction of a pro-inflammatory response by FhCL1 may aid in the migration of *F. hepatica* through host tissues. Furthermore, the inhibition of TLR4 localisation within FhCL1-treated macrophage-associated nanotubes may be associated with the control and containment of inflammatory response in connected cells. The work presented in this thesis has provided insight into the mechanism of action of FhCL1 in human monocyte-derived macrophages. Investigating the immune-modulatory effects of individual helminth-derived molecules is an important step in understanding the mechanisms by which helminths modulate and generally evade host responses, which may ultimately be harnessed therapeutically.

APPENDIX

Appendix 1: Maps of primer positions for RT-qPCR analysis of RPL36AL, IL-1β, IL-10, IFN-β, IL-12B, TLR3 and TLR4 mRNA expression.

```
            HSRPL36AL-F>
  1 CCTTTCCTGT TAGGCGAGAG CTGCGAAAGG CGAGAGCTGC GAAGGGCCAG GTGTCGGGCG
 61 CTGTTTCTCG TTTTCATCAT ATAGACAAAA CAGCCCTGCT GCAAAGATGG TCAACGTACC
          <HSRPL36AL-R
121 TAAAACCCGA AGAACCTTCT GTAAGAAGTG TGGCAAGCAT CAGCCTCACA AAGTGACACA
181 GTATAAGAAG GGCAAGGATT CTTTGTATGC CCAGGGAAGG AGGCGCTATG ATCGGAAGCA
241 GAGTGGCTAT GGTGGGCAGA CAAAGCCAAT TTTCCGGAAG AAGGCTAAGA CCACAAAGAA
301 GATTGTGCTA AGGCTGGAAT GTGTTGAGCC TAACTGCAGA TCCAAGAGGA TGCTGGCCAT
361 TAAGAGATGC AAGCATTTTG AACTGGGAGG AGATAAGAAG AGAAAGGGCC AAGTGATCCA
421 GTTCTAAACT TTGGGATATT TTTCTTCAAT TTTGAAGAGA AAATGGTGAA GCCATAGAAA
481 AGTTACCCGA GGGAAAATAA ATACAGTGAT ATTCTTACGC AAAAAAAAAA AAAAAAAAAA
541 AAAAAAAAA
```

Map of primer positions for RT-qPCR analysis of RPL36AL mRNA expression. Forward and reverse primers for amplification of RPL36AL (NM_001001.3). > indicates forward (F) primer, < indicates reverse (R) primer. Consecutive exons are shown by alternating white and grey background shading. Full primer details are listed in Table 2.2.

```
  1 ACCAAACCTC TTCGAGGCAC AAGGCACAAC AGGCTGCTCT GGGATTCTCT TCAGCCAATC
                                                  HSIL-1β-F>
 61 TTCATTGCTC AAGTGTCTGA AGCAGCCATG GCAGAAGTAC CTGAGCTCGC CAGTGAAATG
121 ATGGCTTATT ACAGTGGCAA TGAGGATGAC TTGTTCTTTG AAGCTGATGG CCCTAAACAG
                                  <HSIL-1β-R
181 ATGAAGTGCT CCTTCCAGGA CCTGGACCTC TGCCCTCTGG ATGGCGGCAT CCAGCTACGA
241 ATCTCCGACC ACCACTACAG CAAGGGCTTC AGGCAGGCCG CGTCAGTTGT TGTGGCCATG
301 GACAAGCTGA GGAAGATGCT GGTTCCCTGC CCACAGACCT TCCAGGAGAA TGACCTGAGC
361 ACCTTCTTTC CCTTCATCTT TGAAGAAGAA CCTATCTTCT TCGACACATG GGATAACGAG
421 GCTTATGTGC ACGATGCACC TGTACGATCA CTGAACTGCA CGCTCCGGGA CTCACAGCAA
481 AAAAGCTTGG TGATGTCTGG TCCATATGAA CTGAAAGCTC TCCACCTCCA GGGACAGGAT
541 ATGGAGCAAC AAGTGGTGTT CTCCATGTCC TTTGTACAAG GAGAAGAAAG TAATGACAAA
601 ATACCTGTGG CCTTGGGCCT CAAGGAAAAG AATCTGTACC TGTCCTGCGT GTTGAAAGAT
661 GATAAGCCCA CTCTACAGCT GGAGAGTGTA GATCCCAAAA ATTACCCAAA GAAGAAGATG
721 GAAAAGCGAT TTGTCTTCAA CAAGATAGAA ATCAATAACA AGCTGGAATT TGAGTCTGCC
781 CAGTTCCCCA ACTGGTACAT CAGCACCTCT CAAGCAGAAA ACATGCCCGT CTTCCTGGGA
841 GGGACCAAAG GCGGCCAGGA TATAACTGAC TTCACCATGC AATTTGTGTC TTCCTAAAGA
901 GAGCTGTACC CAGAGAGTCC TGTGCTGAAT GTGGACTCAA TCCCTAGGGC TGGCAGAAAG
961 GGAACAGAAA GGTTTTTGAG TACGGCTATA GCCTGGACTT TCCTGTTGTC TACACCAATG
1021 CCCAACTGCC TGCCTTAGGG TAGTGCTAAG AGGATCTCCT GTCCATCAGC CAGGACAGTC
1081 AGCTCTCTCC TTTCAGGGCC AATCCCCAGC CCTTTTGTTG AGCCAGGCCT CTCTCACCTC
1141 TCCTACTCAC TTAAAGCCCG CCTGACAGAA ACCACGGCCA CATTTGGTTC TAAGAAACCC
1201 TCTGTCATTC GCTCCCACAT TCTGATGAGC AACCGCTTCC CTATTTATTT ATTTATTTGT
1261 TTGTTTGTTT TATTCATTGG TCTAATTTAT TCAAAGGGGG CAAGAAGTAG CAGTGTCTGT
1321 AAAAGAGCCT AGTTTTTAAT AGCTATGGAA TCAATTCAAT TTGGACTGGT GTGCTCTCTT
1381 TAAATCAAGT CCTTTAATTA AGACTGAAAA TATATAAGCT CAGATTATTT AAATGGGAAT
1441 ATTTATAAAT GAGCAAATAT CATACTGTTC AATGGTTCTG AAATAAACTT CACTGAAG
```

Map of primer positions for RT-qPCR analysis of IL-1β mRNA expression. Forward and reverse primers for amplification of IL-1β (NM_000576.2). > indicates forward (F) primer, < indicates reverse (R) primer. Consecutive exons are shown by alternating white and grey background shading. Full primer details are listed in Table 2.2.

```
   1 ACACATCAGG GGCTTGCTCT TGCAAAACCA AACCACAAGA CAGACTTGCA AAAGAAGGCA
  61 TGCACAGCTC AGCACTGCTC TGTTGCCTGG TCCTCCTGAC TGGGGTGAGG GCCAGCCCAG
 121 GCCAGGGCAC CCAGTCTGAG AACAGCTGCA CCCACTTCCC AGGCAACCTG CCTAACATGC
 181 TTCGAGATCT CCGAGATGCC TTCAGCAGAG TGAAGACTTT CTTTCAAATG AAGGATCAGC
 241 TGGACAACTT GTTGTTAAAG GAGTCCTTGC TGGAGGACTT TAAGGGTTAC CTGGGTTGCC
 301 AAGCCTTGTC TGAGATGATC CAGTTTTACC TGGAGGAGGT GATGCCCCAA GCTGAGAACC
 361 AAGACCCAGA CATCAAGGCG CATGTGAACT CCCTGGGGGA GAACCTGAAG ACCCTCAGGC
                                                    HSIL-10-F>
 421 TGAGGCTACG GCGCTGTCAT CGATTTCTTC CCTGTGAAAA CAAGAGCAAG GCCGTGGAGC
 481 AGGTGAAGAA TGCCTTTAAT AAGCTCCAAG AGAAAGGCAT CTACAAAGCC ATGAGTGAGT
                                                          <HSIL-10-R
 541 TTGACATCTT CATCAACTAC ATAGAAGCCT ACATGACAAT GAAGATACGA AACTGAGACA
 601 TCAGGGTGGC GACTCTATAG ACTCTAGGAC ATAAATTAGA GGTCTCCAAA ATCGGATCTG
 661 GGGCTCTGGG ATAGCTGACC CAGCCCCTTG AGAAACCTTA TTGTACCTCT CTTATAGAAT
 721 ATTTATTACC TCTGATACCT CAACCCCCAT TTCTATTTAT TTACTGAGCT TCTCTGTGAA
 781 CGATTTAGAA AGAAGCCCAA TATTATAATT TTTTTCAATA TTTATTATTT TCACCTGTTT
 841 TTAAGCTGTT TCCATAGGGT GACACACTAT GGTATTTGAG TGTTTTAAGA TAAATTATAA
 901 GTTACATAAG GGAGGAAAAA AAATGTTCTT TGGGGAGCCA ACAGAAGCTT CCATTCCAAG
 961 CCTGACCACG CTTTCTAGCT GTTGAGCTGT TTTCCCTGAC CTCCCTCTAA TTTATCTTGT
1021 CTCTGGGCTT GGGGCTTCCT AACTGCTACA AATACTCTTA GGAAGAGAAA CCAGGGAGCC
1081 CCTTTGATGA TTAATTCACC TTCCAGTGTC TCGGAGGGAT TCCCCTAACC TCATTCCCCA
1141 ACCACTTCAT TCTTGAAAGC TGTGGCCAGC TTGTTATTTA TAACAACCTA AATTTGGTTC
1201 TAGGCCGGGC GCGGTGGCTC ACGCCTGTAA TCCCAGCACT TTGGGAGGCT GAGGCGGGTG
1261 GATCACTTGA GGTCAGGAGT TCCTAACCAG CCTGGTCAAC ATGGTGAAAC CCCGTCTCTA
1321 CTAAAAATAC AAAAATTAGC CGGGCATGGT GGCGCGCACC TGTAATCCCA GCTACTTGGG
1381 AGGCTGAGGC AAGAGAATTG CTTGAACCCA GGAGATGGAA GTTGCAGTGA GCTGATATCA
1441 TGCCCCTGTA CTCCAGCCTG GGTGACAGAG CAAGACTCTG TCTCAAAAAA TAAAAATAAA
1501 AATAAATTTG GTTCTAATAG AACTCAGTTT TAACTAGAAT TTATTCAATT CCTCTGGGAA
1561 TGTTACATTG TTTGTCTGTC TTCATAGCAG ATTTTAATTT TGAATAAATA AATGTATCTT
1621 ATTCACATC
```

Map of primer positions for RT-qPCR analysis of IL-10 mRNA expression.
Forward and reverse primers for amplification of IL-10 (NM_000572.2). > indicates forward (F) primer, < indicates reverse (R) primer. Consecutive exons are shown by alternating white and grey background shading. Full primer details are listed in Table 2.2.

```
   1 ACATTCTAAC TGCAACCTTT CGAAGCCTTT GCTCTGGCAC AACAGGTAGT AGGCGACACT
  61 GTTCGTGTTG TCAACATGAC CAACAAGTGT CTCCTCCAAA TTGCTCTCCT GTTGTGCTTC
                                                        HSIFN-β-F>
 121 TCCACTACAG CTCTTTCCAT GAGCTACAAC TTGCTTGGAT TCCTACAAAG AAGCAGCAAT
 181 TTTCAGTGTC AGAAGCTCCT GTGGCAATTG AATGGGAGGC TTGAATACTG CCTCAAGGAC
 241 AGGATGAACT TTGACATCCC TGAGGAGATT AAGCAGCTGC AGCAGTTCCA GAAGGAGGAC
   <HSIFN-β-R
 301 GCCGCATTGA CCATCTATGA GATGCTCCAG AACATCTTTG CTATTTTCAG ACAAGATTCA
 361 TCTAGCACTG GCTGGAATGA GACTATTGTT GAGAACCTCC TGGCTAATGT CTATCATCAG
 421 ATAAACCATC TGAAGACAGT CCTGGAAGAA AAACTGGAGA AAGAAGATTT CACCAGGGGA
 481 AAACTCATGA GCAGTCTGCA CCTGAAAAGA TATTATGGGA GGATTCTGCA TTACCTGAAG
 541 GCCAAGGAGT ACAGTCACTG TGCCTGGACC ATAGTCAGAG TGGAAATCCT AAGGAACTTT
 601 TACTTCATTA ACAGACTTAC AGGTTACCTC CGAAACTGAA GATCTCCTAG CCTGTGCCTC
 661 TGGGACTGGA CAATTGCTTC AAGCATTCTT CAACCAGCAG ATGCTGTTTA AGTGACTGAT
 721 GGCTAATGTA CTGCATATGA AAGGACACTA GAAGATTTTG AAATTTTTAT TAAATTATGA
 781 GTTATTTTTA TTTATTTAAA TTTTATTTTG GAAAATAAAT TATTTTTGGT GCAAAAGTCA
```

Map of primer positions for RT-qPCR analysis of IFN-β mRNA expression.
Forward and reverse primers for amplification of IFN-β (NM_002176.2). > indicates forward (F) primer, < indicates reverse (R) primer. Full primer details are listed in Table 2.2.

```
   1 CTGTTTCAGG GCCATTGGAC TCTCCGTCCT GCCCAGAGCA AGATGTGTCA CCAGCAGTTG
  61 GTCATCTCTT GGTTTTCCCT GGTTTTTCTG GCATCTCCCC TCGTGGCCAT ATGGGAACTG
 121 AAGAAAGATG TTTATGTCGT AGAATTGGAT TGGTATCCGG ATGCCCCTGG AGAAATGGTG
 181 GTCCTCACCT GTGACACCCC TGAAGAAGAT GGTATCACCT GGACCTTGGA CCAGAGCAGT
 241 GAGGTCTTAG GCTCTGGCAA AACCCTGACC ATCCAAGTCA AAGAGTTTGG AGATGCTGGC
                HSIL-12B-F>
 301 CAGTACACCT GTCACAAAGG AGGCGAGGTT CTAAGCCATT CGCTCCTGCT GCTTCACAAA
 361 AAGGAAGATG GAATTTGGTC CACTGATATT TTAAAGGACC AGAAAGAACC CAAAAATAAG
                                          <HSIL-12B-R
 421 ACCTTTCTAA GATGCGAGGC CAAGAATTAT TCTGGACGTT TCACCTGCTG GTGGCTGACG
 481 ACAATCAGTA CTGATTTGAC ATTCAGTGTC AAAAGCAGCA GAGGCTCTTC TGACCCCCAA
 541 GGGGTGACGT GCGGAGCTGC TACACTCTCT GCAGAGAGAG TCAGAGGGGA CAACAAGGAG
 601 TATGAGTACT CAGTGGAGTG CCAGGAGGAC AGTGCCTGCC CAGCTGCTGA GGAGAGTCTG
 661 CCCATTGAGG TCATGGTGGA TGCCGTTCAC AAGCTCAAGT ATGAAAACTA CACCAGCAGC
 721 TTCTTCATCA GGGACATCAT CAAACCTGAC CCACCCAAGA ACTTGCAGCT GAAGCCATTA
 781 AAGAATTCTC GGCAGGTGGA GGTCAGCTGG GAGTACCCTG ACACCTGGAG TACTCCACAT
 841 TCCTACTTCT CCCTGACATT CTGCGTTCAG GTCCAGGGCA AGAGCAAGAG AGAAAAGAAA
 901 GATAGAGTCT TCACGGACAA GACCTCAGCC ACGGTCATCT GCCGCAAAAA TGCCAGCATT
 961 AGCGTGCGGG CCCAGGACCG CTACTATAGC TCATCTTGGA GCGAATGGGC ATCTGTGCCC
1021 TGCAGTTAGG TTCTGATCCA GGATGAAAAT TTGGAGGAAA AGTGGAAGAT ATTAAGCAAA
1081 ATGTTTAAAG ACACAACGGA ATAGACCCAA AAAGATAATT TCTATCTGAT TTGCTTTAAA
1141 ACGTTTTTTT AGGATCACAA TGATATCTTT GCTGTATTTG TATAGTTAGA TGCTAAATGC
1201 TCATTGAAAC AATCAGCTAA TTTATGTATA GATTTTCCAG CTCTCAAGTT GCCATGGGCC
1261 TTCATGCTAT TTAAATATTT AAGTAATTTA TGTATTTATT AGTATATTAC TGTTATTTAA
1321 CGTTTGTCTG CCAGGATGTA TGGAATGTTT CATACTCTTA TGACCTGATC CATCAGGATC
1381 AGTCCCTATT ATGCAAAATG TGAATTTAAT TTTATTTGTA CTGACAACTT TTCAAGCAAG
1441 GCTGCAAGTA CATCAGTTTT ATGACAATCA GGAAGAATGC AGTGTTCTGA TACCAGTGCC
1501 ATCATACACT TGTGATGGAT GGGAACGCAA GAGATACTTA CATGGAAACC TGACAATGCA
1561 AACCTGTTGA GAAGATCCAG GAGAACAAGA TGCTAGTTCC CATGTCTGTG AAGACTTCCT
1621 GGAGATGGTG TTGATAAAGC AATTTAGGGC CACTTACACT TCTAAGCAAG TTTAATCTTT
1681 GGATGCCTGA ATTTTAAAAG GGCTAGAAAA AAATGATTGA CCAGCCTGGG AAACATAACA
1741 AGACCCCGTC TCTACAAAAA AAATTTAAAA TTAGCCAGGC GTGGTGGCTC ATGCTTGTGG
1801 TCCCAGCTGT TCAGGAGGAT GAGGCAGGAG GATCTCTTGA GCCCAGGAGG TCAAGGCTAT
1861 GGTGAGCCGT GATTGTGCCA CTGCATACCA GCCTAGGTGA CAGAATGAGA CCCTGTCTCA
1921 AAAAAAAAAA TGATTGAAAT TAAAATTCAG CTTTAGCTTC CATGGCAGTC CTCACCCCCA
1981 CCTCTCTAAA AGACACAGGA GGATGACACA GAAACACCGT AAGTGTCTGG AAGGCAAAAA
2041 GATCTTAAGA TTCAAGAGAG AGGACAAGTA GTTATGGCTA AGGACATGAA ATTGTCAGAA
2101 TGGCAGGTGG CTTCTTAACA GCCCTGTGAG AAGCAGACAG ATGCAAAGAA AATCTGGAAT
2161 CCCTTTCTCA TTAGCATGAA TGAACCTGAT ACACAATTAT GACCAGAAAA TATGGCTCCA
2221 TGAAGGTGCT ACTTTTAAGT AATGTATGTG CGCTCTGTAA AGTGATTACA TTTGTTTCCT
2281 GTTTGTTTAT TTATTTATTT ATTTTTGCAT TCTGAGGCTG AACTAATAAA AACTCTTCTT
2341 TGTAATC
```

Map of primer positions for RT-qPCR analysis of IL-12B mRNA expression.
Forward and reverse primers for amplification of IL-12B (NM_002187.2). > indicates forward (F) primer, < indicates reverse (R) primer. Consecutive exons are shown by alternating white and grey background shading. Full primer details are listed in Table 2.2.

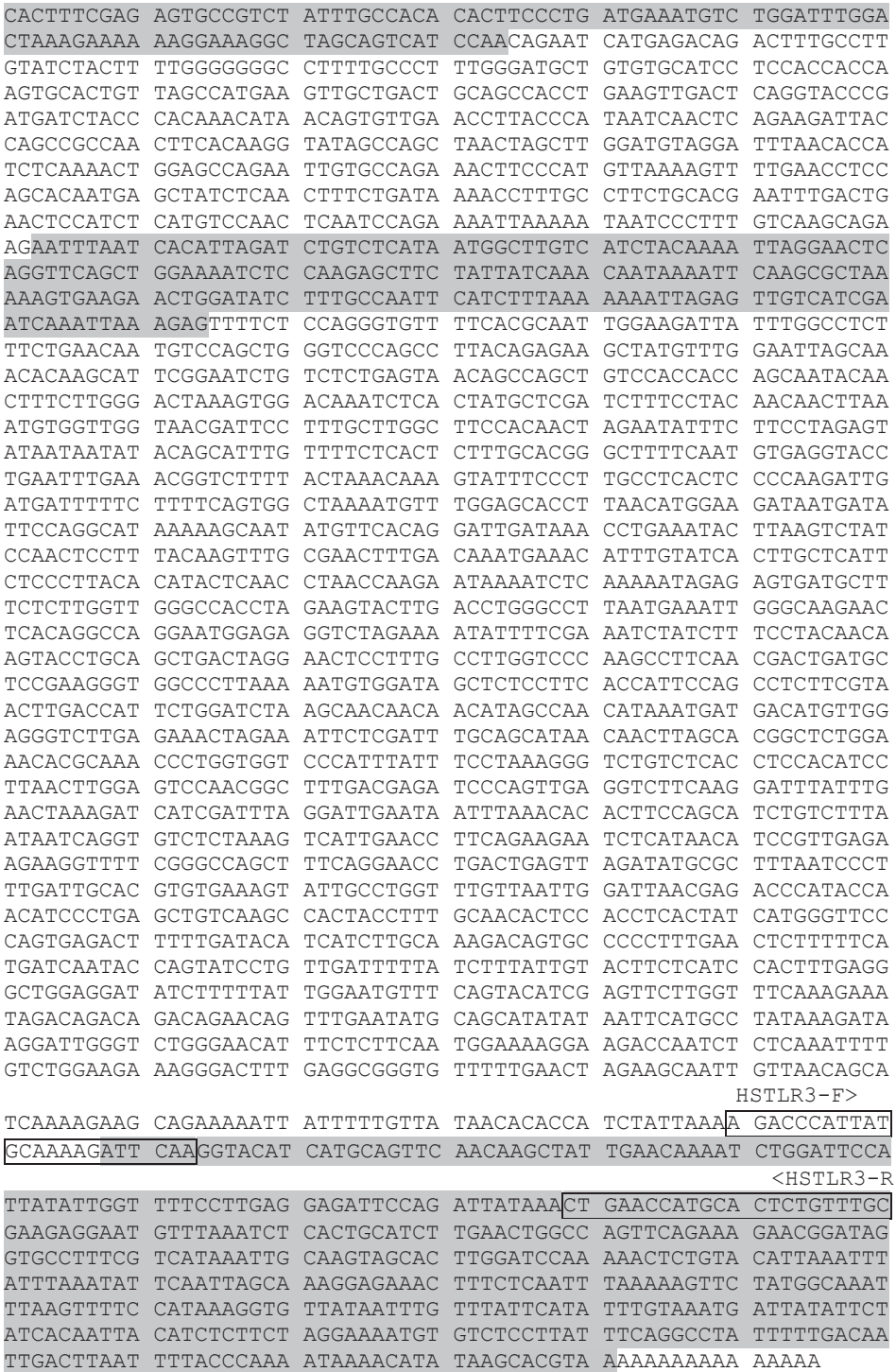

Map of primer positions for RT-qPCR analysis of TLR3 mRNA expression.
Forward and reverse primers for amplification of TLR3 (NM_003265.2). > indicates forward (F) primer, < indicates reverse (R) primer. Consecutive exons are shown by alternating white and grey background shading. Full primer details are listed in Table 2.2.

```
   1 TAGCTTCCTC TTGCTGTTTC TTTAGCCACT GGTCTGCAGG CGTTTTCTTC TTCTAACTTC
  61 CTCTCCTGTG ACAAAAGAGA TAACTATTAG AGAAACAAAA GTCCAGAATG CTAAGGTTGC
 121 CGCTTTCACT TCCTCTCACC CTTTAGCCCA GAACTGCTTT GAATACACCA ATTGCTGTGG
 181 GGCGGCTCGA GGAAGAGAAG ACACCAGTGC CTCAGAAACT GCTCGGTCAG ACGGTGATAG
 241 CGAGCCACGC ATTCACAGGG CCACTGCTGC TCACAGAAGC AGTGAGGATG ATGCCAGGAT
 301 GATGTCTGCC TCGCGCCTGG CTGGGACTCT GATCCCAGCC ATGGCCTTCC TCTCCTGCGT
 361 GAGACCAGAA AGCTGGGAGC CCTGCGTGGA GGTGGTTCCT AATATTACTT ATCAATGCAT
                             HSTLR4-F>
 421 GGAGCTGAAT TTCTACAAAA TCCCCGACAA CCTCCCCTTC TCAACCAAGA ACCTGGACCT
 481 GAGCTTTAAT CCCCTGAGGC ATTTAGGCAG CTATAGCTTC TTCAGTTTCC CAGAACTGCA
                               <HSTLR4-R
 541 GGTGCTGGAT TTATCCAGGT GTGAAATCCA GACAATTGAA GATGGGGCAT ATCAGAGCCT
 601 AAGCCACCTC TCTACCTTAA TATTGACAGG AAACCCCATC CAGAGTTTAG CCCTGGGAGC
 661 CTTTTCTGGA CTATCAAGTT TACAGAAGCT GGTGGCTGTG GAGACAAATC TAGCATCTCT
 721 AGAGAACTTC CCCATTGGAC ATCTCAAAAC TTTGAAAGAA CTTAATGTGG CTCACAATCT
 781 TATCCAATCT TTCAAATTAC CTGAGTATTT TTCTAATCTG ACCAATCTAG AGCACTTGGA
 841 CCTTTCCAGC AACAAGATTC AAAGTATTTA TTGCACAGAC TTGCGGGTTC TACATCAAAT
 901 GCCCCTACTC AATCTCTCTT TAGACCTGTC CCTGAACCCT ATGAACTTTA TCCAACCAGG
 961 TGCATTTAAA GAAATTAGGC TTCATAAGCT GACTTTAAGA AATAATTTTG ATAGTTTAAA
1021 TGTAATGAAA ACTTGTATTC AAGGTCTGGC TGGTTTAGAA GTCCATCGTT TGGTTCTGGG
1081 AGAATTTAGA AATGAAGGAA ACTTGGAAAA GTTTGACAAA TCTGCTCTAG AGGGCCTGTG
1141 CAATTTGACC ATTGAAGAAT TCCGATTAGC ATACTTAGAC TACTACCTCG ATGATATTAT
1201 TGACTTATTT AATTGTTTGA CAAATGTTTC TTCATTTTCC CTGGTGAGTG TGACTATTGA
1261 AAGGGTAAAA GACTTTTCTT ATAATTTCGG ATGGCAACAT TTAGAATTAG TTAACTGTAA
1321 ATTTGGACAG TTTCCCACAT TGAAACTCAA ATCTCTCAAA AGGCTTACTT TCACTTCCAA
1381 CAAAGGTGGG AATGCTTTTT CAGAAGTTGA TCTACCAAGC CTTGAGTTTC TAGATCTCAG
1441 TAGAAATGGC TTGAGTTTCA AAGGTTGCTG TTCTCAAAGT GATTTTGGGA CAACCAGCCT
1501 AAAGTATTTA GATCTGAGCT TCAATGGTGT TATTACCATG AGTTCAAACT TCTTGGGCTT
1561 AGAACAACTA GAACATCTGG ATTTCCAGCA TTCCAATTTG AAACAAATGA GTGAGTTTTC
1621 AGTATTCCTA TCACTCAGAA ACCTCATTTA CCTTGACATT TCTCATACTC ACACCAGAGT
1681 TGCTTTCAAT GGCATCTTCA ATGGCTTGTC CAGTCTCGAA GTCTTGAAAA TGGCTGGCAA
1741 TTCTTTCCAG GAAAACTTCC TTCCAGATAT CTTCACAGAG CTGAGAAACT TGACCTTCCT
1801 GGACCTCTCT CAGTGTCAAC TGGAGCAGTT GTCTCCAACA GCATTTAACT CACTCTCCAG
1861 TCTTCAGGTA CTAAATATGA GCCACAACAA CTTCTTTTCA TTGGATACGT TTCCTTATAA
1921 GTGTCTGAAC TCCCTCCAGG TTCTTGATTA CAGTCTCAAT CACATAATGA CTTCCAAAAA
1981 ACAGGAACTA CAGCATTTTC CAAGTAGTCT AGCTTTCTTA AATCTTACTC AGAATGACTT
2041 TGCTTGTACT TGTGAACACC AGAGTTTCCT GCAATGGATC AAGGACCAGA GGCAGCTCTT
2101 GGTGGAAGTT GAACGAATGG AATGTGCAAC ACCTTCAGAT AAGCAGGGCA TGCCTGTGCT
2161 GAGTTTGAAT ATCACCTGTC AGATGAATAA GACCATCATT GGTGTGTCGG TCCTCAGTGT
UNTIL 5661
```

Map of primer positions for RT-qPCR analysis of TLR4 mRNA expression.
Forward and reverse primers for amplification of TLR4 (NM_138554.4). > indicates forward (F) primer, < indicates reverse (R) primer. Consecutive exons are shown by alternating white and grey background shading. Full primer details are listed in Table 2.2.

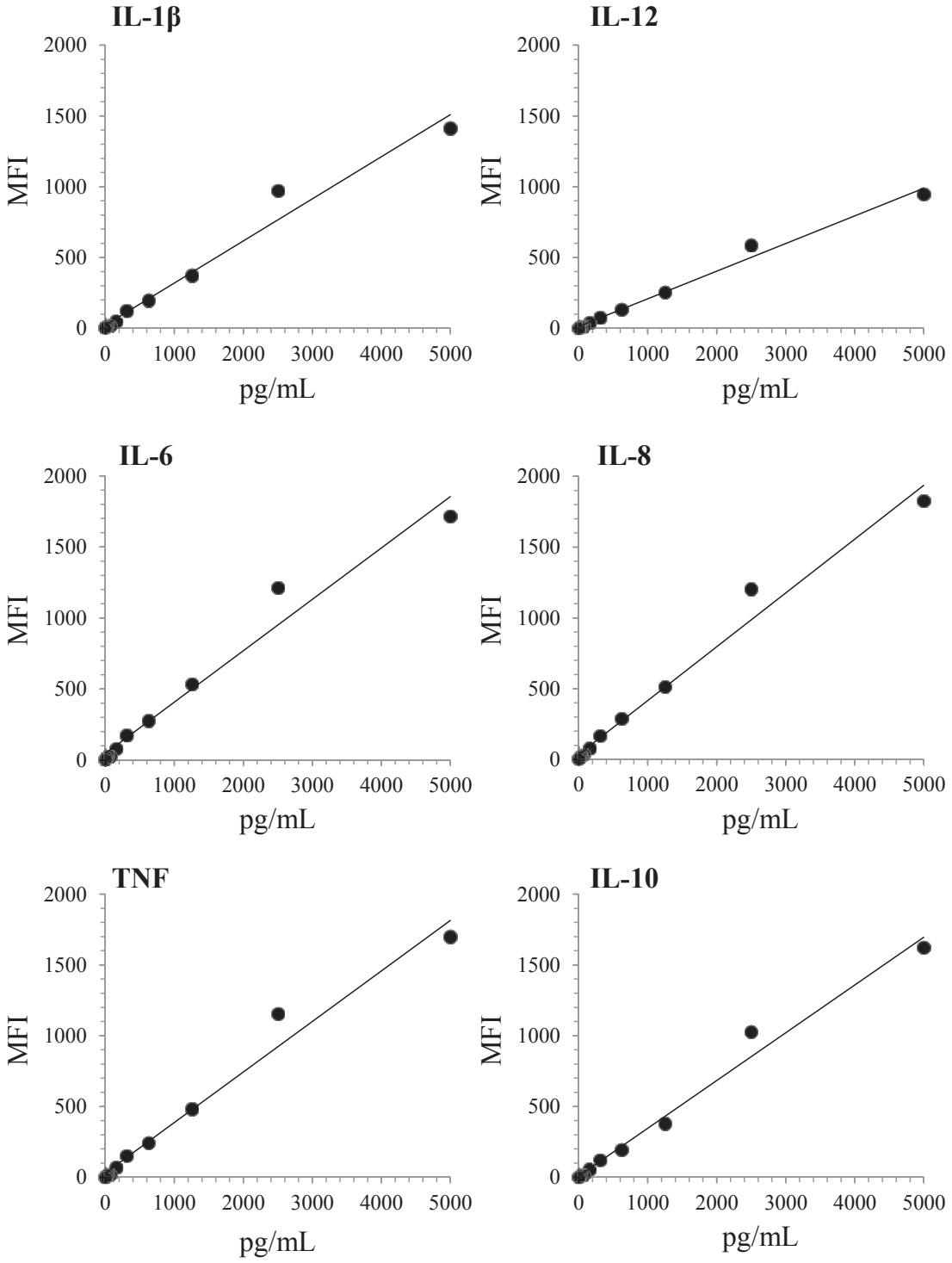

Appendix 2: Standard curves for cytokine quantification by bead array and flow cytometry.

Appendix 3: Mean fluorescence intensity of EEA-1 in macrophage nanotubes compared to connected cell bodies.

PBS-treated replicates			LPS-stimulated replicates					
	MFI	Ratio		MFI	Ratio		MFI	Ratio
Nanotube	45	0.9	**LPS 5 min**			Nanotube	52	0.6
Cell body	53		Nanotube	62	0.5	Cell body	83	
Nanotube	11	0.1	Cell body	128		**LPS 1 h**		
Cell body	131		Nanotube	54	0.4	Nanotube	93	1.0
Nanotube	33	0.2	Cell body	142		Cell body	94	
Cell body	140		Nanotube	30	0.3	Nanotube	25	0.2
Nanotube	33	0.3	Cell body	112		Cell body	162	
Cell body	103		Nanotube	122	0.8	Nanotube	64	0.7
Nanotube	67	0.8	Cell body	156		Cell body	91	
Cell body	88		**LPS 15 min**			**LPS 6 h**		
Nanotube	16	0.2	Nanotube	31	0.2	Nanotube	130	0.9
Cell body	102		Cell body	131		Cell body	141	
Nanotube	58	0.6	Nanotube	59	0.4	Nanotube	89	0.7
Cell body	102		Cell body	140		Cell body	129	
Nanotube	45	0.4	Nanotube	34	0.2	Nanotube	104	0.5
Cell body	108		Cell body	150		Cell body	215	
Nanotube	72	0.9	Nanotube	76	0.5	Nanotube	110	0.5
Cell body	802		Cell body	158		Cell body	215	
Nanotube	5	0.0	Nanotube	71	0.5	Nanotube	55	0.3
Cell body	123		Cell body	143		Cell body	189	
Nanotube	26	0.2	Nanotube	71	0.4	Nanotube	58	0.4
Cell body	168		Cell body	174		Cell body	141	
Nanotube	185	0.1	**LPS 30 min**			Nanotube	74	0.5
Cell body	148		Nanotube	11	0.3	Cell body	166	
Nanotube	89	0.6	Cell body	42		Nanotube	73	0.4
Cell body	141		Nanotube	16	0.3	Cell body	197	
			Cell body	61		Nanotube	155	0.8
			Nanotube	105	0.6	Cell body	197	
			Cell body	170		Nanotube	155	1.0
			Nanotube	90	1.0	Cell body	155	
			Cell body	88				
			Nanotube	43	0.5			
			Cell body	84				

Appendix 4: Mean fluorescence intensity of TLR4 in macrophage nanotubes compared to connected cell bodies.

PBS-treated replicates			LPS-stimulated replicates					
	MFI	Ratio		MFI	Ratio		MFI	Ratio
Nanotube	220	1.8	**LPS 5 min**			**LPS 1 h**		
Cell body	119		Nanotube	102	1.1	Nanotube	149	1.0
Nanotube	48	0.6	Cell body	96		Cell body	148	
Cell body	81		Nanotube	155	1.0	Nanotube	101	0.7
Nanotube	34	0.4	Cell body	162		Cell body	146	
Cell body	95		Nanotube	215	1.8	Nanotube	249	2.3
Nanotube	51	0.5	Cell body	118		Cell body	108	
Cell body	99		Nanotube	459	2.9	Nanotube	499	1.3
Nanotube	51	0.6	Cell body	158		Cell body	381	
Cell body	86		**LPS 15 min**			Nanotube	1008	1.6
Nanotube	236	1.3	Nanotube	162	1.2	Cell body	617	
Cell body	186		Cell body	133		Nanotube	1243	1.9
Nanotube	236	1.4	Nanotube	55	0.4	Cell body	640	
Cell body	174		Cell body	139		**LPS 6 h**		
Nanotube	564	3.3	Nanotube	33	0.3	Nanotube	266	2.5
Cell body	174		Cell body	123		Cell body	106	
Nanotube	71	0.6	Nanotube	138	1.2	Nanotube	153	1.7
Cell body	113		Cell body	116		Cell body	90	
Nanotube	105	1.0	Nanotube	96	0.8	Nanotube	194	1.5
Cell body	106		Cell body	121		Cell body	133	
Nanotube	22	0.2	Nanotube	96	1.0	Nanotube	166	1.3
Cell body	116		Cell body	99		Cell body	133	
Nanotube	135	1.3	**LPS 30 min**			Nanotube	127	1.1
Cell body	108		Nanotube	80	0.9	Cell body	113	
Nanotube	303	1.8	Cell body	92		Nanotube	78	0.7
Cell body	168		Nanotube	81	1.2	Cell body	120	
Nanotube	119	0.9	Cell body	67		Nanotube	78	1.0
Cell body	137		Nanotube	133	0.8	Cell body	79	
			Cell body	159		Nanotube	378	3.0
			Nanotube	254	2.6	Cell body	128	
			Cell body	99		Nanotube	129	1.0
			Nanotube	98	1.0	Cell body	128	
			Cell body	101		Nanotube	129	1.0
			Nanotube	207	1.4	Cell body	129	
			Cell body	145				

Appendix 5: Mean fluorescence intensity of TLR3 in macrophage nanotubes compared to connected cell bodies.

PBS treated replicates		
	MFI	Ratio
Nanotube	322	0.9
Cell body	342	
Nanotube	148	0.4
Cell body	335	
Nanotube	462	2.0
Cell body	230	

Appendix 6: Mean fluorescence intensity of TLR4 in macrophage nanotubes compared to connected cell bodies following FhCL1 treatment.

FhCL1-treated replicates			LPS-stimulated replicates					
	MFI	Ratio		MFI	Ratio		MFI	Ratio
Nanotube	226	1.1	**LPS 5 min**			**LPS 15 min**		
Cell body	213		Nanotube	122	1.1	Nanotube	128	1.2
Nanotube	139	1.2	Cell body	115		Cell body	104	
Cell body	111		Nanotube	124	1.4	Nanotube	128	0.9
Nanotube	72	0.6	Cell body	92		Cell body	143	
Cell body	125		Nanotube	100	0.8	Nanotube	177	1.2
Nanotube	627	1.7	Cell body	125		Cell body	142	
Cell body	368		Nanotube	100	0.7	Nanotube	177	2.0
Nanotube	605	0.9	Cell body	149		Cell body	89	
Cell body	696		Nanotube	94	0.4	**LPS 1 h**		
Nanotube	605	1.5	Cell body	221		Nanotube	58	0.6
Cell body	414		Nanotube	102	0.8	Cell body	97	
Nanotube	238	1.1	Cell body	122		**LPS 6 h**		
Cell body	223		Nanotube	108	0.9	Nanotube	115	1.1
Nanotube	238	0.8	Cell body	119		Cell body	107	
Cell body	294		Nanotube	108	0.5	Nanotube	96	0.8
			Cell body	203		Cell body	113	
			Nanotube	161	1.2	Nanotube	230	2.4
			Cell body	131		Cell body	97	
			Nanotube	161	1.4	Nanotube	127	0.9
			Cell body	115		Cell body	137	
			Nanotube	170	0.9	Nanotube	121	0.7
			Cell body	181		Cell body	173	
			Nanotube	170	1.3	Nanotube	121	1.0
			Cell body	128		Cell body	117	

REFERENCES

Abdollahi-Roodsaz, S., Joosten, L.A., Koenders, M.I., Devesa, I., Roelofs, M.F., Radstake, T.R., Heuvelmans-Jacobs, M., Akira, S., Nicklin, M.J., Ribeiro-Dias, F. & van den Berg, W.B. (2008) Stimulation of TLR2 and TLR4 differentially skews the balance of T cells in a mouse model of arthritis, *The Journal of Clinical Investigation*, 118 (1): 205-16.

Abounit, S. & Zurzolo, C. (2012) Wiring through tunneling nanotubes - from electrical signals to organelle transfer, *Journal of Cell Science*, 125 (Pt 5): 1089-98.

Aderem, A. & Ulevitch, R.J. (2000) Toll-like receptors in the induction of the innate immune response, *Nature*, 406 (6797): 782-7.

Aderem, A. & Underhill, D.M. (1999) Mechanisms of phagocytosis in macrophages, *Annual Review of Immunology*, 17: 593-623.

Adjobimey, T. & Hoerauf, A. (2010) Induction of immunoglobulin G4 in human filariasis: an indicator of immunoregulation, *Annals of Tropical Medicine and Parasitology*, 104 (6): 455-64.

Aggarwal, S., Ghilardi, N., Xie, M.H., de Sauvage, F.J. & Gurney, A.L. (2003) Interleukin-23 promotes a distinct CD4 T cell activation state characterized by the production of interleukin-17, *The Journal of Biological Chemistry*, 278 (3): 1910-4.

Aida, Y. & Pabst, M.J. (1990) Removal of endotoxin from protein solutions by phase separation using Triton X-114, *Journal of Immunological Methods*, 132 (2): 191-5.

Akira, S. & Takeda, K. (2004) Toll-like receptor signalling, *Nature Reviews Immunology*, 4 (7): 499-511.

Akira, S., Uematsu, S. & Takeuchi, O. (2006) Pathogen recognition and innate immunity, *Cell*, 124 (4): 783-801.

Aksoy, E., Zouain, C.S., Vanhoutte, F., Fontaine, J., Pavelka, N., Thieblemont, N., Willems, F., Ricciardi-Castagnoli, P., Goldman, M., Capron, M., Ryffel, B. & Trottein, F. (2005) Double-stranded RNAs from the helminth parasite Schistosoma activate TLR3 in dendritic cells, *The Journal of Biological Chemistry*, 280 (1): 277-83.

Alexopoulou, L., Holt, A.C., Medzhitov, R. & Flavell, R.A. (2001) Recognition of double-stranded RNA and activation of NF-kappaB by Toll-like receptor 3, *Nature*, 413 (6857): 732-8.

Aliprantis, A.O., Yang, R.B., Mark, M.R., Suggett, S., Devaux, B., Radolf, J.D., Klimpel, G.R., Godowski, P. & Zychlinsky, A. (1999) Cell activation and apoptosis by bacterial lipoproteins through toll-like receptor-2, *Science*, 285 (5428): 736-9.

Allen, J.E. & Maizels, R.M. (2011) Diversity and dialogue in immunity to helminths, *Nature Reviews Immunology*, 11 (6): 375-88.

Alonso, A. & Hernan, M.A. (2008) Temporal trends in the incidence of multiple sclerosis: a systematic review, *Neurology*, 71 (2): 129-35.

Amu, S., Saunders, S.P., Kronenberg, M., Mangan, N.E., Atzberger, A. & Fallon, P.G. (2010) Regulatory B cells prevent and reverse allergic airway inflammation via FoxP3-positive T regulatory cells in a murine model, *The Journal of Allergy and Clinical Immunology*, 125 (5): 1114-24.

Anderson, C.F. & Mosser, D.M. (2002) A novel phenotype for an activated macrophage: the type 2 activated macrophage, *Journal of Leukocyte Biology*, 72 (1): 101-6.

Anderson, M.S. & Bluestone, J.A. (2005) The NOD mouse: a model of immune dysregulation, *Annual Review of Immunology*, 23: 447-85.

Andrews, S.J. 1999, The life cycle of Fasciola hepatica, in *Fasciolosis*, J.P. Dalton (ed.), CABI Publishing, Wallingford.

Anthony, R.M., Urban, J.F., Jr., Alem, F., Hamed, H.A., Rozo, C.T., Boucher, J.L., Van Rooijen, N. & Gause, W.C. (2006) Memory T(H)2 cells induce alternatively activated macrophages to mediate protection against nematode parasites, *Nature Medicine*, 12 (8): 955-60.

Arkwright, P.D., Luchetti, F., Tour, J., Roberts, C., Ayub, R., Morales, A.P., Rodriguez, J.J., Gilmore, A., Canonico, B., Papa, S. & Esposti, M.D. (2010) Fas stimulation of T lymphocytes promotes rapid intercellular exchange of death signals via membrane nanotubes, *Cell Research*, 20 (1): 72-88.

Asano, M., Toda, M., Sakaguchi, N. & Sakaguchi, S. (1996) Autoimmune disease as a consequence of developmental abnormality of a T cell subpopulation, *The Journal of Experimental Medicine*, 184 (2): 387-96.

Atochina, O., Da'dara, A.A., Walker, M. & Harn, D.A. (2008) The immunomodulatory glycan LNFPIII initiates alternative activation of murine macrophages in vivo, *Immunology*, 125 (1): 111-21.

Awomoyi, A.A., Marchant, A., Howson, J.M., McAdam, K.P., Blackwell, J.M. & Newport, M.J. (2002) Interleukin-10, polymorphism in SLC11A1 (formerly NRAMP1), and susceptibility to tuberculosis, *The Journal of Infectious Diseases*, 186 (12): 1808-14.

Babu, S., Blauvelt, C.P., Kumaraswami, V. & Nutman, T.B. (2005) Diminished expression and function of TLR in lymphatic filariasis: a novel mechanism of immune dysregulation, *The Journal of Immunology*, 175 (2): 1170-6.

Bachetti, T., Di Zanni, E., Balbi, P., Ravazzolo, R., Sechi, G. & Ceccherini, I. (2012) Beneficial effects of curcumin on GFAP filament organization and down-regulation of GFAP expression in an in vitro model of Alexander disease, *Experimental Cell Research*, 318 (15): 1844-54.

Badolato, R., Ponzi, A.N., Millesimo, M., Notarangelo, L.D. & Musso, T. (1997) Interleukin-15 (IL-15) induces IL-8 and monocyte chemotactic protein 1 production in human monocytes, *Blood*, 90 (7): 2804-9.

Baquerizo, H. & Rabinovitch, A. (1990) Interferon-gamma sensitizes rat pancreatic islet cells to lysis by cytokines and cytotoxic cells, *Journal of Autoimmunity*, 3 Suppl 1: 123-30.

Barrett, A.J. & Kirschke, H. (1981) Cathepsin B, Cathepsin H, and Cathepsin L, *Methods in Enzymology*, 80 Pt C: 535-61.

Bassuny, W.M., Ihara, K., Sasaki, Y., Kuromaru, R., Kohno, H., Matsuura, N. & Hara, T. (2003) A functional polymorphism in the promoter/enhancer region of the FOXP3/Scurfin gene associated with type 1 diabetes, *Immunogenetics*, 55 (3): 149-56.

Beer, R.J. (1976) The relationship between Trichuris trichiura (Linnaeus 1758) of man and Trichuris suis (Schrank 1788) of the pig, *Research in Veterinary Science*, 20 (1): 47-54.

Beg, A.A., Finco, T.S., Nantermet, P.V. & Baldwin, A.S., Jr. (1993) Tumor necrosis factor and interleukin-1 lead to phosphorylation and loss of I kappa B alpha: a mechanism for NF-kappa B activation, *Molecular and Cellular Biology*, 13 (6): 3301-10.

Berasain, P., Goni, F., McGonigle, S., Dowd, A., Dalton, J.P., Frangione, B. & Carmona, C. (1997) Proteinases secreted by Fasciola hepatica degrade extracellular matrix and basement membrane components, *The Journal of Parasitology*, 83 (1): 1-5.

Bettelli, E., Carrier, Y., Gao, W., Korn, T., Strom, T.B., Oukka, M., Weiner, H.L. & Kuchroo, V.K. (2006) Reciprocal developmental pathways for the generation of pathogenic effector TH17 and regulatory T cells, *Nature*, 441 (7090): 235-8.

Beutler, B. (2000) Tlr4: central component of the sole mammalian LPS sensor, *Current Opinion in Immunology*, 12 (1): 20-6.

Beutler, B. (2004) Inferences, questions and possibilities in Toll-like receptor signalling, *Nature*, 430 (6996): 257-63.

Bhattacharyya, A., Pathak, S., Datta, S., Chattopadhyay, S., Basu, J. & Kundu, M. (2002) Mitogen-activated protein kinases and nuclear factor-kappaB regulate Helicobacter pylori-mediated interleukin-8 release from macrophages, *The Biochemical Journal*, 368 (Pt 1): 121-9.

Bonifacio, E., Scirpoli, M., Kredel, K., Fuchtenbusch, M. & Ziegler, A.G. (1999) Early autoantibody responses in prediabetes are IgG1 dominated and suggest antigen-specific regulation, *The Journal of Immunology*, 163 (1): 525-32.

Boonstra, A., Rajsbaum, R., Holman, M., Marques, R., Asselin-Paturel, C., Pereira, J.P., Bates, E.E., Akira, S., Vieira, P., Liu, Y.J., Trinchieri, G. & O'Garra, A. (2006) Macrophages and myeloid dendritic cells, but not plasmacytoid dendritic cells, produce IL-10 in response to MyD88- and TRIF-dependent TLR signals, and TLR-independent signals, *The Journal of Immunology*, 177 (11): 7551-8.

Boulton, T.G., Gregory, J.S. & Cobb, M.H. (1991a) Purification and properties of extracellular signal-regulated kinase 1, an insulin-stimulated microtubule-associated protein 2 kinase, *Biochemistry*, 30 (1): 278-86.

Boulton, T.G., Nye, S.H., Robbins, D.J., Ip, N.Y., Radziejewska, E., Morgenbesser, S.D., DePinho, R.A., Panayotatos, N., Cobb, M.H. & Yancopoulos, G.D. (1991b) ERKs: a family of protein-serine/threonine kinases that are activated and tyrosine phosphorylated in response to insulin and NGF, *Cell*, 65 (4): 663-75.

Broadhurst, M.J., Leung, J.M., Kashyap, V., McCune, J.M., Mahadevan, U., McKerrow, J.H. & Loke, P. (2010) IL-22+ CD4+ T cells are associated with therapeutic trichuris trichiura infection in an ulcerative colitis patient, *Science Translational Medicine*, 2 (60): 60ra88.

Brodsky, F.M. (1988) Living with clathrin: its role in intracellular membrane traffic, *Science*, 242 (4884): 1396-402.

Brosnan, C.F., Selmaj, K. & Raine, C.S. (1988) Hypothesis: a role for tumor necrosis factor in immune-mediated demyelination and its relevance to multiple sclerosis, *Journal of Neuroimmunology*, 18 (1): 87-94.

Bruscia, E.M., Zhang, P.X., Satoh, A., Caputo, C., Medzhitov, R., Shenoy, A., Egan, M.E. & Krause, D.S. (2011) Abnormal trafficking and degradation of TLR4 underlie the elevated inflammatory response in cystic fibrosis, *The Journal of Immunology*, 186 (12): 6990-8.

Bundy, D.A. & Cooper, E.S. (1989) Trichuris and trichuriasis in humans, *Advances in Parasitology*, 28: 107-73.

Butler, C.A., McQuaid, S., Taggart, C.C., Weldon, S., Carter, R., Skibinski, G., Warke, T.J., Choy, D.F., McGarvey, L.P., Bradding, P., Arron, J.R. & Heaney, L.G. (2012) Glucocorticoid receptor beta and histone deacetylase 1 and 2 expression in the airways of severe asthma, *Thorax*, 67 (5): 392-8.

Cammer, W., Bloom, B.R., Norton, W.T. & Gordon, S. (1978) Degradation of basic protein in myelin by neutral proteases secreted by stimulated macrophages: a possible mechanism of inflammatory demyelination, *Proceedings of the National Academy of Sciences of the United States of America*, 75 (3): 1554-8.

Cancado, G.G., Fiuza, J.A., de Paiva, N.C., Lemos Lde, C., Ricci, N.D., Gazzinelli-Guimaraes, P.H., Martins, V.G., Bartholomeu, D.C., Negrao-Correa, D.A., Carneiro, C.M. & Fujiwara, R.T. (2011) Hookworm products ameliorate dextran sodium sulfate-induced colitis in BALB/c mice, *Inflammatory Bowel Diseases*, 17 (11): 2275-86.

Canfield, S.M. & Morrison, S.L. (1991) The binding affinity of human IgG for its high affinity Fc receptor is determined by multiple amino acids in the CH2 domain and is modulated by the hinge region, *The Journal of Experimental Medicine*, 173 (6): 1483-91.

Carranza, F., Falcon, C.R., Nunez, N., Knubel, C., Correa, S.G., Bianco, I., Maccioni, M., Fretes, R., Triquell, M.F., Motran, C.C. & Cervi, L. (2012) Helminth Antigens Enable CpG-Activated Dendritic Cells to Inhibit the Symptoms of Collagen-induced Arthritis through Foxp3+ Regulatory T Cells, *PLoS One*, 7 (7): e40356.

Carson, D., Metzger, H. & Bloch, K.J. (1975) Serum IgE levels during the potentiated reagin response to egg albumin in rats infected with Nippostrongylus brasiliensis, *The Journal of Immunology*, 114 (1 Pt 2): 521-3.

Cella, M., Scheidegger, D., Palmer-Lehmann, K., Lane, P., Lanzavecchia, A. & Alber, G. (1996) Ligation of CD40 on dendritic cells triggers production of high levels of interleukin-12 and enhances T cell stimulatory capacity: T-T help via APC activation, *The Journal of Experimental Medicine*, 184 (2): 747-52.

Cervi, L., MacDonald, A.S., Kane, C., Dzierszinski, F. & Pearce, E.J. (2004) Cutting edge: dendritic cells copulsed with microbial and helminth antigens undergo modified maturation, segregate the antigens to distinct intracellular compartments, and concurrently induce microbe-specific Th1 and helminth-specific Th2 responses, *The Journal of Immunology*, 172 (4): 2016-20.

Cervi, L., Rubinstein, H. & Masih, D.T. (1996) Involvement of excretion-secretion products from Fasciola hepatica inducing suppression of the cellular immune responses, *Veternary Parasitology*, 61 (1-2): 97-111.

Chan, M.S., Medley, G.F., Jamison, D. & Bundy, D.A. (1994) The evaluation of potential global morbidity attributable to intestinal nematode infections, *Parasitology*, 109 (3): 373-87.

Chang, E.Y., Guo, B., Doyle, S.E. & Cheng, G. (2007) Cutting edge: involvement of the type I IFN production and signaling pathway in lipopolysaccharide-induced IL-10 production, *The Journal of Immunology*, 178 (11): 6705-9.

Chaturvedi, A. & Pierce, S.K. (2009) How location governs toll-like receptor signaling, *Traffic*, 10 (6): 621-8.

Chaudhri, G., Quah, B.J., Wang, Y., Tan, A.H., Zhou, J., Karupiah, G. & Parish, C.R. (2009) T cell receptor sharing by cytotoxic T lymphocytes facilitates efficient virus control, *Proceedings of the National Academy of Sciences of the United States of America*, 106 (35): 14984-9.

Chauveau, A., Aucher, A., Eissmann, P., Vivier, E. & Davis, D.M. (2010) Membrane nanotubes facilitate long-distance interactions between natural killer cells and target cells, *Proceedings of the National Academy of Sciences of the United States of America*, 107 (12): 5545-50.

Chen, C., Gault, A., Shen, L. & Nabavi, N. (1994) Molecular cloning and expression of early T cell costimulatory molecule-1 and its characterization as B7-2 molecule, *The Journal of Immunology*, 152 (10): 4929-36.

Chen, R.H., Sarnecki, C. & Blenis, J. (1992) Nuclear localization and regulation of erk- and rsk-encoded protein kinases, *Molecular and Cellular Biology*, 12 (3): 915-27.

Chen, W., Jin, W., Hardegen, N., Lei, K.J., Li, L., Marinos, N., McGrady, G. & Wahl, S.M. (2003) Conversion of peripheral CD4+CD25- naive T cells to CD4+CD25+ regulatory T cells by TGF-beta induction of transcription factor Foxp3, *The Journal of Experimental Medicine*, 198 (12): 1875-86.

Chen, Y.L., Huang, Y.L., Lin, N.Y., Chen, H.C., Chiu, W.C. & Chang, C.J. (2006) Differential regulation of ARE-mediated TNFalpha and IL-1beta mRNA stability by lipopolysaccharide in RAW264.7 cells, *Biochemical and Biophysical Research Communications*, 346 (1): 160-8.

Chia, L.S., Thompson, J.E. & Moscarello, M.A. (1983) Disorder in human myelin induced by superoxide radical: an in vitro investigation, *Biochemical and Biophysical Research Communications*, 117 (1): 141-6.

Chinnery, H.R., Pearlman, E. & McMenamin, P.G. (2008) Cutting edge: Membrane nanotubes in vivo: a feature of MHC class II+ cells in the mouse cornea, *The Journal of Immunology*, 180 (9): 5779-83.

Cho, M.K., Lee, C.H. & Yu, H.S. (2011) Amelioration of intestinal colitis by macrophage migration inhibitory factor isolated from intestinal parasites through toll-like receptor 2, *Parasite Immunology*, 33 (5): 265-75.

Chou, Y.H. & Chien, C.T. (2002) Scabrous controls ommatidial rotation in the Drosophila compound eye, *Developmental Cell*, 3 (6): 839-50.

Collins, P.R., Stack, C.M., O'Neill, S.M., Doyle, S., Ryan, T., Brennan, G.P., Mousley, A., Stewart, M., Maule, A.G., Dalton, J.P. & Donnelly, S. (2004) Cathepsin L1, the major protease involved in liver fluke (Fasciola hepatica) virulence: propetide cleavage sites and autoactivation of the zymogen secreted from gastrodermal cells, *The Journal of Biological Chemistry*, 279 (17): 17038-46.

Cooke, A., Tonks, P., Jones, F.M., O'Shea, H., Hutchings, P., Fulford, A.J. & Dunne, D.W. (1999) Infection with Schistosoma mansoni prevents insulin dependent diabetes mellitus in non-obese diabetic mice, *Parasite Immunology*, 21 (4): 169-76.

Correale, J. & Farez, M. (2007) Association between parasite infection and immune responses in multiple sclerosis, *Annals of Neurology*, 61 (2): 97-108.

Correale, J., Farez, M. & Razzitte, G. (2008) Helminth infections associated with multiple sclerosis induce regulatory B cells, *Annals of Neurology*, 64 (2): 187-99.

Correale, J. & Farez, M.F. (2011) The impact of parasite infections on the course of multiple sclerosis, *Journal of Neuroimmunology*, 233 (1-2): 6-11.

Crispin, J.C., Martinez, A. & Alcocer-Varela, J. (2003) Quantification of regulatory T cells in patients with systemic lupus erythematosus, *Journal of Autoimmunity*, 21 (3): 273-6.

Croese, J., O'Neil, J., Masson, J., Cooke, S., Melrose, W., Pritchard, D. & Speare, R. (2006) A proof of concept study establishing Necator americanus in Crohn's patients and reservoir donors, *Gut*, 55 (1): 136-7.

Crompton, D.W. & Tulley, J.J. (1987) How much Ascariasis is there in Africa?, *Parasitology Today*, 3 (4): 123-7.

Dafa'alla, T.H., Ghalib, H.W., Abdelmageed, A. & Williams, J.F. (1992) The profile of IgG and IgG subclasses of onchocerciasis patients, *Clinical and Experimental Immunology*, 88 (2): 258-63.

Dahlen, E., Dawe, K., Ohlsson, L. & Hedlund, G. (1998) Dendritic cells and macrophages are the first and major producers of TNF-alpha in pancreatic islets in the nonobese diabetic mouse, *The Journal of Immunology*, 160 (7): 3585-93.

Daigneault, M., Preston, J.A., Marriott, H.M., Whyte, M.K. & Dockrell, D.H. (2010) The identification of markers of macrophage differentiation in PMA-stimulated THP-1 cells and monocyte-derived macrophages, *PLoS One*, 5 (1): e8668.

Dainichi, T., Maekawa, Y., Ishii, K., Zhang, T., Nashed, B.F., Sakai, T., Takashima, M. & Himeno, K. (2001) Nippocystatin, a cysteine protease inhibitor from Nippostrongylus brasiliensis, inhibits antigen processing and modulates antigen-specific immune response, *Infection and Immunity*, 69 (12): 7380-6.

Dalton, J.P., Caffrey, C.R., Sajid, M., Stack, C., Donnelly, S., Loukas, A., Don, T., McKerrow, J., Halton, D.W., Brindley, P.J. 2006, Proteases in Trematode Biology, in *Parasitic Flatworms: Molecular Biology, Biochemistry, Immunology and Physiology.*, A.G. Maule, Marks, N.J. (ed.), CABI Publishing, Wallingford, Oxfordshire, GBR, pp. 348-63.

Dalton, J.P., Neill, S.O., Stack, C., Collins, P., Walshe, A., Sekiya, M., Doyle, S., Mulcahy, G., Hoyle, D., Khaznadji, E., Moire, N., Brennan, G., Mousley, A., Kreshchenko, N., Maule, A.G. & Donnelly, S.M. (2003) Fasciola hepatica cathepsin L-like proteases: biology, function, and potential in the development of first generation liver fluke vaccines, *International Journal for Parasitology*, 33 (11): 1173-81.

Daveson, A.J., Jones, D.M., Gaze, S., McSorley, H., Clouston, A., Pascoe, A., Cooke, S., Speare, R., Macdonald, G.A., Anderson, R., McCarthy, J.S., Loukas, A. & Croese, J. (2011) Effect of hookworm infection on wheat challenge in celiac disease - a randomised double-blinded placebo controlled trial, *PLoS One*, 6 (3): e17366.

de Forges, H., Bouissou, A. & Perez, F. (2012) Interplay between microtubule dynamics and intracellular organization, *The International Journal of Biochemistry and Cell Biology*, 44 (2): 266-74.

de Silva, N.R., Brooker, S., Hotez, P.J., Montresor, A., Engels, D. & Savioli, L. (2003) Soil-transmitted helminth infections: updating the global picture, *Trends in Parasitology*, 19 (12): 547-51.

Delcroix, M., Medzihradsky, K., Caffrey, C.R., Fetter, R.D. & McKerrow, J.H. (2007) Proteomic analysis of adult S. mansoni gut contents, *Molecular and Biochemical Parasitology*, 154 (1): 95-7.

Demontis, F. & Dahmann, C. (2007) Apical and lateral cell protrusions interconnect epithelial cells in live Drosophila wing imaginal discs, *Developmental Dynamics*, 236 (12): 3408-18.

Devaraj, S., Cheung, A.T., Jialal, I., Griffen, S.C., Nguyen, D., Glaser, N. & Aoki, T. (2007) Evidence of increased inflammation and microcirculatory abnormalities in patients with type 1 diabetes and their role in microvascular complications, *Diabetes*, 56 (11): 2790-6.

Di Guglielmo, G.M., Le Roy, C., Goodfellow, A.F. & Wrana, J.L. (2003) Distinct endocytic pathways regulate TGF-beta receptor signalling and turnover, *Nature Cell Biology*, 5 (5): 410-21.

DIAMOND Project Group (2006) Incidence and trends of childhood Type 1 diabetes worldwide 1990-1999, *Diabetic Medicine*, 23 (8): 857-66.

Diaz, A. & Allen, J.E. (2007) Mapping immune response profiles: the emerging scenario from helminth immunology, *European Journal of Immunology*, 37 (12): 3319-26.

Diebold, S.S., Kaisho, T., Hemmi, H., Akira, S. & Reis e Sousa, C. (2004) Innate antiviral responses by means of TLR7-mediated recognition of single-stranded RNA, *Science*, 303 (5663): 1529-31.

Dittel, B.N., Visintin, I., Merchant, R.M. & Janeway, C.A., Jr. (1999) Presentation of the self antigen myelin basic protein by dendritic cells leads to experimental autoimmune encephalomyelitis, *The Journal of Immunology*, 163 (1): 32-9.

Doenhoff, M.J. (1997) A role for granulomatous inflammation in the transmission of infectious disease: schistosomiasis and tuberculosis, *Parasitology*, 115 (7): 113-25.

Doherty, G.J. & McMahon, H.T. (2008) Mediation, modulation, and consequences of membrane-cytoskeleton interactions, *Annual Review of Biophysics*, 37: 65-95.

Domhan, S., Ma, L., Tai, A., Anaya, Z., Beheshti, A., Zeier, M., Hlatky, L. & Abdollahi, A. (2011) Intercellular communication by exchange of cytoplasmic material via tunneling nano-tube like structures in primary human renal epithelial cells, *PLoS One*, 6 (6): e21283.

Dong, C., Davis, R.J. & Flavell, R.A. (2002) MAP kinases in the immune response, *Annual Review of Immunology*, 20: 55-72.

Donnelly, S., O'Neill, S.M., Sekiya, M., Mulcahy, G. & Dalton, J.P. (2005) Thioredoxin peroxidase secreted by Fasciola hepatica induces the alternative activation of macrophages, *Infection and Immunity*, 73 (1): 166-73.

Donnelly, S., O'Neill, S.M., Stack, C.M., Robinson, M.W., Turnbull, L., Whitchurch, C. & Dalton, J.P. (2010) Helminth cysteine proteases inhibit TRIF-dependent activation of macrophages via degradation of TLR3, *The Journal of Biological Chemistry*, 285 (5): 3383-92.

Donnelly, S., Stack, C.M., O'Neill, S.M., Sayed, A.A., Williams, D.L. & Dalton, J.P. (2008) Helminth 2-Cys peroxiredoxin drives Th2 responses through a mechanism involving alternatively activated macrophages, *The FASEB Journal*, 22 (11): 4022-32.

Donskow-Lysoniewska, K., Krawczak, K. & Doligalska, M. (2012) Heligmosomoides polygyrus: EAE remission is correlated with different systemic cytokine profiles provoked by L4 and adult nematodes, *Experimental Parasitology*, 132 (2): 243-8.

Dorner, T., Jacobi, A.M. & Lipsky, P.E. (2009) B cells in autoimmunity, *Arthritis Research and Therapy*, 11 (5): 247.

Dowling, D.J., Hamilton, C.M., Donnelly, S., La Course, J., Brophy, P.M., Dalton, J. & O'Neill, S.M. (2010) Major secretory antigens of the helminth Fasciola hepatica activate a suppressive dendritic cell phenotype that attenuates Th17 cells but fails to activate Th2 immune responses, *Infection and Immunity*, 78 (2): 793-801.

Downing, K.H. & Nogales, E. (1998) Tubulin and microtubule structure, *Current Opinion in Cell Biology*, 10 (1): 16-22.

Du, L., Tang, H., Ma, Z., Xu, J., Gao, W., Chen, J., Gan, W., Zhang, Z., Yu, X., Zhou, X. & Hu, X. (2011) The protective effect of the recombinant 53-kDa protein of Trichinella spiralis on experimental colitis in mice, *Digestive Diseases and Sciences*, 56 (10): 2810-7.

Duncan, E.M., Muratore-Schroeder, T.L., Cook, R.G., Garcia, B.A., Shabanowitz, J., Hunt, D.F. & Allis, C.D. (2008) Cathepsin L proteolytically processes histone H3 during mouse embryonic stem cell differentiation, *Cell*, 135 (2): 284-94.

Edwards, J.P., Zhang, X., Frauwirth, K.A. & Mosser, D.M. (2006) Biochemical and functional characterization of three activated macrophage populations, *Journal of Leukocyte Biology*, 80 (6): 1298-307.

Eisenberg, E. & Levanon, E.Y. (2003) Human housekeeping genes are compact, *Trends in Genetics*, 19 (7): 362-5.

Elliott, C., Lindner, M., Arthur, A., Brennan, K., Jarius, S., Hussey, J., Chan, A., Stroet, A., Olsson, T., Willison, H., Barnett, S.C., Meinl, E. & Linington, C. (2012) Functional identification of pathogenic autoantibody responses in patients with multiple sclerosis, *Brain*, 135 (Pt 6): 1819-33.

Elliott, D.E., Li, J., Blum, A., Metwali, A., Qadir, K., Urban, J.F., Jr. & Weinstock, J.V. (2003) Exposure to schistosome eggs protects mice from TNBS-induced colitis, *American Journal of Physiology - Gastrointestinal and Liver Physiology*, 284 (3): G385-91.

Elliott, D.E., Metwali, A., Leung, J., Setiawan, T., Blum, A.M., Ince, M.N., Bazzone, L.E., Stadecker, M.J., Urban, J.F., Jr. & Weinstock, J.V. (2008) Colonization with Heligmosomoides polygyrus suppresses mucosal IL-17 production, *The Journal of Immunology*, 181 (4): 2414-9.

Elliott, D.E., Setiawan, T., Metwali, A., Blum, A., Urban, J.F., Jr. & Weinstock, J.V. (2004) Heligmosomoides polygyrus inhibits established colitis in IL-10-deficient mice, *European Journal of Immunology*, 34 (10): 2690-8.

Erb, K.J. (2007) Helminths, allergic disorders and IgE-mediated immune responses: where do we stand?, *European Journal of Immunology*, 37 (5): 1170-3.

Esser, C. & Radbruch, A. (1990) Immunoglobulin class switching: molecular and cellular analysis, *Annual Review of Immunology*, 8: 717-35.

Eugenin, E.A., Gaskill, P.J. & Berman, J.W. (2009) Tunneling nanotubes (TNT) are induced by HIV-infection of macrophages: a potential mechanism for intercellular HIV trafficking, *Cellular Immunology*, 254 (2): 142-8.

Everts, B., Perona-Wright, G., Smits, H.H., Hokke, C.H., van der Ham, A.J., Fitzsimmons, C.M., Doenhoff, M.J., van der Bosch, J., Mohrs, K., Haas, H., Mohrs, M., Yazdanbakhsh, M. & Schramm, G. (2009) Omega-1, a glycoprotein secreted by Schistosoma mansoni eggs, drives Th2 responses, *The Journal of Experimental Medicine*, 206 (8): 1673-80.

Faulk, W.P. & Taylor, G.M. (1971) An immunocolloid method for the electron microscope, *Immunochemistry*, 8 (11): 1081-3.

Ferluga, J., Doenhoff, M.J. & Allison, A.C. (1979) Increased hepatotoxicity of bacterial lipopolysaccharide in mice infected with Schistosoma mansoni, *Parasite Immunology*, 1 (4): 289-94.

Ferru, I., Roye, O., Delacre, M., Auriault, C. & Wolowczuk, I. (1998) Infection of B-cell-deficient mice by the parasite Schistosoma mansoni: demonstration of the participation of B cells in granuloma modulation, *Scandinavian Journal of Immunology*, 48 (3): 233-40.

Finco, T.S., Beg, A.A. & Baldwin, A.S., Jr. (1994) Inducible phosphorylation of I kappa B alpha is not sufficient for its dissociation from NF-kappa B and is inhibited by protease inhibitors, *Proceedings of the National Academy of Sciences of the United States of America*, 91 (25): 11884-8.

Finkelman, F.D., Katona, I.M., Mosmann, T.R. & Coffman, R.L. (1988) IFN-gamma regulates the isotypes of Ig secreted during in vivo humoral immune responses, *The Journal of Immunology*, 140 (4): 1022-7.

Fitzgerald, K.A., McWhirter, S.M., Faia, K.L., Rowe, D.C., Latz, E., Golenbock, D.T., Coyle, A.J., Liao, S.M. & Maniatis, T. (2003) IKKepsilon and TBK1 are essential components of the IRF3 signaling pathway, *Nature Immunology*, 4 (5): 491-6.

Flannagan, R.S., Harrison, R.E., Yip, C.M., Jaqaman, K. & Grinstein, S. (2010) Dynamic macrophage "probing" is required for the efficient capture of phagocytic targets, *The Journal of Cell Biology*, 191 (6): 1205-18.

Fleming, J.O. & Cook, T.D. (2006) Multiple sclerosis and the hygiene hypothesis, *Neurology*, 67 (11): 2085-6.

Fleming, J.O., Isaak, A., Lee, J.E., Luzzio, C.C., Carrithers, M.D., Cook, T.D., Field, A.S., Boland, J. & Fabry, Z. (2011) Probiotic helminth administration in relapsing-remitting multiple sclerosis: a phase 1 study, *Multiple Sclerosis*, 17 (6): 743-54.

Fontenot, J.D., Gavin, M.A. & Rudensky, A.Y. (2003) Foxp3 programs the development and function of CD4+CD25+ regulatory T cells, *Nature Immunology*, 4 (4): 330-6.

Foster, J.R. (1984) Bacterial infection of the common bile duct in chronic fascioliasis in the rat, *Journal of Comparative Pathology*, 94 (2): 175-81.

Fox, J.G., Beck, P., Dangler, C.A., Whary, M.T., Wang, T.C., Shi, H.N. & Nagler-Anderson, C. (2000) Concurrent enteric helminth infection modulates inflammation and gastric immune responses and reduces helicobacter-induced gastric atrophy, *Nature Medicine*, 6 (5): 536-42.

Frasnelli, M.E., Tarussio, D., Chobaz-Peclat, V., Busso, N. & So, A. (2005) TLR2 modulates inflammation in zymosan-induced arthritis in mice, *Arthritis Research and Therapy*, 7 (2): R370-9.

Freeman, G.J., Long, A.J., Iwai, Y., Bourque, K., Chernova, T., Nishimura, H., Fitz, L.J., Malenkovich, N., Okazaki, T., Byrne, M.C., Horton, H.F., Fouser, L., Carter, L., Ling, V., Bowman, M.R., Carreno, B.M., Collins, M., Wood, C.R. & Honjo, T. (2000) Engagement of the PD-1 immunoinhibitory receptor by a novel B7 family member leads to negative regulation of lymphocyte activation, *The Journal of Experimental Medicine*, 192 (7): 1027-34.

Fujiwara, N. & Kobayashi, K. (2005) Macrophages in inflammation, *Current Drug Targets - Inflammation & Allergy*, 4 (3): 281-6.

Furuno, K., Yuge, T., Kusuhara, K., Takada, H., Nishio, H., Khajoee, V., Ohno, T. & Hara, T. (2004) CD25+CD4+ regulatory T cells in patients with Kawasaki disease, *The Journal of Pediatrics*, 145 (3): 385-90.

Fuss, I.J., Neurath, M., Boirivant, M., Klein, J.S., de la Motte, C., Strong, S.A., Fiocchi, C. & Strober, W. (1996) Disparate CD4+ lamina propria (LP) lymphokine secretion profiles in inflammatory bowel disease. Crohn's disease LP cells manifest increased secretion of IFN-gamma, whereas ulcerative colitis LP cells manifest increased secretion of IL-5, *The Journal of Immunology*, 157 (3): 1261-70.

Gale, E.A. (2002) The rise of childhood type 1 diabetes in the 20th century, *Diabetes*, 51 (12): 3353-61.

Garnon, J., Lachance, C., Di Marco, S., Hel, Z., Marion, D., Ruiz, M.C., Newkirk, M.M., Khandjian, E.W. & Radzioch, D. (2005) Fragile X-related protein FXR1P regulates proinflammatory cytokine tumor necrosis factor expression at the post-transcriptional level, *The Journal of Biological Chemistry*, 280 (7): 5750-63.

Gause, W.C., Urban, J.F., Jr. & Stadecker, M.J. (2003) The immune response to parasitic helminths: insights from murine models, *Trends in Immunology*, 24 (5): 269-77.

Geisow, M.J. & Evans, W.H. (1984) pH in the endosome. Measurements during pinocytosis and receptor-mediated endocytosis, *Experimental Cell Research*, 150 (1): 36-46.

Gerber, J.S. & Mosser, D.M. (2001) Reversing lipopolysaccharide toxicity by ligating the macrophage Fc gamma receptors, *The Journal of Immunology*, 166 (11): 6861-8.

Gerdes, H.H. & Carvalho, R.N. (2008) Intercellular transfer mediated by tunneling nanotubes, *Current Opinion in Cell Biology*, 20 (4): 470-5.

Gessner, A., Blum, H. & Rollinghoff, M. (1993) Differential regulation of IL-9-expression after infection with Leishmania major in susceptible and resistant mice, *Immunobiology*, 189 (5): 419-35.

Gibson, M.C. & Schubiger, G. (2000) Peripodial cells regulate proliferation and patterning of Drosophila imaginal discs, *Cell*, 103 (2): 343-50.

Gillan, V., Lawrence, R.A. & Devaney, E. (2005) B cells play a regulatory role in mice infected with the L3 of Brugia pahangi, *International Immunology*, 17 (4): 373-82.

Gohda, J., Matsumura, T. & Inoue, J. (2004) Cutting edge: TNFR-associated factor (TRAF) 6 is essential for MyD88-dependent pathway but not toll/IL-1 receptor domain-containing adaptor-inducing IFN-beta (TRIF)-dependent pathway in TLR signaling, *The Journal of Immunology*, 173 (5): 2913-7.

Gonzalez, F.A., Seth, A., Raden, D.L., Bowman, D.S., Fay, F.S. & Davis, R.J. (1993) Serum-induced translocation of mitogen-activated protein kinase to the cell surface ruffling membrane and the nucleus, *The Journal of Cell Biology*, 122 (5): 1089-101.

Goodridge, H.S., Marshall, F.A., Else, K.J., Houston, K.M., Egan, C., Al-Riyami, L., Liew, F.Y., Harnett, W. & Harnett, M.M. (2005) Immunomodulation via novel use of TLR4 by the filarial nematode phosphorylcholine-containing secreted product, ES-62, *The Journal of Immunology*, 174 (1): 284-93.

Goral, J., Choudhry, M.A. & Kovacs, E.J. (2004) Acute ethanol exposure inhibits macrophage IL-6 production: role of p38 and ERK1/2 MAPK, *Journal of Leukocyte Biology*, 75 (3): 553-9.

Gordon, S. & Taylor, P.R. (2005) Monocyte and macrophage heterogeneity, *Nature Reviews Immunology*, 5 (12): 953-64.

Gorelik, L., Fields, P.E. & Flavell, R.A. (2000) Cutting edge: TGF-beta inhibits Th type 2 development through inhibition of GATA-3 expression, *The Journal of Immunology*, 165 (9): 4773-7.

Grandvaux, N., Servant, M.J., tenOever, B., Sen, G.C., Balachandran, S., Barber, G.N., Lin, R. & Hiscott, J. (2002) Transcriptional profiling of interferon regulatory factor 3 target genes: direct involvement in the regulation of interferon-stimulated genes, *Journal of Virology*, 76 (11): 5532-9.

Gratchev, A., Guillot, P., Hakiy, N., Politz, O., Orfanos, C.E., Schledzewski, K. & Goerdt, S. (2001) Alternatively activated macrophages differentially express fibronectin and its splice variants and the extracellular matrix protein betaIG-H3, *Scandinavian Journal of Immunology*, 53 (4): 386-92.

Grencis, R.K., Hultner, L. & Else, K.J. (1991) Host protective immunity to Trichinella spiralis in mice: activation of Th cell subsets and lymphokine secretion in mice expressing different response phenotypes, *Immunology*, 74 (2): 329-32.

Groenendijk, B.C., Benus, G.F., Klous, A., Pacheco, Y.M., Volger, O.L., Fledderus, J.O., Ferreira, V., Engelse, M.A., Pannekoek, H., ten Dijke, P., Horrevoets, A.J. & de Vries, C.J. (2011) Activin A induces a non-fibrotic phenotype in smooth muscle cells in contrast to TGF-beta, *Experimental Cell Research*, 317 (2): 131-42.

Gruenberg, J., Griffiths, G. & Howell, K.E. (1989) Characterization of the early endosome and putative endocytic carrier vesicles in vivo and with an assay of vesicle fusion in vitro, *The Journal of Cell Biology*, 108 (4): 1301-16.

Grzych, J.M., Pearce, E., Cheever, A., Caulada, Z.A., Caspar, P., Heiny, S., Lewis, F. & Sher, A. (1991) Egg deposition is the major stimulus for the production of Th2 cytokines in murine schistosomiasis mansoni, *The Journal of Immunology*, 146 (4): 1322-7.

Guillou, F., Roger, E., Mone, Y., Rognon, A., Grunau, C., Theron, A., Mitta, G., Coustau, C. & Gourbal, B.E. (2007) Excretory-secretory proteome of larval Schistosoma mansoni and Echinostoma caproni, two parasites of Biomphalaria glabrata, *Molecular and Biochemical Parasitology*, 155 (1): 45-56.

Gurke, S., Barroso, J.F. & Gerdes, H.H. (2008) The art of cellular communication: tunneling nanotubes bridge the divide, *Histochemistry and Cell Biology*, 129 (5): 539-50.

Gustafson, T. & Wolpert, L. (1967) Cellular movement and contact in sea urchin morphogenesis, *Biological Reviews of the Cambridge Philosophical Society*, 42 (3): 442-98.

Hacker, H., Redecke, V., Blagoev, B., Kratchmarova, I., Hsu, L.C., Wang, G.G., Kamps, M.P., Raz, E., Wagner, H., Hacker, G., Mann, M. & Karin, M. (2006) Specificity in Toll-like receptor signalling through distinct effector functions of TRAF3 and TRAF6, *Nature*, 439 (7073): 204-7.

Hambleton, J., Weinstein, S.L., Lem, L. & DeFranco, A.L. (1996) Activation of c-Jun N-terminal kinase in bacterial lipopolysaccharide-stimulated macrophages, *Proceedings of the National Academy of Sciences of the United States of America*, 93 (7): 2774-8.

Hamilton, C.M., Dowling, D.J., Loscher, C.E., Morphew, R.M., Brophy, P.M. & O'Neill, S.M. (2009) The Fasciola hepatica tegumental antigen suppresses dendritic cell maturation and function, *Infection and Immunity*, 77 (6): 2488-98.

Hang, L., Setiawan, T., Blum, A.M., Urban, J., Stoyanoff, K., Arihiro, S., Reinecker, H.C. & Weinstock, J.V. (2010) Heligmosomoides polygyrus infection can inhibit colitis through direct interaction with innate immunity, *The Journal of Immunology*, 185 (6): 3184-9.

Hansen, A., Lipsky, P.E. & Dorner, T. (2003) New concepts in the pathogenesis of Sjogren syndrome: many questions, fewer answers, *Current Opinion in Rheumatology*, 15 (5): 563-70.

Harn, D.A., McDonald, J., Atochina, O. & Da'dara, A.A. (2009) Modulation of host immune responses by helminth glycans, *Immunological Reviews*, 230 (1): 247-57.

Harrington, L.E., Hatton, R.D., Mangan, P.R., Turner, H., Murphy, T.L., Murphy, K.M. & Weaver, C.T. (2005) Interleukin 17-producing CD4+ effector T cells develop via a lineage distinct from the T helper type 1 and 2 lineages, *Nature Immunology*, 6 (11): 1123-32.

Hartmann, S. & Lucius, R. (2003) Modulation of host immune responses by nematode cystatins, *International Journal for Parasitology*, 33 (11): 1291-302.

Hartung, H.P., Jung, S., Stoll, G., Zielasek, J., Schmidt, B., Archelos, J.J. & Toyka, K.V. (1992) Inflammatory mediators in demyelinating disorders of the CNS and PNS, *Journal of Neuroimmunology*, 40 (2-3): 197-210.

Hatada, E.N., Naumann, M. & Scheidereit, C. (1993) Common structural constituents confer I kappa B activity to NF-kappa B p105 and I kappa B/MAD-3, *The EMBO Journal*, 12 (7): 2781-8.

Hathcock, K.S., Laszlo, G., Pucillo, C., Linsley, P. & Hodes, R.J. (1994) Comparative analysis of B7-1 and B7-2 costimulatory ligands: expression and function, *The Journal of Experimental Medicine*, 180 (2): 631-40.

Hausmann, M., Kiessling, S., Mestermann, S., Webb, G., Spottl, T., Andus, T., Scholmerich, J., Herfarth, H., Ray, K., Falk, W. & Rogler, G. (2002) Toll-like receptors 2 and 4 are up-regulated during intestinal inflammation, *Gastroenterology*, 122 (7): 1987-2000.

Hawa, M.I., Fava, D., Medici, F., Deng, Y.J., Notkins, A.L., De Mattia, G. & Leslie, R.D. (2000) Antibodies to IA-2 and GAD65 in type 1 and type 2 diabetes: isotype restriction and polyclonality, *Diabetes Care*, 23 (2): 228-33.

Hayashi, F., Smith, K.D., Ozinsky, A., Hawn, T.R., Yi, E.C., Goodlett, D.R., Eng, J.K., Akira, S., Underhill, D.M. & Aderem, A. (2001) The innate immune response to bacterial flagellin is mediated by Toll-like receptor 5, *Nature*, 410 (6832): 1099-103.

Hayashi, N., Matsui, K., Tsutsui, H., Osada, Y., Mohamed, R.T., Nakano, H., Kashiwamura, S., Hyodo, Y., Takeda, K., Akira, S., Hada, T., Higashino, K., Kojima, S. & Nakanishi, K. (1999) Kupffer cells from Schistosoma mansoni-infected mice participate in the prompt type 2 differentiation of hepatic T cells in response to worm antigens, *The Journal of Immunology*, 163 (12): 6702-11.

Haziot, A., Ferrero, E., Kontgen, F., Hijiya, N., Yamamoto, S., Silver, J., Stewart, C.L. & Goyert, S.M. (1996) Resistance to endotoxin shock and reduced dissemination of gram-negative bacteria in CD14-deficient mice, *Immunity*, 4 (4): 407-14.

He, Y., Li, J., Zhuang, W., Yin, L., Chen, C., Chi, F., Bai, Y. & Chen, X.P. (2010) The inhibitory effect against collagen-induced arthritis by Schistosoma japonicum infection is infection stage-dependent, *BMC Immunology*, 11: 28.

Heil, F., Ahmad-Nejad, P., Hemmi, H., Hochrein, H., Ampenberger, F., Gellert, T., Dietrich, H., Lipford, G., Takeda, K., Akira, S., Wagner, H. & Bauer, S. (2003) The Toll-like receptor 7 (TLR7)-specific stimulus loxoribine uncovers a strong relationship within the TLR7, 8 and 9 subfamily, *European Journal of Immunology*, 33 (11): 2987-97.

Heil, F., Hemmi, H., Hochrein, H., Ampenberger, F., Kirschning, C., Akira, S., Lipford, G., Wagner, H. & Bauer, S. (2004) Species-specific recognition of single-stranded RNA via toll-like receptor 7 and 8, *Science*, 303 (5663): 1526-9.

Heinz, S., Haehnel, V., Karaghiosoff, M., Schwarzfischer, L., Muller, M., Krause, S.W. & Rehli, M. (2003) Species-specific regulation of Toll-like receptor 3 genes in men and mice, *The Journal of Biological Chemistry*, 278 (24): 21502-9.

Herbert, D.R., Holscher, C., Mohrs, M., Arendse, B., Schwegmann, A., Radwanska, M., Leeto, M., Kirsch, R., Hall, P., Mossmann, H., Claussen, B., Forster, I. & Brombacher, F. (2004) Alternative macrophage activation is essential for survival during schistosomiasis and downmodulates T helper 1 responses and immunopathology, *Immunity*, 20 (5): 623-35.

Herbert, D.R., Yang, J.Q., Hogan, S.P., Groschwitz, K., Khodoun, M., Munitz, A., Orekov, T., Perkins, C., Wang, Q., Brombacher, F., Urban, J.F., Jr., Rothenberg, M.E. & Finkelman, F.D. (2009) Intestinal epithelial cell secretion of RELM-beta protects against gastrointestinal worm infection, *The Journal of Experimental Medicine*, 206 (13): 2947-57.

Hewitson, J.P., Grainger, J.R. & Maizels, R.M. (2009) Helminth immunoregulation: the role of parasite secreted proteins in modulating host immunity, *Molecular and Biochemical Parasitology*, 167 (1): 1-11.

Hewitson, J.P., Harcus, Y., Murray, J., van Agtmaal, M., Filbey, K.J., Grainger, J.R., Bridgett, S., Blaxter, M.L., Ashton, P.D., Ashford, D.A., Curwen, R.S., Wilson, R.A., Dowle, A.A. & Maizels, R.M. (2011) Proteomic analysis of secretory products from the model gastrointestinal nematode Heligmosomoides polygyrus reveals dominance of venom allergen-like (VAL) proteins, *Journal of Proteomics*, 74 (9): 1573-94.

Hirschfeld, M., Kirschning, C.J., Schwandner, R., Wesche, H., Weis, J.H., Wooten, R.M. & Weis, J.J. (1999) Cutting edge: inflammatory signaling by Borrelia burgdorferi lipoproteins is mediated by toll-like receptor 2, *The Journal of Immunology*, 163 (5): 2382-6.

Hiscott, J., Pitha, P., Genin, P., Nguyen, H., Heylbroeck, C., Mamane, Y., Algarte, M. & Lin, R. (1999) Triggering the interferon response: the role of IRF-3 transcription factor, *Journal of Interferon & Cytokine Research*, 19 (1): 1-13.

Hochrein, H., Schlatter, B., O'Keeffe, M., Wagner, C., Schmitz, F., Schiemann, M., Bauer, S., Suter, M. & Wagner, H. (2004) Herpes simplex virus type-1 induces IFN-alpha production via Toll-like receptor 9-dependent and -independent pathways, *Proceedings of the National Academy of Sciences of the United States of America*, 101 (31): 11416-21.

Hoebe, K., Du, X., Georgel, P., Janssen, E., Tabeta, K., Kim, S.O., Goode, J., Lin, P., Mann, N., Mudd, S., Crozat, K., Sovath, S., Han, J. & Beutler, B. (2003) Identification of Lps2 as a key transducer of MyD88-independent TIR signalling, *Nature*, 424 (6950): 743-8.

Holland, M.J., Harcus, Y.M., Riches, P.L. & Maizels, R.M. (2000) Proteins secreted by the parasitic nematode Nippostrongylus brasiliensis act as adjuvants for Th2 responses, *European Journal of Immunology*, 30 (7): 1977-87.

Hong, J., Leung, E., Fraser, A.G., Merriman, T.R., Vishnu, P. & Krissansen, G.W. (2007) TLR2, TLR4 and TLR9 polymorphisms and Crohn's disease in a New Zealand Caucasian cohort, *Journal of Gastroenterology and Hepatology*, 22 (11): 1760-6.

Hori, S., Nomura, T. & Sakaguchi, S. (2003) Control of regulatory T cell development by the transcription factor Foxp3, *Science*, 299 (5609): 1057-61.

Hoshino, K., Takeuchi, O., Kawai, T., Sanjo, H., Ogawa, T., Takeda, Y., Takeda, K. & Akira, S. (1999) Cutting edge: Toll-like receptor 4 (TLR4)-deficient mice are hyporesponsive to lipopolysaccharide: evidence for TLR4 as the Lps gene product, *The Journal of Immunology*, 162 (7): 3749-52.

Hsieh, C.S., deRoos, P., Honey, K., Beers, C. & Rudensky, A.Y. (2002) A role for cathepsin L and cathepsin S in peptide generation for MHC class II presentation, *The Journal of Immunology*, 168 (6): 2618-25.

Hsieh, C.S., Heimberger, A.B., Gold, J.S., O'Garra, A. & Murphy, K.M. (1992) Differential regulation of T helper phenotype development by interleukins 4 and 10 in an alpha beta T-cell-receptor transgenic system, *Proceedings of the National Academy of Sciences of the United States of America*, 89 (13): 6065-9.

Hsieh, C.S., Macatonia, S.E., Tripp, C.S., Wolf, S.F., O'Garra, A. & Murphy, K.M. (1993) Development of TH1 CD4+ T cells through IL-12 produced by Listeria-induced macrophages, *Science*, 260 (5107): 547-9.

Huang, Y.M., Xiao, B.G., Ozenci, V., Kouwenhoven, M., Teleshova, N., Fredrikson, S. & Link, H. (1999) Multiple sclerosis is associated with high levels of circulating dendritic cells secreting pro-inflammatory cytokines, *Journal of Neuroimmunology*, 99 (1): 82-90.

Hubner, M.P., Shi, Y., Torrero, M.N., Mueller, E., Larson, D., Soloviova, K., Gondorf, F., Hoerauf, A., Killoran, K.E., Stocker, J.T., Davies, S.J., Tarbell, K.V. & Mitre, E. (2012) Helminth protection against autoimmune diabetes in nonobese diabetic mice is independent of a type 2 immune shift and requires TGF-beta, *The Journal of Immunology*, 188 (2): 559-68.

Hubner, M.P., Stocker, J.T. & Mitre, E. (2009) Inhibition of type 1 diabetes in filaria-infected non-obese diabetic mice is associated with a T helper type 2 shift and induction of FoxP3+ regulatory T cells, *Immunology*, 127 (4): 512-22.

Husebye, H., Halaas, O., Stenmark, H., Tunheim, G., Sandanger, O., Bogen, B., Brech, A., Latz, E. & Espevik, T. (2006) Endocytic pathways regulate Toll-like receptor 4 signaling and link innate and adaptive immunity, *The EMBO Journal*, 25 (4): 683-92.

Hussaarts, L., van der Vlugt, L.E., Yazdanbakhsh, M. & Smits, H.H. (2011) Regulatory B-cell induction by helminths: implications for allergic disease, *The Journal of Allergy and Clinical Immunology*, 128 (4): 733-9.

Hussain, R., Hamilton, R.G., Kumaraswami, V., Adkinson, N.F., Jr. & Ottesen, E.A. (1981) IgE responses in human filariasis. I. Quantitation of filaria-specific IgE, *The Journal of Immunology*, 127 (4): 1623-9.

Hussain, R. & Ottesen, E.A. (1986) IgE responses in human filariasis. IV. Parallel antigen recognition by IgE and IgG4 subclass antibodies, *The Journal of Immunology*, 136 (5): 1859-63.

Hussain, R., Poindexter, R.W. & Ottesen, E.A. (1992) Control of allergic reactivity in human filariasis. Predominant localization of blocking antibody to the IgG4 subclass, *The Journal of Immunology*, 148 (9): 2731-7.

Imai, S. & Fujita, K. (2004) Molecules of parasites as immunomodulatory drugs, *Current Topics in Medicinal Chemistry*, 4 (5): 539-52.

Imai, S., Tezuka, H. & Fujita, K. (2001) A factor of inducing IgE from a filarial parasite prevents insulin-dependent diabetes mellitus in nonobese diabetic mice, *Biochemical and Biophysical Research Communications*, 286 (5): 1051-8.

Inoue, J., Kerr, L.D., Rashid, D., Davis, N., Bose, H.R., Jr. & Verma, I.M. (1992) Direct association of pp40/I kappa B beta with rel/NF-kappa B transcription factors: role of ankyrin repeats in the inhibition of DNA binding activity, *Proceedings of the National Academy of Sciences of the United States of America*, 89 (10): 4333-7.

Ishizaka, K., Ishizaka, T. & Lee, E.H. (1970) Biologic function of the Fc fragments of E myeloma protein, *Immunochemistry*, 7 (8): 687-702.

Ishizaka, T., Urban, J.F., Jr. & Ishizaka, K. (1976) IgE formation in the rat following infection with Nippostrongylus brasiliensis. I. Proliferation and differentiation of IgE-bearing cells, *Cellular Immunology*, 22 (2): 248-61.

Iyer, S.S., Ghaffari, A.A. & Cheng, G. (2010) Lipopolysaccharide-mediated IL-10 transcriptional regulation requires sequential induction of type I IFNs and IL-27 in macrophages, *The Journal of Immunology*, 185 (11): 6599-607.

Izaguirre, A., Barnes, B.J., Amrute, S., Yeow, W.S., Megjugorac, N., Dai, J., Feng, D., Chung, E., Pitha, P.M. & Fitzgerald-Bocarsly, P. (2003) Comparative analysis of IRF and IFN-alpha expression in human plasmacytoid and monocyte-derived dendritic cells, *Journal of Leukocyte Biology*, 74 (6): 1125-38.

Jacinto, A., Wood, W., Balayo, T., Turmaine, M., Martinez-Arias, A. & Martin, P. (2000) Dynamic actin-based epithelial adhesion and cell matching during Drosophila dorsal closure, *Current Biology*, 10 (22): 1420-6.

Jankovic, D., Kullberg, M.C., Caspar, P. & Sher, A. (2004) Parasite-induced Th2 polarization is associated with down-regulated dendritic cell responsiveness to Th1 stimuli and a transient delay in T lymphocyte cycling, *The Journal of Immunology*, 173 (4): 2419-27.

Jansen, A., Homo-Delarche, F., Hooijkaas, H., Leenen, P.J., Dardenne, M. & Drexhage, H.A. (1994) Immunohistochemical characterization of monocytes-macrophages and dendritic cells involved in the initiation of the insulitis and beta-cell destruction in NOD mice, *Diabetes*, 43 (5): 667-75.

Jaramillo, A., Gill, B.M. & Delovitch, T.L. (1994) Insulin dependent diabetes mellitus in the non-obese diabetic mouse: a disease mediated by T cell anergy?, *Life Sciences*, 55 (15): 1163-77.

Jarrett, E. & Bazin, H. (1974) Elevation of total serum IgE in rats following helminth parasite infection, *Nature*, 251 (5476): 613-4.

Jiang, W., Reich, I.C. & Pisetsky, D.S. (2004) Mechanisms of activation of the RAW264.7 macrophage cell line by transfected mammalian DNA, *Cellular Immunology*, 229 (1): 31-40.

Jiang, Z., Georgel, P., Du, X., Shamel, L., Sovath, S., Mudd, S., Huber, M., Kalis, C., Keck, S., Galanos, C., Freudenberg, M. & Beutler, B. (2005) CD14 is required for MyD88-independent LPS signaling, *Nature Immunology*, 6 (6): 565-70.

Jing, Q., Huang, S., Guth, S., Zarubin, T., Motoyama, A., Chen, J., Di Padova, F., Lin, S.C., Gram, H. & Han, J. (2005) Involvement of microRNA in AU-rich element-mediated mRNA instability, *Cell*, 120 (5): 623-34.

Johnston, M.J., Wang, A., Catarino, M.E., Ball, L., Phan, V.C., MacDonald, J.A. & McKay, D.M. (2010) Extracts of the rat tapeworm, Hymenolepis diminuta, suppress macrophage activation in vitro and alleviate chemically induced colitis in mice, *Infection and Immunity*, 78 (3): 1364-75.

Jonuleit, H., Schmitt, E., Schuler, G., Knop, J. & Enk, A.H. (2000) Induction of interleukin 10-producing, nonproliferating CD4(+) T cells with regulatory properties by repetitive stimulation with allogeneic immature human dendritic cells, *The Journal of Experimental Medicine*, 192 (9): 1213-22.

Juarez, E., Nunez, C., Sada, E., Ellner, J.J., Schwander, S.K. & Torres, M. (2010) Differential expression of Toll-like receptors on human alveolar macrophages and autologous peripheral monocytes, *Respiratory Research*, 11: 2.

Kadiu, I. & Gendelman, H.E. (2011a) Human immunodeficiency virus type 1 endocytic trafficking through macrophage bridging conduits facilitates spread of infection, *Journal of Neuroimmune Pharmacology: The Official Journal of the Society on NeuroImmune Pharmacology*, 6 (4): 658-75.

Kadiu, I. & Gendelman, H.E. (2011b) Macrophage bridging conduit trafficking of HIV-1 through the endoplasmic reticulum and Golgi network, *Journal of Proteome Research*, 10 (7): 3225-38.

Kagan, J.C. & Medzhitov, R. (2006) Phosphoinositide-mediated adaptor recruitment controls Toll-like receptor signaling, *Cell*, 125 (5): 943-55.

Kagan, J.C., Su, T., Horng, T., Chow, A., Akira, S. & Medzhitov, R. (2008) TRAM couples endocytosis of Toll-like receptor 4 to the induction of interferon-beta, *Nature Immunology*, 9 (4): 361-8.

Kaisho, T., Takeuchi, O., Kawai, T., Hoshino, K. & Akira, S. (2001) Endotoxin-induced maturation of MyD88-deficient dendritic cells, *The Journal of Immunology*, 166 (9): 5688-94.

Kanter, J.L., Narayana, S., Ho, P.P., Catz, I., Warren, K.G., Sobel, R.A., Steinman, L. & Robinson, W.H. (2006) Lipid microarrays identify key mediators of autoimmune brain inflammation, *Nature Medicine*, 12 (1): 138-43.

Karaghiosoff, M., Steinborn, R., Kovarik, P., Kriegshauser, G., Baccarini, M., Donabauer, B., Reichart, U., Kolbe, T., Bogdan, C., Leanderson, T., Levy, D., Decker, T. & Muller, M. (2003) Central role for type I interferons and Tyk2 in lipopolysaccharide-induced endotoxin shock, *Nature Immunology*, 4 (5): 471-7.

Karin, M. (1995) The regulation of AP-1 activity by mitogen-activated protein kinases, *The Journal of Biological Chemistry*, 270 (28): 16483-6.

Karvonen, M., Tuomilehto, J., Libman, I. & LaPorte, R. (1993) A review of the recent epidemiological data on the worldwide incidence of type 1 (insulin-dependent) diabetes

mellitus. World Health Organization DIAMOND Project Group, *Diabetologia*, 36 (10): 883-92.

Kawai, T. & Akira, S. (2006) TLR signaling, *Cell Death and Differentiation*, 13 (5): 816-25.

Kawai, T. & Akira, S. (2007) Signaling to NF-kappaB by Toll-like receptors, *Trends in Molecular Medicine*, 13 (11): 460-9.

Kawai, T., Takeuchi, O., Fujita, T., Inoue, J., Muhlradt, P.F., Sato, S., Hoshino, K. & Akira, S. (2001) Lipopolysaccharide stimulates the MyD88-independent pathway and results in activation of IFN-regulatory factor 3 and the expression of a subset of lipopolysaccharide-inducible genes, *The Journal of Immunology*, 167 (10): 5887-94.

Khan, W.I., Blennerhasset, P.A., Varghese, A.K., Chowdhury, S.K., Omsted, P., Deng, Y. & Collins, S.M. (2002) Intestinal nematode infection ameliorates experimental colitis in mice, *Infection and Immunity*, 70 (11): 5931-7.

Kikutani, H. & Makino, S. (1992) The murine autoimmune diabetes model: NOD and related strains, *Advances in Immunology*, 51: 285-322.

Kim, H.S., Han, M.S., Chung, K.W., Kim, S., Kim, E., Kim, M.J., Jang, E., Lee, H.A., Youn, J., Akira, S. & Lee, M.S. (2007) Toll-like receptor 2 senses beta-cell death and contributes to the initiation of autoimmune diabetes, *Immunity*, 27 (2): 321-33.

Kim, J.H., Kim, S.J., Lee, I.S., Lee, M.S., Uematsu, S., Akira, S. & Oh, K.I. (2009) Bacterial endotoxin induces the release of high mobility group box 1 via the IFN-beta signaling pathway, *The Journal of Immunology*, 182 (4): 2458-66.

Kim, Y.J., Sapp, E., Cuiffo, B.G., Sobin, L., Yoder, J., Kegel, K.B., Qin, Z.H., Detloff, P., Aronin, N. & DiFiglia, M. (2006) Lysosomal proteases are involved in generation of N-terminal huntingtin fragments, *Neurobiology of Disease*, 22 (2): 346-56.

Kimpimaki, T., Kupila, A., Hamalainen, A.M., Kukko, M., Kulmala, P., Savola, K., Simell, T., Keskinen, P., Ilonen, J., Simell, O. & Knip, M. (2001) The first signs of beta-cell autoimmunity appear in infancy in genetically susceptible children from the general population: the Finnish Type 1 Diabetes Prediction and Prevention Study, *The Journal of Clinical Endocrinology and Metabolism*, 86 (10): 4782-8.

Kitchens, R.L. (2000) Role of CD14 in cellular recognition of bacterial lipopolysaccharides, *Chemical Immunology*, 74: 61-82.

Kitchens, R.L., Wang, P. & Munford, R.S. (1998) Bacterial lipopolysaccharide can enter monocytes via two CD14-dependent pathways, *The Journal of Immunology*, 161 (10): 5534-45.

Klotz, C., Ziegler, T., Figueiredo, A.S., Rausch, S., Hepworth, M.R., Obsivac, N., Sers, C., Lang, R., Hammerstein, P., Lucius, R. & Hartmann, S. (2011) A helminth immunomodulator exploits host signaling events to regulate cytokine production in macrophages, *PLoS Pathogens*, 7 (1): e1001248.

Kobayashi, M., Saitoh, S., Tanimura, N., Takahashi, K., Kawasaki, K., Nishijima, M., Fujimoto, Y., Fukase, K., Akashi-Takamura, S. & Miyake, K. (2006) Regulatory roles

for MD-2 and TLR4 in ligand-induced receptor clustering, *The Journal of Immunology*, 176 (10): 6211-8.

Kolb, H. & Elliott, R.B. (1994) Increasing incidence of IDDM a consequence of improved hygiene?, *Diabetologia*, 37 (7): 729.

Konat, G.W. & Wiggins, R.C. (1985) Effect of reactive oxygen species on myelin membrane proteins, *Journal of Neurochemistry*, 45 (4): 1113-8.

Korn, T., Bettelli, E., Gao, W., Awasthi, A., Jager, A., Strom, T.B., Oukka, M. & Kuchroo, V.K. (2007) IL-21 initiates an alternative pathway to induce proinflammatory T(H)17 cells, *Nature*, 448 (7152): 484-7.

Korn, T., Bettelli, E., Oukka, M. & Kuchroo, V.K. (2009) IL-17 and Th17 Cells, *Annual Review of Immunology*, 27: 485-517.

Koyanagi, M., Brandes, R.P., Haendeler, J., Zeiher, A.M. & Dimmeler, S. (2005) Cell-to-cell connection of endothelial progenitor cells with cardiac myocytes by nanotubes: a novel mechanism for cell fate changes?, *Circulation Research*, 96 (10): 1039-41.

Kreider, T., Anthony, R.M., Urban, J.F., Jr. & Gause, W.C. (2007) Alternatively activated macrophages in helminth infections, *Current Opinion in Immunology*, 19 (4): 448-53.

Kristiansen, M., Graversen, J.H., Jacobsen, C., Sonne, O., Hoffman, H.J., Law, S.K. & Moestrup, S.K. (2001) Identification of the haemoglobin scavenger receptor, *Nature*, 409 (6817): 198-201.

Krug, A., French, A.R., Barchet, W., Fischer, J.A., Dzionek, A., Pingel, J.T., Orihuela, M.M., Akira, S., Yokoyama, W.M. & Colonna, M. (2004a) TLR9-dependent recognition of MCMV by IPC and DC generates coordinated cytokine responses that activate antiviral NK cell function, *Immunity*, 21 (1): 107-19.

Krug, A., Luker, G.D., Barchet, W., Leib, D.A., Akira, S. & Colonna, M. (2004b) Herpes simplex virus type 1 activates murine natural interferon-producing cells through toll-like receptor 9, *Blood*, 103 (4): 1433-7.

Krull, W.H. & Jackson, R.S. (1943) Observations on the route of migration of the common liver fluke, Fasciola hepatica, in the definitive host., *Journal of the Washington Academy of Sciences*, 33: 79-82.

Kuijk, L.M., Klaver, E.J., Kooij, G., van der Pol, S.M., Heijnen, P., Bruijns, S.C., Kringel, H., Pinelli, E., Kraal, G., de Vries, H.E., Dijkstra, C.D., Bouma, G. & van Die, I. (2012) Soluble helminth products suppress clinical signs in murine experimental autoimmune encephalomyelitis and differentially modulate human dendritic cell activation, *Molecular Immunology*, 51 (2): 210-8.

Kuo, Y.C. & Chen, H.H. (2010) Effect of electromagnetic field on endocytosis of cationic solid lipid nanoparticles by human brain-microvascular endothelial cells, *Journal of Drug Targeting*, 18 (6): 447-56.

Kurniawan, A., Yazdanbakhsh, M., van Ree, R., Aalberse, R., Selkirk, M.E., Partono, F. & Maizels, R.M. (1993) Differential expression of IgE and IgG4 specific antibody

responses in asymptomatic and chronic human filariasis, *The Journal of Immunology*, 150 (9): 3941-50.

La Flamme, A.C., Ruddenklau, K. & Backstrom, B.T. (2003) Schistosomiasis decreases central nervous system inflammation and alters the progression of experimental autoimmune encephalomyelitis, *Infection and Immunity*, 71 (9): 4996-5004.

Lamaze, C. & Schmid, S.L. (1995) The emergence of clathrin-independent pinocytic pathways, *Current Opinion in Cell Biology*, 7 (4): 573-80.

Lambertucci, J.R. (2010) Acute schistosomiasis mansoni: revisited and reconsidered, *Memorias do Instituto Oswaldo Cruz*, 105 (4): 422-35.

Langrish, C.L., Chen, Y., Blumenschein, W.M., Mattson, J., Basham, B., Sedgwick, J.D., McClanahan, T., Kastelein, R.A. & Cua, D.J. (2005) IL-23 drives a pathogenic T cell population that induces autoimmune inflammation, *The Journal of Experimental Medicine*, 201 (2): 233-40.

Latz, E., Schoenemeyer, A., Visintin, A., Fitzgerald, K.A., Monks, B.G., Knetter, C.F., Lien, E., Nilsen, N.J., Espevik, T. & Golenbock, D.T. (2004) TLR9 signals after translocating from the ER to CpG DNA in the lysosome, *Nature Immunology*, 5 (2): 190-8.

Le Roy, C. & Wrana, J.L. (2005) Clathrin- and non-clathrin-mediated endocytic regulation of cell signalling, *Nature Reviews Molecular Cell Biology*, 6 (2): 112-26.

Lee, H.K., Dunzendorfer, S., Soldau, K. & Tobias, P.S. (2006) Double-stranded RNA-mediated TLR3 activation is enhanced by CD14, *Immunity*, 24 (2): 153-63.

Lee, J., Chuang, T.H., Redecke, V., She, L., Pitha, P.M., Carson, D.A., Raz, E. & Cottam, H.B. (2003) Molecular basis for the immunostimulatory activity of guanine nucleoside analogs: activation of Toll-like receptor 7, *Proceedings of the National Academy of Sciences of the United States of America*, 100 (11): 6646-51.

Lenormand, P., Sardet, C., Pages, G., L'Allemain, G., Brunet, A. & Pouyssegur, J. (1993) Growth factors induce nuclear translocation of MAP kinases (p42mapk and p44mapk) but not of their activator MAP kinase kinase (p45mapkk) in fibroblasts, *The Journal of Cell Biology*, 122 (5): 1079-88.

Libermann, T.A. & Baltimore, D. (1990) Activation of interleukin-6 gene expression through the NF-kappa B transcription factor, *Molecular and Cellular Biology*, 10 (5): 2327-34.

Lien, E., Sellati, T.J., Yoshimura, A., Flo, T.H., Rawadi, G., Finberg, R.W., Carroll, J.D., Espevik, T., Ingalls, R.R., Radolf, J.D. & Golenbock, D.T. (1999) Toll-like receptor 2 functions as a pattern recognition receptor for diverse bacterial products, *The Journal of Biological Chemistry*, 274 (47): 33419-25.

Lightowlers, M.W. & Rickard, M.D. (1988) Excretory-secretory products of helminth parasites: effects on host immune responses, *Parasitology*, 96 Suppl: S123-66.

Like, A.A., Guberski, D.L. & Butler, L. (1991) Influence of environmental viral agents on frequency and tempo of diabetes mellitus in BB/Wor rats, *Diabetes*, 40 (2): 259-62.

Liu, M.F., Wang, C.R., Fung, L.L. & Wu, C.R. (2004) Decreased CD4+CD25+ T cells in peripheral blood of patients with systemic lupus erythematosus, *Scandinavian Journal of Immunology*, 59 (2): 198-202.

Liu, Q., Sundar, K., Mishra, P.K., Mousavi, G., Liu, Z., Gaydo, A., Alem, F., Lagunoff, D., Bleich, D. & Gause, W.C. (2009) Helminth infection can reduce insulitis and type 1 diabetes through CD25- and IL-10-independent mechanisms, *Infection and Immunity*, 77 (12): 5347-58.

Livak, K.J. & Schmittgen, T.D. (2001) Analysis of relative gene expression data using real-time quantitative PCR and the 2(-Delta Delta C(T)) Method, *Methods*, 25 (4): 402-8.

Locksley, R.M., Heinzel, F.P., Sadick, M.D., Holaday, B.J. & Gardner, K.D., Jr. (1987) Murine cutaneous leishmaniasis: susceptibility correlates with differential expansion of helper T-cell subsets, *Annales de l'Institut Pasteur Immunology*, 138 (5): 744-9.

Loke, P., MacDonald, A.S. & Allen, J.E. (2000a) Antigen-presenting cells recruited by Brugia malayi induce Th2 differentiation of naive CD4(+) T cells, *European Journal of Immunology*, 30 (4): 1127-35.

Loke, P., MacDonald, A.S., Robb, A., Maizels, R.M. & Allen, J.E. (2000b) Alternatively activated macrophages induced by nematode infection inhibit proliferation via cell-to-cell contact, *European Journal of Immunology*, 30 (9): 2669-78.

Loke, P., Nair, M.G., Parkinson, J., Guiliano, D., Blaxter, M. & Allen, J.E. (2002) IL-4 dependent alternatively-activated macrophages have a distinctive in vivo gene expression phenotype, *BMC Immunology*, 3: 7.

Londei, M., Savill, C.M., Verhoef, A., Brennan, F., Leech, Z.A., Duance, V., Maini, R.N. & Feldmann, M. (1989) Persistence of collagen type II-specific T-cell clones in the synovial membrane of a patient with rheumatoid arthritis, *Proceedings of the National Academy of Sciences of the United States of America*, 86 (2): 636-40.

Lou, E., Fujisawa, S., Morozov, A., Barlas, A., Romin, Y., Dogan, Y., Gholami, S., Moreira, A.L., Manova-Todorova, K. & Moore, M.A. (2012) Tunneling nanotubes provide a unique conduit for intercellular transfer of cellular contents in human malignant pleural mesothelioma, *PLoS One*, 7 (3): e33093.

Lowther, J., Robinson, M.W., Donnelly, S.M., Xu, W., Stack, C.M., Matthews, J.M. & Dalton, J.P. (2009) The importance of pH in regulating the function of the Fasciola hepatica cathepsin L1 cysteine protease, *PLoS Neglected Tropical Diseases*, 3 (1): e369.

Lu, J.Y., Sadri, N. & Schneider, R.J. (2006) Endotoxic shock in AUF1 knockout mice mediated by failure to degrade proinflammatory cytokine mRNAs, *Genes & development*, 20 (22): 3174-84.

Luchetti, F., Canonico, B., Arcangeletti, M., Guescini, M., Cesarini, E., Stocchi, V., Degli Esposti, M. & Papa, S. (2012) Fas signalling promotes intercellular communication in T cells, *PLoS One*, 7 (4): e35766.

Ludewig, B., Odermatt, B., Landmann, S., Hengartner, H. & Zinkernagel, R.M. (1998) Dendritic cells induce autoimmune diabetes and maintain disease via de novo formation of local lymphoid tissue, *The Journal of Experimental Medicine*, 188 (8): 1493-501.

Lund, J., Sato, A., Akira, S., Medzhitov, R. & Iwasaki, A. (2003) Toll-like receptor 9-mediated recognition of Herpes simplex virus-2 by plasmacytoid dendritic cells, *The Journal of Experimental Medicine*, 198 (3): 513-20.

Lundberg, A.M., Drexler, S.K., Monaco, C., Williams, L.M., Sacre, S.M., Feldmann, M. & Foxwell, B.M. (2007) Key differences in TLR3/poly I:C signaling and cytokine induction by human primary cells: a phenomenon absent from murine cell systems, *Blood*, 110 (9): 3245-52.

MacDonald, A.S., Straw, A.D., Bauman, B. & Pearce, E.J. (2001) CD8- dendritic cell activation status plays an integral role in influencing Th2 response development, *The Journal of Immunology*, 167 (4): 1982-8.

Macian, F., Lopez-Rodriguez, C. & Rao, A. (2001) Partners in transcription: NFAT and AP-1, *Oncogene*, 20 (19): 2476-89.

Mahieu, T. & Libert, C. (2007) Should we inhibit type I interferons in sepsis?, *Infection and Immunity*, 75 (1): 22-9.

Mahieu, T., Park, J.M., Revets, H., Pasche, B., Lengeling, A., Staelens, J., Wullaert, A., Vanlaere, I., Hochepied, T., van Roy, F., Karin, M. & Libert, C. (2006) The wild-derived inbred mouse strain SPRET/Ei is resistant to LPS and defective in IFN-beta production, *Proceedings of the National Academy of Sciences of the United States of America*, 103 (7): 2292-7.

Maizels, R.M., Balic, A., Gomez-Escobar, N., Nair, M., Taylor, M.D. & Allen, J.E. (2004) Helminth parasites - masters of regulation, *Immunological Reviews*, 201: 89-116.

Makino, S., Kunimoto, K., Muraoka, Y., Mizushima, Y., Katagiri, K. & Tochino, Y. (1980) Breeding of a non-obese, diabetic strain of mice, *Jikken Dobutsu*, 29 (1): 1-13.

Marcos, L.A., Terashima, A. & Gotuzzo, E. (2008) Update on hepatobiliary flukes: fascioliasis, opisthorchiasis and clonorchiasis, *Current Opinion in Infectious Diseases*, 21 (5): 523-30.

Maron, R., Palanivel, V., Weiner, H.L. & Harn, D.A. (1998) Oral administration of schistosome egg antigens and insulin B-chain generates and enhances Th2-type responses in NOD mice, *Clinical Immunology and Immunopathology*, 87 (1): 85-92.

Martin, P. & Leibovich, S.J. (2005) Inflammatory cells during wound repair: the good, the bad and the ugly, *Trends in Cell Biology*, 15 (11): 599-607.

Martinez, F.O., Gordon, S., Locati, M. & Mantovani, A. (2006) Transcriptional profiling of the human monocyte-to-macrophage differentiation and polarization: new molecules and patterns of gene expression, *The Journal of Immunology*, 177 (10): 7303-11.

Martinez, F.O., Helming, L. & Gordon, S. (2009) Alternative activation of macrophages: an immunologic functional perspective, *Annual Review of Immunology*, 27: 451-83.

Marzo, L., Gousset, K. & Zurzolo, C. (2012) Multifaceted roles of tunneling nanotubes in intercellular communication, *Frontiers in Physiology*, 3: 72.

Mathey, E.K., Derfuss, T., Storch, M.K., Williams, K.R., Hales, K., Woolley, D.R., Al-Hayani, A., Davies, S.N., Rasband, M.N., Olsson, T., Moldenhauer, A., Velhin, S., Hohlfeld, R., Meinl, E. & Linington, C. (2007) Neurofascin as a novel target for autoantibody-mediated axonal injury, *The Journal of Experimental Medicine*, 204 (10): 2363-72.

Matsumoto, M., Funami, K., Tanabe, M., Oshiumi, H., Shingai, M., Seto, Y., Yamamoto, A. & Seya, T. (2003) Subcellular localization of Toll-like receptor 3 in human dendritic cells, *The Journal of Immunology*, 171 (6): 3154-62.

Matteoni, R. & Kreis, T.E. (1987) Translocation and clustering of endosomes and lysosomes depends on microtubules, *The Journal of Cell Biology*, 105 (3): 1253-65.

McCoy, K.D. & Le Gros, G. (1999) The role of CTLA-4 in the regulation of T cell immune responses, *Immunology and Cell Biology*, 77 (1): 1-10.

McCusker, K. & Hoidal, J. (1989) Characterization of scavenger receptor activity in resident human lung macrophages, *Experimental Lung Research*, 15 (4): 651-61.

McGonigle, L., Mousley, A., Marks, N.J., Brennan, G.P., Dalton, J.P., Spithill, T.W., Day, T.A. & Maule, A.G. (2008) The silencing of cysteine proteases in Fasciola hepatica newly excysted juveniles using RNA interference reduces gut penetration, *International Journal for Parasitology*, 38 (2): 149-55.

McInnes, I.B., al-Mughales, J., Field, M., Leung, B.P., Huang, F.P., Dixon, R., Sturrock, R.D., Wilkinson, P.C. & Liew, F.Y. (1996) The role of interleukin-15 in T-cell migration and activation in rheumatoid arthritis, *Nature Medicine*, 2 (2): 175-82.

McInnes, I.B., Leung, B.P., Harnett, M., Gracie, J.A., Liew, F.Y. & Harnett, W. (2003) A novel therapeutic approach targeting articular inflammation using the filarial nematode-derived phosphorylcholine-containing glycoprotein ES-62, *The Journal of Immunology*, 171 (4): 2127-33.

McInnes, I.B., Leung, B.P., Sturrock, R.D., Field, M. & Liew, F.Y. (1997) Interleukin-15 mediates T cell-dependent regulation of tumor necrosis factor-alpha production in rheumatoid arthritis, *Nature Medicine*, 3 (2): 189-95.

McLean, A. 2011, *Densitometry of western blots using Image J software*, Neural Regeneration Laboratory, Ottawa Institute of Systems Biology, Ottawa, viewed 08/07/2012 2012, <http://137.122.232.177/Protocols/ImageJ%28ACM%20revisedv5%29.pdf>.

McSorley, H.J., Gaze, S., Daveson, J., Jones, D., Anderson, R.P., Clouston, A., Ruyssers, N.E., Speare, R., McCarthy, J.S., Engwerda, C.R., Croese, J. & Loukas, A. (2011) Suppression of inflammatory immune responses in celiac disease by experimental hookworm infection, *PLoS One*, 6 (9): e24092.

Medzhitov, R., Preston-Hurlburt, P. & Janeway, C.A., Jr. (1997) A human homologue of the Drosophila Toll protein signals activation of adaptive immunity, *Nature*, 388 (6640): 394-7.

Medzhitov, R., Preston-Hurlburt, P., Kopp, E., Stadlen, A., Chen, C., Ghosh, S. & Janeway, C.A., Jr. (1998) MyD88 is an adaptor protein in the hToll/IL-1 receptor family signaling pathways, *Molecular Cell*, 2 (2): 253-8.

Meinl, E., Derfuss, T., Krumbholz, M., Probstel, A.K. & Hohlfeld, R. (2011) Humoral autoimmunity in multiple sclerosis, *Journal of the Neurological Sciences*, 306 (1-2): 180-2.

Menard, R., Carmona, E., Takebe, S., Dufour, E., Plouffe, C., Mason, P. & Mort, J.S. (1998) Autocatalytic processing of recombinant human procathepsin L. Contribution of both intermolecular and unimolecular events in the processing of procathepsin L in vitro, *The Journal of Biological Chemistry*, 273 (8): 4478-84.

Mendoza-Villanueva, D., Deng, W., Lopez-Camacho, C. & Shore, P. (2010) The Runx transcriptional co-activator, CBFbeta, is essential for invasion of breast cancer cells, *Molecular Cancer*, 9: 171.

Metwali, A., Setiawan, T., Blum, A.M., Urban, J., Elliott, D.E., Hang, L. & Weinstock, J.V. (2006) Induction of CD8+ regulatory T cells in the intestine by Heligmosomoides polygyrus infection, *American Journal of Physiology - Gastrointestinal and Liver Physiology*, 291 (2): G253-9.

Michaelsson, E., Holmdahl, M., Engstrom, A., Burkhardt, H., Scheynius, A. & Holmdahl, R. (1995) Macrophages, but not dendritic cells, present collagen to T cells, *European Journal of Immunology*, 25 (8): 2234-41.

Miller, J., Fraser, S.E. & McClay, D. (1995) Dynamics of thin filopodia during sea urchin gastrulation, *Development*, 121 (8): 2501-11.

Mills, K.H. (2011) TLR-dependent T cell activation in autoimmunity, *Nature Reviews Immunology*, 11 (12): 807-22.

Miltenburg, A.M., van Laar, J.M., de Kuiper, R., Daha, M.R. & Breedveld, F.C. (1992) T cells cloned from human rheumatoid synovial membrane functionally represent the Th1 subset, *Scandinavian Journal of Immunology*, 35 (5): 603-10.

Misgeld, T., Burgess, R.W., Lewis, R.M., Cunningham, J.M., Lichtman, J.W. & Sanes, J.R. (2002) Roles of neurotransmitter in synapse formation: development of neuromuscular junctions lacking choline acetyltransferase, *Neuron*, 36 (4): 635-48.

Miyamoto, S., Maki, M., Schmitt, M.J., Hatanaka, M. & Verma, I.M. (1994) Tumor necrosis factor alpha-induced phosphorylation of I kappa B alpha is a signal for its degradation but not dissociation from NF-kappa B, *Proceedings of the National Academy of Sciences of the United States of America*, 91 (26): 12740-4.

Mizoguchi, A. & Bhan, A.K. (2006) A case for regulatory B cells, *The Journal of Immunology*, 176 (2): 705-10.

Mo, H.M., Liu, W.Q., Lei, J.H., Cheng, Y.L., Wang, C.Z. & Li, Y.L. (2007) Schistosoma japonicum eggs modulate the activity of CD4+ CD25+ Tregs and prevent development of colitis in mice, *Experimental Parasitology*, 116 (4): 385-9.

Mosmann, T.R., Cherwinski, H., Bond, M.W., Giedlin, M.A. & Coffman, R.L. (1986) Two types of murine helper T cell clone. I. Definition according to profiles of lymphokine activities and secreted proteins, *The Journal of Immunology*, 136 (7): 2348-57.

Mosser, D.M. & Edwards, J.P. (2008) Exploring the full spectrum of macrophage activation, *Nature Reviews Immunology*, 8 (12): 958-69.

Motomura, Y., Wang, H., Deng, Y., El-Sharkawy, R.T., Verdu, E.F. & Khan, W.I. (2009) Helminth antigen-based strategy to ameliorate inflammation in an experimental model of colitis, *Clinical and Experimental Immunology*, 155 (1): 88-95.

Mu, F.T., Callaghan, J.M., Steele-Mortimer, O., Stenmark, H., Parton, R.G., Campbell, P.L., McCluskey, J., Yeo, J.P., Tock, E.P. & Toh, B.H. (1995) EEA1, an early endosome-associated protein. EEA1 is a conserved alpha-helical peripheral membrane protein flanked by cysteine "fingers" and contains a calmodulin-binding IQ motif, *The Journal of Biological Chemistry*, 270 (22): 13503-11.

Mukaida, N., Shiroo, M. & Matsushima, K. (1989) Genomic structure of the human monocyte-derived neutrophil chemotactic factor IL-8, *The Journal of Immunology*, 143 (4): 1366-71.

Mulvenna, J., Hamilton, B., Nagaraj, S.H., Smyth, D., Loukas, A. & Gorman, J.J. (2009) Proteomics analysis of the excretory/secretory component of the blood-feeding stage of the hookworm, Ancylostoma caninum, *Molecular and Cellular Proteomics*, 8 (1): 109-21.

Murray, P.J. & Wynn, T.A. (2011) Protective and pathogenic functions of macrophage subsets, *Nature Reviews Immunology*, 11 (11): 723-37.

Nair, M.G., Cochrane, D.W. & Allen, J.E. (2003) Macrophages in chronic type 2 inflammation have a novel phenotype characterized by the abundant expression of Ym1 and Fizz1 that can be partly replicated in vitro, *Immunology Letters*, 85 (2): 173-80.

Nair, M.G., Du, Y., Perrigoue, J.G., Zaph, C., Taylor, J.J., Goldschmidt, M., Swain, G.P., Yancopoulos, G.D., Valenzuela, D.M., Murphy, A., Karow, M., Stevens, S., Pearce, E.J. & Artis, D. (2009) Alternatively activated macrophage-derived RELM-alpha is a negative regulator of type 2 inflammation in the lung, *The Journal of Experimental Medicine*, 206 (4): 937-52.

Nair, M.G., Gallagher, I.J., Taylor, M.D., Loke, P., Coulson, P.S., Wilson, R.A., Maizels, R.M. & Allen, J.E. (2005) Chitinase and Fizz family members are a generalized feature of nematode infection with selective upregulation of Ym1 and Fizz1 by antigen-presenting cells, *Infection and Immunity*, 73 (1): 385-94.

Nair, M.G., Guild, K.J. & Artis, D. (2006) Novel effector molecules in type 2 inflammation: lessons drawn from helminth infection and allergy, *The Journal of Immunology*, 177 (3): 1393-9.

Neininger, A., Kontoyiannis, D., Kotlyarov, A., Winzen, R., Eckert, R., Volk, H.D., Holtmann, H., Kollias, G. & Gaestel, M. (2002) MK2 targets AU-rich elements and regulates biosynthesis of tumor necrosis factor and interleukin-6 independently at different post-transcriptional levels, *The Journal of Biological Chemistry*, 277 (5): 3065-8.

Newlands, G.F., Skuce, P.J., Knox, D.P. & Smith, W.D. (2001) Cloning and expression of cystatin, a potent cysteine protease inhibitor from the gut of Haemonchus contortus, *Parasitology*, 122 (Pt 3): 371-8.

Nguyen, H.B., Rivers, E.P., Abrahamian, F.M., Moran, G.J., Abraham, E., Trzeciak, S., Huang, D.T., Osborn, T., Stevens, D. & Talan, D.A. (2006) Severe sepsis and septic shock: review of the literature and emergency department management guidelines, *Annals of Emergency Medicine*, 48 (1): 28-54.

Niehaus, A., Shi, J., Grzenkowski, M., Diers-Fenger, M., Archelos, J., Hartung, H.P., Toyka, K., Bruck, W. & Trotter, J. (2000) Patients with active relapsing-remitting multiple sclerosis synthesize antibodies recognizing oligodendrocyte progenitor cell surface protein: implications for remyelination, *Annals of Neurology*, 48 (3): 362-71.

Nishiya, T. & DeFranco, A.L. (2004) Ligand-regulated chimeric receptor approach reveals distinctive subcellular localization and signaling properties of the Toll-like receptors, *The Journal of Biological Chemistry*, 279 (18): 19008-17.

Nurieva, R., Yang, X.O., Martinez, G., Zhang, Y., Panopoulos, A.D., Ma, L., Schluns, K., Tian, Q., Watowich, S.S., Jetten, A.M. & Dong, C. (2007) Essential autocrine regulation by IL-21 in the generation of inflammatory T cells, *Nature*, 448 (7152): 480-3.

O'Doherty, U., Peng, M., Gezelter, S., Swiggard, W.J., Betjes, M., Bhardwaj, N. & Steinman, R.M. (1994) Human blood contains two subsets of dendritic cells, one immunologically mature and the other immature, *Immunology*, 82 (3): 487-93.

O'Neill, S.M., Brady, M.T., Callanan, J.J., Mulcahy, G., Joyce, P., Mills, K.H. & Dalton, J.P. (2000) Fasciola hepatica infection downregulates Th1 responses in mice, *Parasite Immunology*, 22 (3): 147-55.

O'Neill, S.M., Mills, K.H. & Dalton, J.P. (2001) Fasciola hepatica cathepsin L cysteine proteinase suppresses Bordetella pertussis-specific interferon-gamma production in vivo, *Parasite Immunology*, 23 (10): 541-7.

Obermajer, N., Doljak, B. & Kos, J. (2006) Cysteine cathepsins: regulators of antitumour immune response, *Expert Opinion on Biological Therapy*, 6 (12): 1295-309.

Oda, T. & Maeda, H. (1986) A new simple fluorometric assay for phagocytosis, *Journal of Immunological Methods*, 88 (2): 175-83.

Odegaard, J.I. & Chawla, A. (2011) Alternative macrophage activation and metabolism, *Annual Review of Pathology*, 6: 275-97.

Ogunrinade, A. & Adegoke, G.O. (1982) Bovine fascioliasis in Nigeria - intercurrent parasitic and bacterial infections, *Tropical Animal Health and Production*, 14 (2): 121-5.

Ohashi, K., Burkart, V., Flohe, S. & Kolb, H. (2000) Cutting edge: heat shock protein 60 is a putative endogenous ligand of the toll-like receptor-4 complex, *The Journal of Immunology*, 164 (2): 558-61.

Ohashi, K., Naruto, M., Nakaki, T. & Sano, E. (2003) Identification of interleukin-8 converting enzyme as cathepsin L, *Biochimica et Biophysica Acta*, 1649 (1): 30-9.

Okamura, Y., Watari, M., Jerud, E.S., Young, D.W., Ishizaka, S.T., Rose, J., Chow, J.C. & Strauss, J.F., 3rd (2001) The extra domain A of fibronectin activates Toll-like receptor 4, *The Journal of Biological Chemistry*, 276 (13): 10229-33.

Okano, M., Satoskar, A.R., Nishizaki, K., Abe, M. & Harn, D.A., Jr. (1999) Induction of Th2 responses and IgE is largely due to carbohydrates functioning as adjuvants on Schistosoma mansoni egg antigens, *The Journal of Immunology*, 163 (12): 6712-7.

Onfelt, B., Nedvetzki, S., Benninger, R.K., Purbhoo, M.A., Sowinski, S., Hume, A.N., Seabra, M.C., Neil, M.A., French, P.M. & Davis, D.M. (2006) Structurally distinct membrane nanotubes between human macrophages support long-distance vesicular traffic or surfing of bacteria, *The Journal of Immunology*, 177 (12): 8476-83.

Onfelt, B., Nedvetzki, S., Yanagi, K. & Davis, D.M. (2004) Cutting edge: Membrane nanotubes connect immune cells, *The Journal of Immunology*, 173 (3): 1511-3.

Orrenius, S., Gogvadze, V. & Zhivotovsky, B. (2007) Mitochondrial oxidative stress: implications for cell death, *Annual Review of Pharmacology and Toxicology*, 47: 143-83.

Osada, Y., Shimizu, S., Kumagai, T., Yamada, S. & Kanazawa, T. (2009) Schistosoma mansoni infection reduces severity of collagen-induced arthritis via down-regulation of pro-inflammatory mediators, *International Journal for Parasitology*, 39 (4): 457-64.

Ottesen, E.A., Skvaril, F., Tripathy, S.P., Poindexter, R.W. & Hussain, R. (1985) Prominence of IgG4 in the IgG antibody response to human filariasis, *The Journal of Immunology*, 134 (4): 2707-12.

Park, H., Li, Z., Yang, X.O., Chang, S.H., Nurieva, R., Wang, Y.H., Wang, Y., Hood, L., Zhu, Z., Tian, Q. & Dong, C. (2005) A distinct lineage of CD4 T cells regulates tissue inflammation by producing interleukin 17, *Nature Immunology*, 6 (11): 1133-41.

Park, Y., Park, S., Yoo, E., Kim, D. & Shin, H. (2004) Association of the polymorphism for Toll-like receptor 2 with type 1 diabetes susceptibility, *Annals of the New York Academy of Sciences*, 1037: 170-4.

Paschoud, S., Dogar, A.M., Kuntz, C., Grisoni-Neupert, B., Richman, L. & Kuhn, L.C. (2006) Destabilization of interleukin-6 mRNA requires a putative RNA stem-loop structure, an AU-rich element, and the RNA-binding protein AUF1, *Molecular and Cellular Biology*, 26 (22): 8228-41.

Patschan, S., Chen, J., Gealekman, O., Krupincza, K., Wang, M., Shu, L., Shayman, J.A. & Goligorsky, M.S. (2008a) Mapping mechanisms and charting the time course of premature cell senescence and apoptosis: lysosomal dysfunction and ganglioside

accumulation in endothelial cells, *American Journal of Physiology - Renal Physiology*, 294 (1): F100-9.

Patschan, S., Chen, J., Polotskaia, A., Mendelev, N., Cheng, J., Patschan, D. & Goligorsky, M.S. (2008b) Lipid mediators of autophagy in stress-induced premature senescence of endothelial cells, *American Journal of Physiology - Heart and Circulatory Physiology*, 294 (3): H1119-29.

Payne, D.M., Rossomando, A.J., Martino, P., Erickson, A.K., Her, J.H., Shabanowitz, J., Hunt, D.F., Weber, M.J. & Sturgill, T.W. (1991) Identification of the regulatory phosphorylation sites in pp42/mitogen-activated protein kinase (MAP kinase), *The EMBO Journal*, 10 (4): 885-92.

Pearce, E.J. (2005) Priming of the immune response by schistosome eggs, *Parasite Immunology*, 27 (7-8): 265-70.

Peden, A.A., Schonteich, E., Chun, J., Junutula, J.R., Scheller, R.H. & Prekeris, R. (2004) The RCP-Rab11 complex regulates endocytic protein sorting, *Molecular Biology of the Cell*, 15 (8): 3530-41.

Pesce, J.T., Ramalingam, T.R., Mentink-Kane, M.M., Wilson, M.S., El Kasmi, K.C., Smith, A.M., Thompson, R.W., Cheever, A.W., Murray, P.J. & Wynn, T.A. (2009) Arginase-1-expressing macrophages suppress Th2 cytokine-driven inflammation and fibrosis, *PLoS pathogens*, 5 (4): e1000371.

Pihoker, C., Gilliam, L.K., Hampe, C.S. & Lernmark, A. (2005) Autoantibodies in diabetes, *Diabetes*, 54 Suppl 2: S52-61.

Pilling, D., Fan, T., Huang, D., Kaul, B. & Gomer, R.H. (2009) Identification of markers that distinguish monocyte-derived fibrocytes from monocytes, macrophages, and fibroblasts, *PLoS One*, 4 (10): e7475.

Pinet, V., Vergelli, M., Martin, R., Bakke, O. & Long, E.O. (1995) Antigen presentation mediated by recycling of surface HLA-DR molecules, *Nature*, 375 (6532): 603-6.

Plotnikov, E.Y., Khryapenkova, T.G., Galkina, S.I., Sukhikh, G.T. & Zorov, D.B. (2010) Cytoplasm and organelle transfer between mesenchymal multipotent stromal cells and renal tubular cells in co-culture, *Experimental Cell Research*, 316 (15): 2447-55.

Plotnikov, E.Y., Khryapenkova, T.G., Vasileva, A.K., Marey, M.V., Galkina, S.I., Isaev, N.K., Sheval, E.V., Polyakov, V.Y., Sukhikh, G.T. & Zorov, D.B. (2008) Cell-to-cell cross-talk between mesenchymal stem cells and cardiomyocytes in co-culture, *Journal of Cellular and Molecular Medicine*, 12 (5A): 1622-31.

Pociot, F., D'Alfonso, S., Compasso, S., Scorza, R. & Richiardi, P.M. (1995) Functional analysis of a new polymorphism in the human TNF alpha gene promoter, *Scandinavian Journal of Immunology*, 42 (4): 501-4.

Poltorak, A., He, X., Smirnova, I., Liu, M.Y., Van Huffel, C., Du, X., Birdwell, D., Alejos, E., Silva, M., Galanos, C., Freudenberg, M., Ricciardi-Castagnoli, P., Layton, B. & Beutler, B. (1998) Defective LPS signaling in C3H/HeJ and C57BL/10ScCr mice: mutations in Tlr4 gene, *Science*, 282 (5396): 2085-8.

Porcheray, F., Viaud, S., Rimaniol, A.C., Leone, C., Samah, B., Dereuddre-Bosquet, N., Dormont, D. & Gras, G. (2005) Macrophage activation switching: an asset for the resolution of inflammation, *Clinical and Experimental Immunology*, 142 (3): 481-9.

Prinz, M., Garbe, F., Schmidt, H., Mildner, A., Gutcher, I., Wolter, K., Piesche, M., Schroers, R., Weiss, E., Kirschning, C.J., Rochford, C.D., Bruck, W. & Becher, B. (2006) Innate immunity mediated by TLR9 modulates pathogenicity in an animal model of multiple sclerosis, *The Journal of Clinical Investigation*, 116 (2): 456-64.

Puri, C. (2009) Loss of myosin VI no insert isoform (NoI) induces a defect in clathrin-mediated endocytosis and leads to caveolar endocytosis of transferrin receptor, *The Journal of Biological Chemistry*, 284 (50): 34998-5014.

Quah, B.J., Barlow, V.P., McPhun, V., Matthaei, K.I., Hulett, M.D. & Parish, C.R. (2008) Bystander B cells rapidly acquire antigen receptors from activated B cells by membrane transfer, *Proceedings of the National Academy of Sciences of the United States of America*, 105 (11): 4259-64.

Quayle, A.J., Chomarat, P., Miossec, P., Kjeldsen-Kragh, J., Forre, O. & Natvig, J.B. (1993) Rheumatoid inflammatory T-cell clones express mostly Th1 but also Th2 and mixed (Th0-like) cytokine patterns, *Scandinavian Journal of Immunology*, 38 (1): 75-82.

Rabinovitch, A., Sumoski, W., Rajotte, R.V. & Warnock, G.L. (1990) Cytotoxic effects of cytokines on human pancreatic islet cells in monolayer culture, *The Journal of Clinical Endocrinology and Metabolism*, 71 (1): 152-6.

Raes, G., Brys, L., Dahal, B.K., Brandt, J., Grooten, J., Brombacher, F., Vanham, G., Noel, W., Bogaert, P., Boonefaes, T., Kindt, A., Van den Bergh, R., Leenen, P.J., De Baetselier, P. & Ghassabeh, G.H. (2005) Macrophage galactose-type C-type lectins as novel markers for alternatively activated macrophages elicited by parasitic infections and allergic airway inflammation, *Journal of Leukocyte Biology*, 77 (3): 321-7.

Raes, G., De Baetselier, P., Noel, W., Beschin, A., Brombacher, F. & Hassanzadeh Gh, G. (2002) Differential expression of FIZZ1 and Ym1 in alternatively versus classically activated macrophages, *Journal of Leukocyte Biology*, 71 (4): 597-602.

Ramirez-Weber, F.A. & Kornberg, T.B. (1999) Cytonemes: cellular processes that project to the principal signaling center in Drosophila imaginal discs, *Cell*, 97 (5): 599-607.

Rapoport, M.J., Lazarus, A.H., Jaramillo, A., Speck, E. & Delovitch, T.L. (1993) Thymic T cell anergy in autoimmune nonobese diabetic mice is mediated by deficient T cell receptor regulation of the pathway of p21ras activation, *The Journal of Experimental Medicine*, 177 (4): 1221-6.

Ray, A., Sassone-Corsi, P. & Sehgal, P.B. (1989) A multiple cytokine- and second messenger-responsive element in the enhancer of the human interleukin-6 gene: similarities with c-fos gene regulation, *Molecular and Cellular Biology*, 9 (12): 5537-47.

Reardon, C., Sanchez, A., Hogaboam, C.M. & McKay, D.M. (2001) Tapeworm infection reduces epithelial ion transport abnormalities in murine dextran sulfate sodium-induced colitis, *Infection and Immunity*, 69 (7): 4417-23.

Rebuffat, S.A., Nguyen, B., Robert, B., Castex, F. & Peraldi-Roux, S. (2008) Antithyroperoxidase antibody-dependent cytotoxicity in autoimmune thyroid disease, *The Journal of Clinical Endocrinology and Metabolism*, 93 (3): 929-34.

Reis e Sousa, C., Hieny, S., Scharton-Kersten, T., Jankovic, D., Charest, H., Germain, R.N. & Sher, A. (1997) In vivo microbial stimulation induces rapid CD40 ligand-independent production of interleukin 12 by dendritic cells and their redistribution to T cell areas, *The Journal of Experimental Medicine*, 186 (11): 1819-29.

Rewers, M., Bugawan, T.L., Norris, J.M., Blair, A., Beaty, B., Hoffman, M., McDuffie, R.S., Jr., Hamman, R.F., Klingensmith, G., Eisenbarth, G.S. & Erlich, H.A. (1996) Newborn screening for HLA markers associated with IDDM: diabetes autoimmunity study in the young (DAISY), *Diabetologia*, 39 (7): 807-12.

Rink, J., Ghigo, E., Kalaidzidis, Y. & Zerial, M. (2005) Rab conversion as a mechanism of progression from early to late endosomes, *Cell*, 122 (5): 735-49.

Rissoan, M.C., Soumelis, V., Kadowaki, N., Grouard, G., Briere, F., de Waal Malefyt, R. & Liu, Y.J. (1999) Reciprocal control of T helper cell and dendritic cell differentiation, *Science*, 283 (5405): 1183-6.

Ritzenthaler, S. & Chiba, A. (2003) Myopodia (postsynaptic filopodia) participate in synaptic target recognition, *Journal of Neurobiology*, 55 (1): 31-40.

Ritzenthaler, S., Suzuki, E. & Chiba, A. (2000) Postsynaptic filopodia in muscle cells interact with innervating motoneuron axons, *Nature Neuroscience*, 3 (10): 1012-7.

Robinson, M.W., Alvarado, R., To, J., Hutchinson, A.T., Dowdell, S.N., Lund, M., Turnbull, L., Whitchurch, C.B., O'Brien, B.A., Dalton, J.P. & Donnelly, S. (2012) A helminth cathelicidin-like protein suppresses antigen processing and presentation in macrophages via inhibition of lysosomal vATPase, *The FASEB Journal*, 26 (11): 4614-27.

Robinson, M.W. & Connolly, B. (2005) Proteomic analysis of the excretory-secretory proteins of the Trichinella spiralis L1 larva, a nematode parasite of skeletal muscle, *Proteomics*, 5 (17): 4525-32.

Robinson, M.W., Corvo, I., Jones, P.M., George, A.M., Padula, M.P., To, J., Cancela, M., Rinaldi, G., Tort, J.F., Roche, L. & Dalton, J.P. (2011a) Collagenolytic activities of the major secreted cathepsin L peptidases involved in the virulence of the helminth pathogen, Fasciola hepatica, *PLoS Neglected Tropical Diseases*, 5 (4): e1012.

Robinson, M.W., Donnelly, S., Hutchinson, A.T., To, J., Taylor, N.L., Norton, R.S., Perugini, M.A. & Dalton, J.P. (2011b) A family of helminth molecules that modulate innate cell responses via molecular mimicry of host antimicrobial peptides, *PLoS Pathogens*, 7 (5): e1002042.

Rodriguez-Sosa, M., Satoskar, A.R., Calderon, R., Gomez-Garcia, L., Saavedra, R., Bojalil, R. & Terrazas, L.I. (2002) Chronic helminth infection induces alternatively

activated macrophages expressing high levels of CCR5 with low interleukin-12 production and Th2-biasing ability, *Infection and Immunity*, 70 (7): 3656-64.

Roux, P.P. & Blenis, J. (2004) ERK and p38 MAPK-activated protein kinases: a family of protein kinases with diverse biological functions, *Microbiology and Molecular Biology Reviews*, 68 (2): 320-44.

Ruddy, S. & Austen, K.F. (1975) Activation of the complement and properdin systems in rheumatoid arthritis, *Annals of the New York Academy of Sciences*, 256: 96-104.

Rudick, R.A., Ransohoff, R.M., Peppler, R., VanderBrug Medendorp, S., Lehmann, P. & Alam, J. (1996) Interferon beta induces interleukin-10 expression: relevance to multiple sclerosis, *Annals of Neurology*, 40 (4): 618-27.

Rustom, A., Saffrich, R., Markovic, I., Walther, P. & Gerdes, H.H. (2004) Nanotubular highways for intercellular organelle transport, *Science*, 303 (5660): 1007-10.

Ruyssers, N.E., De Winter, B.Y., De Man, J.G., Loukas, A., Herman, A.G., Pelckmans, P.A. & Moreels, T.G. (2008) Worms and the treatment of inflammatory bowel disease: are molecules the answer?, *Clinical and Developmental Immunology*, 2008: 567314.

Ruyssers, N.E., De Winter, B.Y., De Man, J.G., Loukas, A., Pearson, M.S., Weinstock, J.V., Van den Bossche, R.M., Martinet, W., Pelckmans, P.A. & Moreels, T.G. (2009) Therapeutic potential of helminth soluble proteins in TNBS-induced colitis in mice, *Inflammatory Bowel Diseases*, 15 (4): 491-500.

Rzepecka, J., Rausch, S., Klotz, C., Schnoller, C., Kornprobst, T., Hagen, J., Ignatius, R., Lucius, R. & Hartmann, S. (2009) Calreticulin from the intestinal nematode Heligmosomoides polygyrus is a Th2-skewing protein and interacts with murine scavenger receptor-A, *Molecular Immunology*, 46 (6): 1109-19.

Sadowski, L., Pilecka, I. & Miaczynska, M. (2009) Signaling from endosomes: location makes a difference, *Experimental Cell Research*, 315 (9): 1601-9.

Saitoh, S. (2009) Chaperones and transport proteins regulate TLR4 trafficking and activation, *Immunobiology*, 214 (7): 594-600.

Saitoh, S., Akashi, S., Yamada, T., Tanimura, N., Kobayashi, M., Konno, K., Matsumoto, F., Fukase, K., Kusumoto, S., Nagai, Y., Kusumoto, Y., Kosugi, A. & Miyake, K. (2004) Lipid A antagonist, lipid IVa, is distinct from lipid A in interaction with Toll-like receptor 4 (TLR4)-MD-2 and ligand-induced TLR4 oligomerization, *International Immunology*, 16 (7): 961-9.

Salinas-Carmona, M.C., de la Cruz-Galicia, G., Perez-Rivera, I., Solis-Soto, J.M., Segoviano-Ramirez, J.C., Vazquez, A.V. & Garza, M.A. (2009) Spontaneous arthritis in MRL/lpr mice is aggravated by Staphylococcus aureus and ameliorated by Nippostrongylus brasiliensis infections, *Autoimmunity*, 42 (1): 25-32.

Samson, F., Donoso, J.A., Heller-Bettinger, I., Watson, D. & Himes, R.H. (1979) Nocodazole action on tubulin assembly, axonal ultrastructure and fast axoplasmic transport, *The Journal of Pharmacology and Experimental Therapeutics*, 208 (3): 411-7.

Sartor, R.B. & Hoentjen, F. 2005, Proinflammatory cytokines and signaling pathways in intestinal innate immune cells, in *Mucosal Immunology*, J. Mestecky (ed.), Elsevier, Philadelphia, pp. 681-701.

Sato, S., Sugiyama, M., Yamamoto, M., Watanabe, Y., Kawai, T., Takeda, K. & Akira, S. (2003) Toll/IL-1 receptor domain-containing adaptor inducing IFN-beta (TRIF) associates with TNF receptor-associated factor 6 and TANK-binding kinase 1, and activates two distinct transcription factors, NF-kappa B and IFN-regulatory factor-3, in the Toll-like receptor signaling, *The Journal of Immunology*, 171 (8): 4304-10.

Saunders, K.A., Raine, T., Cooke, A. & Lawrence, C.E. (2007a) Inhibition of autoimmune type 1 diabetes by gastrointestinal helminth infection, *Infection and Immunity*, 75 (1): 397-407.

Saunders, K.A., Raine, T., Cooke, A. & Lawrence, C.E. (2007b) Inhibition of autoimmune type 1 diabetes by gastrointestinal helminth infection, *Infect Immun*, 75 (1): 397-407.

Schmid, S.L., McNiven, M.A. & De Camilli, P. (1998) Dynamin and its partners: a progress report, *Current Opinion in Cell Biology*, 10 (4): 504-12.

Schnoeller, C., Rausch, S., Pillai, S., Avagyan, A., Wittig, B.M., Loddenkemper, C., Hamann, A., Hamelmann, E., Lucius, R. & Hartmann, S. (2008) A helminth immunomodulator reduces allergic and inflammatory responses by induction of IL-10-producing macrophages, *The Journal of Immunology*, 180 (6): 4265-72.

Schonemeyer, A., Lucius, R., Sonnenburg, B., Brattig, N., Sabat, R., Schilling, K., Bradley, J. & Hartmann, S. (2001) Modulation of human T cell responses and macrophage functions by onchocystatin, a secreted protein of the filarial nematode Onchocerca volvulus, *The Journal of Immunology*, 167 (6): 3207-15.

Schook, L.B., Albrecht, H., Gallay, P. & Jongeneel, C.V. (1994) Cytokine regulation of TNF-alpha mRNA and protein production by unprimed macrophages from C57Bl/6 and NZW mice, *Journal of Leukocyte Biology*, 56 (4): 514-20.

Schramm, G., Mohrs, K., Wodrich, M., Doenhoff, M.J., Pearce, E.J., Haas, H. & Mohrs, M. (2007) Cutting edge: IPSE/alpha-1, a glycoprotein from Schistosoma mansoni eggs, induces IgE-dependent, antigen-independent IL-4 production by murine basophils in vivo, *The Journal of Immunology*, 178 (10): 6023-7.

Schroder, M. & Bowie, A.G. (2005) TLR3 in antiviral immunity: key player or bystander?, *Trends in Immunology*, 26 (9): 462-8.

Schubert, L.A., Jeffery, E., Zhang, Y., Ramsdell, F. & Ziegler, S.F. (2001) Scurfin (FOXP3) acts as a repressor of transcription and regulates T cell activation, *The Journal of Biological Chemistry*, 276 (40): 37672-9.

Searle, S. & Blackwell, J.M. (1999) Evidence for a functional repeat polymorphism in the promoter of the human NRAMP1 gene that correlates with autoimmune versus infectious disease susceptibility, *Journal of Medical Genetics*, 36 (4): 295-9.

Sebbag, M., Parry, S.L., Brennan, F.M. & Feldmann, M. (1997) Cytokine stimulation of T lymphocytes regulates their capacity to induce monocyte production of tumor

necrosis factor-alpha, but not interleukin-10: possible relevance to pathophysiology of rheumatoid arthritis, *European Journal of Immunology*, 27 (3): 624-32.

Seder, R.A., Paul, W.E., Davis, M.M. & Fazekas de St Groth, B. (1992) The presence of interleukin 4 during in vitro priming determines the lymphokine-producing potential of CD4+ T cells from T cell receptor transgenic mice, *The Journal of Experimental Medicine*, 176 (4): 1091-8.

Segura, M., Su, Z., Piccirillo, C. & Stevenson, M.M. (2007) Impairment of dendritic cell function by excretory-secretory products: a potential mechanism for nematode-induced immunosuppression, *European Journal of Immunology*, 37 (7): 1887-904.

Selmaj, K.W. & Raine, C.S. (1988) Tumor necrosis factor mediates myelin and oligodendrocyte damage in vitro, *Annals of Neurology*, 23 (4): 339-46.

Semnani, R.T., Venugopal, P.G., Leifer, C.A., Mostbock, S., Sabzevari, H. & Nutman, T.B. (2008) Inhibition of TLR3 and TLR4 function and expression in human dendritic cells by helminth parasites, *Blood*, 112 (4): 1290-8.

Serafini, B., Columba-Cabezas, S., Di Rosa, F. & Aloisi, F. (2000) Intracerebral recruitment and maturation of dendritic cells in the onset and progression of experimental autoimmune encephalomyelitis, *The American Journal of Pathology*, 157 (6): 1991-2002.

Seroogy, C.M., Soares, L., Ranheim, E.A., Su, L., Holness, C., Bloom, D. & Fathman, C.G. (2004) The gene related to anergy in lymphocytes, an E3 ubiquitin ligase, is necessary for anergy induction in CD4 T cells, *The Journal of Immunology*, 173 (1): 79-85.

Setiawan, T., Metwali, A., Blum, A.M., Ince, M.N., Urban, J.F., Jr., Elliott, D.E. & Weinstock, J.V. (2007) Heligmosomoides polygyrus promotes regulatory T-cell cytokine production in the murine normal distal intestine, *Infection and Immunity*, 75 (9): 4655-63.

Sever, S., Altintas, M.M., Nankoe, S.R., Moller, C.C., Ko, D., Wei, C., Henderson, J., del Re, E.C., Hsing, L., Erickson, A., Cohen, C.D., Kretzler, M., Kerjaschki, D., Rudensky, A., Nikolic, B. & Reiser, J. (2007) Proteolytic processing of dynamin by cytoplasmic cathepsin L is a mechanism for proteinuric kidney disease, *The Journal of Clinical Investigation*, 117 (8): 2095-104.

Shen, H., Tesar, B.M., Walker, W.E. & Goldstein, D.R. (2008) Dual signaling of MyD88 and TRIF is critical for maximal TLR4-induced dendritic cell maturation, *The Journal of Immunology*, 181 (3): 1849-58.

Sherer, N.M., Lehmann, M.J., Jimenez-Soto, L.F., Horensavitz, C., Pypaert, M. & Mothes, W. (2007) Retroviruses can establish filopodial bridges for efficient cell-to-cell transmission, *Nature Cell Biology*, 9 (3): 310-5.

Shi, M., Wang, A., Prescott, D., Waterhouse, C.C., Zhang, S., McDougall, J.J., Sharkey, K.A. & McKay, D.M. (2011) Infection with an intestinal helminth parasite reduces Freund's complete adjuvant-induced monoarthritis in mice, *Arthritis and Rheumatism*, 63 (2): 434-44.

Shieh, J.C., Schaar, B.T., Srinivasan, K., Brodsky, F.M. & McConnell, S.K. (2011) Endocytosis regulates cell soma translocation and the distribution of adhesion proteins in migrating neurons, *PLoS One*, 6 (3): e17802.

Sioud, M. (2005) Induction of inflammatory cytokines and interferon responses by double-stranded and single-stranded siRNAs is sequence-dependent and requires endosomal localization, *Journal of Molecular Biology*, 348 (5): 1079-90.

Skapenko, A., Leipe, J., Lipsky, P.E. & Schulze-Koops, H. (2005) The role of the T cell in autoimmune inflammation, *Arthritis Research and Therapy*, 7 Suppl 2: S4-14.

Smith, A.M., Dowd, A.J., Heffernan, M., Robertson, C.D. & Dalton, J.P. (1993a) Fasciola hepatica: a secreted cathepsin L-like proteinase cleaves host immunoglobulin, *International Journal for Parasitology*, 23 (8): 977-83.

Smith, A.M., Dowd, A.J., McGonigle, S., Keegan, P.S., Brennan, G., Trudgett, A. & Dalton, J.P. (1993b) Purification of a cathepsin L-like proteinase secreted by adult Fasciola hepatica, *Molecular and Biochemical Parasitology*, 62 (1): 1-8.

Smith, P., Fallon, R.E., Mangan, N.E., Walsh, C.M., Saraiva, M., Sayers, J.R., McKenzie, A.N., Alcami, A. & Fallon, P.G. (2005) Schistosoma mansoni secretes a chemokine binding protein with antiinflammatory activity, *The Journal of Experimental Medicine*, 202 (10): 1319-25.

Smith, P., Mangan, N.E., Walsh, C.M., Fallon, R.E., McKenzie, A.N., van Rooijen, N. & Fallon, P.G. (2007) Infection with a helminth parasite prevents experimental colitis via a macrophage-mediated mechanism, *The Journal of Immunology*, 178 (7): 4557-66.

Smith, P., Walsh, C.M., Mangan, N.E., Fallon, R.E., Sayers, J.R., McKenzie, A.N. & Fallon, P.G. (2004) Schistosoma mansoni worms induce anergy of T cells via selective up-regulation of programmed death ligand 1 on macrophages, *The Journal of Immunology*, 173 (2): 1240-8.

Smith, P.D., Janoff, E.N., Mosteller-Barnum, M., Merger, M., Orenstein, J.M., Kearney, J.F. & Graham, M.F. (1997) Isolation and purification of CD14-negative mucosal macrophages from normal human small intestine, *Journal of Immunological Methods*, 202 (1): 1-11.

Smith, P.D., Smythies, L.E., Mosteller-Barnum, M., Sibley, D.A., Russell, M.W., Merger, M., Sellers, M.T., Orenstein, J.M., Shimada, T., Graham, M.F. & Kubagawa, H. (2001) Intestinal macrophages lack CD14 and CD89 and consequently are down-regulated for LPS- and IgA-mediated activities, *The Journal of Immunology*, 167 (5): 2651-6.

Smythies, L.E., Sellers, M., Clements, R.H., Mosteller-Barnum, M., Meng, G., Benjamin, W.H., Orenstein, J.M. & Smith, P.D. (2005) Human intestinal macrophages display profound inflammatory anergy despite avid phagocytic and bacteriocidal activity, *The Journal of Clinical Investigation*, 115 (1): 66-75.

Snapper, C.M. & Paul, W.E. (1987a) B cell stimulatory factor-1 (interleukin 4) prepares resting murine B cells to secrete IgG1 upon subsequent stimulation with bacterial lipopolysaccharide, *The Journal of Immunology*, 139 (1): 10-7.

Snapper, C.M. & Paul, W.E. (1987b) Interferon-gamma and B cell stimulatory factor-1 reciprocally regulate Ig isotype production, *Science*, 236 (4804): 944-7.

Snapper, C.M., Peschel, C. & Paul, W.E. (1988) IFN-gamma stimulates IgG2a secretion by murine B cells stimulated with bacterial lipopolysaccharide, *The Journal of Immunology*, 140 (7): 2121-7.

Sojka, D.K., Huang, Y.H. & Fowell, D.J. (2008) Mechanisms of regulatory T-cell suppression - a diverse arsenal for a moving target, *Immunology*, 124 (1): 13-22.

Sowinski, S., Jolly, C., Berninghausen, O., Purbhoo, M.A., Chauveau, A., Kohler, K., Oddos, S., Eissmann, P., Brodsky, F.M., Hopkins, C., Onfelt, B., Sattentau, Q. & Davis, D.M. (2008) Membrane nanotubes physically connect T cells over long distances presenting a novel route for HIV-1 transmission, *Nature Cell Biology*, 10 (2): 211-9.

Spang, A. (2009) On the fate of early endosomes, *The Journal of Biological Chemistry*, 390 (8): 753-9.

Spees, J.L., Olson, S.D., Whitney, M.J. & Prockop, D.J. (2006) Mitochondrial transfer between cells can rescue aerobic respiration, *Proceedings of the National Academy of Sciences of the United States of America*, 103 (5): 1283-8.

Sprent, J. & Kishimoto, H. (2001) The thymus and central tolerance, *Philosophical transactions of the Royal Society of London. Series B, Biological sciences*, 356 (1409): 609-16.

Stack, C.M., Dalton, J.P., Cunneen, M. & Donnelly, S. (2005) De-glycosylation of Pichia pastoris-produced Schistosoma mansoni cathepsin B eliminates non-specific reactivity with IgG in normal human serum, *Journal of Immunological Methods*, 304 (1-2): 151-7.

Stanworth, D.R., Humphrey, J.H., Bennich, H. & Johansson, S.G. (1968) Inhibition of Prausnitz-Kustner reaction by proteolytic-cleavage fragments of a human myeloma protein of immunoglobulin class E, *Lancet*, 2 (7558): 17-8.

Stein, M., Keshav, S., Harris, N. & Gordon, S. (1992) Interleukin-4 potently enhances murine macrophage mannose receptor activity - A marker of alternative immunological macrophage activation, *The Journal of Experimental Medicine*, 176 (1): 287-92.

Steinfelder, S., Andersen, J.F., Cannons, J.L., Feng, C.G., Joshi, M., Dwyer, D., Caspar, P., Schwartzberg, P.L., Sher, A. & Jankovic, D. (2009) The major component in schistosome eggs responsible for conditioning dendritic cells for Th2 polarization is a T2 ribonuclease (omega-1), *The Journal of Experimental Medicine*, 206 (8): 1681-90.

Stoecklin, G., Tenenbaum, S.A., Mayo, T., Chittur, S.V., George, A.D., Baroni, T.E., Blackshear, P.J. & Anderson, P. (2008) Genome-wide analysis identifies interleukin-10 mRNA as target of tristetraprolin, *The Journal of Biological Chemistry*, 283 (17): 11689-99.

Su, A.I., Cooke, M.P., Ching, K.A., Hakak, Y., Walker, J.R., Wiltshire, T., Orth, A.P., Vega, R.G., Sapinoso, L.M., Moqrich, A., Patapoutian, A., Hampton, G.M., Schultz, P.G. & Hogenesch, J.B. (2002) Large-scale analysis of the human and mouse

transcriptomes, *Proceedings of the National Academy of Sciences of the United States of America*, 99 (7): 4465-70.

Sugawara, S., Sugiyama, A., Nemoto, E., Rikiishi, H. & Takada, H. (1998) Heterogeneous expression and release of CD14 by human gingival fibroblasts: characterization and CD14-mediated interleukin-8 secretion in response to lipopolysaccharide, *Infection and Immunity*, 66 (7): 3043-9.

Summers, R.W., Elliott, D.E., Qadir, K., Urban, J.F., Jr., Thompson, R. & Weinstock, J.V. (2003) Trichuris suis seems to be safe and possibly effective in the treatment of inflammatory bowel disease, *The American Journal of Gastroenterology*, 98 (9): 2034-41.

Summers, R.W., Elliott, D.E., Urban, J.F., Jr., Thompson, R.A. & Weinstock, J.V. (2005) Trichuris suis therapy for active ulcerative colitis: a randomized controlled trial, *Gastroenterology*, 128 (4): 825-32.

Sun, S.C., Ganchi, P.A., Beraud, C., Ballard, D.W. & Greene, W.C. (1994) Autoregulation of the NF-kappa B transactivator RelA (p65) by multiple cytoplasmic inhibitors containing ankyrin motifs, *Proceedings of the National Academy of Sciences of the United States of America*, 91 (4): 1346-50.

Sutton, T.L., Zhao, A., Madden, K.B., Elfrey, J.E., Tuft, B.A., Sullivan, C.A., Urban, J.F., Jr. & Shea-Donohue, T. (2008) Anti-inflammatory mechanisms of enteric Heligmosomoides polygyrus infection against trinitrobenzene sulfonic acid-induced colitis in a murine model, *Infection and Immunity*, 76 (10): 4772-82.

Tabeta, K., Georgel, P., Janssen, E., Du, X., Hoebe, K., Crozat, K., Mudd, S., Shamel, L., Sovath, S., Goode, J., Alexopoulou, L., Flavell, R.A. & Beutler, B. (2004) Toll-like receptors 9 and 3 as essential components of innate immune defense against mouse cytomegalovirus infection, *Proceedings of the National Academy of Sciences of the United States of America*, 101 (10): 3516-21.

Takaesu, G., Surabhi, R.M., Park, K.J., Ninomiya-Tsuji, J., Matsumoto, K. & Gaynor, R.B. (2003) TAK1 is critical for IkappaB kinase-mediated activation of the NF-kappaB pathway, *Journal of Molecular Biology*, 326 (1): 105-15.

Takeda, K. & Akira, S. (2004) TLR signaling pathways, *Seminars in Immunology*, 16 (1): 3-9.

Takeuchi, O. & Akira, S. (2010) Pattern recognition receptors and inflammation, *Cell*, 140 (6): 805-20.

Takeuchi, O., Kawai, T., Muhlradt, P.F., Morr, M., Radolf, J.D., Zychlinsky, A., Takeda, K. & Akira, S. (2001) Discrimination of bacterial lipoproteins by Toll-like receptor 6, *International Immunology*, 13 (7): 933-40.

Takeuchi, O., Sato, S., Horiuchi, T., Hoshino, K., Takeda, K., Dong, Z., Modlin, R.L. & Akira, S. (2002) Cutting edge: role of Toll-like receptor 1 in mediating immune response to microbial lipoproteins, *The Journal of Immunology*, 169 (1): 10-4.

Tamai, R., Sakuta, T., Matsushita, K., Torii, M., Takeuchi, O., Akira, S., Akashi, S., Espevik, T., Sugawara, S. & Takada, H. (2002) Human gingival CD14(+) fibroblasts

primed with gamma interferon increase production of interleukin-8 in response to lipopolysaccharide through up-regulation of membrane CD14 and MyD88 mRNA expression, *Infection and Immunity*, 70 (3): 1272-8.

Taniguchi, T., Ogasawara, K., Takaoka, A. & Tanaka, N. (2001) IRF family of transcription factors as regulators of host defense, *Annual Review of Immunology*, 19: 623-55.

Tanimura, N., Saitoh, S., Matsumoto, F., Akashi-Takamura, S. & Miyake, K. (2008) Roles for LPS-dependent interaction and relocation of TLR4 and TRAM in TRIF-signaling, *Biochemical and Biophysical Research Communications*, 368 (1): 94-9.

Tarkowski, A., Klareskog, L., Carlsten, H., Herberts, P. & Koopman, W.J. (1989) Secretion of antibodies to types I and II collagen by synovial tissue cells in patients with rheumatoid arthritis, *Arthritis Rheum*, 32 (9): 1087-92.

Taylor, J.J., Krawczyk, C.M., Mohrs, M. & Pearce, E.J. (2009a) Th2 cell hyporesponsiveness during chronic murine schistosomiasis is cell intrinsic and linked to GRAIL expression, *The Journal of Clinical Investigation*, 119 (4): 1019-28.

Taylor, M.D., Harris, A., Babayan, S.A., Bain, O., Culshaw, A., Allen, J.E. & Maizels, R.M. (2007) CTLA-4 and CD4+ CD25+ regulatory T cells inhibit protective immunity to filarial parasites in vivo, *The Journal of Immunology*, 179 (7): 4626-34.

Taylor, M.D., Harris, A., Nair, M.G., Maizels, R.M. & Allen, J.E. (2006) F4/80+ alternatively activated macrophages control CD4+ T cell hyporesponsiveness at sites peripheral to filarial infection, *The Journal of Immunology*, 176 (11): 6918-27.

Taylor, M.D., LeGoff, L., Harris, A., Malone, E., Allen, J.E. & Maizels, R.M. (2005) Removal of regulatory T cell activity reverses hyporesponsiveness and leads to filarial parasite clearance in vivo, *The Journal of Immunology*, 174 (8): 4924-33.

Taylor, M.D., van der Werf, N., Harris, A., Graham, A.L., Bain, O., Allen, J.E. & Maizels, R.M. (2009b) Early recruitment of natural CD4+ Foxp3+ Treg cells by infective larvae determines the outcome of filarial infection, *European Journal of Immunology*, 39 (1): 192-206.

Taylor, P.R., Brown, G.D., Reid, D.M., Willment, J.A., Martinez-Pomares, L., Gordon, S. & Wong, S.Y. (2002) The beta-glucan receptor, dectin-1, is predominantly expressed on the surface of cells of the monocyte/macrophage and neutrophil lineages, *The Journal of Immunology*, 169 (7): 3876-82.

Teft, W.A., Kirchhof, M.G. & Madrenas, J. (2006) A molecular perspective of CTLA-4 function, *Annual Review of Immunology*, 24: 65-97.

Termeer, C., Benedix, F., Sleeman, J., Fieber, C., Voith, U., Ahrens, T., Miyake, K., Freudenberg, M., Galanos, C. & Simon, J.C. (2002) Oligosaccharides of Hyaluronan activate dendritic cells via toll-like receptor 4, *The Journal of Experimental Medicine*, 195 (1): 99-111.

Terrazas, L.I., Montero, D., Terrazas, C.A., Reyes, J.L. & Rodriguez-Sosa, M. (2005) Role of the programmed Death-1 pathway in the suppressive activity of alternatively

activated macrophages in experimental cysticercosis, *International Journal for Parasitology*, 35 (13): 1349-58.

Thomas, K.E., Galligan, C.L., Newman, R.D., Fish, E.N. & Vogel, S.N. (2006) Contribution of interferon-beta to the murine macrophage response to the toll-like receptor 4 agonist, lipopolysaccharide, *The Journal of Biological Chemistry*, 281 (41): 31119-30.

Thomas, P.G., Carter, M.R., Atochina, O., Da'Dara, A.A., Piskorska, D., McGuire, E. & Harn, D.A. (2003) Maturation of dendritic cell 2 phenotype by a helminth glycan uses a Toll-like receptor 4-dependent mechanism, *The Journal of Immunology*, 171 (11): 5837-41.

Thomas, R., Davis, L.S. & Lipsky, P.E. (1994) Rheumatoid synovium is enriched in mature antigen-presenting dendritic cells, *The Journal of Immunology*, 152 (5): 2613-23.

Tivol, E.A., Borriello, F., Schweitzer, A.N., Lynch, W.P., Bluestone, J.A. & Sharpe, A.H. (1995) Loss of CTLA-4 leads to massive lymphoproliferation and fatal multiorgan tissue destruction, revealing a critical negative regulatory role of CTLA-4, *Immunity*, 3 (5): 541-7.

Trentham, D.E., Dynesius-Trentham, R.A., Orav, E.J., Combitchi, D., Lorenzo, C., Sewell, K.L., Hafler, D.A. & Weiner, H.L. (1993) Effects of oral administration of type II collagen on rheumatoid arthritis, *Science*, 261 (5129): 1727-30.

Triantafilou, M. & Triantafilou, K. (2002) Lipopolysaccharide recognition: CD14, TLRs and the LPS-activation cluster, *Trends in Immunology*, 23 (6): 301-4.

Turner, K.J., Feddema, L. & Quinn, E.H. (1979) Non-specific potentiation of IgE by parasitic infections in man, *International Archives of Allergy and Applied Immunology*, 58 (2): 232-6.

Ueda, H., Howson, J.M., Esposito, L., Heward, J., Snook, H., Chamberlain, G., Rainbow, D.B., Hunter, K.M., Smith, A.N., Di Genova, G., Herr, M.H., Dahlman, I., Payne, F., Smyth, D., Lowe, C., Twells, R.C., Howlett, S., Healy, B., Nutland, S., Rance, H.E., Everett, V., Smink, L.J., Lam, A.C., Cordell, H.J., Walker, N.M., Bordin, C., Hulme, J., Motzo, C., Cucca, F., Hess, J.F., Metzker, M.L., Rogers, J., Gregory, S., Allahabadia, A., Nithiyananthan, R., Tuomilehto-Wolf, E., Tuomilehto, J., Bingley, P., Gillespie, K.M., Undlien, D.E., Ronningen, K.S., Guja, C., Ionescu-Tirgoviste, C., Savage, D.A., Maxwell, A.P., Carson, D.J., Patterson, C.C., Franklyn, J.A., Clayton, D.G., Peterson, L.B., Wicker, L.S., Todd, J.A. & Gough, S.C. (2003) Association of the T-cell regulatory gene CTLA4 with susceptibility to autoimmune disease, *Nature*, 423 (6939): 506-11.

Ulevitch, R.J. & Tobias, P.S. (1995) Receptor-dependent mechanisms of cell stimulation by bacterial endotoxin, *Annual Review of Immunology*, 13: 437-57.

Uronen-Hansson, H., Allen, J., Osman, M., Squires, G., Klein, N. & Callard, R.E. (2004) Toll-like receptor 2 (TLR2) and TLR4 are present inside human dendritic cells, associated with microtubules and the Golgi apparatus but are not detectable on the cell surface: integrity of microtubules is required for interleukin-12 production in response to internalized bacteria, *Immunology*, 111 (2): 173-8.

Valero, M.A., Navarro, M., Garcia-Bodelon, M.A., Marcilla, A., Morales, M., Hernandez, J.L., Mengual, P. & Mas-Coma, S. (2006) High risk of bacterobilia in advanced experimental chronic fasciolosis, *Acta Tropica*, 100 (1-2): 17-23.

van der Kleij, D., Latz, E., Brouwers, J.F., Kruize, Y.C., Schmitz, M., Kurt-Jones, E.A., Espevik, T., de Jong, E.C., Kapsenberg, M.L., Golenbock, D.T., Tielens, A.G. & Yazdanbakhsh, M. (2002) A novel host-parasite lipid cross-talk. Schistosomal lyso-phosphatidylserine activates toll-like receptor 2 and affects immune polarization, *The Journal of Biological Chemistry*, 277 (50): 48122-9.

van der Kleij, D., van den Biggelaar, A.H., Kruize, Y.C., Retra, K., Fillie, Y., Schmitz, M., Kremsner, P.G., Tielens, A.G. & Yazdanbakhsh, M. (2004) Responses to Toll-like receptor ligands in children living in areas where schistosome infections are endemic, *The Journal of Infectious Diseases*, 189 (6): 1044-51.

van der Neut Kolfschoten, M., Schuurman, J., Losen, M., Bleeker, W.K., Martinez-Martinez, P., Vermeulen, E., den Bleker, T.H., Wiegman, L., Vink, T., Aarden, L.A., De Baets, M.H., van de Winkel, J.G., Aalberse, R.C. & Parren, P.W. (2007) Anti-inflammatory activity of human IgG4 antibodies by dynamic Fab arm exchange, *Science*, 317 (5844): 1554-7.

van der Zee, J.S., van Swieten, P. & Aalberse, R.C. (1986) Inhibition of complement activation by IgG4 antibodies, *Clinical and Experimental Immunology*, 64 (2): 415-22.

van Liempt, E., van Vliet, S.J., Engering, A., Garcia Vallejo, J.J., Bank, C.M., Sanchez-Hernandez, M., van Kooyk, Y. & van Die, I. (2007) Schistosoma mansoni soluble egg antigens are internalized by human dendritic cells through multiple C-type lectins and suppress TLR-induced dendritic cell activation, *Molecular Immunology*, 44 (10): 2605-15.

van Riet, E., Everts, B., Retra, K., Phylipsen, M., van Hellemond, J.J., Tielens, A.G., van der Kleij, D., Hartgers, F.C. & Yazdanbakhsh, M. (2009) Combined TLR2 and TLR4 ligation in the context of bacterial or helminth extracts in human monocyte derived dendritic cells: molecular correlates for Th1/Th2 polarization, *BMC Immunology*, 10: 9.

Vanhoutte, F., Breuilh, L., Fontaine, J., Zouain, C.S., Mallevaey, T., Vasseur, V., Capron, M., Goriely, S., Faveeuw, C., Ryffel, B. & Trottein, F. (2007) Toll-like receptor (TLR)2 and TLR3 sensing is required for dendritic cell activation, but dispensable to control Schistosoma mansoni infection and pathology, *Microbes and Infection*, 9 (14-15): 1606-13.

Venugopal, P.G., Nutman, T.B. & Semnani, R.T. (2009) Activation and regulation of toll-like receptors (TLRs) by helminth parasites, *Immunologic Research*, 43 (1-3): 252-63.

Verge, C.F., Gianani, R., Kawasaki, E., Yu, L., Pietropaolo, M., Jackson, R.A., Chase, H.P. & Eisenbarth, G.S. (1996) Prediction of type I diabetes in first-degree relatives using a combination of insulin, GAD, and ICA512bdc/IA-2 autoantibodies, *Diabetes*, 45 (7): 926-33.

Vyas, J.M., Kim, Y.M., Artavanis-Tsakonas, K., Love, J.C., Van der Veen, A.G. & Ploegh, H.L. (2007) Tubulation of class II MHC compartments is microtubule dependent and involves multiple endolysosomal membrane proteins in primary dendritic cells, *The Journal of Immunology*, 178 (11): 7199-210.

Waalen, K., Forre, O. & Natvig, J.B. (1988) Dendritic cells in rheumatoid inflammation, *Springer Seminars in Immunopathology*, 10 (2-3): 141-56.

Walker, L.S. & Abbas, A.K. (2002) The enemy within: keeping self-reactive T cells at bay in the periphery, *Nature Reviews Immunology*, 2 (1): 11-9.

Wang, X. & Gerdes, H.H. (2011a) Long-distance electrical coupling via tunneling nanotubes, *Biochimica et Biophysica Acta*, 1818 (8): 2082-6.

Wang, X., Veruki, M.L., Bukoreshtliev, N.V., Hartveit, E. & Gerdes, H.H. (2010) Animal cells connected by nanotubes can be electrically coupled through interposed gap-junction channels, *Proceedings of the National Academy of Sciences of the United States of America*, 107 (40): 17194-9.

Wang, Y., Cui, J., Sun, X. & Zhang, Y. (2011b) Tunneling-nanotube development in astrocytes depends on p53 activation, *Cell Death and Differentiation*, 18 (4): 732-42.

Wang, Y., Yang, Y., Liu, X., Wang, N., Cao, H., Lu, Y., Zhou, H. & Zheng, J. (2012) Inhibition of clathrin/dynamin-dependent internalization interferes with LPS-mediated TRAM-TRIF-dependent signaling pathway, *Cellular Immunology*, 274 (1-2): 121-9.

Waskiewicz, A.J. & Cooper, J.A. (1995) Mitogen and stress response pathways: MAP kinase cascades and phosphatase regulation in mammals and yeast, *Current Opinion in Cell Biology*, 7 (6): 798-805.

Watanabe, H., Numata, K., Ito, T., Takagi, K. & Matsukawa, A. (2004) Innate immune response in Th1- and Th2-dominant mouse strains, *Shock*, 22 (5): 460-6.

Watkins, S.C. & Salter, R.D. (2005) Functional connectivity between immune cells mediated by tunneling nanotubules, *Immunity*, 23 (3): 309-18.

Watts, C. (2008) Location, location, location: identifying the neighborhoods of LPS signaling, *Nature Immunology*, 9 (4): 343-5.

Whelan, J.T., Hollis, S.E., Cha, D.S., Asch, A.S. & Lee, M.H. (2012) Post-transcriptional regulation of the Ras-ERK/MAPK signaling pathway, *Journal of Cellular Physiology*, 227 (3): 1235-41.

Whelan, M., Harnett, M.M., Houston, K.M., Patel, V., Harnett, W. & Rigley, K.P. (2000) A filarial nematode-secreted product signals dendritic cells to acquire a phenotype that drives development of Th2 cells, *The Journal of Immunology*, 164 (12): 6453-60.

Wiesemann, E., Deb, M., Trebst, C., Hemmer, B., Stangel, M. & Windhagen, A. (2008) Effects of interferon-beta on co-signaling molecules: upregulation of CD40, CD86 and PD-L2 on monocytes in relation to clinical response to interferon-beta treatment in patients with multiple sclerosis, *Multiple Sclerosis*, 14 (2): 166-76.

Wilberz, S., Partke, H.J., Dagnaes-Hansen, F. & Herberg, L. (1991) Persistent MHV (mouse hepatitis virus) infection reduces the incidence of diabetes mellitus in non-obese diabetic mice, *Diabetologia*, 34 (1): 2-5.

Wildin, R.S., Smyk-Pearson, S. & Filipovich, A.H. (2002) Clinical and molecular features of the immunodysregulation, polyendocrinopathy, enteropathy, X linked (IPEX) syndrome, *Journal of Medical Genetics*, 39 (8): 537-45.

Wilson, A.G., Symons, J.A., McDowell, T.L., McDevitt, H.O. & Duff, G.W. (1997) Effects of a polymorphism in the human tumor necrosis factor alpha promoter on transcriptional activation, *Proceedings of the National Academy of Sciences of the United States of America*, 94 (7): 3195-9.

Winzen, R., Thakur, B.K., Dittrich-Breiholz, O., Shah, M., Redich, N., Dhamija, S., Kracht, M. & Holtmann, H. (2007) Functional analysis of KSRP interaction with the AU-rich element of interleukin-8 and identification of inflammatory mRNA targets, *Molecular and Cellular Biology*, 27 (23): 8388-400.

Wood, W., Jacinto, A., Grose, R., Woolner, S., Gale, J., Wilson, C. & Martin, P. (2002) Wound healing recapitulates morphogenesis in Drosophila embryos, *Nature Cell Biology*, 4 (11): 907-12.

World Health Organization 2008, *Atlas multiple sclerosis resources in the world 2008*, World Health Organization, Geneva.

Wright, S.D., Ramos, R.A., Tobias, P.S., Ulevitch, R.J. & Mathison, J.C. (1990) CD14, a receptor for complexes of lipopolysaccharide (LPS) and LPS binding protein, *Science*, 249 (4975): 1431-3.

Wubbolts, R., Fernandez-Borja, M., Jordens, I., Reits, E., Dusseljee, S., Echeverri, C., Vallee, R.B. & Neefjes, J. (1999) Opposing motor activities of dynein and kinesin determine retention and transport of MHC class II-containing compartments, *Journal of Cell Science*, 112 (6): 785-95.

Xu, D., Liu, H., Komai-Koma, M., Campbell, C., McSharry, C., Alexander, J. & Liew, F.Y. (2003) CD4+CD25+ regulatory T cells suppress differentiation and functions of Th1 and Th2 cells, Leishmania major infection, and colitis in mice, *The Journal of Immunology*, 170 (1): 394-9.

Yamada, M., Nakazawa, M., Kamata, I. & Arizono, N. (1992) Low-level infection with the nematode Nippostrongylus brasiliensis induces significant and sustained specific and non-specific IgE antibody responses in rats, *Immunology*, 75 (1): 36-40.

Yamamoto, M., Sato, S., Hemmi, H., Hoshino, K., Kaisho, T., Sanjo, H., Takeuchi, O., Sugiyama, M., Okabe, M., Takeda, K. & Akira, S. (2003) Role of adaptor TRIF in the MyD88-independent toll-like receptor signaling pathway, *Science*, 301 (5633): 640-3.

Yamamoto, M., Sato, S., Hemmi, H., Sanjo, H., Uematsu, S., Kaisho, T., Hoshino, K., Takeuchi, O., Kobayashi, M., Fujita, T., Takeda, K. & Akira, S. (2002) Essential role for TIRAP in activation of the signalling cascade shared by TLR2 and TLR4, *Nature*, 420 (6913): 324-9.

Yasuda, K., Khandare, A., Burianovskyy, L., Maruyama, S., Zhang, F., Nasjletti, A. & Goligorsky, M.S. (2011) Tunneling nanotubes mediate rescue of prematurely senescent endothelial cells by endothelial progenitors: exchange of lysosomal pool, *Aging*, 3 (6): 597-608.

Yasuda, K., Park, H.C., Ratliff, B., Addabbo, F., Hatzopoulos, A.K., Chander, P. & Goligorsky, M.S. (2010) Adriamycin nephropathy: a failure of endothelial progenitor cell-induced repair, *The American Journal of Pathology*, 176 (4): 1685-95.

Yazdanbakhsh, M. (1999) Common features of T cell reactivity in persistent helminth infections: lymphatic filariasis and schistosomiasis, *Immunology Letters*, 65 (1-2): 109-15.

Zaahl, M.G., Robson, K.J., Warnich, L. & Kotze, M.J. (2004) Expression of the SLC11A1 (NRAMP1) 5'-(GT)n repeat: opposite effect in the presence of -237C-->T, *Blood Cells, Molecules and Diseases*, 33 (1): 45-50.

Zaccone, P., Burton, O., Miller, N., Jones, F.M., Dunne, D.W. & Cooke, A. (2009) Schistosoma mansoni egg antigens induce Treg that participate in diabetes prevention in NOD mice, *European Journal of Immunology*, 39 (4): 1098-107.

Zaccone, P., Burton, O.T., Gibbs, S., Miller, N., Jones, F.M., Dunne, D.W. & Cooke, A. (2010) Immune modulation by Schistosoma mansoni antigens in NOD mice: effects on both innate and adaptive immune systems, *Journal of Biomedicine and Biotechnology*, 2010: 795210.

Zaccone, P., Burton, O.T., Gibbs, S.E., Miller, N., Jones, F.M., Schramm, G., Haas, H., Doenhoff, M.J., Dunne, D.W. & Cooke, A. (2011) The S. mansoni glycoprotein omega-1 induces Foxp3 expression in NOD mouse CD4(+) T cells, *European Journal of Immunology*, 41 (9): 2709-18.

Zaccone, P., Fehérvári, Z., Jones, F.M., Sidobre, S., Kronenberg, M., Dunne, D.W. & Cooke, A. (2003) Schistosoma mansoni antigens modulate the activity of the innate immune response and prevent onset of type 1 diabetes, *European Journal of Immunology*, 33 (5): 1439-49.

Zanoni, I., Ostuni, R., Marek, L.R., Barresi, S., Barbalat, R., Barton, G.M., Granucci, F. & Kagan, J.C. (2011) CD14 controls the LPS-induced endocytosis of Toll-like receptor 4, *Cell*, 147 (4): 868-80.

Zhang, T., Kruys, V., Huez, G. & Gueydan, C. (2002) AU-rich element-mediated translational control: complexity and multiple activities of trans-activating factors, *Biochemical Society Transactions*, 30 (Pt 6): 952-8.

Zhang, Y. (2011) Tunneling-nanotube: A new way of cell-cell communication, *Communicative and Integrative Biology*, 4 (3): 324-5.

Zheng, X., Hu, X., Zhou, G., Lu, Z., Qiu, W., Bao, J. & Dai, Y. (2008) Soluble egg antigen from Schistosoma japonicum modulates the progression of chronic progressive experimental autoimmune encephalomyelitis via Th2-shift response, *Journal of Neuroimmunology*, 194 (1-2): 107-14.

Zhou, L., Lopes, J.E., Chong, M.M., Ivanov, II, Min, R., Victora, G.D., Shen, Y., Du, J., Rubtsov, Y.P., Rudensky, A.Y., Ziegler, S.F. & Littman, D.R. (2008) TGF-beta-induced Foxp3 inhibits T(H)17 cell differentiation by antagonizing RORgammat function, *Nature*, 453 (7192): 236-40.

Zhu, D., Tan, K.S., Zhang, X., Sun, A.Y., Sun, G.Y. & Lee, J.C. (2005) Hydrogen peroxide alters membrane and cytoskeleton properties and increases intercellular connections in astrocytes, *Journal of Cell Science*, 118 (Pt 16): 3695-703.

Zhu, J. & Paul, W.E. (2008) CD4 T cells: fates, functions, and faults, *Blood*, 112 (5): 1557-69.

Zhu, Z., Zheng, T., Homer, R.J., Kim, Y.K., Chen, N.Y., Cohn, L., Hamid, Q. & Elias, J.A. (2004) Acidic mammalian chitinase in asthmatic Th2 inflammation and IL-13 pathway activation, *Science*, 304 (5677): 1678-82.

Ziegelbauer, K., Speich, B., Mausezahl, D., Bos, R., Keiser, J. & Utzinger, J. (2012) Effect of sanitation on soil-transmitted helminth infection: systematic review and meta-analysis, *PLoS Medicine*, 9 (1): e1001162.

Ziegler, A.G., Hummel, M., Schenker, M. & Bonifacio, E. (1999) Autoantibody appearance and risk for development of childhood diabetes in offspring of parents with type 1 diabetes: the 2-year analysis of the German BABYDIAB Study, *Diabetes*, 48 (3): 460-8.

Zinchuk, V., Zinchuk, O. & Okada, T. (2007) Quantitative colocalization analysis of multicolor confocal immunofluorescence microscopy images: pushing pixels to explore biological phenomena, *Acta Histochemica et Cytochemica*, 40 (4): 101-11.

Zipris, D., Lazarus, A.H., Crow, A.R., Hadzija, M. & Delovitch, T.L. (1991) Defective thymic T cell activation by concanavalin A and anti-CD3 in autoimmune nonobese diabetic mice. Evidence for thymic T cell anergy that correlates with the onset of insulitis, *The Journal of Immunology*, 146 (11): 3763-71.

Zvaifler, N.J., Steinman, R.M., Kaplan, G., Lau, L.L. & Rivelis, M. (1985) Identification of immunostimulatory dendritic cells in the synovial effusions of patients with rheumatoid arthritis, *The Journal of Clinical Investigation*, 76 (2): 789-800.